SUDAAR NO. 482

STANFORD UNIVERSITY

CENTER FOR SYSTEMS RESEARCH

Design of State-Feedback Controllers Including Sensitivity Reduction, with Applications to Precision Pointing

by

Zeev Hadass

Guidance and Control Laboratory

August 1974

This research was supported by
The Government of Israel
and partially supported by the
National Aeronautics and Space Administration
Contract NGR 05-020-019
and the
Air Force Avionics Laboratory
under Contract F33615-72-C-1297

SUDAAR 482

DESIGN OF STATE-FEEDBACK CONTROLLERS INCLUDING SENSITIVITY REDUCTION, WITH APPLICATIONS TO PRECISION POINTING

by

Zeev Hadass

Guidance and Control Laboratory
Department of Aeronautics and Astronautics
STANFORD UNIVERSITY
Stanford, California 94305

This research was supported by

The Government of Israel

and partially supported by the
National Aeronautics & Space Administration
Contract NGR 05-020-019

and the
Air Force Avionics Laboratory
under Contract F33615-72-C-1297

August 1974

ABSTRACT

State feedback controllers have been researched extensively in the last decade and computational tools have been developed for their design. In spite of the better system performance that can be obtained with these controllers, their application has not been widespread. This is mainly due to insufficient practical design experience and to the scarceness of general design guidelines in the published literature. Also, in many high-performance applications, especially if state estimates rather than states are used for feedback, the system is found to be excessively sensitive to parameter variations.

The purpose of this research is to develop a better engineering insight into the design process of state feedback controllers and to provide a method for the reduction of their sensitivity to parameter variations.

In this work the design procedure of feedback controllers is described and the considerations for the selection of the design parameters are given. The frequency domain properties of single-input single-output systems using state feedback controllers are analyzed, and desirable phase and gain margin properties are demonstrated. Special consideration is given to the design of controllers for tracking systems, especially those that are designed to track polynomial commands.

As an application example, a controller is designed for a tracking telescope. The telescope has a polynomial tracking requirement and possesses some special features such as actuator saturation and multiple measurements, one of which is sampled. The resulting system has a tracking performance that compares favorably with a much more complicated digital aided tracker.

The problem of parameter sensitivity reduction is treated by considering the variable parameters as random variables. A performance index is defined as a weighted sum of the state and control covariances that stem from both the random system disturbances and the parameter uncertainties. This performance index is minimized numerically by adjusting a set of free parameters.

A computer program implementing this method was developed and is applied to the sensitivity reduction of several initially sensitive tracking systems. Sensitivity reduction factors of 2-3 are typically obtained with modest increases in output rms and control effort.

ACKNOWLEDGMENTS

I wish to extend my gratitude to my adviser, Professor J. David Powell for his advice and guidance throughout the course of this research and for his many helpful suggestions. I also wish to thank Professor John V. Breakwell for his many useful comments, and Professors Dan DeBra and Arthur Bryson for their thorough review and constructive criticisms as readers.

My appreciation is extended to Ms. Ida Lee for her conscientious typing and editing.

I thank Mr. John Palmer of the Department of Computer Science at Stanford for his advice and aid in the development of the computer programs.

Particular gratitude is expressed to the Government of Israel who provided my finanical support, to the NASA for partial support under Contract NGR 05-020-019, and to Stanford University who financed my computer expenses.

Special thanks go to my wife, Rina, who gave me much support and encouragement during the period of this research.

TABLE OF CONTENTS

TABLE OF CONTENTS (Cont)

TABLE OF CONTENTS (Cont)

LIST OF FIGURES

LIST OF FIGURES (Cont)

LIST OF FIGURES (Cont)

LIST OF TABLES

LIST OF SYMBOLS

a	Ch. II	coefficient vector of the open loop characteristic polynomial
a	Ch. V	inner azimuth gimbal acceleration
a_o		gyro torquer position gain
a_1		gyro torquer integral gain
a_{ij}		ij element of the state weighting matrix
A		state weighting matrix
A	App. C	hydraulic actuator area
A_o		integral state weighting matrix
A_1	Ch. II	state weighting matrix for augmented system
A_1, A_2	App. C	hydraulic actuator areas
b	Ch. II	control weight for single input system
b	App. C	viscous friction coefficient
b_i $i=1,\ldots,5$	Ch. V	constants in the telescope dynamic matrix
b_{ij}		ij element of the control weighting matrix
B		control weighting matrix
B	Ch. V, App. C	bulk modulus of hydraulic fluid
B_r		partition of reduced estimator dynamic matrix
c		gyroscope damping coefficient
c_o		control amplifier gain
c_i $i=1,m$		components of feedback gain matrix for single input systems
c_1	App. C	proportionality constant

C		state feedback gain matrix
C_o	Ch. II	equilibrium control gain matrix
C_1	Ch. IV	state feedback gain matrix
C_2	Ch. IV	sensitivity feedback gain matrix
C_E		state estimate feedback gain matrix
C_r		state estimate feedback gain matrix
C_y		output feedback gain matrix
$\mathcal{C}$	Ch. II	controllability matrix
d	Ch. II	vector used in the definition of the model PI
d_1	Ch. III	thrustor noise torque
D		gyro drift torque
$D(s)$		system characteristic equation
$D_m(s)$		model characteristic equation
D_A	Ch. V App. C	characteristic volume of hydraulic actuator
DX		change in X due to free parameter perturbation
DF_c		change in F_c due to free parameter perturbation
DY		change in Y due to free parameter perturbation
$D(\delta X)$		change in δX due to free parameter perturbation
e		error state vector
$E[\ ]$		expected value
E_z		expected value over the distribution of z
E_w		expected value over the distribution of w
f_o		sampling rate of sampler and hold
F		system matrix

F_o		system matrix of observable system
F_1		system matrix of actual plant
F_c		closed loop system matrix
F_n		system matrix of non-measured states
F_r		system matrix of measured states
F_μ		derivative of system matrix with respect to the variable parameter μ
g		control distribution vector for single input systems
g(w,z)		function of z and w obtained by the relationship $f[x(w_1 z), u(w,z)] = g(w,z)$
g(i,j)		i,j element of the G matrix
G		control distribution matrix
G_i		control distribution matrix of the integral state
G_n		control distribution matrix of the measured states
G_r		control distribution matrix of the non-measured states
G_μ		derivative of control distribution matrix with respect to the variable parameter μ
G(s)	Ch. II	plant transfer function
$G_p(s)$	Ch. III	plant transfer function
$G_o(s)$		open loop transfer function
$G_c(s)$		compensator transfer function
H		output matrix
H	Ch. V App. H	gyro angular momentum
H_r		artificial output matrix for the non-measured states
H(s)		compensator transfer function

$H_c(s)$		equivalent series compensator transfer function
$H_u(s)$		transfer function from control to estimator output
$H_y(s)$		transfer function from measurement to estimator output
i		integral state
I		unity matrix
I_e		$e \times e$ unity matrix
$\{I_1, I_2, I_3, I_4,$		moments of inertia
J		performance index (PI)
J_o		nominal PI
J_A		additional PI
J_{AO}		additional PI for normalized parameter covariance matrix
J_{oi}		initial value of nominal PI
J_{SD}		deterministic sensitivity PI
J_{SS}		stochastic sensitivity PI
k	Ch. III, Ch. IV	spring constant of reduced Relativity Satellite
k	App. H	gyro loop gain
k_A	Ch. V App. C	gain in hydraulic actuator
k_A	App. H	gyro amplifier gain
k_D		gyro scale factor
k_g		rate gyro scale factor
k_i $i=1,\ldots,n$		components of the estimator gain matrix for single output systems

k_L		leakage coefficient of hydraulic actuator
k_T		gyro torquer scale factor
k_α		spring constant of soft spring in Relativity Satellite
k_γ		spring constant of stiff spring in Relativity Satellite
K		estimator gain matrix
K_A		acceleration coefficient
K_r		estimator gain matrix for reduced order estimator
ℓ		order of polynomial that can be tracked with constant control
m		number of controls
m	Ch. II-B-3	order of the numerator
m	Ch. II-D-3	vector of coefficients of polynomial reference output or disturbance
m_v		spool mass of electrohydraulic valve
m_1		damping of hydraulic actuator
m_2		natural frequency of hydraulic actuator
M_1, M_2, M_3		measurement noise distribution coefficients for system with reduced order estimator
M_α, M_ϵ, M_ψ		moments about axes of tracking telescope
n		dimension of system
n_q		dimension of free parameter vector
n_z	Ch. II	dimension of integral state vector
n_z	Ch. IV	dimension of variable parameter vector
N(s)		numerator of open loop transfer function
p		dimension of output vector
p	Ch. V	outer azimuth gimbal rate

p_i $i=1,\ldots,n$		ith root of characteristic equation
$p(\ )$		probability density function
p, p_1, p_2		pressures in hydraulic actuator
p_c, p_{c1}, p_{c2}		commanded pressures in hydraulic actuator
P		covariance matrix of the estimate error
P(s)		polynomial used for model PI
q		dimension of the state disturbance vector
q	Ch. IV	free parameter vector
q	Ch. V	torquer state
q	App. C	load flow rate of hydraulic torquer
q_n^t		last row of the inverse of the controllability matrix
Q		intensity matrix of the state disturbance
Q_w		intensity matrix of the state disturbance for the reduced Stanford Relativity Satellite
r	II-B-3	order of model for model PI
r	II-D-3	order of tracked polynomial
r	Ch. V	inner azimuth gimbal acceleration rate
r_d	Ch. V	detector measurement noise intensity
r_n	Ch. III	measurement noise intensity
R		measurement noise intensity matrix
R	App. E	minimum distance of target from tracker
s		Laplace transform operator
S		Ricatti matrix
S_λ		Eigenvalue sensitivity

S_s		transfer function sensitivity
t		time
t_f		final time
t_i		initial time
T	Ch. V	torquer generated torques about gyro output axis
$T(s,\mu)$	Ch. III	closed loop transfer function depending on variable parameter μ
u		control vector
u_o		external control
u_1		inner azimuth gimbal control
u_2		outer azimuth gimbal control
u_w		control required to eliminate effect of disturbances
U		control covariance
$U(\infty)$		equilibrium value of U
$U(s)$		inverse of transfer matrix from control to output
v		measurement noise vector
v	App. E	target velocity
v_e		volume of hydraulic actuator chamber
v_r		measurement noise of the artificial measurement in the reduced order estimator
v_{ii}		variance of the ith variable parameter
V	Ch. IV	covariance matrix of the variable parameters
V	App. F	potential energy
V_o		normalized covariance matrix of the variable parameters

w		state disturbance vector
w_i $i=1,q$		components of the state disturbance vector
W		weighting matrix for sensitivity PI
x		state vector
x_A		augmented state vector
x_c		state vector of the controllable canonical form
x_n	Ch. IV	nominal state vector
x_n	App. J	state vector of the measured states in the reduced order estimator
x_r		state vector of the non-measured states in the reduced order estimator
x_u		state vector of system with non-white disturbance
x_v		spool displacement of the hydraulic actuator
X		state covariance matrix
$X(\infty)$, X_∞		equilibrium value of X
X_A		covariance matrix of the augmented system
X_n		nominal covariance matrix
y		output vector
y_r		artificial measurement vector for reduced order estimator
Y		auxiliary covariance matrix defined by Eq. (4.26a)
Y_i		The Y matrix for the ith variable parameter
$Y(s)$		transfer matrix from the control to the state
$Y_i(s)$		transfer function from scalar n to the ith component of the state vector

z	Ch. II	state vector of the integral states
z	Ch. IV	variable parameter vector
z_i $i=1,\ldots,m$		ith root of numerator polynomial
z_n		expected value of the variable parameter vector
$Z(s)$		transfer matrix from the state disturbance to the output

Greek Symbols

α	Ch. II	coefficient vector of the required closed loop characteristic polynomial
α	Ch. III	ratio between outer inertia and total inertia of reduced Stanford Relativity Satellite
α	Ch. V	total angle of inner azimuth gimbal
α_c		commanded angle of inner azimuth gimbal
α_N		noise torque between outer and middle body
α_i $i=1,\ldots,m$		contribution of the ith control in a multi-input system
β		linearized state of zero order hold
γ_i $i=1,\ldots,r$		ith coefficient of model characteristic equation
Γ		disturbance distribution matrix
δ_d		tracking error
δx		state vector perturbation due to a system parameter perturbation
δF		system matrix perturbation due to a system parameter perturbation
δX		addition to the covariance matrix due to a system parameter perturbation

$\delta\omega_L$		lower frequency margin
$\delta\omega_n$		upper frequency margin
ϵ	Ch. IV	sensitivity weighting coefficient
ϵ	V-D, V-E, App. J App. K	output error
ϵ	V-B, App. C App. E	elevation angle
ζ		damping coefficient
λ		number of integrations required for polynomial tracking
λ_i		ith eigenvalue
Λ_{λ_j}		super diagonal unity matrix of order λ_j
μ		variable parameter
π		number of integrations required for rejecting polynomial disturbances
ρ		distance of target from tracker
σ_p		the rms value of p
σ_{az}		tracking error defined in Eq. (5.19)
σ_d		detector rms noise
σ_{FC}		tracking error of system with feedback controller
σ_N		torquer rms noise
σ_T		disturbance torques on inner gimbal
$\sigma(t)$		trajectory sensitivity
τ		nondimensional time
τ_v		time constant of the hydraulic actuator

φ	Ch. III	attitude angle of outer body in reduced Relativity Satellite phase angle
φ	App. G	phase angle
φ	Ch. V	inner azimuth gimbal angle
$\begin{cases}\varphi_A, \varphi_B, \\ \varphi_C\end{cases}$		phase angles
Φ		state transition matrix
ψ		outer azimuth gimbal angle
ω		inner azimuth gimbal rate
ω_o	Ch. II	distance of Butterworth configuration eigenvalues from origin
ω_o	Chs. III, IV, V	natural frequency
ω_o	App. G	sampling frequency

Subscripts

A	augmented
D	disturbance system
e	error system
o	nominal system
n	nominal system
r	reference system
s	equilibrium

Superscripts

o	optimal
T	transpose
-1	inverse

$\hat{}$	estimate
$\sim$	estimate error
-	time average

Abbreviations Used In Text

adj	adjoint matrix (in equations)
det	determinant (in equations)
PI	performance index
RIG	rate integrating gyro
rms	root mean square
RO	reference output
SEF	state estimate feedback
SISO	single-input single-output
SRP	sensitivity reduction program
SRS	Stanford Relativity Satellite, or Relativity Satellite
tr	trace operator
ZOH	zero order hold

Computer Programs

OPTSYS	Optimal System Design program
PAROPT	Parameter Sensitivity Minimization program
SIMUL	Time Response Simulation program
XAGSA	General Stability Analysis program

I. INTRODUCTION

A. BACKGROUND

State feedback controllers have been researched intensively in the last decade. Design methods for these controllers have been developed, the most important among them being quadratic synthesis [BRY-1]. The application of these methods to all but the simplest systems requires computer aid and in recent years, efficient computer programs for their implementation have become available [BRY-3].

In applying these methods, it is observed in many cases that the resulting systems have better performance capabilities than those that are designed using classical frequency domain techniques, especially for multivariable systems [BU-1]. In spite of this, the application of state feedback to practical design problems is not yet widespread, mainly due to the fact that this method is relatively new and designers are therefore not familiar with its potential.

In classical frequency domain techniques, a considerable body of design experience has accumulated over the years. Based on this experience, designers can express the system specifications in terms of the controller structure and parameters. No comparable experience exists for state feedback controllers and it is therefore difficult, at times, to relate the system specifications to design parameters such as state and control weights.

Most of the publications on the subject of state feedback control either treat its theoretical aspects or describe the results of specific applications. Only few publications such as Bull's [BU-1] give some general insight into the design process and provide practical guidelines for the selection of the design parameters. Designers experienced in the classical techniques are therefore reluctant to use these methods.

In attempting to apply state feedback to practical designs, the problems of sensitivity to parameter variations may be encountered. In

most applications of state feedback, almost all the states are estimated and not measured. High performance systems using state estimates for feedback are typically sensitive to parameter variations.

The subject of sensitivity has been treated extensively in the literature. A collection of papers dealing with this subject has been published recently by Cruz [CR-1]. Most of the publications, however, treat various theoretical aspects of the problem. Design papers, in which practical methods for sensitivity reduction are described, are relatively scarce. Some of the sensitivity reduction methods that are applicable to quadratic synthesis designs are reviewed in Chapter IV of this work. None of these methods, however, seems to be directly applicable to relatively high order multiinput-output systems in which several plant parameters may be variable. The designer is therefore apt to compromise on a system that has lower performance but also lower sensitivity and will thus not be able to take advantage of the full potential of state feedback controllers.

A better engineering insight into the design process of state feedback controllers, and a general method for their sensitivity reduction may therefore increase the applicability of these controllers to realistic systems. In this thesis, an attempt is made to treat these two problems.

B. THESIS OUTLINE

In Chapter II the design process of feedback controllers and state estimators is reviewed. Various methods for determining the state feedback and estimator gains are given and the selection of state and control weights for quadratic synthesis is described.

Some frequency domain properties of single-input single-output state feedback controllers are derived. These properties show that these controllers, especially if they are designed by quadratic synthesis, have advantages over other methods of compensation.

The application of state feedback to systems with tracking requirements is also described in this chapter. The state augmentations that

are required for tracking specific time functions are derived.

Most of the material in this chapter is taken from sources in the literature. Some parts, however, such as the infinite gain margin property of full state feedback controllers and the determination of the state augmentation required for polynomial tracking, are believed to be original.

In Chapter III, the parameter sensitivity of state estimate feedback controllers is examined and illustrated by means of an example. The system in this example is a simplified version of the Stanford Relativity Satellite which is a satellite-mounted tracking telescope. For this system, it is shown that the sensitivity stems from the use of state estimates instead of states for feedback. A stability criterion, which is expressed as a frequency margin, is developed for this system.

In Chapter IV, a method is derived for the sensitivity reduction of systems represented in state variable form. The method is applicable to multivariable systems with several variable parameters, subject to arbitrary inputs. It is an extension of the quadratic synthesis method and is based on a method developed by Palsson and Whittaker [PA-1] for single-input single-output systems. A computer program implementing this method was developed and the results of its application to two systems are described. These systems are the simplified and full version of the Stanford Relativity Satellite [BU-1]. Considerable sensitivity reduction is obtained in both cases, at a modest cost in performance and control effort.

In Chapter V, a state feedback controller for a ground-based tracking telescope is designed. This system was selected as an example for the application of the design methods of Chapter II. It has some special features such as control through a flexible element, several measurements, polynomial tracking requirements, and nonlinear elements. Several variants of the controller and estimator design are investigated and their performances are compared. The sensitivity is reduced using the methods derived in Chapter IV, and a nonlinear network is introduced for the improvement of the large signal stability. The tracking performance is compared to that of an aided tracker designed for a similar system.

Conclusions and a summary are given in Chapter VI.

C. CONTRIBUTIONS

The principal contributions of this thesis are as follows.

C.1 State Feedback Control

(1) Investigation of engineering properties of state feedback controllers. Determination of state augmentations required for polynomial tracking.

(2) Application of a state estimate feedback controller to a high performance tracker.

C.2 Sensitivity Reduction

(1) Analysis of the sensitivity of state estimate feedback controllers and derivation of the frequency margin stability criterion.

(2) Development of a method for the reduction of sensitivity to parameter variations, and of a computer program for the implementation of this method.

(3) Application of the method to estimator design, including the reduced sensitivity design of the attitude control of the Stanford Relativity Satellite.

II. FEEDBACK CONTROLLER DESIGN

A. INTRODUCTION

In this chapter, the design of state feedback controllers for linear systems is described and some guidelines are given for their application to realistic systems. It is an attempt to fill a gap in the literature between the theoretical treatments which typically deal with the mathematical steps of designing a controller and the application papers which typically describe specific results without discussing the design steps and the considerations involved in the design procedure.

Familiarity with the state variable representation of systems and its various conomical forms is assumed. This subject is treated extensively in various texts [CA-1, SC-1].

Only linear time invariant systems are considered. This is not as restrictive as it may seem since the design of feedback controllers for nonlinear systems is, in general, very complicated and therefore in many cases an open loop controller is designed for the nominal trajectory and a feedback controller for the perturbations about this trajectory [BRY-2]. The perturbation equations are linear. They may not have constant coefficients but in many cases it is preferred to use an average value of the coefficients and design a constant gain controller instead of the much more complex time-varying controller. If the range of variation of the coefficients is large and the variation sufficiently slow, a switchable gain controller may be used.

In the following section, B, regulator design procedures are described, using both pole placement and quadratic synthesis. In the quadratic synthesis procedure, the judgement of the designer is involved mainly in the selection of state and control weights. Some methods are given for this selection based on system requirements.

In Section C, some properties of systems using state feedback are examined. There seems to be a notion among control designers that state feedback may have an advantage over classical design methods for multi-input multi-output systems but that it offers no such advantage for single-input single-output (SISO) systems. The properties described in this Section show that in many cases, state feedback may have considerable advantages over classical design techniques even for SISO systems.

In Section D, the more complex problems of tracking and nonzero mean disturbances are treated and multivariable integral control is introduced.

B. REGULATOR DESIGN

B.1 Description of the Design Procedure

The basic controller for a linear time invariant system is the regulator. It is designed to keep the states of the system in an acceptable vicinity of zero with an acceptable amount of control, while the system is subject to random zero-mean disturbances and the measurements are contaminated by random zero-mean noise.

The system is described by

$$\begin{aligned} \dot{x} &= Fx + Gu + \Gamma w \\ y &= Hx + v \end{aligned} \tag{2.1}$$

where

- x = state vector ($n \times 1$)
- F = system matrix ($n \times n$)
- u = control vector ($m \times 1$)
- G = control distribution matrix ($n \times m$)
- w = state disturbance ($q \times 1$)
- Γ = disturbance distribution matrix ($n \times q$)
- y = output vector ($p \times 1$)

H = output matrix ($p \times n$)

v = measurement noise ($p \times 1$).

The regulator design procedure consists of two steps: (1) design of a state feedback controller, and (2) design of a state estimator. These two design steps are performed independently.

The state feedback controller has the form

$$u = -Cx .$$

In its design, all the states are assumed to be available for feedback. The design consists in selecting the feedback gain matrix $C(m \times n)$. Two principal methods are available for this selection: (1) pole placement; (2) quadratic synthesis.

In the first method, the system requirements, such as rise time, overshoot, damping ratio, phase margin, etc., are translated into desirable locations of the closed loop eigenvalues and the feedback gains required to obtain these eigenvalues are found. Only for SISO systems are the gains determined uniquely by the eigenvalues. For multivariable systems, additional constraints have to be imposed. Methods for selecting the gains for given eigenvalues are described in Section B.2.

In the second method, the gains are determined so as to minimize a performance index of the form

$$J = \int_0^\infty (x^T Ax + u^T Bu)dt$$

where the weighting matrices A and B are determined by the designer. The methods for selection of the weighting matrices and for determining the gains for given weighting matrices are described in Section B.3.

The estimator generates estimates of the non-measured states which are then used for feedback in the controller instead of the real states. In many cases, especially when the system is subject to noise, all the

states required for feedback, and not just the non-measured ones, are obtained from the estimator. The structure of the estimator and the methods for its design are described in Section B.4.

The engineering properties of systems designed by this method are described in Section C. The regulator as described above will keep the states of the system in the vicinity of zero when the system is subject to random, zero mean disturbances. If the disturbances have a constant or slowly time-varying component, or if the output of the system is required to follow a command input, regulator type controllers may not be able to prevent output errors. State augmentation techniques as described in Section D may in some cases extend the regulator design procedures to such cases.

B.2 Feedback Gain Determination by Pole Placement

In general, the system specifications will call for either a specified time response (rise time, overshoot) to inputs (or recovery from non-zero initial conditions) or for a maximum rms level of output and control when the system is subject to random disturbances and sensor noise of a known intensity.

Typically, pole placement will be used in the first case since it is difficult to correlate the closed loop eigenvalue location with the resulting rms value in the outputs and the controls. For single input systems, several methods exist for the determination of the gains. If the system is in its controllable canonical form [CA-1] the feedback gains are simply the differences between the coefficients of the open loop characteristic equation and the required closed loop characteristic equation [CA-1]. If the system matrix has arbitrary form the gain matrix C is obtained from the equation

$$C = [a - \alpha]^T P \qquad (2.2)$$

where $a - \alpha$ is the vector of the differences between the coefficients of the open loop and the required closed loop characteristic equations, P is the transformation matrix from the given form into the controllable canonical form [$x_c = Px$]. Ackerman [AC-1] has provided a formula for finding the feedback gains without calculating the open loop characteristic polynomial. It is

$$C = q_n^T \alpha(F)$$

where

$q_n^T = [0, \ldots, 0, 1]\mathcal{C}^{-1}$,

F = the system dynamic matrix

$\alpha(s)$ = the desired closed loop characteristic polynomial,

$\mathcal{C} = [G, FG, \ldots, F^{n-1}G]$, is the controllability matrix.

Some algorithms for gain determination in multi-input system have also been developed. Anderson & Luenberger [AN-1] transform the system into a canonical form that is composed of blocks in the controller canonical form on the diagonal and zero blocks above it. The required closed loop eigenvalues can be obtained by adjusting the coefficients of each block separately by the corresponding control. The arbitrariness in the determination of the gains is resolved by engineering considerations where the designer selects the controls that he prefers to apply. Other controls are applied only if the system is uncontrollable by those that are preferred.

Gopinath [GO-1] describes an algorithm for determining the gains in which the uniqueness is achieved by restraining the C matrix to rank 1. It then has the form

$$C = \begin{bmatrix} \alpha_1 \\ \vdots \\ \alpha_m \end{bmatrix} [c_1, \ldots, c_n]$$

where α_1 to α_m represent the relative contributions of the different controls and are determined by the designer. For multiple controls, the designer may find it difficult to translate his physical insight into the desirable relative contribution of each control.

Gain determination by pole placement has some basic deficiencies: (1) It is convenient to define time response criteria in terms of second, or at most, third-order models. The determination of the roots of a higher order model that satisfies given criteria is more difficult. For a high order system, therefore, there are two possibilities: (a) To place all the eigenvalues of the system in the region of the required eigenvalues (maybe by assigning double or triple eigenvalues), accepting the resulting uncertainty in the time response. (b) To assign all the eigenvalues except two or three that are required for the determined time response to regions in the s-plane that are far from the imaginary axis and thus give faster time responses. This assures that the time response will be dominated by the two or three slow eigenvalues. This possibility will require higher gains and therefore may saturate the controller for even small deflection of the states. (2) In multi-input systems, the additional criteria imposed in order to obtain unique gains may result in undesirable solutions. For high order systems, pole placement therefore does not exploit fully the possibilities of state feedback controllers. In general, better designs can be obtained using quadratic synthesis.

B.3 Feedback Gain Determination by Quadratic Synthesis

In this method the feedback gains are selected so as to minimize a quadratic performance index (PI). For systems which are required to recover from non-zero initial conditions and are not subject to further

disturbances, the PI is

$$J = \int_{t_o}^{\infty} (x^T Ax + u^T Bu)dt \ . \qquad (2.3)$$

For systems which are subject to random disturbances, the PI is

$$J = \lim_{t_f \to \infty} \frac{1}{t_f - t_o} \int_{t_o}^{t_f} (x^T Ax + u^T Bu)dt \ . \qquad (2.4)$$

The second case is the more realistic one. A physical interpretation of the PI for this case can be obtained by rewriting Eq. (2.4) as

$$J \approx tr[AX(\infty)] + tr[BU(\infty)] \qquad (2.5)$$

where

$X(\infty)$ = the steady state state covariance

$U(\infty)$ = the steady state control covariance

tr = the trace operator.

The steady state covariance matrices exists since the system is assumed to be stable. The PI of (2.5) is thus a weighted sum of the state and control covariances where the weighting matrices A and B are selected by the designer.

The quadratic synthesis design procedure consists of two steps: (1) selection of the weighting matrices A and B; (2) determination of the gains so as to minimize the PI for the selected weighting matrices.

These steps will now be described.

(1) Selection of the weighting matrices. The selection of the A and B matrices constitutes the actual design in the quadratic synthesis method since the determination of the gains after these matrices are selected is a purely computational step. Unfortunately, no set rules exist for the selection of

these matrices so as to obtain desired time responses or closed loop eigenvalue locations. The selection is, in many cases, a matter of designer experience. One of the reasons for the scant use of state feedback in actual systems is the lack of a sufficient body of this experience among working designers.

In general, the design is iterative, with the weighting matrices modified at each step so as to approach the required performance.

Some general guidelines for the initial selection and subsequent modification of these matrices can, however, be given. The most convenient rule for the initial selection of the weighting matrices is probably Bryson's Rule [BRY-1]. It is

$$a_{ii} = \frac{1}{(x_{i_{max}})^2} \qquad a_{ij} = 0, \quad i \neq j;$$

$$b_{ii} = \frac{1}{(u_{i_{max}})^2} \qquad b_{ij} = 0, \quad i \neq j; \tag{2.11}$$

where $x_{i_{max}}$ and $u_{i_{max}}$ are the maximum permissible values of the respective states and controls. For systems subject to random disturbances, they are the rms values of the permissible uncertainties in the states and controls.

This method was used, among others, by Gupta and Bryson [GUP-1] and by Bull [BU-1] for the design of controllers. In general, it is recommended to weight in the first iteration only the outputs and the controls. In most cases, some changes in the weights are required after their initial determination.

For multivariable systems, no general rules can be given for the effect of these changes and in general, the selection has to be made by trial and error. In some cases, it is possible to decouple approximately the system and determine

the weights or even design the controllers for the decoupled systems. The performance of the overall coupled system has to be verified. This method is used by Gupta and Bryson [GUP-1].

For single input systems, the effect of weight changes on the closed loop eigenvalues can be determined by the root square locus method. This method is described in detail in Appendix J. It is based on one of the formulations of the quadratic synthesis method due to Rynaski and Whitbeck [RY-1]. According to this formulation, a system designed by quadratic synthesis satisfies the equation

$$[B + Y^T(-s)AY(s)]u(s) = 0 , \qquad (2.6)$$

where $Y(s) = (sI - F)^{-1}G$.

For SISO systems, this equation has 2n roots that are symmetric about the imaginary axis. For a given A and B (a scalar for SISO systems), the left half plane roots of this equation are the closed loop eigenvalues of the system.

The effect of weight changes on the closed loop eigenvalue locations is determined by fixing the control weight and all the state weight except one. A root locus is constructed as a function of this weight. If all the weights are varied in turn with different values assigned to the remaining weights, a grid is obtained that shows the closed loop eigenvalue locations as a function of the state weights. The method becomes cumbersome if more than two or three states are weighted and is totally impractical for multi-input systems because of the (m-1)n extraneous roots that are introduced where

m is the number of controls,

n is the state dimension.

A design example using this method is presented in Chapter V.

The advantage of using the root square locus method instead of arbitrary pole placement is that the non-dominant eigenvalues are not positioned arbitrarily but are located so as to optimize the performance according to a PI such as given by Eq. (2.3). The dominant eigenvalues have to be determined in both cases according to the system specifications.

Another method that is applicable to SISO systems and that does not require the separate examination of the weighting of each state is the model performance index method. In this method, the state and control weights are determined so that the closed loop response of the controlled system approaches that of a system having prescribed eigenvalues. It is essentially an eigenvalue placement procedure in which only the dominant eigenvalues and those that are required for the cancellation of the zeros are assigned. All others are removed to regions of non-dominancy in a predictable way. The method is based on Eq. (2.6). Several versions of its implementation are described in the literature [SC-1, RE-1]. The version presented here is an extension of the method given by Anderson & Moore [AN-2, Sec. 5.4].

Given the open loop transfer function of the system

$$\frac{y(s)}{u(s)} = \frac{k \prod_{i=1}^{m} (s + z_i)}{\prod_{i=1}^{n} (s + p_i)} = \frac{kN(s)}{D(s)} ; \qquad (2.7)$$

The steps for the determination of A are (b, the scalar control weight, is assumed to be unity without loss of generality):

(a) Define the characteristic equation of the model as

$$D_M(s) = s^r + \gamma_1 s^{r-1} + \ldots \gamma_r .$$

The degree of the model must be such that $r < n - m - 1$.

(b) Define a polynomial

$$P(s) = D_m(s)N(s) .$$

(c) Find a vector d such that

$$d^T(sI - F)^{-1}g = \frac{P(s)}{D(s)} \qquad (2.8)$$

or $$d^T \text{ adj}(sI - F)g = P(s).$$

The restriction on the dimension of $D_M(s)$ is now clear since the dimension of $d^T \text{ adj}(sI - F)g$ is less than $n - 1$.

(d) Define

$$A = dd^T. \qquad (2.9)$$

The results of this procedure can be evaluated using Eq. (2.6) (with scalar b). Substituting A from Eq. (2.9) into (2.6), it is transformed into

$$\begin{aligned} & b + Y^T(-s)\, dd^T Y(s) \\ = \; & b + g^T(-sI-F^T)^{-1}\, dd^T(sI-F)^{-1}g \\ = \; & b + \frac{P(-s)P(s)}{D(-s)D(s)} \quad . \end{aligned}$$

The closed loop eigenvalues for a given value of b will be the left half plane eigenvalues of

$$bD(-s)D(s) + P(-s)P(s) .$$

By constructing a root locus as a function of b, conclusions can be drawn about its influence on the closed loop eigenvalue locations: (i) For $b \to \infty$ (high cost of control), the closed loop eigenvalues become the stable open loop eigenvalues and the mirror images about the imaginary axis of the unstable open loop eigenvalues. (ii) For $b \to 0$ (low cost of control): r eigenvalues tend towards the eigenvalues of $D_M(s)$; m eigenvalues tend towards the left half plane open loop zeros and the mirror images of the right half plane open loop zeros; $n - m - r$ eigenvalues form a

Butterworth configuration that recedes from the origin as b decreases. The distance of the Butterworth eigenvalues from the origin tends to [KW-2, Sec. 3.8]:

$$\omega_0 = \left(\frac{k^2}{b}\right)^{\frac{1}{2(n-m-r)}} \qquad (2.10)$$

for low b.

For sufficiently low b the closed loop response of a system with left half plane zeros (minimum phase system) will therefore approach the model response. The residues of the eigenvalues that approach the zeros are small, and the n - m - r eigenvalues of the Butterworth configuration are sufficiently removed from the origin so as not to influence the time response. The value of b which will assure the dominancy of the model eigenvalues has to be determined for each system individually.

It is important to note that for systems with right half plane zeros (non-minimum phase systems), it is, in general, not possible to approach the model response since the m eigenvalues that approach the mirror images of the right half plane zeros will, in general, have large residues. This is a fundamental deficiency of non-minimum phase systems.

It is also important to bear in mind that the system will have the desirable response only to inputs for which the numerator of the transfer function is the same as the numerator of the open loop transfer functions y(s)/u(s). This includes response to set point changes but does not include recovery from nonzero initial conditions or disturbances. The time response to these latter inputs will generally contain modes corresponding to all the eigenvalues of the system, and therefore, in many cases, will be much slower than the response to set point changes.

For high order systems, it may be undesirable to attempt the removal of the Butterworth roots from the region of dominancy, since this may require excessive amounts of control (recall Sec. B.2). In this case, a zero order model may be used which is equivalent to weighting the output only. Obviously this is the same as using the root square locus method with output weighting only. The time response for low values of b will, in this case, be dominated by the $n - m$ ordered Butterworth configuration, with m roots approaching the m open loop zeros. The time response of Butterworth configurations is described in many control texts (e.g., KW-2, Sec. 3.8). The relative weighting of the output and the control for this case may be determined by Eq. (2.10).

There is, at present, no apparent generalization of the model PI method to multivariable systems. Anderson and Moore [AN-2] suggest a generalization to multi-input systems: by determining the ratios of the m components of the control vector, an equivalent single input control is created and the method may be applied. This is the same constraint that is given by Gopinath [GO-1]. The resulting system, however, will not be optimal in the sense that the same closed loop behavior can be obtained with lower values of the control. In some cases, it may be advantageous to sacrifice this optimality in order to have a simpler design method.

The guidelines for the selection of the weighting matrices are summarized below.

(a) Weight only the outputs and the controls for the initial iteration. Note that the weight of one of the outputs or controls can be set arbitrarily since it is only the ratio of the state-to-control weights that is important. The initial determination of the weights is most conveniently done by Bryson's rule.

(b) For multivariable systems, little can be said about the effect of weighting changes except that, in general, increasing the ratio of output-to-control weighting will increase the bandwidth and increasing the weighting on states that are derivatives of the outputs will increase the damping of the roots.

(c) For single input systems, root square locus can be used for determining the effect of changing the weights of the output and perhaps one or two more states. If more states have to be weighted, the model PI can be used.

It is clear from this section that since the weight selection is an iterative procedure, it is important to have a fast computer program that repeatedly determines the gains and eigenvalues for many values of the weights. Such programs have only become available in the last few years.

(2) Feedback gain determination. The optimal feedback gain matrix that minimizes a PI as given in Eq. (2.3) or (2.4) is [BRY-2]

$$C^o = B^{-1}G^T S^o \qquad (2.12)$$

where S^o is the positive definite steady state solution of the Ricatti matrix equation:

$$\dot{S} = -SF - F^T S + SGB^{-1}G^T S - A \; . \qquad (2.13)$$

The optimal feedback is always a full state feedback.

There exist several computational methods for calculating the S^o matrix. These methods are described by Bryson & Ho [BRY-2], and Bull [BU-1]. It seems that currently the most efficient method for time invariant systems is the eigenvector decomposition method, which has been implemented as a computer program (OPTSYS) by Bryson and Hall [BRY-3]. This program determines the optimal feedback gain matrix and the resulting closed loop eigenvalues and eigenvectors from given F, G, A and B matrices. Since it is a very fast and inexpensive program, it is convenient for determining the state weights

iteratively. In general, a satisfactory system will be obtained after four to five iterations [BU-1].

For low order SISO systems, the gains can also be found by hand calculation using an addition to Eq. (2.6) [BRY-1], viz.,

$$[B+Y^T(-s)AY(s)] = [I+C(-sI-F)^{-1}G]^T B[I+C(sI-F)^{-1}G].$$

For SISO systems, the unique value of C is found by comparing the coefficients of the polynomial that is formed from the left half plane roots of the left side to those of $1 + C(sI-F)^{-1}G$.

B.4 Design of Linear Estimators

As explained in Section B.1, the design of a state feedback controller is composed of two distinct steps: (a) controller design, and (b) state estimator design. In this section, the design methods for the state estimator will be described.

A full state estimator is a model of the system, the output of which is compared to the system output. The difference between the outputs is fed back to the estimator through a gain matrix K. For the system (repeated from Eq. 2.1)

$$\dot{x} = Fx + Gu + \Gamma w$$

$$y = Hx + v ,$$

the estimator has the form

$$\dot{\hat{x}} = F\hat{x} + Gu + K(y - H\hat{x}) , \qquad (2.17)$$

where $\hat{x}$ is the state estimate, and K is the estimator gain matrix. From Eq. (2.5) it can be seen that the governing equation for the estimate error $\tilde{x} = x - \hat{x}$ is

$$\dot{\tilde{x}} = (F - KH)\tilde{x} + \Gamma w - Kv. \qquad (2.18)$$

The rate of decay of this error is therefore determined by the n eigenvalues of $F - KH$ which can be determined arbitrarily by the selection of the $n \times p$ matrix K, whenever $[F, H]$ is observable. p is the number of measurements. Only for $p = 1$ will the eigenvalues determine the components of K uniquely.

The design of the full state estimator consists of the selection of the gain matrix K. Various criteria exist for the determination of K. The principal ones are: noise filtration, rate of error decay, and sensitivity to plant parameter variations. If the main criterion is noise filtration, and if both the process and measurement noise are white and Gaussian, the gains can be selected by minimizing a performance index of the form [BU-1]

$$J_e = \lim_{t_f \to \infty} \frac{1}{t_f - t_o} \int_{t_o}^{t_f} (w^T Q^{-1} w + v^T R^{-1} v) dt. \qquad (2.19)$$

The estimator that is obtained by this method is a Kalman filter. This is an optimal estimator since it generates the least squares estimate of x. The Kalman filter gain matrix K^o is [BRY-2]

$$K^o = -P^o H^T R^{-1} \qquad (2.20)$$

where P^o is the steady state positive definite solution of the equation

$$\dot{P} = FP + PF^T + Q - PH^T R^{-1} HP. \qquad (2.21)$$

P is the covariance matrix of the estimation error $\tilde{x}$. P^o can be computed by different methods which are similar to those used for solving the Ricatti equation (2.13). Here, too, the most efficient method seems to be eigenvector decomposition. The program OPTSYS contains an option for evaluating Kalman filter gains. The estimator gains that are obtained by this method depend on the relative magnitude of the process and measurement noises. Two extreme cases will now be considered.

(a) $Q = 0$; no process noise. In this case, for stable plants, $P^o = 0$ and $K^o = 0$ are obtained from Eq. (2.21). Since the system is not disturbed, the estimate is exact and the noisy error feedback can only contaminate it. If the initial state of the plant is not identical to that of the estimator, the error decay rate is determined by the plant dynamics solely.

(b) $R = 0$; no measurement noise. In this case, $K^o \to \infty$; i.e., all the eigenvalues of $F - K^oH$ tend to $-\infty$, which means that the estimates are obtained by differentiating the output $n - 1$ times. This differentiation can be performed since the output contains no noise whatsoever.

From these extreme cases, it can be seen that as the measurement noises decrease relative to the process noises, the estimate error eigenvalues of the Kalman filter become faster. If the dominant estimate error eigenvalues are much faster than the dominant controller eigenvalues, noise criteria cease to be important for the determination of the estimator gains. In this case the filtering action provided by the estimator is not better than that provided by the controller itself. The estimator gains can, in this case, be determined by other criteria such as error decay rate or parameter sensitivity.

If error decay rate is the principal criterion, the estimator gains may be determined by pole placement. Methods similar to those described in Section B.1 may be used for this placement. However, if a computational method for determining the Kalman filter gains is available, it may be more convenient to determine the gains that are required for the placement by using this method with artificial noises. The noises in this case are merely a computational tool for the determination of the gains.

For single output systems, the influence of the noises on the eigenvalue locations can be determined by a root square locus procedure. In this case the closed loop eigenvalues are the left half plane roots of

$$R + Z(s)QZ^T(-s) = 0,$$

where

$Z(s) = H(sI - F)^{-1}\Gamma$

R = the measurement noise covariance

Q = the process noise covariance.

For multioutput systems, the eigenvalue locations as a function of the noises have to be determinated by trial and error. The method of artificial noises can also be used when the eigenvalues obtained from the Kalman filter gains are inconveniently located. An example of such a problem is given by Bull [BU-1]. In this case the Kalman filter had very low damping and could easily become unstable if the filter gains were not implemented precisely. The roots obtained by using artificial noises are more conveniently located. The resulting system is not optimal for the real noises but its rms values are only slightly higher than those of the optimal systems. The property of low sensitivity of the noise changes to estimator gains has been observed in several systems but its generality has not been established. The determination of estimator gains from sensitivity considerations is described in Chapter IV.

For a system with p measurements, a full state estimator is actually not required for the estimation of all the states. Luenberger [LU-2] has developed the concept of the reduced order observer which has $n - p$ states and which, together with the p measurements, provides an estimate of all the n plant states. A method for designing the observer by transformation into a canonical form is described in the same paper. Gopinath [GO-1] developed a design method which does not require such a transformation. This method is described in Appendix E. An example of the use of such an observer is given in Chapter V.

If the measurements are noisy, the use of a reduced order observer instead of a full state estimator results in larger output and control noises. This is so because the noisy measurements are fed into the controller directly without being filtered by the estimator.

B.5 Performance Index Evaluation

For a system of the form of Eq. (2.1), which is subject to the white Gaussian disturbance vector, w, and for which the measurement of the output is contaminated by the white Gaussian noise vector, v, the optimal controller is obtained by

(a) using the optimal feedback gain C^o from Eq. (2.12), with the feedback obtained from an estimator. Note that the optimal feedback is independent of the process and measurement noise.

(b) using the optimal estimator gain K^o from Eq. (2.20). Note that K^o is independent of the weighting matrices A and B.

This is the certainty equivalence principle [BRY-2]. The system is optimal in the sense that it minimizes the PI of Eq. (2.5)

$$J = \mathrm{tr}(AX) + \mathrm{tr}(BU).$$

It is of interest in many cases to evaluate the consequences of using nonoptimal K or C matrices. This can be done by comparing the resulting PI.

The expressions for X and U that are required for evaluating J are given below. If $K = K^o$, we have

$$X = \hat{X} + P , \tag{2.23}$$

where

$X = \lim_{t\to\infty} E[x(t)x^T(t)]$ is the steady state covariance matrix of the state

$\hat{X} = \lim_{t\to\infty} E[\hat{x}(t)\hat{x}^T(t)]$ is the steady state covariance matrix of the estimate

$P = \lim_{t\to\infty} E[\tilde{x}(t)\tilde{x}^T(t)]$ is the steady state covariance matrix of the estimation error.

Equation (2.23) is valid because for an optimal estimator

$$E[\tilde{x}(t)\hat{x}^T(t)] = 0 .$$

The governing equations for $\hat{X}$ and P are [BRY-2]

$$(F - GC)\hat{X} + \hat{X}(F - GC)^T + KRK^T = 0 \tag{2.24}$$

and

$$(F - KH)P + P(F - KH)^T + KRK^T + Q = 0. \tag{2.25}$$

Note that Eqs. (2.24) and (2.25) are valid for both optimal and non-optimal systems but for systems with nonoptimal filters, Eq. (2.23) is not valid. For systems with an optimal filter, the covariance of the estimate error may also be determined by Eq. (2.21).

For systems with nonoptimal filters, the state covariance is given by

$$X = \hat{X} + P + \lim_{t\to\infty} E[\tilde{x}(t)\hat{x}^T(t)] . \tag{2.26}$$

In this case, X has to be calculated by using the augmented system

$$x_A = \begin{bmatrix} x \\ \tilde{x} \end{bmatrix} , \tag{2.27}$$

for which the covariance is given by (2.28)

$$F_A X_A + X_A F_A^T + \Gamma_A Q \Gamma_A^T + K_A R K_A^T , \tag{2.28}$$

where

$$F_A = \begin{bmatrix} F - GC & GC \\ 0 & F - KH \end{bmatrix} [2n \times 2n]$$

$$X_A = \begin{bmatrix} X & E(x\tilde{x}^T) \\ E(x\tilde{x}^T) & P \end{bmatrix} [2n \times 2n]$$

$$\Gamma_A = \begin{bmatrix} \Gamma \\ \Gamma \end{bmatrix} \quad [2n \times q]$$

$$K_A = \begin{bmatrix} 0 \\ K \end{bmatrix} \quad [2n \times p] \quad .$$

X is determined from the upper left $n \times n$ partition of X_A. The equation for U is

$$U = C\hat{X}C^T \quad . \tag{2.29}$$

This equation is always valid but if Eq. (2.28) is used to find X, $\hat{X}$ may not be available. In this case

$$U = C_A X_A C_A^T \quad , \tag{2.30}$$

where

$$C_A = [C, -C] \qquad m \times 2n.$$

C. ENGINEERING PROPERTIES OF STATE FEEDBACK CONTROLLERS

In this section, some frequency domain properties of systems with state and state estimate feedback controllers are examined. These properties make it possible to compare the results of this design method to those of classical frequency domain techniques. This comparison is most meaningful for SISO systems, which are the principal domain of application of the classical techniques. The eigenvalue separation property of state estimate feedback controllers is used in this section. This property is derived in most modern control texts [AN-2]. It is apparent from the state equation for the augmented system of Eq. (2.27), which is

$$\begin{bmatrix} \dot{x} \\ \dot{\tilde{x}} \end{bmatrix} = \begin{bmatrix} F-GC & GC \\ 0 & F-KH \end{bmatrix} \begin{bmatrix} x \\ \tilde{x} \end{bmatrix} + \begin{bmatrix} G \\ 0 \end{bmatrix} u_o + \begin{bmatrix} \Gamma \\ \Gamma \end{bmatrix} w + \begin{bmatrix} 0 \\ K \end{bmatrix} v \,, \qquad (2.31)$$

where u_o is an external input that is applied to both the plant and the estimator.

From Eq. (2.31), the characteristic equation of the augmented system is

$$\Delta(s) = \det(sI - F + KH) \times \det(sI - F + GC). \qquad (2.32)$$

This characteristic equation contains two separate groups of eigenvalues.
(a) n eigenvalues of the controller (F - GC) that are the same as those obtained with feedback from the states instead of from the estimates.
(b) n eigenvalues of the estimate error system (F - KH).

It is because of this separation of the eigenvalues that the controller can be designed as if full state feedback were available and the estimator can then be designed separately. Note that this property does not depend on the method by which the estimator and feedback gains are obtained, but only on the estimator having the structure of Eq. (2.17).

C.1 Transfer Matrices and Tracking Properties

The transfer matrices from the various inputs to the outputs y are found from Eq. (2.31). Defining

$$N \triangleq sI - F + GC$$

$$M \triangleq sI - F + KH \,,$$

the system output is obtained as

$$\begin{aligned} y = {} & HN^{-1}Gu_o + HN^{-1}(sI - F + GC + KH)M^{-1}\Gamma w \\ & + HN^{-1}GCM^{-1}Kv \,. \end{aligned} \qquad (2.33)$$

From this equation it can be seen that for inputs applied to both the

plant and the estimator, the characteristic equation of the transfer matrix contains the eigenvalues of the closed loop system only, (F - GC), i.e., for these inputs, the system behaves as if the feedback gains were obtained from the states and not from their estimates.

This is a remarkable property of state estimate feedback design. It can also be seen from Eq. (2.36) that the estimate error $\tilde{x}$ is not excited by the input u_o. For all other inputs (disturbances and measurement noises), the characteristic equations of the transfer matrices contain both the controller eigenvalues and the estimate error eigenvalues.

These different transfer matrices are important for tracker design, which is discussed in Section D.

C.2 Equivalent Compensators

For SISO systems, it is sometimes of interest to compare the structure of the state estimate feedback controller to that of compensating networks obtained by classical design techniques. For this purpose, the equivalent compensating networks of the state estimate feedback controller are determined. Block diagram representations of the state estimate feedback (SEF) controllers are given in Fig. II-1.

Figure II-1a is obtained from Eq. (2.1) and (2.17). Figure II-1b is obtained from Fig. II-1a by defining

$$G(s) = H(sI - F)^{-1}G \tag{2.34}$$

$$H_u(s) = C(sI - F + KH)^{-1}G \tag{2.35}$$

$$H_y(s) = C(sI - F + KH)^{-1}K \ . \tag{2.36}$$

Figure II-1c is obtained from Fig. II-1b by defining

$$H_c(s) = [1 + H_u(s)]^{-1} \ . \tag{2.37}$$

Using two linear algebraic relations [GA-1],

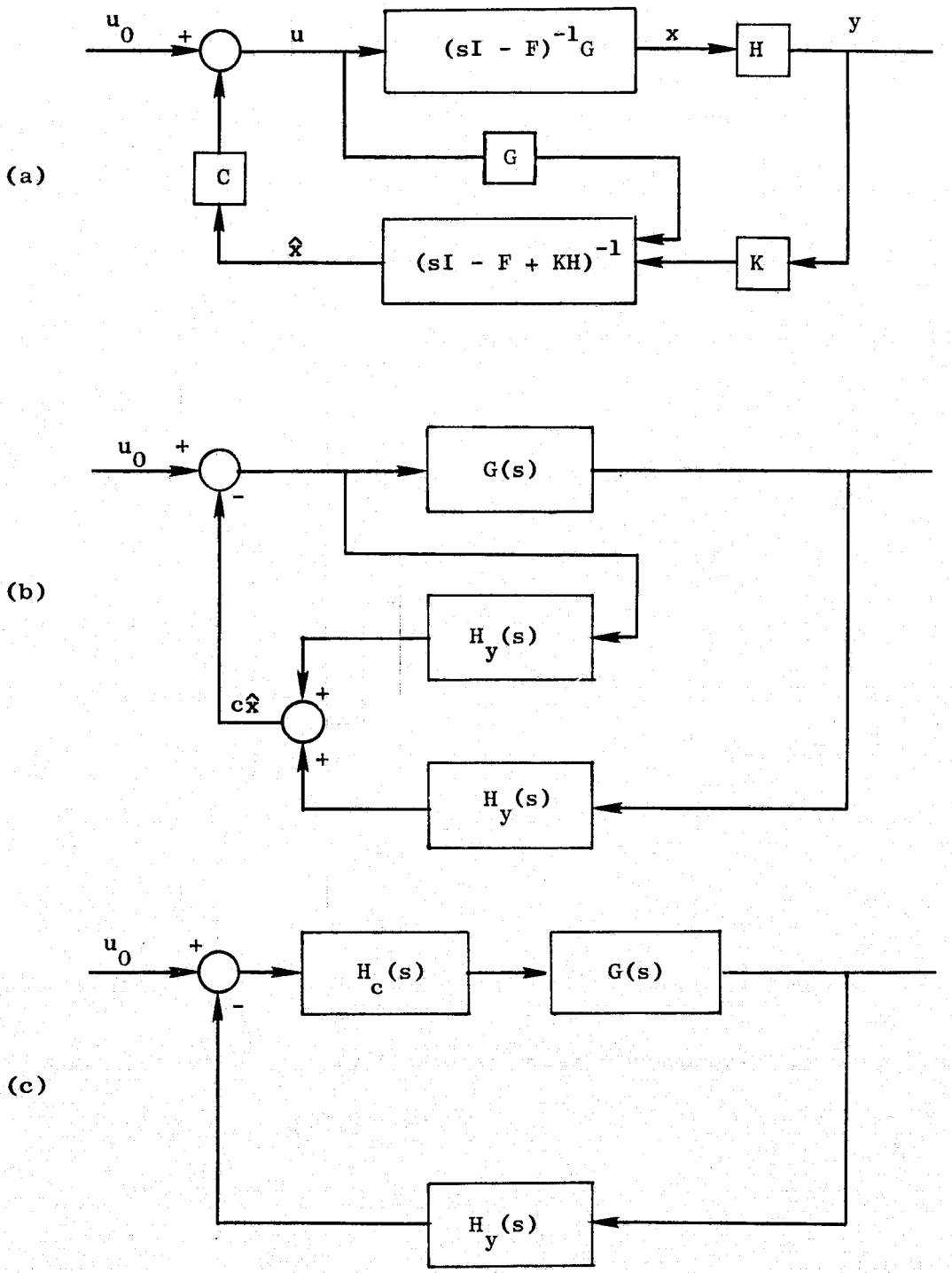

FIG. II-1 BLOCK DIAGRAMS OF THE STATE ESTIMATE FEEDBACK CONTROLLER.

$$[I + C(sI - A)B]^{-1} = 1 - C(sI - A + BC)^{-1}B \qquad (2.38a)$$

$$1 - CB = \det(I - BC) . \qquad (2.38b)$$

Equation (2.37) can be further written as

$$\begin{aligned} H_c(s) &= [1 + C(sI - F + KH)^{-1}G]^{-1} \\ &= 1 - C(sI - F + KH + GC)^{-1}G \\ &= \det[I - GC(sI - F + KH + GC)^{-1}] \\ &= \frac{\det(sI - F + KH)}{\det(sI-F+KH+GC)} . \end{aligned} \qquad (2.39)$$

Using

$$H_y(s) = C(sI - F + KH)^{-1}K = \frac{C\ adj(sI - F + KH)K}{\det(sI - F + KH)} , \qquad (2.40)$$

the open loop transfer function is

$$G_o(s) = \frac{C\ adj(sI - F + KH)K}{\det(sI - F+ KH+ GC)}\ G(s) = H(s)G(s) . \qquad (2.41)$$

The eigenvalues of $F - KH$ do not appear in this transfer function. The compensating networks $H_y(s)$ and $H_c(s)$ and the open loop transfer function $G_o(s)$ can now be used to compare the design with classical frequency domain designs.

C.3 Gain and Phase Margin

Single-input single-output (SISO) systems with full state feedback controllers have some desirable gain and phase margin properties. Consider the SISO system

$$\dot{x} = Fx + c_o Gu$$

$$u = -Cx$$

where C is a full state feedback. c_o is a variable scalar (it may be the gain of the control amplifier) with nominal value of unity. For such a controller

(a) The system has infinite gain margin for changes in c_o if the zeros of $C(sI - F)^{-1}G$ are in the left half plane. This result remains valid if state estimate instead of state feedback is used. The proof of this result is given in Appendix A. The system, however, may still be conditionally stable, ie., a decrease in c_o may cause it to become unstable.

(b) If the feedback gains are found by quadratic synthesis, the inequality

$$\left|1 - C(j\omega I - F)^{-1}G\right| \geq 1 \qquad (2.42)$$

is satisfied [AN-2, Sec. 5.3]. In fact, it can be shown that whenever (2.42) is satisfied, some A and B matrices can be found such that the given gains minimize a quadratic performance index of the form (2.3).

If (2.42) is satisfied, the distance of the polar plot of $C(j\omega I - F)^{-1}G$ from the $-1 + j0$ point is at least unity. Since $C(j\omega I-F)^{-1}G$ is the open loop transfer function, the following results are obtained [AN-2]: (1) the gain margin to changes in c_o is infinite; (b) the phase margin is at least $60°$ (This is important for determining the tolerance of such systems to time delays); (c) conditionally stable systems will remain stable for $c_o > \frac{1}{2} c_{o_{nom}}$.

As an example, the polar plot of a $1/s^3$ plant which has an optimal controller is shown in Fig. II-2. This system has infinite gain

margin but is conditionally stable.

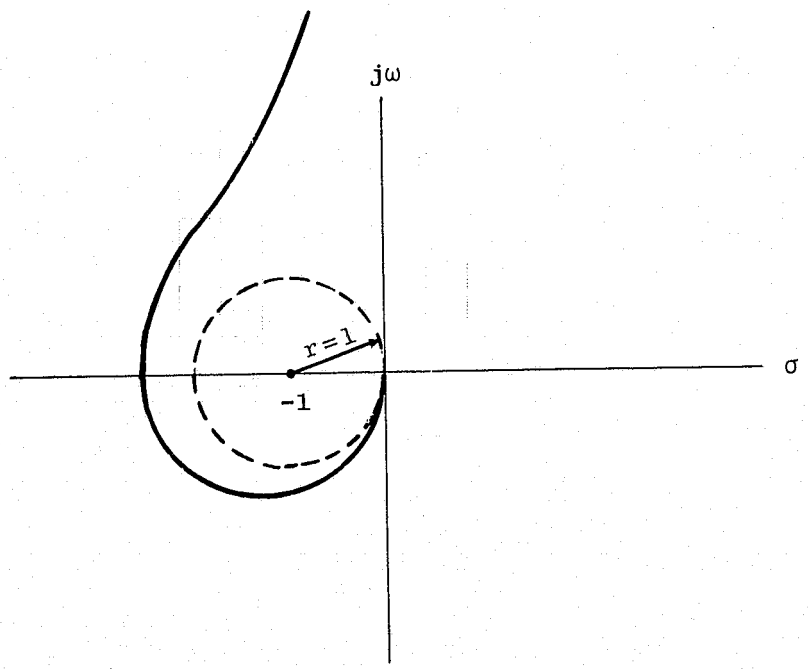

FIG. II-2 POLAR PLOT OF A $1/s^3$ PLANT WITH OPTIMAL CONTROLLER

D. TRACKERS AND SYSTEMS SUBJECT TO TIME CORRELATED DISTURBANCES

D.1 General

If a system is subject to time correlated disturbances or if it is required to track a given reference output, some modification to the regulator structure may be required. In this section, reference outputs and disturbances are considered which may be represented as outputs of linear systems driven by white noise. They are given by

$$\dot{x}_r = F_r x_r + \Gamma_r w_r$$
$$y_r = H_r x_r \qquad (2.43)$$

and

$$\dot{x}_D = F_D x_D + \Gamma_D w_D$$
$$w = H_D x_D \,. \qquad (2.44)$$

For such reference outputs and disturbances, the response may be improved by augmenting the state vector and designing a controller for the augmented state. The required augmentations and the meaning of the improvement in the controller are discussed in Section D.2. The design of a regulator (no tracking requirements) for a system subject to this type of disturbance is described by Johnson and Shelton [JO-2].

If the intensities of w_r and w_D are zero, a deterministic tracking problem or a regulator with deterministic disturbance result. Only the class of F_r and F_D matrices that cause sustained reference outputs or disturbances are of interest in this case; it is treated in Section D.3.

D.2 Stochastic Tracking and Disturbances

Consider the system of Eq. (2.1), which is required to track a reference output of the form of Eq. (2.43) and is subject to disturbances of the form of Eq. (2.44).

An optimal controller can be found for the augmented system

$$\dot{x}_A = \begin{bmatrix} \dot{x} \\ \dot{x}_r \\ \dot{x}_D \end{bmatrix} = \begin{bmatrix} F & 0 & \Gamma H_D \\ 0 & F_r & 0 \\ 0 & 0 & F_D \end{bmatrix} \begin{bmatrix} x \\ x_r \\ x_D \end{bmatrix} + \begin{bmatrix} 0 & 0 \\ \Gamma_r & 0 \\ 0 & \Gamma_D \end{bmatrix} \begin{bmatrix} 0 \\ w_r \\ w_D \end{bmatrix} + \begin{bmatrix} G \\ 0 \\ 0 \end{bmatrix} u \qquad (2.45)$$

$$y_a = y - y_r = [H \,, -H_r] \begin{bmatrix} x \\ x_r \end{bmatrix} + v \,.$$

So as to minimize the performance index:

$$J = \int_0^\infty [(y - y_r)^T A_1 (y - y_r) + u^T B u]dt.$$

The solution of this problem is given by Kwakernaak and Sivan [KW-2]. A partitioned Ricatti matrix is obtained and from it the augmented feedback gain matrix can be determined as

$$u = [C, \; C_r, \; C_D] \begin{bmatrix} x \\ x_r \\ x_D \end{bmatrix}. \qquad (2.47)$$

C is the feedback matrix from the states of the unaugmented system that minimizes the PI

$$J = \int_0^\infty (y^T A_1 y + u^T B u)dt \; .$$

The optimal feedback is not changed by the tracking requirements or the time correlated disturbance.

C_r and C_D are feedforward matrices from the reference and disturbance states. These states do not, of course, exist in reality and have to be estimated. The block diagram for this system using estimators for the states, the disturbances, and the reference states is shown in Fig. II-3.

In Fig. II-3, estimator No. 2 estimates the states x_u which are defined by

$$F_A = \begin{bmatrix} F & \Gamma H_D \\ 0 & F_D \end{bmatrix}$$

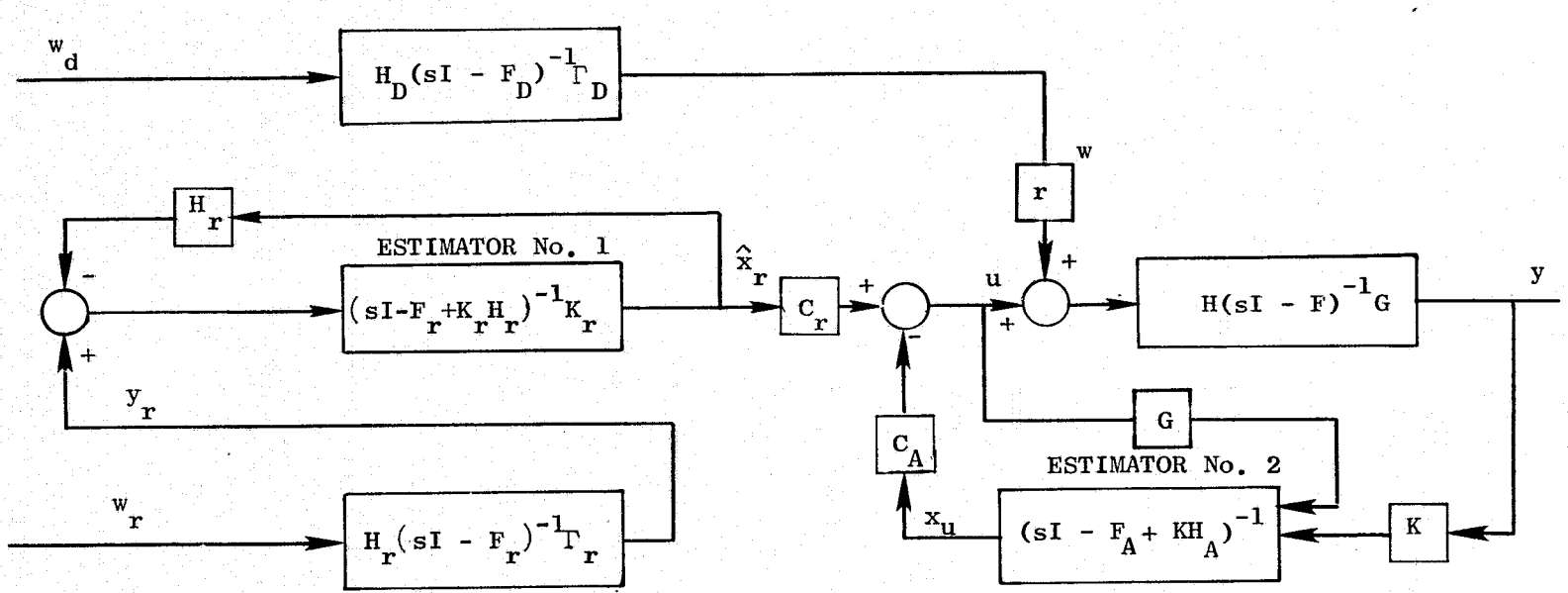

FIG. II-3 SYSTEM WITH FEEDFORWARD AND FEEDBACK CONTROLLERS

$$\dot{x}_u = \begin{bmatrix} \dot{x} \\ \dot{x}_D \end{bmatrix} = \begin{bmatrix} F & \Gamma H_D \\ 0 & F_D \end{bmatrix} \begin{bmatrix} x \\ x_D \end{bmatrix} + \begin{bmatrix} G \\ 0 \end{bmatrix} u + \begin{bmatrix} 0 \\ \Gamma_D \end{bmatrix} w_D$$

$$y_u = [H, \; 0] \begin{bmatrix} x \\ x_D \end{bmatrix}$$

$$C_A = [C, \; C_D] \; .$$

The optimal estimator gains K and K_r can be found separately since the reference model and the system are not connected.

It is important to recognize that a configuration such as shown in Fig. II-3 is not essential for accommodating disturbances given in by Eq. (2.43) or tracking reference outputs given by Eq. (2.44), but is is the configuration that will give the minimum of the PI of Eq. (2.46). Physically that means that the deviations of the output from the reference output will tend to be smaller when feedforward as per Eq. (2.47) is used. In many cases, the reference output and the outputs of the system are not measurable separately and only the error $y_e = y - y_r$ is measured. In that case feedforward from the reference output cannot be used. A regulator configuration may be used with the output error fed back to the estimator. This is shown in Fig. II-4 (with the disturbance omitted).

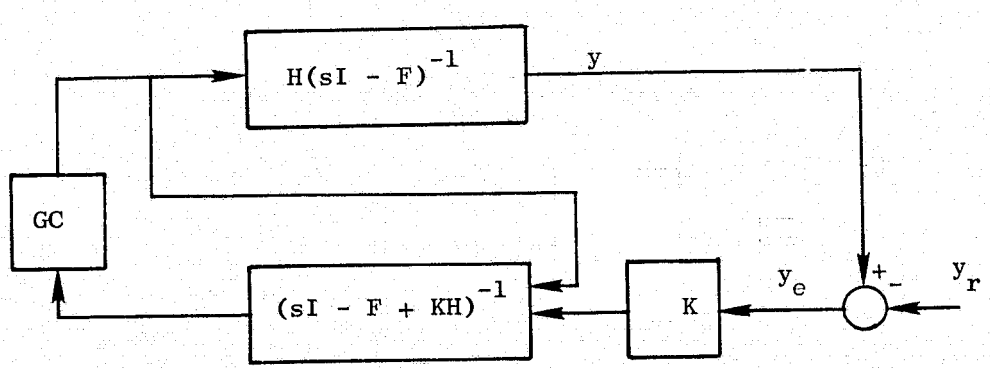

FIG. II-4 ESTIMATOR WITH OUTPUT ERROR MEASUREMENT

The transfer matrix from y_r to y for this case will be the same as the transfer matrix from the measurement noise v to y (Eq. 2.38).

$$y = H(sI - F + GC)^{-1}GC(sI - F + KH)^{-1}Ky_r , \qquad (2.48)$$

i.e., in this case, the system has no way of distinguishing between the reference output and the measurement noise since it has no information about the reference model. In general, the output error for this configuration will be greater than for the optimal configuration of Fig. II-6.

An exception is the case of complete reducibility of the reference output [RA-1, KR-1]. This is defined as the case in which an error state vector $e = x - x_r$ can be defined such that

$$\dot{e} = Fe + Gu \qquad (2.49)$$

$$y_e = He.$$

For a completely reducible reference output, the error state therefore has the same dynamics as the system. The condition for complete reducibility is that all the eigenvalues of F_r have to be among those of F. A state transformation may be required in order to obtain the form of Eq. (2.49). If the reference output is completely reducible, feedback from the error states (or their estimates): $u = -Ce$ will minimize the PI of Eq. (2.46). The configuration of Fig. II-4 is therefore optimal for this case.

D.3 Deterministic Tracking and Disturbances

If w_r and w_D in Eq. (2.43) and (2.44) vanish, a deterministic tracking problem results. This problem can be solved by state augmentation in the same way as described in the previous Section, but the resulting solutions for most forms of F_r and F_D matrices represent controls that are optimal for specific reference outputs and disturbances only and therefore have little general interest.

A class of reference outputs and disturbances that is of general interest is the class of polynomials in time. They can be considered as outputs of models of the form

$$F_r = \left[\begin{array}{c|c} 0 & I_{r-1} \\ \hline 0 & 0 \end{array}\right].$$

The order of the model is determined by the order of the highest polynomial output. This output is the first state of the model. The coefficients of the polynomial are determined by the initial conditions. This class of reference outputs includes steps, ramps, constant accelerations, etc. Systems that are required to track this type of reference output or are subject to this type of disturbance generally are required to have zero output error at equilibrium.

The interest in this class of inputs comes from the fact that if a system is designed for error free tracking of a polynomial reference output, it will also track error free all polynomial reference outputs of lower order. It is therefore adapted to an entire class of reference outputs and not just for one specific function of time. The same is true for polynomial disturbances.

The consideration of polynomial tracking in conjunction with state feedback follows the classical design approach in which the type of a system is defined as the order of polynomial that it can track with finite error.

The following points now have to be determined.† (a) What are the requirements in the structure of the system such that it shall be capable of error free tracking of a polynomial? (b) What are the additions to state feedback required in the controller in order to obtain the error free tracking?

† The material in this part is an extension of Ch. 3.7, Ref. KW-2.

The equilibrium condition of a system tracking a polynomial reference output is defined as the condition in which the error has vanished. In this condition

$$\begin{aligned} \dot{x}_s(t) &= Fx_s(t) + Gu_s(t) \\ y_s(t) &= Hx_s(t) = mt^r , \end{aligned} \tag{2.50}$$

where $x_s(t)$ is the equilibrium solution of Eq. (2.1) for the given reference output and m is an arbitrary vector $[1 \times p]$.

Whether such a condition can be reached depends on whether Eq. (2.50) can be solved for $u_s(t)$ for given $y = mt^r$. To determine the conditions for the existence of $u_s(t)$, Eq. (2.50) is rewritten in the form

$$\begin{bmatrix} sI - F & G \\ H & 0 \end{bmatrix} \begin{bmatrix} x_s \\ u_s \end{bmatrix} = \begin{bmatrix} 0 \\ \dfrac{m}{s^{r+1}} \end{bmatrix} . \tag{2.51}$$

A solution for u_s and x_s can be obtained if the matrix

$$\begin{bmatrix} sI-F & G \\ H & 0 \end{bmatrix}$$

is square and has full rank. This condition is fulfilled if (a) the number of controls equals the number of outputs, and (b) the system is controllable and observable. In this case,

$$u_s(s) = [H(sI - F)^{-1}G]^{-1} \frac{m}{s^{r+1}} . \tag{2.52}$$

If $p > m$ (more outputs than controls), no solution exists for u_s. If $m > p$ (more controls than outputs), additional outputs may be defined or u_s can be optimized for some performance index. Holley & Bryson [HO-1] describe such an optimization for a steady reference output.

The conditions (a) and (b) above guarantee the existence of $u_s(t)$. However, for this control to reach an equilibrium state which is a polynomial of time, one more condition is required. The matrix

$$U(s) = [H(sI - F)^{-1}G]^{-1}$$

has to be stable. If this is not so, the equilibrium state of zero output error is achieved but the control diverges. The additional condition can also be posed as the requirement for the open loop transfer matrix

$$Y(s) = H(sI - F)^{-1}G$$

to have minimum phase which means that all the roots of the numerator polynomial

$$\det[H \text{ adj}(sI - F)G]$$

are required to be in the left half plane.

It is important to bear in mind that no real system can track indefinitely a polynomial reference output that results in polynomial u of order greater than zero, since all controllers are subject to saturation. Two cases are therefore of practical importance. (1) The tracking of function of time that can be assumed to be composed of polynomial segments of such length that the controller is not saturated. (2) the tracking of polynomials that result in constant control.

If u_s exists, an error system can be defined as

$$\begin{aligned} e(t) &= x(t) - x_s(t) \\ u_e(t) &= u(t) - u_s(t) \\ y_e(t) &= y(t) - y_s(t) \ . \end{aligned} \tag{2.53}$$

Substituting Eq. (2.53) into Eq. (2.1) and using (2.50), the error equation is obtained as

$$\begin{aligned} \dot{e} &= Fe + Gu_e \\ y_e &= He \ . \end{aligned} \tag{2.54}$$

This is a regulator problem for which a state feedback gain can be found in the form

$$u_e = -Ce \ . \tag{2.55}$$

The total control that is required for error free tracking is therefore the sum of the error feedback and the equilibrium control

$$u(t) = -Ce(t) + u_s(t) \ . \tag{2.56}$$

According to Eq. (2.54) the error feedback can be obtained from an estimator that has the dynamics of the system and the output of which is compared to the error output y_e.

Zero equilibrium output error is assured if the equilibrium control is obtained by feeding back integrals of the output error. The number of integrations that is required can be determined by finding the number λ for which the solution of the following equation (which is obtained from Eq. 2.52) exists:

$$\lim_{s\to o} s^{\lambda} u_s = \lim_{s\to o} s^{\lambda}[H(sI - F)^{-1}G]^{-1} m \frac{1}{s^{r+1}} = \text{const.} \tag{2.58}$$

By assigning a nonzero value to the $\underline{j}$th component of m only, the number of integrations n_j of the $\underline{j}$th output error is found as

$$n_j = \lambda_j \ . \tag{2.59}$$

If $u_e = \text{const}$ is imposed in (2.57), the order of polynomials that can be tracked with constant control is obtained.

$$\lim_{s\to o} s[H(sI - F)^{-1}G]^{-1} \; m \frac{1}{s^{\ell+1}} = \text{const} . \qquad (2.58)$$

The constant control u is obtained by one integration of the output.

For SISO systems, ℓ is the number of roots at the origin (free integrations) of the open loop transfer functions. Comparing this condition with the condition for complete reducibility (Eq. 2.49) it results that for polynomial reference output, complete reducibility is equivalent to the possibility of error free tracking with constant control.

In order to determine the gains from the error integrals, a state vector z is defined such that

$$\dot{z} = F_i z + G_i (y - y_r) . \qquad (2.60)$$

The order of z is

$$n_z = \sum_{j=1}^{p} \lambda_j .$$

The matrix $F_i[n_z \times n_z]$ is defined as

$$F_i = \begin{bmatrix} \Lambda_{\lambda_1} & 0 \cdots\cdots & 0 \\ 0 & \ddots & 0 \\ 0 \vdots & \ddots & 0 \\ 0 \cdots\cdots & 0 & \Lambda_{\lambda_p} \end{bmatrix}$$

where

$$\Lambda_{\lambda_j} = \begin{bmatrix} 0 & I_{\lambda_j - 1} \\ 0 & 0 \end{bmatrix} .$$

The matrix $G_i[n_z \times q]$ is defined as

$$\begin{cases} g(\lambda_j, j) = 1 \\ g(i,j) = 0 \end{cases} \qquad i \neq \lambda_j \ .$$

The equilibrium control is therefore obtained as

$$u_s = -C_o z \ .$$

The gain matrix $C_o[m \times n_z]$ may now be determined by quadratic synthesis. The system is augmented by the state z and the control is selected to minimize a PI of the form

$$J = \int_o^\infty (x^T A x + z^T A_o z + u^T B u)dt \ . \qquad (2.61)$$

A different method for determining the integral control gains was developed by Holley and Bryson [HO-1]. In this method the additional roots due to the integral control are determined separately after the system is designed.

The block diagram of the complete tracker is shown in Fig. II-5.

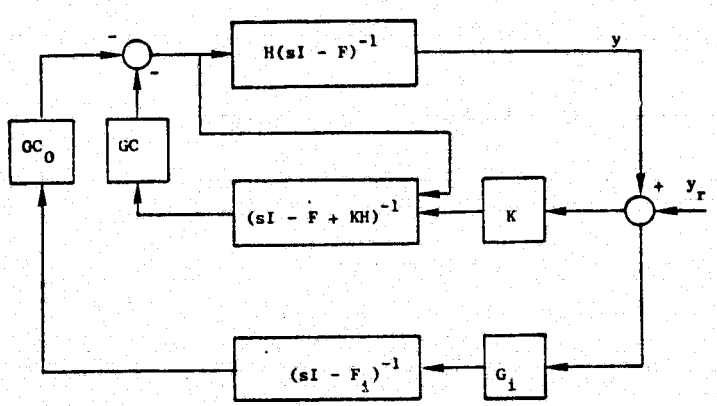

FIG. II-5 TRACKER WITH INTEGRAL CONTROL

In Fig. II-5 the integral control is applied to both the plant and the estimator. The application to the estimator is not essential, but if it is done the eigenvalue separation between the controller and the estimator is preserved. The eigenvalues of the controller are now those of the augmented system

$$\left[\begin{array}{c|c} F_i & G_i H \\ \hline -GC_o & F-GC \end{array}\right] . \tag{2.62}$$

The design of systems that are subject to polynomial disturbances is done along the same lines. Note, however, that it is rare to have polynomial disturbances of order higher than zero (constant disturbances).

For the sake of completeness, the development for the general case is given below.

It is required to determine: (a) the system structure that will permit the output error to remain zero when the system is subject to polynomial disturbances; (b) the additions to the feedback required in order to keep the error at zero.

The system is defined by

$$\begin{aligned} \dot{x} &= Fx + Gu + \Gamma w \\ y &= Hx , \end{aligned} \tag{2.63}$$

where $w = m t^r$. In the steady state

$$Hx = 0 . \tag{2.64}$$

Using (2.64) and the Laplace transform of (2.63), we obtain

$$H(sI - F)^{-1}(Gu_w + \Gamma w) = 0. \tag{2.65}$$

u_w can now be determined for a given w if the conditions for the

existence of Eq. (2.52) are satisfied. For u_w to be non-divergent, the minimum phase condition also has to be satisfied. u_w is then given by

$$u_w = [H(sI - F)^{-1}G]^{-1}H(sI - F)^{-1}\Gamma w \ . \qquad (2.66)$$

u_w can be obtained, as for polynomial reference output, by feeding back integrals of the output error. The number of required integrations π is determined by solving

$$\lim s^{\pi}[H(sI - F)^{-1}G]^{-1} H(sI - F)^{-1}\Gamma \frac{m}{s^{r+1}} = \text{const.} \qquad (2.67)$$

The controller shown in Fig. II-5 can therefore be used for this case without change if the number of integrations is determined as the larger of those required to track the reference output and to reject the disturbances. If the integral control is used for cancelling disturbances only, and is applied to the estimator, a steady state error in the estimator output results [TA-1]. The system output will, however, be maintained at zero.

III. SENSITIVITY OF CONTROLLERS TO PLANT PARAMETER VARIATIONS

A. INTRODUCTION

The design procedure of state feedback controllers and some of their engineering properties were described in Chapter II. The controller and estimator gains depend on the structure of the system matrices and on the values of their parameters. If the actual values of these parameters differ from those that were assumed in the design, some of the system properties described in Section II-C may not be preserved. In most engineering problems, the system matrices are only an approximate description of the actual system structure and the values of their parameters are, in many cases, ill defined and may also vary in time. The sensitivity of the controller to plant parameter perturbations is therefore of great importance to the designer. Some aspects of this problem have been treated extensively in the literature, using the various definitions of sensitivity given in Section III-B. One aspect that has received extensive treatment is the sensitivity comparison of open loop and closed loop controllers[e.g, KR-2], especially if the loop is closed by full state feedback or by full state estimate feedback [KW-1].

This problem, however, is not especially relevant to the designer. The decision to use a feedback controller instead of an open loop controller is, in general, made for various reasons other than sensitivity. The problem is then to compare the sensitivities of various types of applicable feedback schemes. There is no general solution to this problem and each system has to be examined individually.

In the context of this work, the sensitivity of state estimate feedback controllers is of special interest. It is important to distinguish, in this respect, between state feedback and state estimate feedback controllers. While the nominal properties of these types of controllers

may be close, their sensitivies are generally totally different. In most cases, the state estimate feedback (SEF) controllers will be more sensitive but this is not a meaningful comparison since the estimates are only used because the states are not measured. Therefore the choice is not between state feedback and SEF controllers but between SEF controllers and other applicable feedback schemes.

In Section III-C the sensitivity of a SEF controller is analyzed and in Section III-D the sensitivities of such a controller and a classical compensation network are compared for a specific case.

B. MEASURES OF SENSITIVITY

The functionally most significant measure of sensitivity which is also most frequently used in time domain design is trajectory sensitivity. It is defined as the vector

$$\sigma(t) = \frac{dx(t)}{d\mu} \tag{3.1}$$

where μ is a scalar variable parameter [KR-3]. If there is more than one variable parameter, a sensitivity vector is defined for each parameter.

In order to get a scalar, time independent measure of sensitivity, the time average of a weighted square of this expression is used in stochastic systems and its time integral in deterministic systems. These integrals or average values are then defined as sensitivity performance indices [KR-3].

For deterministic systems

$$J_{SD} = \int_o^\infty \sigma^T(t) W \sigma(t) dt = tr\left\{ W \int_o^\infty \sigma(t)\sigma^T(t) dt \right\}. \tag{3.2}$$

For stochastic systems

$$J_{SS} = \lim_{t_f \to \infty} \frac{1}{t_f} \int_0^{t_f} E[\sigma^T(t) W \sigma(t)]dt$$

$$= \mathrm{tr}\left\{W \lim_{t_f \to \infty} \frac{1}{t_f} \int_0^{t_f} E[\sigma(t)\sigma^T(t)]dt\right\} \tag{3.3}$$

where W is an arbitrary weighting matrix. For a stable stochastic system, the approximate value of the performance index is

$$J_{SS} \cong \mathrm{tr}\left\{WE[\sigma(\infty)\sigma^T(\infty)]\right\}, \tag{3.4}$$

where $\sigma(\infty)$ is the steady state value of the sensitivity vector. The governing equations for $\sigma(t)$ are given in Chapter IV-A.

Trajectory sensitivity and the sensitivity performance index (PI) related to it are good measures of sensitivity but they are difficult to evaluate and therefore a simpler measure is often required, especially for preliminary design. One such measure is the eigenvalue sensitivity defined as [PO-1, Sec. 32]

$$S_\lambda = \frac{d\lambda_k}{d\mu}, \tag{3.5}$$

where λ_k is the kth eigenvalue.

This measure of sensitivity is not as closely related to the system time response as the trajectory sensitivity because: (a) only the dominant eigenvalues influence the time response; (b) the time response perturbation depends not only on perturbations of the eigenvalues but also on those of the eigenvectors. In many cases, however, especially when different controllers for the same system are compared, a sufficient measure of their relative sensitivity can be obtained by comparing the parameter perturbations required to induce instability. For this case, eigenvalue sensitivites are adequate.

A numerical approximation of the eigenvalue sensitivities can be

obtained by computing the eigenvalues of the nominal and perturbed dynamic matrices. The QR Algorithm by Francis [FR-1] is a very efficient method for this computation and it has been incorporated into a variety of computer programs, among them the OPTSYS program used for optimal controller design.

In frequency domain design, transfer function sensitivity is often used. It is defined by Bode [BO-1] as

$$S_s = \frac{d \ell n\, T(s,\mu)}{d \ell n\, \mu} , \tag{3.6}$$

where

$$T(s,\mu) = \frac{G(s,\mu)}{1 + G(s,\mu)\, H(s,\mu)}$$

is the closed loop transfer function. This sensitivity measure is not used in this work.

C. STATE ESTIMATE FEEDBACK CONTROLLERS WITH PERTURBED PARAMETERS

Consider the system of Eq. (2.1) and (2.17) with the system matrices perturbed as follows:

$$\begin{aligned} F &= F_0 + \delta F \\ G &= G_0 + \delta G \\ H &= H_0 + \delta H . \end{aligned} \tag{3.7}$$

The dynamic equations are now

$$\begin{bmatrix} \dot{x} \\ \dot{\hat{x}} \end{bmatrix} = \begin{bmatrix} F_o+\delta F & -(G_o+\delta G)C \\ K(H_o+\delta H) & F_o-G_oC-KH_o \end{bmatrix} + \begin{bmatrix} \Gamma \\ 0 \end{bmatrix} w + \begin{bmatrix} 0 \\ K \end{bmatrix} v + \begin{bmatrix} G_o+\delta G \\ G_o \end{bmatrix} u_o . \tag{3.8}$$

It is assumed here that the errors occur only in the matrices F, G, and H over which the designer has no control. No errors are assumed in the gain matrices K and C. If such errors exist, their influence can be analyzed by replacing δGC by $\delta(GC)$, and $K\delta H$ by $\delta(KH)$ in Eq. (3.8).

Using the transformation

$$\begin{bmatrix} x \\ \tilde{x} \end{bmatrix} = \begin{bmatrix} I & 0 \\ I & -I \end{bmatrix} \begin{bmatrix} x \\ \hat{x} \end{bmatrix} ,$$

Eq. (3.8) is changed to

$$\begin{bmatrix} \dot{x} \\ \dot{\tilde{x}} \end{bmatrix} = \begin{bmatrix} F_o+\delta F-(G_o+\delta G)C & (G_o+\delta G)C \\ \delta F-\delta GC-K\delta H & F_o-KH_o+\delta GC \end{bmatrix} \begin{bmatrix} x \\ \tilde{x} \end{bmatrix} + \begin{bmatrix} \Gamma \\ \Gamma \end{bmatrix} w - \begin{bmatrix} 0 \\ K \end{bmatrix} v + \begin{bmatrix} G_o+\delta G \\ \delta G \end{bmatrix} u_o . \quad (3.9)$$

The salient fact that can be observed from comparing Eq. (3.9) and (2.36) is that the parameter perturbations couple the state into the estimate error equation and therefore destroy the separation of the controller and the estimate error eigenvalues. As demonstrated in III-D, this coupling may lead to instability for even relatively small perturbations if the original eigenvalues have low damping.

The characteristic equation of the perturbed system may be found by using the expression for the determinant of block matrices [GA-1, Sec. 5]

$$\det \begin{bmatrix} M_1 & M_2 \\ M_3 & M_4 \end{bmatrix} = \det M_1 \det(M_4 - M_3 M_1^{-1} M_2) =$$
$$= \det M_4 \det(M_1 - M_2 M_4^{-1} M_3) .$$

Defining

$$M = sI - F_0 + G_0 C$$
$$N = sI - F_0 + KH_0 - \delta GC .$$

The characteristic equation of (3.9) is obtained as

$$D(s) = \det\begin{bmatrix} M-\delta F+\delta GC & -(G_o+\delta G)C \\ -\delta F+\delta GC+K\delta H & N \end{bmatrix} = 0 \quad , \tag{3.10}$$

which reduces to

$$\begin{aligned} D(s) = \det N \times \det[M - (sI-F_o+KH_o+G_oC)N^{-1}(\delta F-\delta GC) \\ + (G_o+\delta G)CN^{-1}K\delta H] = 0 . \end{aligned} \tag{3.11}$$

The influence of the parameter changes on the system eigenvalues may be determined from Eqs. (3.9) or (3.11). Equation (3.11) can be put in the form of a sum of terms of which one is the unperturbed characteristic equation and the others are the coefficients of the parameter perturbations, viz.,

$$D(s) = D_0(s) + D_1(s)\delta\mu_1 + \ldots, + D_r(s)\delta\mu_r = 0. \tag{3.12}$$

From this form the influence of each parameter may be evaluated by root locus techniques. Computer programs are available for this evaluation. The root loci may also be constructed directly from Eq. (3.9) by perturbing the parameters and computing the eigenvalues.

D. A NUMERICAL EXAMPLE OF THE SENSITIVITY OF STATE ESTIMATE FEEDBACK (SEF) CONTROLLERS

D.1 General

In this section a detailed numerical example is given of a state estimate feedback (SEF) controller for which the parameter sensitivity problem is particularly severe. This same system is used in Chapter IV

for an application of the sensitivity reduction method which is developed there. This system was selected because it demonstrates the sensitivity problem of the class of systems in which there is an elastic element between the controller and the controlled element. Also, it is sufficiently simple so that the underlying reasons for its sensitivity can be perceived.

D.2 Plant Description

The plant used in this example is derived from the Stanford Relativity Satellite, a controller for which was designed by Bull [BU-1]. This Satellite, which is shown in Fig. III-1, consists of an outer body in which a helium filled dewar is mounted elastically. The dewar contains a telescope which is also connected to it elastically. The attitude of the telescope is controlled by means of two controllers: an actuator between the telescope and the dewar, and a thrustor mounted on the outer body. The actuator provides the high bandwidth precision control for the telescope and the thrustor controls the outer body so that the relative attitude between the three bodies remains small. The attitude of the telescope is measured.

A dynamic model of the plant is shown in Fig. III-2. The damping constants b_α and b_γ are very low and can be neglected in the analysis. The spring constants k_α and k_γ are poorly defined and may vary in time. The controller gains, especially for the thrustor, may also vary in time, but the sensitivity to these variations is low and they are therefore not considered here. In this example, a low frequency approximation of this plant is used. For low frequency behavior, it can be assumed that the spring force in the spring k_γ is cancelled by the control u_1 so that no net force is applied by the telescope on the dewar.

The model of the approximated system is shown in Fig. III-3. Its governing equations are

$$\begin{aligned} I_1\ddot{\theta} &= k\varphi + w_1 \\ I_2(\ddot{\varphi} + \ddot{\theta}) &= -k\varphi + u - w_1 + w_2 \,. \end{aligned} \tag{3.13}$$

The state vector x is defined as

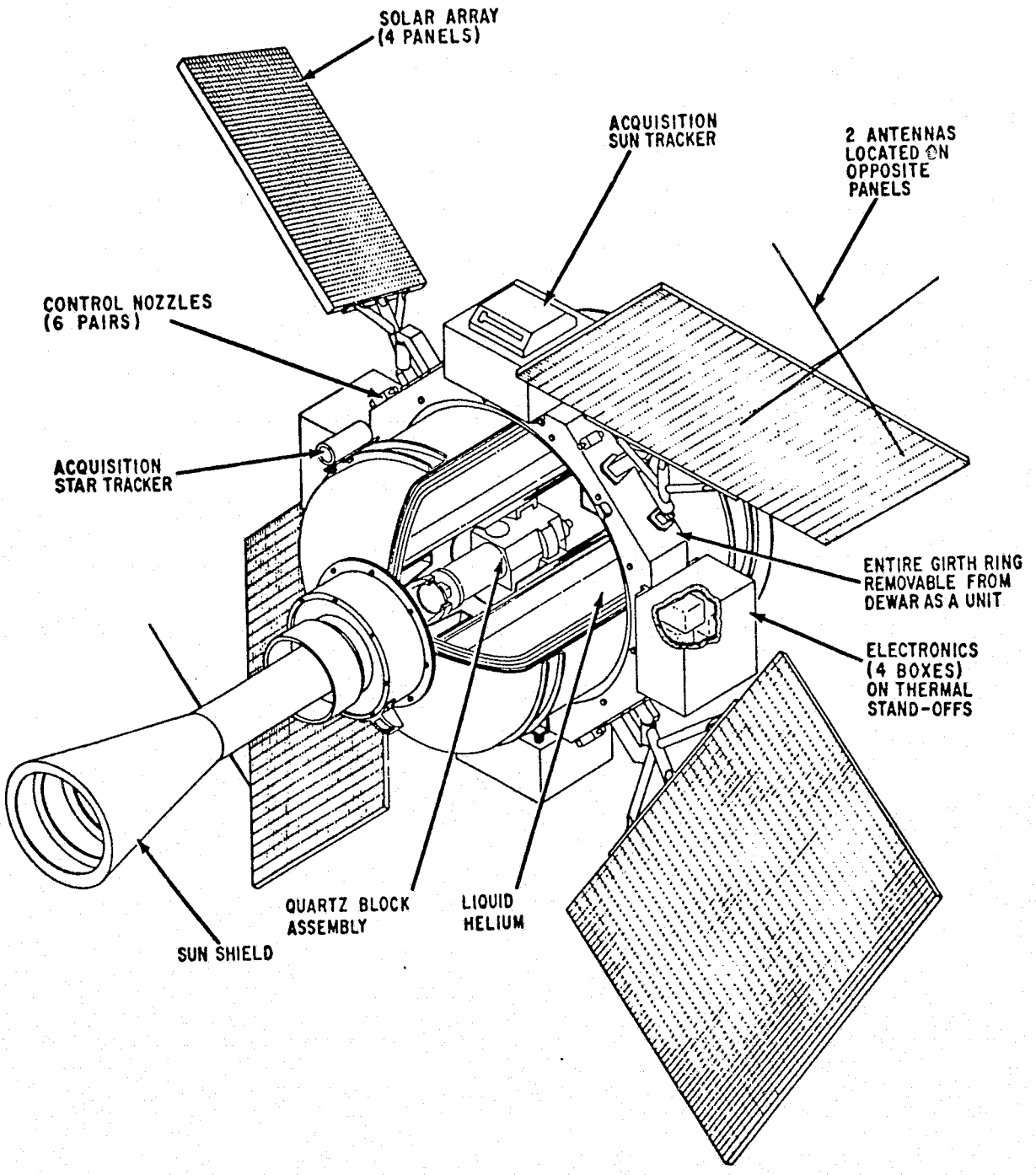

FIG. III-1 LAYOUT OF THE STANFORD RELATIVITY SATELLITE [from BU-1].

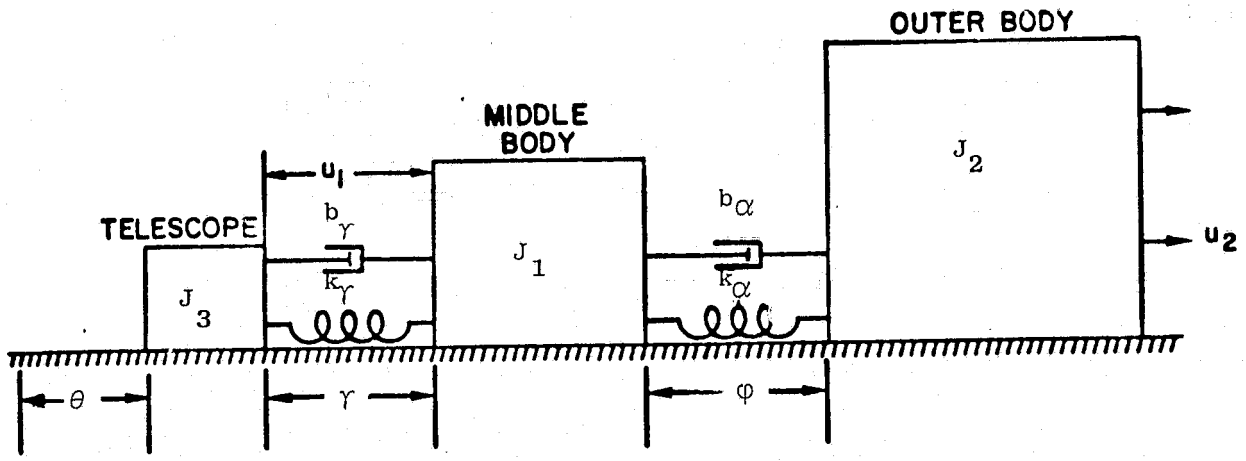

FIG. III-2 MODEL OF THE STANFORD RELATIVITY SATELLITE

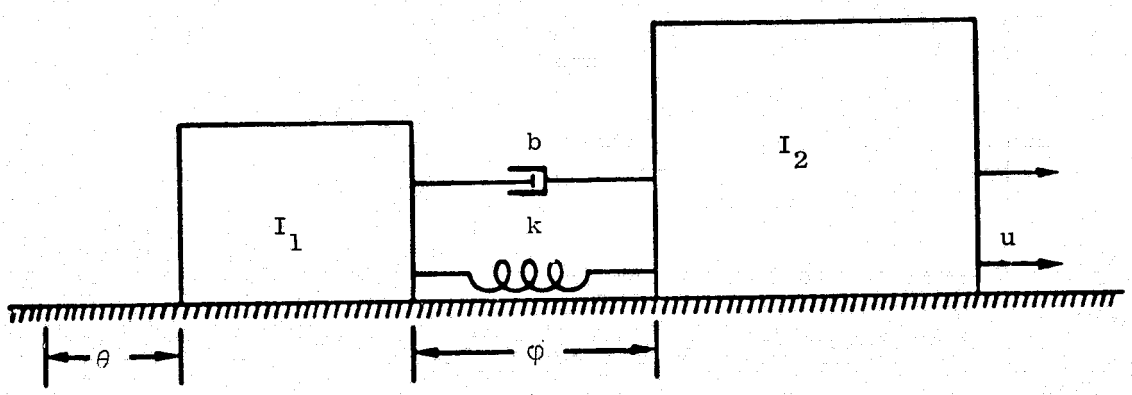

FIG. III-3 SIMPLIFIED MODEL OF THE STANFORD RELATIVITY SATELLITE

$$\mathbf{x} = \begin{bmatrix} x_1 \\ x_2 \\ x_3 \\ x_4 \end{bmatrix} = \begin{bmatrix} \theta \\ \dot{\theta} \\ \varphi \\ \dot{\varphi} \end{bmatrix} .$$

Using $k/I_3 = \omega_o^2$ (the natural frequency of the oscillatory motion), and $k/I_1 = \alpha\omega_o^2$ where $I_3 = (I_1 I_2)/(I_1 + I_2)$, the state representation of Eq. (3.13) is obtained.

$$\begin{bmatrix} \dot{x}_1 \\ \dot{x}_2 \\ \dot{x}_3 \\ \dot{x}_4 \end{bmatrix} = \begin{bmatrix} 0 & 1 & 0 & 0 \\ 0 & 0 & \alpha\omega_o^2 & 0 \\ 0 & 0 & 0 & 1 \\ 0 & 0 & -\omega_o^2 & 0 \end{bmatrix} \begin{bmatrix} x_1 \\ x_2 \\ x_3 \\ x_4 \end{bmatrix} + \begin{bmatrix} 0 \\ 0 \\ 0 \\ 1/I_2 \end{bmatrix} u + \begin{bmatrix} 0 & 0 \\ 1 & 0 \\ 0 & 0 \\ 0 & 1 \end{bmatrix} w \qquad (3.14)$$

$$y = [1 \quad 0 \quad 0 \quad 0]x + v .$$

The disturbances that are acting on this sytem are [BU-1]: (a) d_1, thrustor noise torque acting on the outer body at an equivalent bandwidth of 1 rad/sec. (b) α_N, noise torque between outer and middle body at an equivalent bandwidth of 1 rad/sec.

Their intensity matrix has the form

$$Q_w = \begin{bmatrix} \left(\frac{\alpha_N}{I_1}\right)^2 & -\frac{\alpha_N^2}{I_1 I_3} \\ -\frac{\alpha_N^2}{I_1 I_3} & \left(\frac{\alpha_N}{I_3}\right)^2 + \left(\frac{d_1}{I_2}\right)^2 \end{bmatrix} . \qquad (3.15)$$

The intensities of these disturbances are not well known and in the actual computation of Bull [BU-1], the off-diagonal terms were neglected and the diagonal terms were adjusted so as to obtain desirable pole locations. The intensity matrix is thus considered as a pole placement device.

In order to obtain the same estimator roots and sensitivity properties, this same intensity matrix is used here.

The numerical values of the system parameters and the covariance matrix elements are thus

$$\alpha\omega_0^2 = 19.5 \text{ sec}^{-2}$$

$$\omega_0^2 = 25 \text{ sec}^{-2}$$

$$I_2 = 250 \text{ kg m}^2$$

$$Q_w = \begin{bmatrix} 1.1\text{X}10^{-14} & 0 \\ 0 & 2.3\text{X}10^{-14} \end{bmatrix} [\text{rad}^2 \text{ sec}^{-3}] .$$

The measurement noise intensity is

$$r_n = 5.5 \times 10^{-17} \text{ rad}^2 \text{ sec.}$$

D.3 Contoller and Estimator Design

An optimal controller for the system was designed using the weighting matrices derived from Bull [BU-1]

$$A = \begin{bmatrix} 12\text{X}10^4 & 0 & 0 & 0 \\ 0 & 5 & 0 & 0 \\ 0 & 0 & 6.5\text{X}10^5 & 0 \\ 0 & 0 & 0 & 6.5\text{X}10^3 \end{bmatrix}$$

The control gains were found using the OPTSYS program [BRY-3]. The optimal estimator gains were found using the same program, with the disturbance covariance matrix of Eq. (3.15) and the given measurement noise variance.

The optimal gains are

$$C = [109, \quad 270, \quad 284, \quad 384]$$

and

$$K^T = [18.7, \quad 175, \quad 13.9, \quad -30.5].$$

The eigenvalues are: (a) controller (F - GC)

$$-0.35 \pm 5.0j$$

$$-0.41 \pm 0.41j \ ;$$

(b) estimate error (F - KH)

$$-1.01 \pm 5.11j$$

$$-8.33 \pm 8.35j \ .$$

D.4 Sensitivity Root Locus

Since there is only one significantly varying parameter (the spring constant k), the characteristic equation of the perturbed system can be written in the form of Eq. (3.12) as

$$D(s) = D_0(s) + D_1(s)\delta k \ .$$

The eigenvalues of $D_0(s)$ are those of the optimal controller and estimator. $D_1(s)$ is a sixth order system with the eigenvalues: $-0.41 \pm 0.41j$, $-2.21 \pm 5.26j$, $-7.47 \pm 7.68j$. With these eigenvalues, a root locus as a function of δk was constructed. It is shown in Fig. III-4. Only the regions of the root locus which are in the vicinity of the nominal values are significant since very large parameter perturbations are generally not expected. For this system, the region of $k < 0$ has no meaning.

The range of stability of the system is from the root locus:

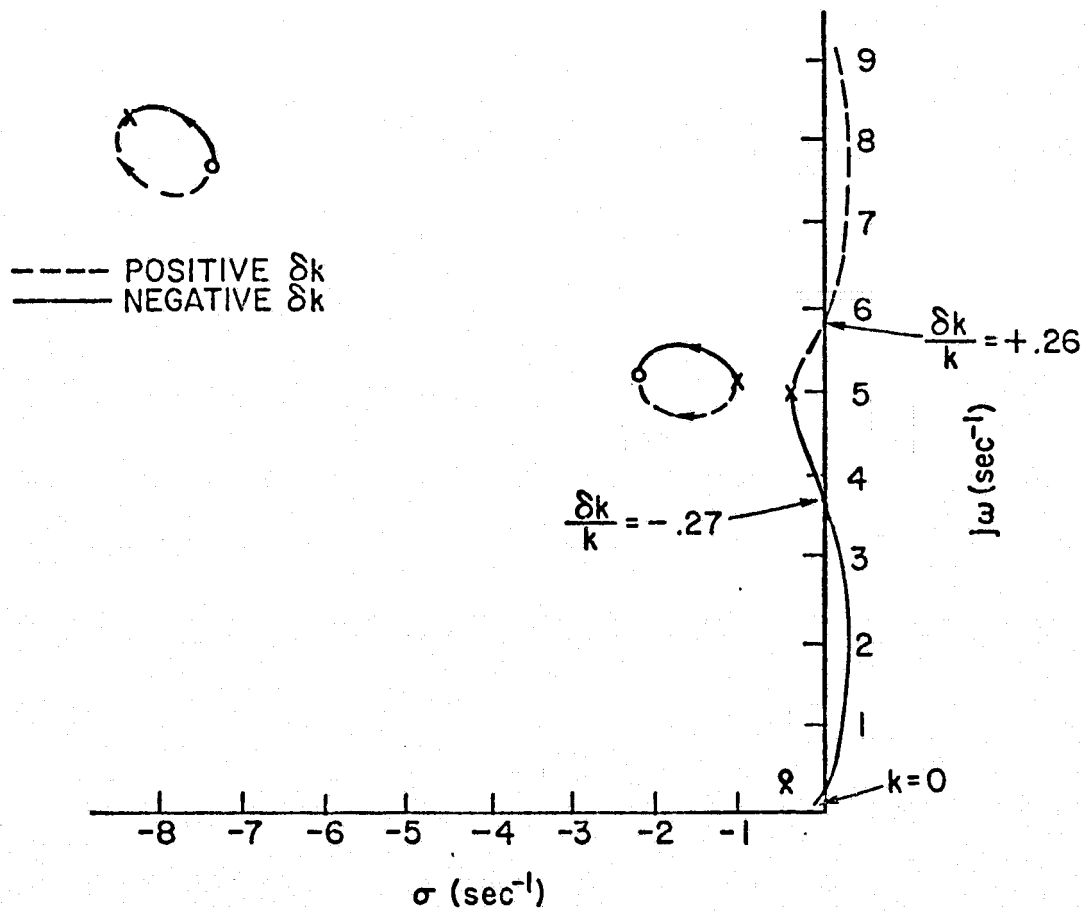

FIG. III-4 SENSITIVITY ROOT LOCUS FOR STATE ESTIMATE FEEDBACK CONTROLLER

$$0.73 < \frac{\delta k}{k_0} < 1.26; \quad \text{or,} \quad 18.1 < k < 31.5. \tag{3.17}$$

It is important to note that this is not the permissible operational range since the performance will generally deteriorate before the system becomes unstable.

While the root locus gives a good representation of the sensitivity problem, it does not provide a method for its solution. It is not obvious how the system eigenvalues have to be modified in order to decrease the sensitivity, especially since the root locus numerator eigenvalues are also determined by the gain matrices K and C, and therefore will change whenever the system eigenvalues are changed.

For a SISO system, more insight can be gained into the sensitivity problem by considering the transfer function and using frequency domain stability criteria. In principle, this representation may also suggest the modifications required for reducing the sensitivity but in practice the implementation of these modifications is difficult.

D.5 Frequency Domain Analysis

From Eq. (2.41) the equivalent open loop transfer function for a system using an estimator is

$$G_o(s) = G_c(s)\, G_p(s) ,$$

where

$$G_p(s) = H(sI - F)^{-1}G$$

is the plant transfer function, and

$$G_c(s) = \frac{C\ \mathrm{adj}[sI - F + KH]G}{\det[sI - F + KH + GC]}$$

is the equivalent compensator transfer function.

For the example, these transfer functions were calculated using

the computer program XAGSA [WI-1]. They are

$$G_p(s) = \frac{0.077}{s^2(s^2 + 25)} \text{ sec}^2$$

$$G_c(s) = \frac{4.1 \times 10^5 (s + 0.37)(s^2 - 1.58s + 5.2^2)}{(s^2 + 3.4s + 5.85^2)(s^2 + 1.65 + 11.8^2)} \text{ sec}^{-2}.$$

$G_0(j\omega)$, the open loop frequency response, is shown in Fig. III-5.

Since the plant is undamped, the frequency response has three zero crossings; i.e., three points at which the gain equals unity (points A, B, C). The frequency domain stability criterion for a system with several zero crossings can be found from its polar plot. The significant parameters for determination of stability are the phase angles at the three zero crossings. They are shown in Fig. III-5

Polar plots are sketched in Fig. III-6 for four different cases of the angles φ_B and φ_C, with $\varphi_A < 180°$ in all cases. The cases are:

(a) $\varphi_B < 180°$; $\varphi_C < 180°$

(b) $\varphi_B > 180°$; $\varphi_C < 180°$

(c) $\varphi_B > 180°$; $\varphi_C > 180°$

(d) $\varphi_B < 180°$; $\varphi_C > 180°$.

Case b is shown in Fig. III-5. Case a is obtained if the gain for this system is increased. Cases c and d cannot be obtained by gain changes. Case c can be obtained by parameter variation (see below). The exact shape of the polar plots is not important for the stability determination as long as the quadrants of the zero crossings are preserved.

From Fig. III-6 it can be seen that only case b is stable. The condition of stability for this system is therefore

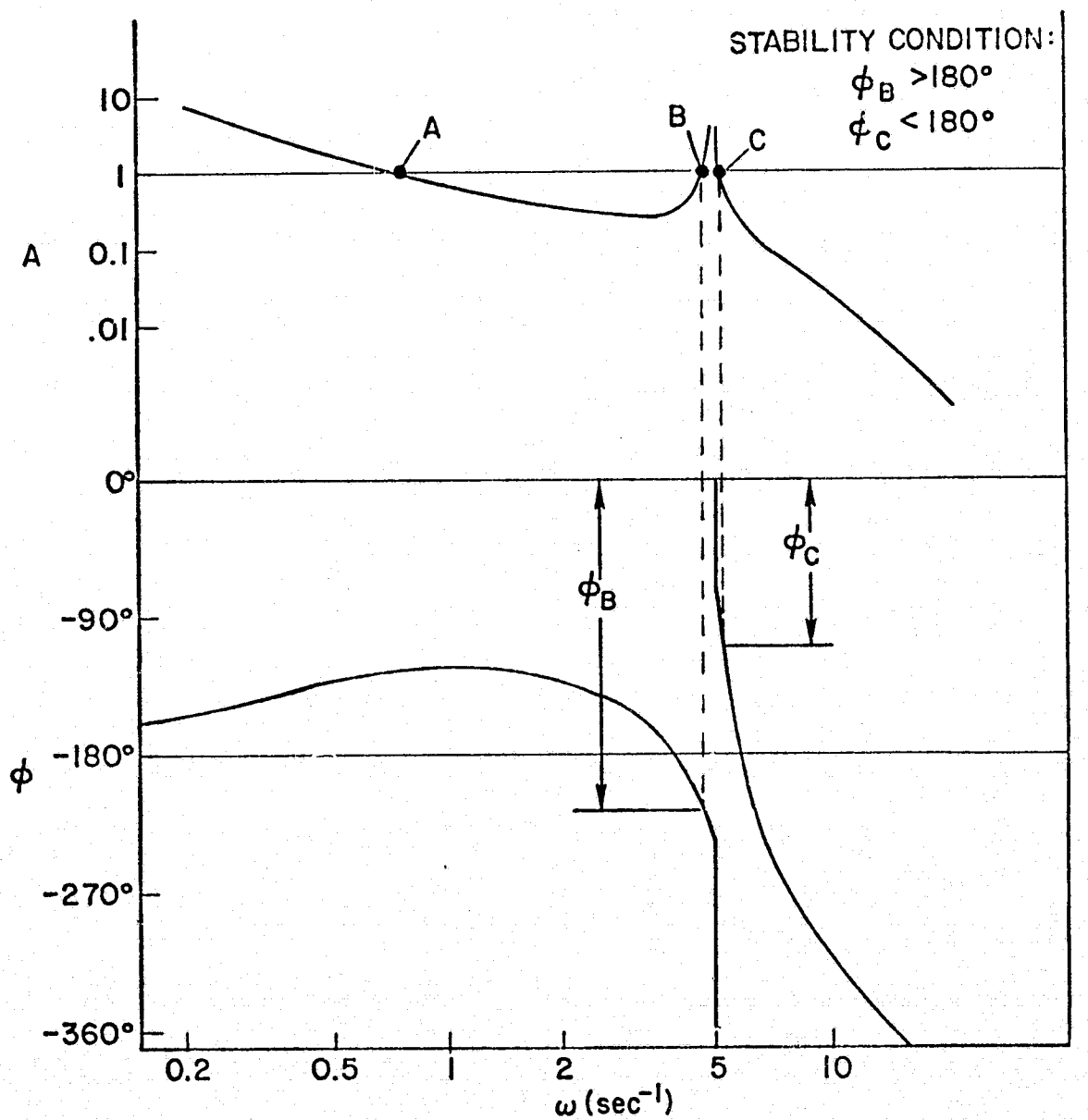

FIG. III-5 OPEN LOOP FREQUENCY RESPONSE OF STATE ESTIMATE FEEDBACK (SEF) CONTROLLER

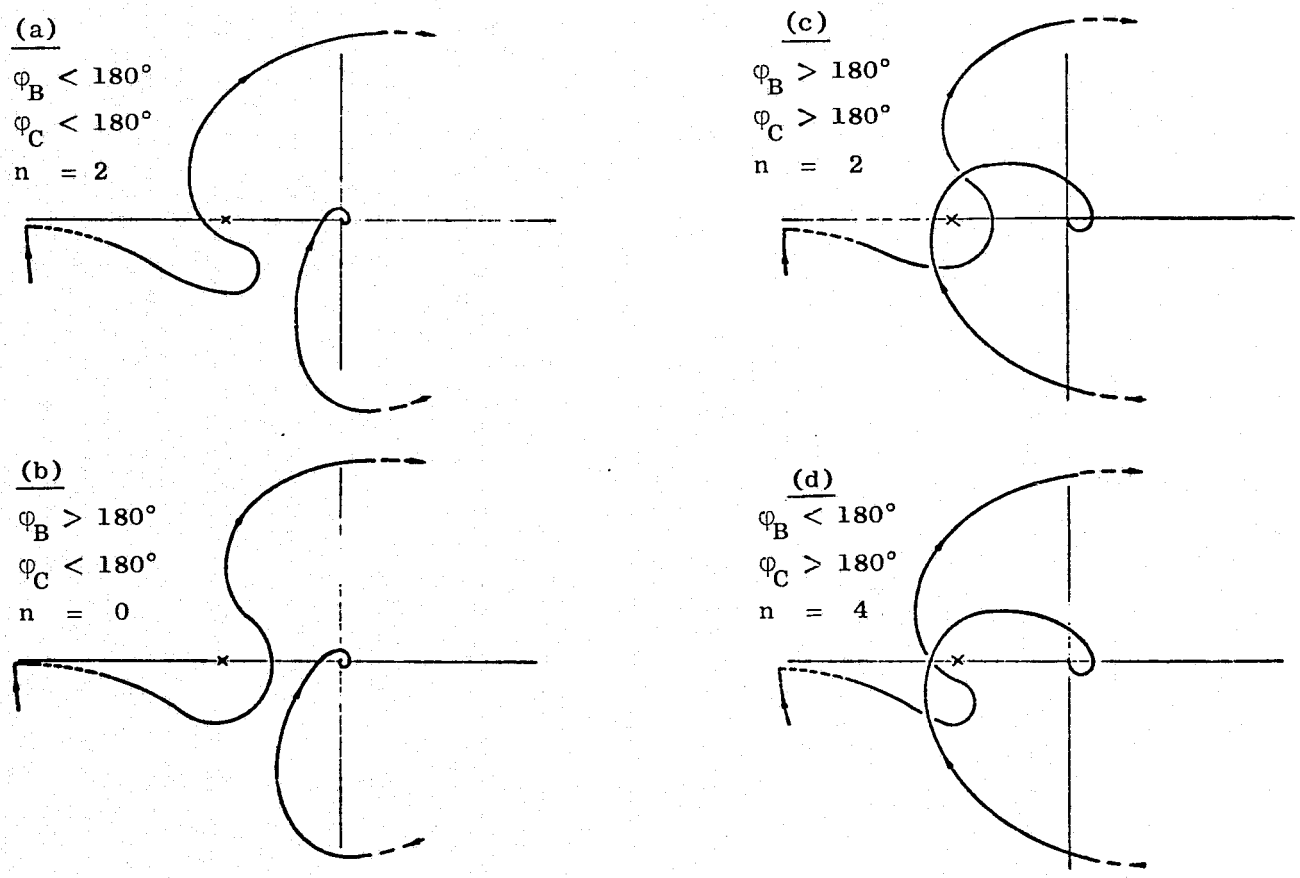

FIG. III-6 POLAR PLOTS FOR DIFFERENT PHASE ANGLES φ_B AND φ_C

$$\varphi_B > 180^\circ$$
$$\varphi_C < 180^\circ \quad . \tag{3.18}$$

The sensitivity to variations in ω_0 can be determined from this criterion.

Figure III-7 is an amplitude frequency plot of the region of $\omega = \omega_0$ with part of the phase-frequency plot overlaid.

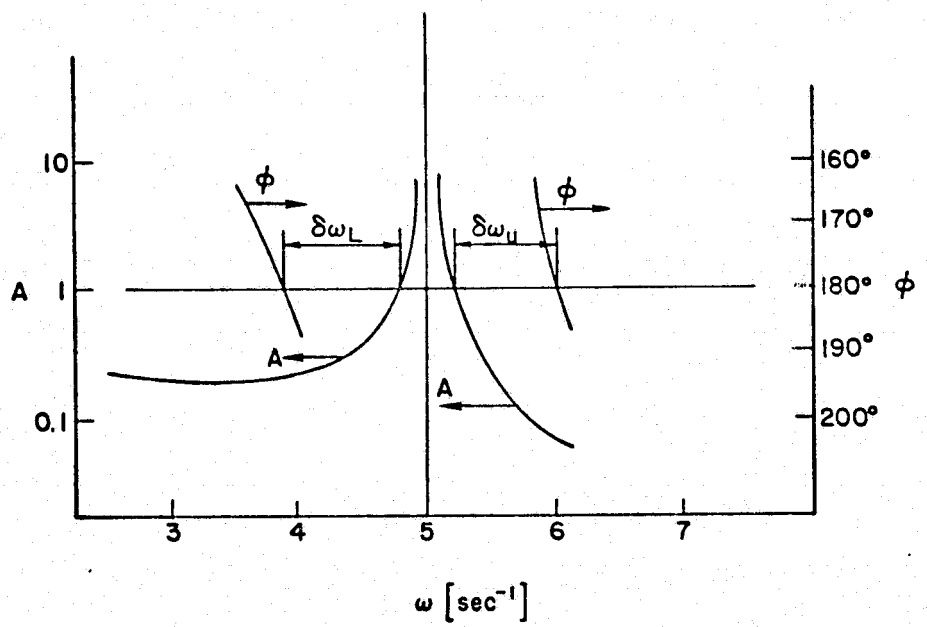

FIG. III-7 FREQUENCY RESPONSE IN THE REGION OF RESONANCE

Since the plant root at $\omega = \omega_0$ has no damping, its influence on the phase frequency plot consists of the addition of a phase lag of 180° at this frequency without modifying the plot at other frequencies. Also, the shape of the amplitude frequency plot in the vicinity of the frequency is determined mostly by this root. Changes in the natural frequency of the plant will therefore cause the amplitude plot to move relative to the phase plot in Fig. III-7 without changing the shape of

the phase plot and with little change in the shape of the amplitude plot. It can be seen from the figure that changes in ω_0 will cause instability as follows: decrease by 1 rad/sec → instability as per Fig. III-6a; increase by 0.8 rad/sec → instability as per Fig. III-6c.

The region of stability found by this method is somewhat larger than that found by the root locus method (Eq. 3.16). In order to decrease the sensitivity, the frequency margins $\delta\omega_L$ and $\delta\omega_u$ have to be increased. This can be done by modifying the compensator roots so that the phase slopes in the region of the zero crossing B and C are decreased. However, decreasing the slope in the vicinity of B will also decrease the phase margin at the first zero crossing A. An acceptable compromise may be difficult to find and no systematic way exists to achieve it, even for this low order system. It is therefore obvious that more powerful methods are needed.

The bandwidth of the system is determined by the selection of the weighting matrices A and B. Theoretically, state feedback controllers can have infinite bandwidth but in practical systems, the desired bandwidth will be limited by considerations such as saturation and noise susceptibility. It is of interest to compare the sensitivities of controllers with the same structure but with different bandwidths, in order to determine whether sensitivity considerations also contribute to the selection of the desired bandwidth. For this comparison, the weighting matrices were changed and systems with two different bandwidths, one higher and one lower than the nominal, were calculated. Q and R were held constant, therefore keeping the estimator unchanged. The stability regions for these systems are shown in Table III-1.

Table III-1

FREQUENCY MARGIN AS A FUNCTION OF SYSTEM BANDWIDTH

System	Bandwidth (sec^{-1})	$\delta\omega_L$	$\delta\omega_u$
Low	0.32	-1.15	+0.9
Nominal	0.8	-1.0	+0.8
High	1.8	-0.65	+0.65

An increase in sensitivity is observed as the bandwidth is increased. Although this effect is not drastic, it is an additional factor that limits the system bandwidth that is achievable in practice.

D.6 Sensitivity Comparison of Different Controllers

In this section the sensitivity of the state estimate feedback (SEF) controller is compared with that of two other controllers that may be used with this plant. They are: (a) a state feedback controller; (b) a classical network compensator. The first controller is only realizable if all the states are measured, which, in general, is not practical. It is used here only in order to emphasize the increase in sensitivity due to the use of SEF instead of state feedback.

(1) State feedback. For this case, the characteristic equation is the determinant of $(sI - F - \delta F + GC)$, viz.,

$$s^4 + \frac{c_4}{I_2} s^3 + \left(\frac{c_3}{I_2} + k\right)s^2 + \frac{c_2}{I_2} \alpha k s + \frac{c_1}{I_2} \alpha k$$

$$+ \left(s^2 + \frac{c_2}{I_2} \alpha s + \frac{c_1}{I_2} \alpha\right) \delta k \ .$$

The root locus as a function of δk is shown in Fig. III-8. From Fig. III-8 it is clear that no sensitivity problem exists for this case. The SEF controller for this system, while equivalent to the state feedback controller in many aspects when the system parameters are at their nominal values, is much more sensitive to parameter perturbations.

(2) Classical compensation. There is no unique compensation network for this system but any network must have the following characteristics: (i) provide lead at the first zero crossing of the system (point A) so as to have an adequate phase margin. (ii) provide an overall phase lag greater than 180° at $\omega = \omega_0$ in order to satisfy the stability requirements of Eq. (3.18). The simplest network which

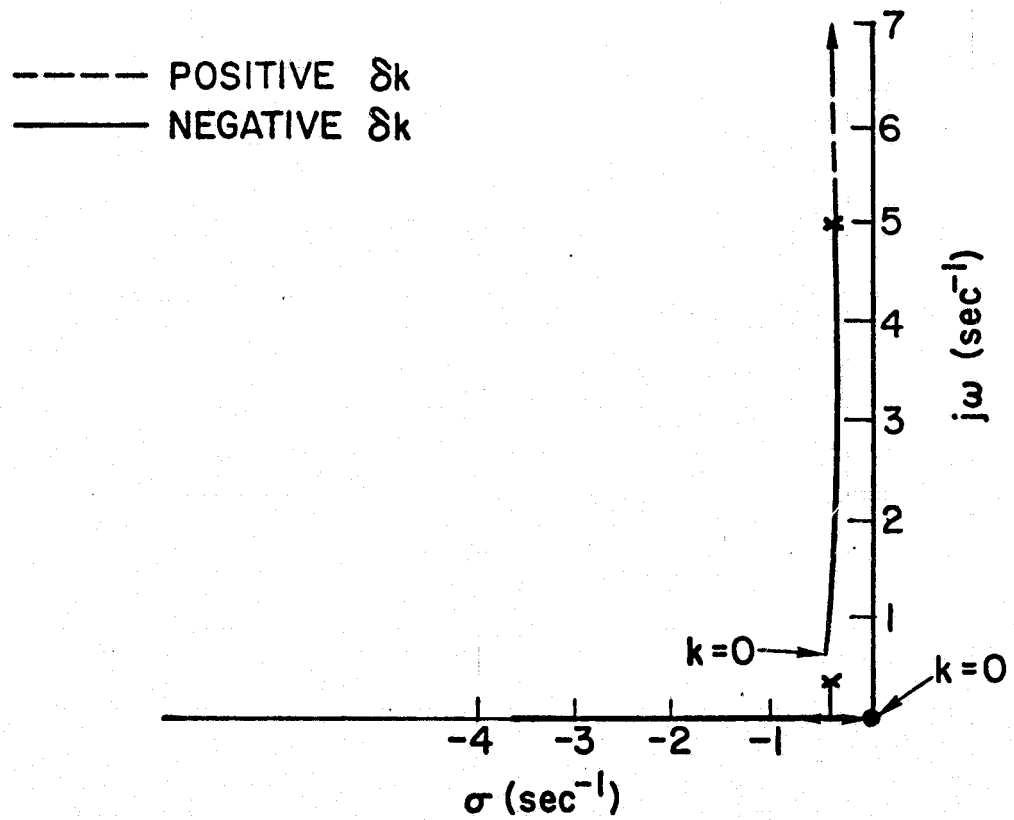

FIG. III-8 SENSITIVITY ROOT LOCUS FOR THE STATE FEEDBACK CONTROLLER

has these characteristics is

$$G_c(s) = c_0 \frac{(s + a)}{(s + b)^2} \tag{3.19}$$

where $a, b < \omega_0$.

In order to determine the values of the parameters c_o, a, and b, a parameter optimization program was used in which these parameters were adjusted so as to minimize a cost function of the form of Eq. (2.3) with the same A and B matrices as were used for the design of the optimal controller for this system (Eq. 3.16). The result is:

$$G_c(s) = \frac{3054(s + 0.23)}{(s + 3.2)^2} . \tag{3.20}$$

Both the nominal response and the sensitivity of this compensator are compared with those of the SEF controller.

The closed loop eigenvalues of the system with the classical compensator are: $-0.07 \pm 4.85j$; $-0.81 \pm 1j$; -4.85; -0.3. Note the low damping of the first eigenvalue.

For time response comparison, the responses to a step command and to a step disturbance were computed. These responses are shown in Figs. III-9 and III-10. The lower damping of the natural frequency in the classical compensator can be seen in the velocity and acceleration responses, especially in the disturbance response. For sensitivity comparison, the movement of the root at $-0.07 \pm 4.85j$ as a function of $\delta k/k_o$ is shown in Fig. III.11. All the other roots move towards stable zeros and therefore cause no instability. Comparing Fig. III-11 and Fig. III-4, it can be seen that the classical compensator (CC) is much less sensitive than the SEF compensator. The stability regions are

	$-\delta k/k$	$+\delta k/k$
SEF	-0.27	+0.26
CC	-0.52	large

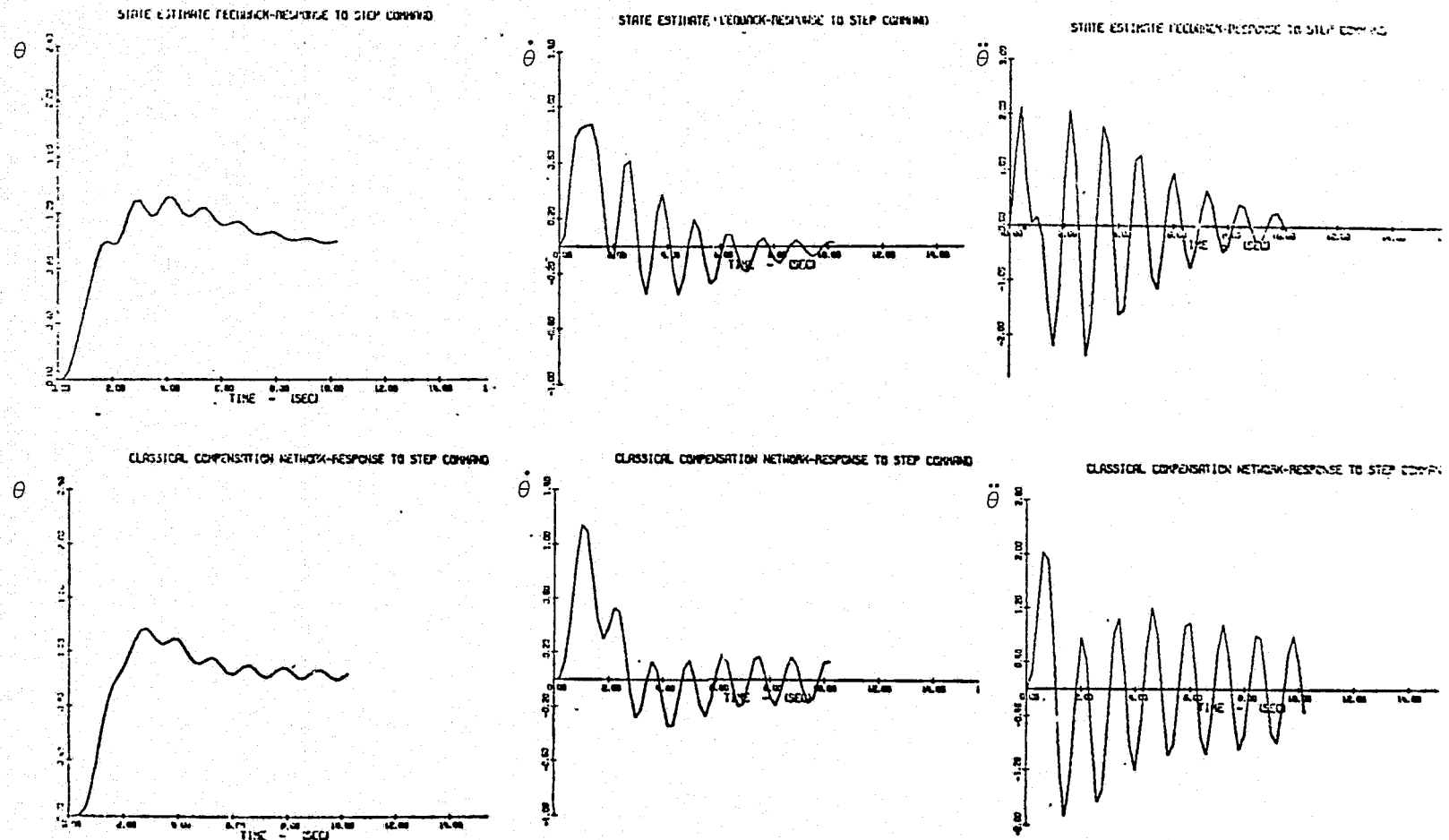

FIG. III-9 RESPONSE TO STEP COMMAND OF STATE ESTIMATE FEEDBACK (SEF) CONTROLLER AND CLASSICAL COMPENSATOR

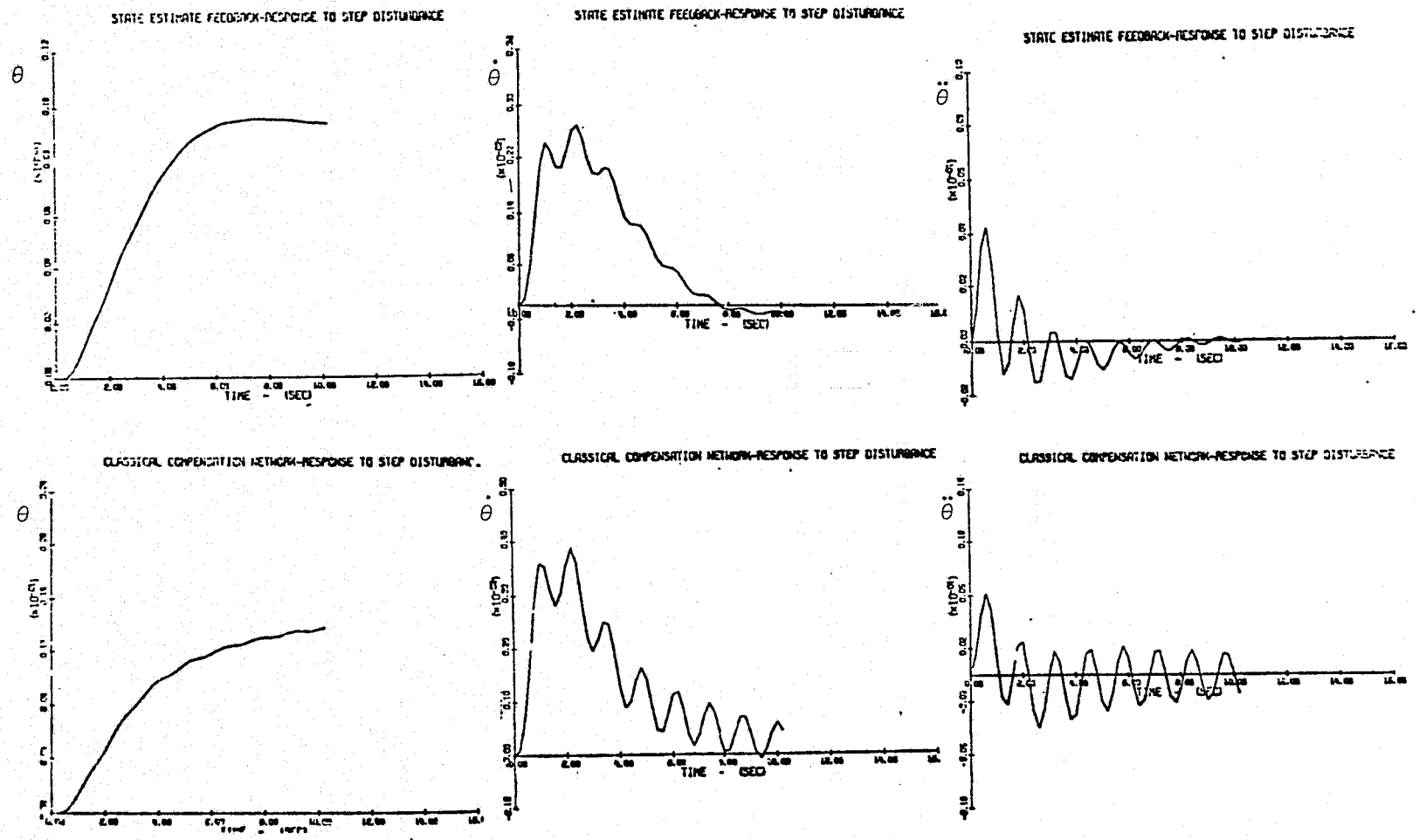

FIG. III-10 RESPONSE TO STEP DISTURBANCE OF STATE ESTIMATE FEEDBACK (SEF) CONTROLLER AND CLASSICAL COMPENSATOR.

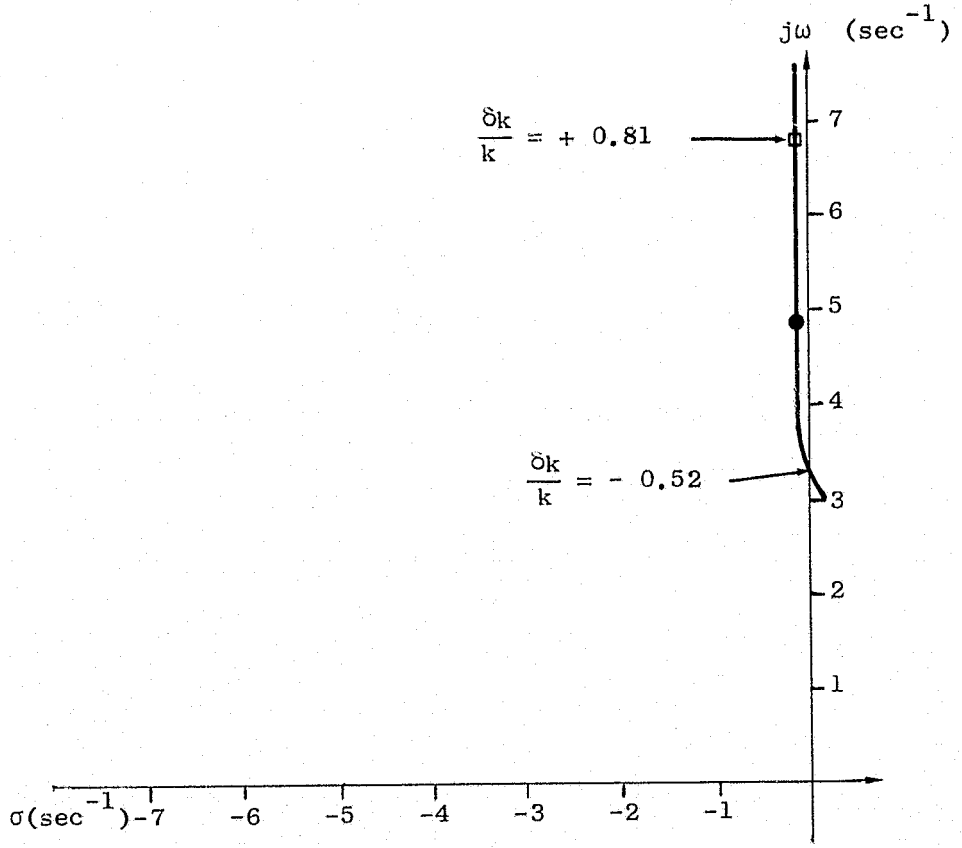

FIG. III-11 SENSITIVITY ROOT LOCUS OF CLASSICAL COMPENSATOR

The classical compensator has very low sensitivity to increase in ω. This can be understood by considering its Bode plot, Fig. III-12. In this plot it can be seen that the phase angle reaches $180°$ only below ω_0, whereas for the SEF controller, it reaches this value both below and above this frequency (see Fig. III-5). For the classical controller, the phase angle φ_c is always less than $180°$.

E. CONCLUSIONS

In this chapter the sensitivity to parameter perturbation of the SEF controller was analyzed and demonstrated by means of an example. In the specific example that was considered, the classical compensator is probably a better choice than the SEF controller since its lower sensitivity seems more important than its less acceptable time behavior. If, however, the full system and not just its low frequency approximation is considered, it was shown by Bull [BU-1] that such a classical compensator will not provide adequate control unless the system bandwidth is lowered considerably. For the required bandwidth, SEF is hard to replace.

The sensitivity problem for this full system is, however, just as severe as for the low frequency approximation. It is therefore clearly desirable to have a general method for the sensitivity reduction of SEF controllers. This method should operate in such a way that while the sensitivity is reduced, the nominal performance is not degraded unduly.

In Chapter IV such a method is developed.

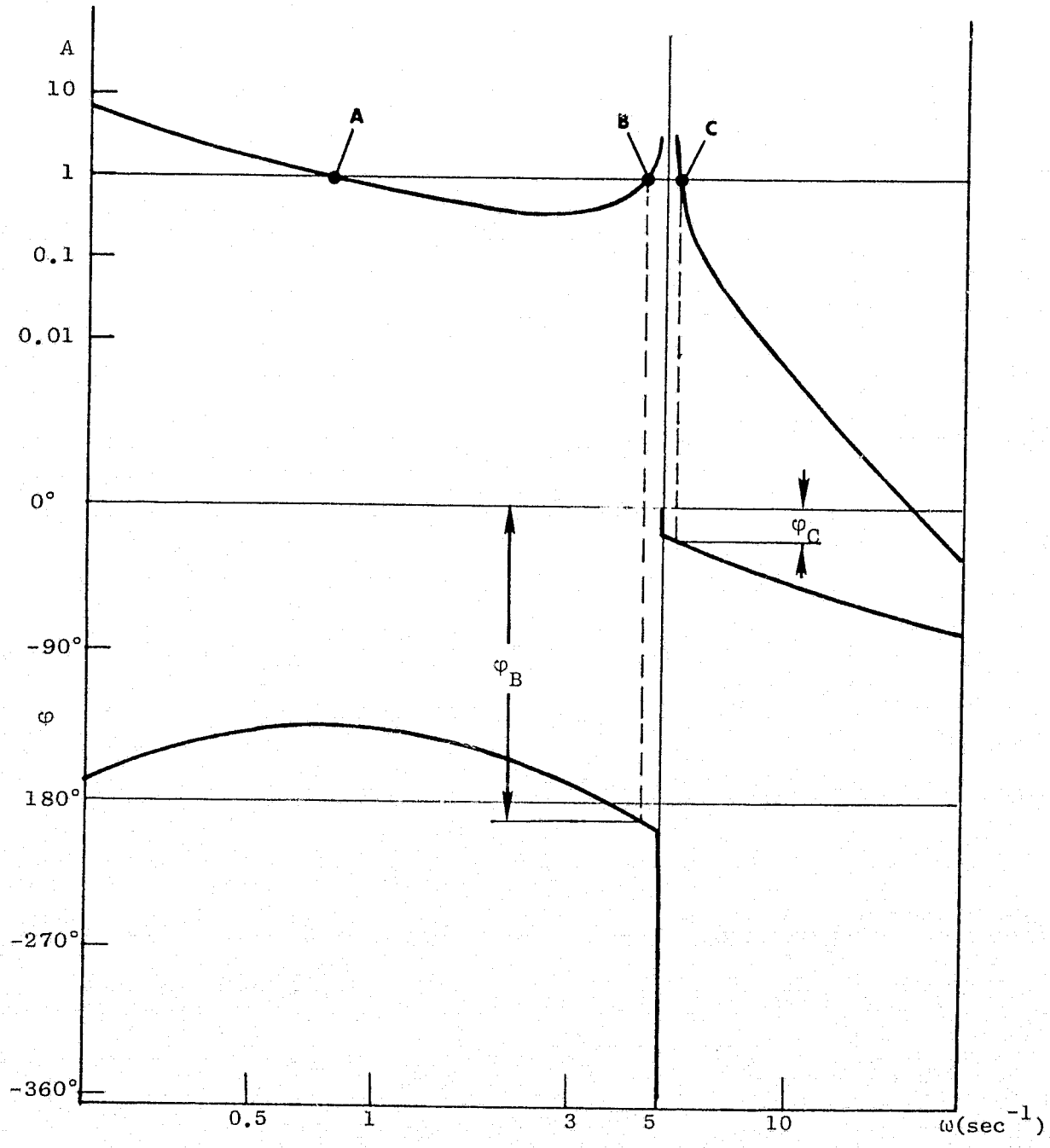

FIG. III-12 OPEN LOOP FREQUENCY RESPONSE OF THE CLASSICAL DESIGN.

IV. A DESIGN METHOD FOR MINIMIZING THE SENSITIVITY TO PARAMETER VARIATIONS

A. INTRODUCTION

Several time domain methods for the minimization of the sensitivity to parameter perturbations are described in the literature. One common approach is to define a sensitivity vector (Eq. 3.1)

$$\sigma = \frac{\partial x}{\partial \mu}$$

for which the governing equation is [LUH-1]

$$\dot{\sigma} = F\sigma + F_\mu x + G_\mu u + G\frac{\partial u}{\partial \mu} \qquad (4.1)$$

$$\sigma(0) = \frac{\partial x(0)}{\partial \mu}$$

where $F_\mu = \frac{\partial F}{\partial \mu}$, $G_\mu = \frac{\partial G}{\partial \mu}$.

As an extension to the regulator problem, an augmented PI can now be formulated [CAS-1, DA-1]

$$J_A = \int_0^\infty (x^T A x + u^T B u + \sigma^T S \sigma)dt ,$$

and a control that minimizes it can be found.

Two separate cases have to be considered: (a) open loop control

and (b) feedback control. If the control is implemented in an open loop fashion, $\partial u/\partial \mu = 0$, and the optimal control can be obtained in a straightforward way by solving the optimal regulator problem for the augmented system with the state vector $x_A^T = [x^T, \sigma^T]$, and the PI of Eq. (4.2). This, however, is hardly a realistic approach since, in general, feedback control will be required.

In order to determine $\partial u/\partial \mu$ for the feedback case the form of the control has to be stipulated. Some authors [CAS-1, DA-1, DO-1, BR-1] stipulate

$$u = C_1 x + C_2 \sigma$$

and solve the optimal control problem for the augmented system. C_1 and C_2 are not obtained from the solution of a Ricatti equation since the dynamic matrix of the augmented system contains C_1 [SA-1].

In addition to some theoretical questions as to the optimality of this solution [SA-1], it is complicated to implement since the sensitivity vector σ has to be obtained from a model. The order of the system is thereby augmented. For single input system algorithms have been developed to augment the order by n only, even if there are several variable parameters in the system [WI-1]. The examples given for the use of this method are of low order and assume that the state is available for feedback [CAS-1, DA-1, DO-1, LA-1, BR-1]. No mention is made of the influence of using the estimate instead of the state. These examples seem to show a definite reduction in their trajectory sensitivity but it is not clear whether this is also true for higher order systems. In one case of a higher order system, no conclusive result was found [RY-2]. Hendricks and D'Angelo [HE-1] use the same augmented system but postulate a control of the form

$$u = Cx$$

and find C by parameter optimization. This method was applied to the sensitivity minimization of a space booster with good results.

Here too, however, all the states are assumed available and the effect of using state estimates instead of states is not considered. This and the following methods have the advantage over the previous methods that the controller does not become more complicated because of the sensitivity requirements and only the values of its parameters are modified. Rillings and Roy [RI-1] postulate the same control but use analog computer simulation to minimize the PI. In another variant of this method, Cassidy and Roy [CAS-1] force the control to have non-zero feedback gains only for the measured states. This is done by solving the inverse problem and defining the weighting matrices that give the desired feedback structure. From the given data, the computation times for this method seem extensively lengthy. More recently, Stravroulakis and Sarachik [ST-1], using the same augmented system, derive iterative governing equations for output feedback or state estimate feedback gains for both the deterministic and the stochastic case. These equations are formulated for a single variable parameter and it is not clear how they can be extended to multiple parameters. The gains that are obtained by this method seem to be applicable to practical state estimate feedback systems but the governing equations are complicated and the computational labor involved in the iterative calculation may be considerable. This problem is not discussed by the authors. Many of the references cited above and other papers that treat various aspects of the sensitivity problem were collected by Cruz in a book published recently [CR-1].

A different approach is used by Palsson and Whittaker [PA-1]. In this approach, the variable parameters are considered as components of a random vector with mean at the nominal value and known covariance. A performance index of the form

$$J = \overline{\int_0^\infty x^T A x dt}$$

is minimized where the average is taken over the values of the variable parameters. The structure of the system is predetermined and the minimization is performed by varying a set of free parameters selected by

the designer. The method as presented is applicable to single-input single-output (SISO) systems only, and is essentially designed to select the parameters of classical compensators. It seeks a balance between the performance at nominal and off-nominal conditions. The relative importance of these two conditions can be determined by the designer. The example presented shows an appreciable reduction in sensitivity without unduly affecting the nominal performance. This method is not suitable for the sensitivity reduction of SEF controllers for several reasons: (a) The natural free parameters for a SEF controller are the feedback and estimator gains. However, since the control is not weighted in the PI, not all the feedback gains can be left free since very high or even infinite gains would result in most cases. The selection of the gains that remain fixed is somewhat arbitrary and may lead to unsatisfactory results. (b) The restriction to SISO systems prevents the selection of the estimator gains as free parameters, if the estimator is a Kalman filter. In that case, at least two inputs are required; one being a disturbance, and the other a sensor noise (Eq. 2.36). If those two inputs cannot be used in the desensitization, the nominal estimator gains will tend to infinity and the estimator may lose its filtering properties. The total number of inputs must therefore be equal to the sum of the number of disturbances and outputs. The method as presented, however, cannot be extended to multivariable systems. (c) The controller has to be transformed into its equivalent compensating network form or alternatively, the closed loop transfer function has to be found. Both these operations are cumbersome and present numerical problems.

In this thesis a sensitivty minimization method is developed that is based on the Palsson-Whittaker [PA-1] method but has none of the drawbacks described above. It is applicable to multivariable systems, both deterministic and stochastic, without restriction on the structure of the system matrices. Although it was motivated by the need for sensitivity reduction of SEF controllers, it is applicable to any system which can be represented in the form of Eq. (2.1). The basic equations are similar to those given by Palsson-Whittaker but the method of solution is totally different.

B. DESCRIPTION OF THE SENSITIVITY MINIMIZATION METHOD

B.1 Problem Statement

Consider the system (repeated from 2.1)

$$\begin{aligned} \dot{x} &= Fx + Gu + \Gamma w \\ y &= Hx + v \ , \end{aligned} \tag{4.3}$$

where the matrices F, G, Γ, and H contain parameters the values of which are uncertain. If these parameters are considered as Gaussian random variables, a Gaussian random vector may be formed of which they are the components. This vector is specified by

$$E(z) = z_n, \tag{4.4}$$

where the components of z_n are the nominal values of the parameters, and by

$$E[(z - z_n)(z - z_n)^T] \tag{4.5}$$

a covariance matrix which is assumed known. Equation (4.3) may then be written as

$$\begin{aligned} \dot{x} &= F(z)x + G(z)u + \Gamma(z)w \\ y &= H(z)x + v, \end{aligned} \tag{4.6}$$

$$x(0) = 0.$$

The control is defined as

$$u = -Cx \tag{4.7}$$

where the values of C may be left free or defined by functional relationships to other parameters of the system. For this definition of

u to be valid, Eq. (4.3) generally is required to describe an augmented system that includes the plant and the compensations. The matrices F, G, H, and Γ then have to be defined accordingly. For SEF controllers, the augmented system is given by Eq. (2.31). For this case, the control is given as

$$u = [0, -C_E][x, \hat{x}]^T = [-C_e, C_E][x, \tilde{x}]^T .$$

A quadratic PI for this system is

$$J = \lim_{t_f \to \infty} \frac{1}{t_f} \int_0^{t_f} E(x^T A x + u^T B u) dt . \tag{4.8}$$

In this expression, the expected value is taken over the probability distributions of x and u that are derived from both the distributions of the random process w and of the random vector z. Note that w is the process noise of the augmented system. Since w and z are independent, the expected value of a function of x and u is

$$\begin{aligned} E[f(x,u)] &= \int_{x,u} f[x(w,z),\ u(w,z)]\ p[x(w,z),\ u(w,z)]dxdy \\ &= \int_w E_z p(w) dw = \int_z E_w p(z) dz , \end{aligned} \tag{4.9}$$

where

$$E_z = \int_z g(w,z)\ p(z)dz$$

is the expected value over the distribution of z and

$$E_w = \int_w g(w,z)\ p(w)dw$$

is the expected value over the distribution of w.

A free parameter vector q is defined by the designer. This

vector consists of n_q parameters of the system matrices that can be varied by the designer.

The problem is now stated as follows: Given the system of Eqs. (4.6), (4.7) in which the system matrices are functions of a variable parameter vector defined by Eqs. (4.4) and (4.5), determine the value of the free parameter vector q so that the PI of Eq. (4.8) is minimized.

B.2 Method of Solution

Using Eq. (4.7) in Eq. (4.8), the PI becomes

$$J = \lim_{t_f \to \infty} \frac{1}{t_f} \int_0^{t_f} E[x^T(A + C^T B C)x]dt$$

Since for any vector v, $v^T v = tr(vv^T)$, this equation can be transformed into

$$J = tr[(A + C^T B C) \lim_{t_f \to \infty} \frac{1}{t_f} \int_0^{t_f} E(xx^T)dt] \; . \qquad (4.10)$$

The state vector x may be written as

$$x(w,z) = x_n(w,z_n) + \delta x(w,\delta z) \qquad (4.11)$$

where x_n is the state vector obtained when the parameters have their nominal values, and δx is the perturbation in the state vector due to a perturbation δz in the variable parameter vector.

Assuming small perturbations in z so that a first order expansion is satisfactory, substituting Eq. (4.7) into (4.6) and defining

$$F_c = F - GC$$

the governing equations for x_n and δx become

$$\dot{x}_n = F_c(z_n)x_n + \Gamma(z_n)w \tag{4.12a}$$

$$\dot{\delta x} = F_c(z_n)\delta x + \delta F_c x_n + \delta\Gamma w \ , \tag{4.12b}$$

$$x_n(0) = 0; \qquad \delta x(0) = 0 \ ; \tag{4.12c}$$

where

$$\delta F_c = \sum_{i=1}^{n_z} \frac{\partial F_c}{\partial z_i}\,\delta z_i$$

$$\delta\Gamma = \sum_{i=1}^{n_z} \frac{\partial \Gamma}{\partial z_i}\,\delta z_i \ .$$

The expected value of Eq. (4.12b) is

$$E(\dot{\delta x}) = F_c(z_n)E(\delta x) + \sum_{i=1}^{n_z} \frac{\partial F_c}{\partial z_i} E(\delta z_i x_n) + \sum_{i=1}^{n_z} \frac{\partial \Gamma}{\partial z_i} E(\delta z_i w) \ .$$

δz is independent of x_n and w, and since $E(\delta z) = 0$, we have

$$E(\delta z_i x_n) = E(\delta z_i w) = 0, \qquad i = 1, n_z \ .$$

From Eq. (4.12c),

$$E[\delta x(0)] = 0$$

and therefore

$$E[\delta x(t)] = 0. \tag{4.13}$$

The expression $E(xx^T)$ in the PI of Eq. (4.10) can now be evaluated in terms of x_n and δx

$$\begin{aligned} E(xx^T) &= E[(x_n + \delta x)(x_n + \delta x)^T] \\ &= E(x_n x_n^T) + E(x_n \delta x^T) + E(\delta x x_n^T) + E(\delta x \delta x^T) \ . \end{aligned} \tag{4.14}$$

To find the value of the second term of this expression, it can be written according to Eq. (4.8) and using Eq. (4.13), as

$$E[x_n(w)\delta x^T(w,z)] = E_w\{E_z[x_n(w)\delta x^T(w,z)]\}$$
$$= E_w\{x_n(w)E[\delta x^T(w,z)]\} = 0 .$$

Similarly,

$$E[\delta x x_n^T] = 0 .$$

We therefore get

$$E(xx^T) = E(x_n x_n^T) + E(\delta x \delta x^T) = X_n + \delta X , \qquad (4.15)$$

where X_n is the covariance matrix of the nominal state. δx can thus be interpreted as the addition to the covariance due to the parameter uncertainties. Substituting Eq. (4.15) into Eq. (4.10) yields

$$J = tr[(A + C^T BC) \lim_{t_f \to \infty} \frac{1}{t_f} \int_0^{t_f} [X_n(t) + \delta X(t)]dt$$
$$= tr[(A + C^T BC)(\bar{X}_n + \overline{\delta X})] \qquad (4.16)$$

where $\bar{X}_n$ and $\overline{\delta X}$ are the time averages over all time of X_n and δX respectively.

For a stable system, X_n and δX tend to constant values $X_n(\infty)$ and $\delta X(\infty)$. Since the averaging in Eq. (4.16) is performed over a large time interval, it can be assumed that $\bar{X}_n \to X_n(\infty)$ and $\overline{\delta X} \to \delta X(\infty)$. The PI therefore becomes

$$J \cong tr\{[A + C^T BC][X_n(\infty) + \delta X(\infty)]\}$$
$$= J_0 + J_A , \qquad (4.17)$$

where

$$J_0 = \mathrm{tr}[(A + C^T B C)\, X_n(\infty)]$$

is the nominal PI, and

$$J_A = \mathrm{tr}[(A + C^T B C)\, \delta X(\infty)]$$

is the additional PI due to the parameter variations. The PI of Eq. (4.17) can be minimized computationally by a two-step sequence: (a) the matrices $X_n(\infty)$ and $\delta X(\infty)$ are found for a given value of the free parameter vector, q. The PI that corresponds to this value is then determined. (b) the q vector is modified in a direction that decreases J. This sequence is repeated until the decrease in J in one cycle is less than a predetermined value.

The two parts of this sequence are independent and computer programs for each one can be developed separately.

B.3 The Governing Equations for X_n and δX.

For brevity, the subscripts of x_n and X_n will now be dropped. To find X use $(d)/(dt)(xx^T)$, viz.,

$$\frac{d}{dt}(xx^T) = \dot{x}x^T + x\dot{x}^T . \tag{4.18}$$

Substituting Eq. (4.12a) into Eq. (4.18) yields

$$\begin{aligned} \frac{d}{dt}(xx^T) &= (F_c x + \Gamma w)x^T + x(F_c x + \Gamma w)^T \\ &= F_c xx^T + \Gamma w x^T + xx^T F_c^T + xw^T\Gamma^T . \end{aligned} \tag{4.19}$$

Taking the expected value of both sides of this equation and using the definition

$$E(xx^T) = X$$

Eq. (4.19) becomes

$$\dot{X} = F_c X + \Gamma E(wx^T) + XF_c^T + E(xw^T)\Gamma^T \quad . \tag{4.20}$$

But,

$$E(xw^T) = E\{[e^{F_c t}x(0) + \int_0^t e^{F_c(t-\tau)}\Gamma w(\tau)d\tau]w(t)\}$$

and

$$E[w(\tau)w^T(t)] = Q\delta(t-\tau)$$

$$E[x(0)w(t)] = 0, \text{for} \quad t \geq 0,$$

therefore

$$\begin{aligned} E(xw^T) &= E\int_0^t e^{F_c(t-\tau)}\Gamma w(\tau)w^T(t)d\tau \\ &= \int_0^t e^{F_c(t-\tau)}\Gamma Q\delta(t-\tau)d\tau \\ &= \underline{\underline{\frac{1}{2}\Gamma Q}} \quad . \end{aligned} \tag{4.21}$$

Similarly,

$$E(wx^T) = \frac{1}{2}Q\Gamma^T \quad . \tag{4.22}$$

Using Eqs. (4.21) and (4.22) in Eq. (4.20), the covariance is

$$\dot{X} = F_c X + XF_c^T + \Gamma Q\Gamma^T \quad . \tag{4.23}$$

In the steady state, $\dot{X} = 0$ and the final equation for X_∞ is

$$F_c X_\infty + X_\infty F_c^T + \Gamma Q\Gamma^T = 0 \quad . \tag{4.24}$$

The governing equation for δX can be found in a similar way. Using

$$\frac{d}{dt}(\delta x \delta x^T) = \delta x \delta\dot{x}^T + \delta\dot{x}\delta x^T \tag{4.25a}$$

and Eq. (4.12b) yields

$$\frac{d}{dt}\left(\delta x \delta x^T\right) = \delta x \delta x^T F_c^T + \delta x x^T \delta F_c^T + \delta x w^T \delta\Gamma^T + F_c \delta x \delta x^T + \delta F_c x \delta x^T + \delta\Gamma w \delta x^T \quad . \tag{4.25b}$$

To determine the expected value of this equation, $E(\delta x w^T)$ has to be evaluated.

$$\begin{aligned} E(\delta x w^T) &= E\left(\left\{e^{F_c t}\delta x_o + \int_o^t e^{F_c(t-\tau)}\left[\delta F_c x(\tau) + \delta\Gamma w(\tau)\right]\delta\tau\right\} w^T(t)\right) \\ &= \int_o^t e^{F_c(t-\tau)}\delta F_c E\left[x(\tau)w^T(t)\right]d\tau \\ &\quad + \int_o^t e^{F_c(t-\tau)}\delta\Gamma E\left[w(\tau)w^T(t)\right]d\tau \\ &= \frac{1}{2}\delta\Gamma Q \quad . \end{aligned} \tag{4.26}$$

The first integral vanishes because

$$E\left[x(\tau)w^T(t)\right] \neq 0 \qquad \text{only for } \tau = t \quad .$$

Using the definitions of X and δX from Eq. (4.15), the expected value of Eq. (4.25b) can now be found.

$$\dot{\delta X} = \delta X F_c^T + F_c \delta X^T + E\left[\delta\Gamma Q \delta\Gamma^T\right] + E\left[\delta x x^T \delta F_c^T\right] + E\left[\delta F_c x \delta x^T\right] \quad . \tag{4.27a}$$

The last term on the right hand side of this equation may be written as

$$E\left[\delta F_c x dx^T\right] = E_z\left[\delta F_c E_w\left(x\delta x^T\right)\right] \quad ,$$

since δF_c is independent of w. Defining

$$Y = E_w(x\delta x^T) , \tag{4.27b}$$

the last term of Eq. (4.27a) is

$$E[\delta F_c x\delta x^T] = E_z[\delta F_c Y] . \tag{4.28}$$

As $t \to \infty$, δX tends to the steady state value, δX_∞.

The final equation for δX_∞ is obtained by substituting Eq. (4.28) into Eq. (4.27a) and putting $\dot{\delta X}_\infty = 0$. Thus

$$\delta X_\infty F_c^T + F_c \delta X_\infty + E_z[\delta\Gamma Q\delta\Gamma^T + Y_\infty^T \delta F_c^T + \delta F_c Y_\infty] = 0 \tag{4.29}$$

To get the governing equation for Y_∞, the identity

$$\begin{aligned} \frac{d}{dt}(x\delta x^T) &= \dot{x}\delta x^T + x\dot{\delta x}^T \\ &= F_c x\delta x^T + \Gamma w\delta x^T + x\delta x^T F_c^T + xx^T\delta F_c^T + xw^T\delta\Gamma^T \end{aligned} \tag{4.30}$$

is used. The expected value of this equation over the distribution of w can now be found using Eq. (4.22) and Eq. (4.26), and the definition of Eq. (4.27b).

$$\dot{Y} = F_c Y + YF_c^T + \Gamma Q\delta\Gamma^T + X\delta F_c^T . \tag{4.31}$$

The steady state value of Y as $t \to \infty$ is given by

$$F_c Y_\infty + Y_\infty F_c^T + \Gamma Q\delta\Gamma^T + X_\infty \delta F_c^T = 0 . \tag{4.32}$$

The governing equations for X_∞ and δX_∞ that have been derived in this section are rewritten

$$F_c X_\infty + X_\infty F_c^T = -\Gamma Q \Gamma^T \tag{4.33a}$$

$$F_c Y_\infty + Y_\infty F_c^T = -\Gamma Q \delta\Gamma^T - X_\infty \delta F_c^T \tag{4.33b}$$

$$F_c \delta X_\infty + \delta X_\infty F_c^T = -E_z\left[\delta\Gamma Q \delta\Gamma^T + Y_\infty^T \delta F_c^T + \delta F_c Y_\infty\right]. \tag{4.33c}$$

These equations all have the same well known form [e.g., GA-1]

$$AX + XA^T = B ,$$

where A and B are given. They must be solved in the order in which they are written because the right hand sides of the second and third equations contain expressions found in the solution of the previous equations. For their actual solution, these equations must be written in a slightly different form. Equation (4.33b) is rewritten as

$$F_c Y_\infty + Y_\infty F_c^T = -\sum_{i=1}^{n_z}\left(\Gamma Q \frac{\partial \Gamma}{\partial z_i} - X_\infty \frac{\partial F_c}{\partial z_i}\right)\delta z_i . \tag{4.34}$$

Y_∞ is therefore obtained in the form of a sum: $Y_\infty = \Sigma\, Y_i \delta z$, where Y_i is the solution of

$$F_c Y_i + Y_i F_c^T = -\Gamma Q \frac{\partial \Gamma}{\partial z_i} - X_\infty \frac{\partial F_c}{\partial z_i} . \tag{4.35}$$

This equation is solved n_z times with different right hand sides. The right hand side of Eq. (4.33c) can be written as

$$E_z\left[\delta\Gamma Q \delta\Gamma^T + \delta F_c Y_\infty + Y_\infty^T \delta F_c^T\right]$$

$$= E_z\left[\sum_{j=1}^{n_z}\sum_{i=1}^{n_z} \frac{\partial\Gamma}{\partial z_i} Q\left(\frac{\partial\Gamma}{\partial z_j}\right)^T + \frac{\partial F_c}{\partial z_i} Y_j + \left(\frac{\partial F_c}{\partial z_i} Y_j\right)^T\right]\delta z_i \delta z_j \qquad (4.36)$$

$$= \sum_{j=1}^{n_z}\sum_{i=1}^{n_z}\left[\frac{\partial\Gamma}{\partial z_i} Q\left(\frac{\partial\Gamma}{\partial z_j}\right)^T + \frac{\partial F_c}{\partial z_i} Y_j + \left(\frac{\partial F_c}{\partial z_i} Y_j\right)^T\right] v_{ij}$$

where V is the parameter covariance matrix (see Eq. 4.5).

Equation (4.36) can be written in a more compact form although this form is not used in the actual computation because of excessive storage requirements.

$$\sum_{j=1}^{n_z}\sum_{i=1}^{n_z}\left[\frac{\partial\Gamma}{\partial z_i} Q\left(\frac{\partial\Gamma}{\partial z_j}\right)^T + \frac{\partial F_c}{\partial z_i} Y_j + \left(\frac{\partial F_c}{\partial z_i} Y_j\right)^T\right] v_{ij} \qquad (4.37)$$

$$= \left[\frac{\partial\Gamma}{\partial z} Q\right]\left[V \otimes I_{np}\right]\frac{\partial\Gamma}{\partial z}^T + \frac{\partial F}{\partial z}(V \otimes I_n)Y + \left[\frac{\partial F}{\partial z}(V \otimes I_n)Y\right]^T$$

where I_n is the $n \times n$ unit matrix,

$$\frac{\partial\Gamma}{\partial z} Q = \left[\frac{\partial\Gamma}{\partial z_1} Q \;\middle|\; \frac{\partial\Gamma}{\partial z_2} Q \;\middle|\; \cdots \frac{\partial\Gamma}{\partial z_{n_z}} Q\right], \quad [n \times (n_p \times n_z)];$$

$$\frac{\partial\Gamma}{\partial z} = \left[\frac{\partial\Gamma}{\partial z_1} \;\middle|\; \cdots \;\middle|\; \frac{\partial\Gamma}{\partial z_{n_z}}\right], \quad [n \times (n_p \times n_z)];$$

$$\frac{\partial F_c}{\partial z} = \left[\frac{\partial F_c}{\partial z_1} \;\vdots\; \cdots \;\vdots\; \frac{\partial F_c}{\partial z_{n_z}}\right] \qquad [n \times (n \times n_z)];$$

$$Y = \begin{bmatrix} Y_1 \\ \vdots \\ Y_{n_z} \end{bmatrix} \qquad [(n \times n_z) \times n] \;;$$

and where

$$A \otimes B$$

is the Kronecker product of A and B. This product is defined for $A[n \times n]$ and $B[m \times m]$ as a $(n \times m) \times (n \times m)$ matrix having as its ijth $m \times m$ block:

$$(A \otimes B)_{ij} = a_{ij} B.$$

There are $n \times n$ such blocks.

Equation (4.33) can now be rewritten in the form

$$F_c X_\infty + X_\infty F_c^T = -\Gamma Q \Gamma^T \tag{4.38a}$$

$$F_c Y_i + Y_i F_c^T = -\Gamma Q \frac{\partial \Gamma}{\partial z_i} - X_\infty \frac{\partial F_c}{\partial z_i} \tag{4.38b}$$

$$F_c \delta X_\infty + \delta X_\infty F_c^T = -\left[\frac{\partial \Gamma}{\partial z} Q\right]\left[V \otimes I_{n_p}\right]\left(\frac{\partial \Gamma}{\partial z}\right)^T$$

$$- \frac{\partial F}{\partial z}(V \otimes I_n)Y - \left[\frac{\partial F}{\partial z}(V \otimes I_n)Y\right]^T. \tag{4.38c}$$

From Equation (4.33c) and (4.36) it can be seen that δX is proportional to the parameter covariance matrix V, i.e., if each element of V is multiplied by a scalar coefficient ϵ, so is each element of δX. From Eq. (4.17) it is clear that the additional performance index J_A is then multiplied by the same coefficient.

In the problem statement the parameter covariance matrix V is assumed known (see Eq. 4.5). Its elements are a measure of the uncertainties in the parameters. In reality, however, these uncertainties are ill defined and the matrix V is considered mainly as a design tool. It can be written as

$$V = \epsilon V_0$$

where ϵ is a scalar weighting coefficient. Equation (4.17) then becomes

$$J = J_0 + J_A = J_0 + \epsilon J_{A0} . \tag{4.39}$$

The coefficient ϵ is selected by the designer for the relative weighting of nominal performance vs sensitivity. The relative magnitude of the elements of V is selected according to the importance of the sensitivity reduction for the respective parameters.

Equations (4.38) remain valid if the system is forced by inputs other than white noise. If the disturbance is colored, it can be modeled by means of a shaping filter forced by white noise. An augmented system can then be formed consisting of the states of the system and of the shaping filter. This augmented system is excited by white noise and Eqs. (4.38) is therefore valid for it.

For deterministic systems which are required to recover from nonzero initial conditions, the white noise vector w is replaced by an impulsive input vector w_i at $t = 0$: $w_i = w_o \delta(t)$. The initial conditions are then represented by the equivalent initial impulses. Equations (4.38) can be used unchanged if the following terms are redefined:

$$
\begin{aligned}
Q &= w_o w_o^T \\
X_\infty &= \int_o^\infty x x^T dt \\
Y_\infty &= \int_o^\infty x \delta x^T dt \\
\delta X_\infty &= \int_o^\infty \delta x \delta x^T dt \ .
\end{aligned}
\tag{4.40}
$$

With these redefined terms the deterministic PI is given by Eq. (4.17).

If the system is to be optimized for some deterministic input other than an initial impulse, this can be handled by state augmentations.

B.4 Description of the Computer Program

The computer program, PAROPT, for the minimization of the PI of Eq. (4.7) is described in detail in Appendix B. Only its main features are described in this section. It consists of two main parts: (1) A search subprogram; (2) A subprogram for the solution of Eq. (4.33) and determination of the PI from Eq. (4.17).

(1) Search subprogram. This subprogram is part of the program library of the Computer Science Department at Stanford University. It was developed by Gill, Murray and Pitfield [GI-1]. It iteratively seeks the minimum value of a scalar function $F(q)$, where q is a vector of dimension n_q, by modifying the components of q. The value of $F(q)$ for a given q is an input to the subprogram. For the current problem, it is the performance index J of Eq. (4.17).

The mode of operation of this program is as follows. For given initial values of q and J, the approximate direction of the gradient of J with respect to the vector q is found by perturbing the components of q one at a time and determining J for the perturbed vector. The components

of the approximate gradient vector are proportional to

$$\frac{J_i - J_0}{\Delta q_i}$$

The direction of the conjugate gradient [BRY-2 for definition] is then determined and a linear search is performed along this direction. In general, three to four evaluations of J are required to determine the minimum of J along a direction. At the minimum, the gradient is again found and a new linear search direction is determined.

One iteration is defined as a gradient determination and linear search. This iterative procedure is continued until termination criteria are satisfied. (See Appendix B for more details.)

(2) Subprogram for the evaluation of J. It is obvious from the description of the search subprogram that the value of J must be computed a large number of times. In one iteration, n_q evaluations are required for the gradient determination and 3 to 4 for the linear search. In an average program, 8 to 10 iterations may be expected and therefore it may be required to compute J 100 to 200 times. For the program to be of any practical usefulness, a very efficient method for this computation must therefore be developed.

The principal part of this evaluation is the solution of Eqs (4.38). The same equation with different right hand sides is to be solved $2 + n_z$ times. It is to be noted, however, that Eq. (4.38a) and (4.38c) have symmetric right hand sides and therefore symmetric solutions (Lyapunov equations), whereas the right hand side of Eq. (4.38b) is not symmetric. Several methods are available for the solution of these equations. These methods are compared by Hagander [HA-1]

and Pace and Barnett [PA-1]. The recommendation of Hagander is to use a direct method (described below) for systems of order smaller than 6 or 7, and other methods above this order. The reason for the recommendation for a different method for large systems, despite the better precision of the direct method, is that the computation time of the direct method increases as $n^6/3$ and becomes prohibitively large for large systems. Pace and Barnett recommend the direct method up to order 10 approximately. The direct method consists of transforming an equation of the form

$$AZ + ZA^T = B \tag{4.41}$$

into the form

$$\alpha z = -\beta , \tag{4.42}$$

where $z(\ell \times 1)$ is the n^2 vector of the coefficients of Z, and β is the n^2 vector of the coefficient of B. α is obtained from A by [BE-1]

$$\alpha = A \otimes I_n + I_n \otimes A$$

For symmetric Z, the dimension of z need only be $\ell = \frac{1}{2}(n + 1)n$. An algorithm to obtain α for this case is given by Bingoulac [BI-1].

For antisymmetric Z, the dimension of z is $\ell = \frac{1}{2}(n-1)n$. A transformation algorithm for this case was developed as part of this program.

The method commonly used for the solution of linear equations of the form of (4.42) is Gaussian elimination [FO-1]. It consists of two steps: (a) forward elimination ($\ell^3/3$ operations), and (b) back substitution ($\ell^2/2$ operation). By comparing the number of operations, it is obvious that to

solve a general equation of type (4.41) by the direct method, it is advantageous to decompose the right hand side into symmetric and antisymmetric parts and to obtain two separate solutions, the sum of which is the required solution. This is important for the solution of Eq. (4.38b). In the solution of (4.42), forward elimination is only required if α is changed. If only β is changed, the much less costly back-substitution is required.

In our case, for one evaluation of the PI, only one forward elimination of order $\frac{1}{2}(n+1)n$ is required (for X), and one of order $\frac{1}{2}(n-1)n$ (for the antisymmetric part of Y_1). This considerably reduces the average computation time for the direct method and makes it attractive for much larger systems. Moreover, since the points at which the cost is computed for the gradient determination correspond to only slightly perturbed q vectors, the changes in X and δX that stem from these perturbations can be obtained by expanding Eqs. (4.38) about the nominal point and neglecting second order terms. Equation (4.38a) at the perturbed point is

$$F_{c1}X_1 + X_1F_{c1}^T = -\Gamma_1 Q \Gamma_1^T \qquad (4.43)$$

where the subscript 1 refers to this point. Expanding Eq. (4.43) yields

$$(F_c+DF_c)(X+DX) + (X+DX)(F_c+DF_c)^T = -\Gamma_1 Q \Gamma_1^T$$

where the prefix D indicates the change between the nominal and perturbed points. Neglecting the product $(DF_c)(DX)$, Eq. (4.43) becomes

$$F_c DX + DXF_c^T = -F_{c1}X - XF_{c1}^T - \Gamma_1 Q \Gamma_1^T \qquad (4.44a)$$

The coefficients of the left hand side of this equation are

the same as for Eq. (4.38a) at the nominal point. Similarly, for DY and D(δX),

$$F_c DY + DYF_c^T = F_{c1}Y + YF_{c1}^T - \Gamma_1 Q \delta\Gamma_1^T - X_1 \delta F_{c1} \tag{4.44b}$$

$$F_c D(\delta X) + D(\delta X) = -F_{c1}\delta X - \delta X F_{c1}^T - E_z(\delta F_{c1} Y_1 + Y_1 \delta F_{c1}^T + \delta\Gamma_1 Q \delta\Gamma_1^T) \tag{4.44c}$$

This approximation was compared to the exact method of evaluating the perturbed PI and no significant difference was observed.

The evaluation of the PI and its gradient, therefore, can be done with only one forward elimination of order $\frac{1}{2}(n + 1)n$ and one of order $\frac{1}{2}(n - 1)n$. This method was implemented in PAROPT, which has been applied to the sensitivity reduction of several systems. Results of its application are described in Section IV-C.

The largest system to which it was applied is of 12th order with 2 variable and 20 free parameters.

One iteration for this system (gradient evaluation plus linear search) required about 40 sec on an IBM 360/67 computer. This method therefore seems practical for even fairly large systems. The computation time increases as the fourth power (approximately) of the system order and is almost independent of the number of free and variable parameters.

C. APPLICATIONS

C.1 Introduction

In this Section the application of the sensitivity reduction program (SRP) to two systems will be described. The systems are: (a) low frequency approximation of the Stanford Relativity Satellite (SRS)

as described in Section III-D. (b) full Stanford Relativity Satellite (per III-D).

The design considerations for the nominal optimal controllers for these systems will not be given since they are described in detail by Bull [BU-1] for the full system and remain valid for the low frequency approximation. Since the purpose of this section is to investigate the operation of the sensitivity reduction program (SRP), several designs with different program parameters were made and the results are presented in considerable detail, particularly for the first example. The criteria that are used for the comparison of different designs for the same system are:

- Sensitivity criterion: the range of variation of the variable parameter for which the system is still stable (high range ≡ low sensitivity);
- Nominal performance criteria: output and control rms values and the square root of the nominal PI, which is a weighted rms value.

Some points have to be kept in mind when using these criteria: (a) The stability range of the variable parameters should not be construed as defining the actual permitted range of variation of these parameters. In general, the performance will become unacceptable for variations that are considerably less than those that cause instability. (b) The rms values of the outputs and the controls depend on the assumed covariance matrices of the process and measurement noises. These covariance matrices are generally not well known and in some cases, they are artificially determined in order to get acceptably damped roots of the estimator. Small differences (less than a factor of 2) in the rms values of different designs cannot, therefore, be considered as significant. The criteria that are used in this section are therefore unrefined but can still give a valid comparison between different designs.

More precise criteria are difficult to define, in general, although for specific cases they may exist. In some cases the time response envelope to a specific input may be restricted, or limits may be posed on the phase and gain margins. It is important to verify, whenever

such criteria are used, that they reflect actual system requirements and do not pose artificial restraints on the design.

The initial point in the application of the SRP must be a stable one for Eq. (4.33) to be valid. In the examples of this Section, the nominal optimal point that was found without considering sensitivity was selected as the initial point. This is not required but it is an easy point to calculate since the weighting and covariance matrices are also required for the SRP. The systems that are used in the SRP are the augmented systems given by

$$\begin{bmatrix} \dot{x} \\ \dot{\tilde{x}} \end{bmatrix} = \begin{bmatrix} F_1 - GC & GC \\ F_1 - F & F - KH \end{bmatrix} \begin{bmatrix} x \\ \tilde{x} \end{bmatrix} + \begin{bmatrix} \Gamma & 0 \\ \Gamma & -K \end{bmatrix} \begin{bmatrix} v \\ w \end{bmatrix} . \qquad (4.45)$$

where F_1 is the actual plant, F is the assumed plant in estimator. At the initial point $F_1 = F$. The weighting matrices are the same as those that were used for the nominal design.

For the application of the program, the parameter covariance matrix and the sensitivity coefficient ϵ have to be determined and the free parameters have to be defined. The parameters that are controlled by the designer and some or all of which can be used as free variables are: C, the feedback gains; K, the estimator gains; and F, the representations of the variable parameters in the estimator. The last item may require some clarification. If there are no variable parameters, the estimator parameters will obviously be selected to be the same as the plant parameters. If, however, some plant parameters are variable, it has been found that the sensitivity can be decreased, in some cases, if their representations in the estimator differ from their nominal values. It is therefore desirable to include these representations among the free parameters. The actual selection of the program parameters will be discussed for each example separately.

C-2 Example 1: Low Frequency Approximation of the Stanford Relativity Satellite (SRS)

This system was described in Chapter III-D. The augmented system is an 8th order system for which the initial dynamic and state weight matrices are shown in Fig. IV-1.

(1) Program parameters. The only variable parameter for this case is the spring stiffness, k. The parameter covariance matrix is therefore a scalar and only its product with the sensitivity coefficient ϵ is important. Various values of this product have been used in the different designs as described below. Only the estimator gains and the variable parameter representations in the estimator were used as free parameters since it was found in preliminary runs that the feedback gains do not vary appreciably. The application of the SRP (sensitivity reduction program) in this case is therefore a redesign of the estimator.

Four designs were executed with the design parameters varied as described below. The weighting coefficients ϵ and V (a scalar in this case) define the assumed rms value of the spring constant k

$$\sigma_k = \sqrt{\epsilon V} \tag{4.46}$$

As explained in IV-B-3, this rms value does not represent an actual expected uncertainty in the variable parameter but is used as a design tool for the relative weighting of the nominal and additional performance indices. The designs are:

Design No. 1: $\sigma_k/k = 0.28$ ($J_A/J_o = 1$ at the initial point)

Design No. 2: $\sigma_k/k = 0.9$ ($J_A/J_o = 10$ at the initial point)

Design No. 3: $\sigma_k/k = 0.9$, $R = 0$

Design No. 4: $\sigma_k/k = 0.9$, $Q = 0$.

THE INITIAL DYNAMICS MATRIX...

ROW	COL. 1	COL. 2	COL. 3	COL. 4	COL. 5	COL. 6	COL. 7
1	0.0	1.0000000CD 00	0.0	0.0	0.0	0.0	0.0
2	0.0	0.0	1.937500000 01	1.317500000-02	0.0	0.0	0.0
3	0.0	0.0	0.0	1.000000000 00	0.0	0.0	0.0
4	-4.380C0C00-01	-1.082000000 00	-2.613120000 01	-1.547400000 00	4.380000000-01	1.082000000 00	1.131200000 00
5	0.0	0.0	0.0	0.0	-1.870000000 01	1.000000000 00	0.0
6	0.0	0.0	0.0	0.0	-1.754000000 02	0.0	1.937500000 01
7	0.0	0.0	0.0	0.0	-1.390000000 01	0.0	0.0
8	0.0	0.0	0.0	0.0	3.050000000 01	0.0	-2.500000000 01

ROW	COL. 8	COL.
1	0.0	
2	0.0	
3	0.0	
4	1.530400000 00	
5	0.0	
6	1.317500000-02	
7	1.000000000 00	
8	-1.700000000-02	

THE STATE WEIGHT...

ROW	COL. 1	COL. 2	COL. 3	COL. 4	COL. 5	COL. 6	COL. 7
1	1.200000000 04	0.0	0.0	0.0	0.0	0.0	0.0
2	0.0	5.000000000 00	0.0	0.0	0.0	0.0	0.0
3	0.0	0.0	6.500000000 05	0.0	0.0	0.0	0.0
4	0.0	0.0	0.0	6.500000000 03	0.0	0.0	0.0
5	0.0	0.0	0.0	0.0	0.0	0.0	0.0
6	0.0	0.0	0.0	0.0	0.0	0.0	0.0
7	0.0	0.0	0.0	0.0	0.0	0.0	0.0
8	0.0	0.0	0.0	0.0	0.0	0.0	0.0

ROW	COL. 8	COL.
1	0.0	
2	0.0	
3	0.0	
4	0.0	
5	0.0	
6	0.0	
7	0.0	
8	0.0	

FIG. IV-1 DYNAMIC AND WEIGHTING MATRICES FOR THE REDUCED STANFORD RELATIVITY SATELLITE

In Designs 1 and 2, the estimator is a Kalman filter and the SRP seeks a balance between the nominally optimal estimator parameters and those required for minimum sensitivity. In Design 3 it is assumed that there is no measurement noise. The minimum nominal PI is obtained for $K \to \infty$, since for this gain, the estimate error covariance $P \to 0$ and the system behaves as if state feedback instead of state estimate feedback were used. The estimator gains are therefore determined by sensitivity considerations only. Similarly, in Design 4, where no process noise is assumed, the minimum nominal PI is obtained for $K = 0$. Here, too, the estimator gains are determined by sensitivity considerations only.

(2) Results. The values of the estimator parameters for the different designs are given in Table IV-1. These include the estimator gains and the value of the spring constant

Table IV-1

ESTIMATOR PARAMETERS OF THE
REDUCED STANFORD RELATIVITY SATELLITE (SRS) DESIGNS

	Nominal	Design No. 1	Design No. 2	Design No. 3	Design No. 4
k_1	18.7	4.46	31.1	26.3	45.6
k_2	175.4	166.2	162.9	163.7	179.5
k_3	13.9	19.8	107.8	108.7	134.6
k_4	-30.5	-111.6	-50.5	-49.6	-34.4
Assumed Value of $k(\omega_0^2)$	25.0	26.4	22.3	22.4	31.6

used in the estimator $(\hat{k})$. The nominal performance criteria are given in Table IV-2. These are the average, output and control rms values that result from the process and measurement noises given in Chapter III-C.

The eigenvalues are shown in Table IV-3 and in Fig. IV-2. The sensitivity root loci for the sensitive eigenvalue are given in Fig. IV-3. The frequency margin for the nominal design (from Fig. III-7) and for Design 2 are shown in Fig. IV-4. The sensitivity properties are compared in Table IV-3.

Table IV-2

NOMINAL PERFORMANCE CRITERIA OF THE REDUCED SRS DESIGNS
(scaled to initial value)

	Nominal	Design No. 1	Design No. 2	Design No. 3	Design No. 4
Nominal PI (J_o/J_{oi})	1.0	1.18	1.59	1.57	1.32
Weighted rms $(\sqrt{J_o/J_{oi}})$	1.0	1.09	1.26	1.25	1.15
Output rms* $(\sigma_\theta/\sigma_{\theta i})$	1.0	1.14	1.72	1.70	1.74
Control rms* (σ_u/σ_{ul})	1.0	1.12	1.11	1.15	1.11

* Note: The output and control rms values for all the designs were found using the same process and measurement noises (given in Sec. III-D-2)

Table IV-3

EIGENVALUES OF THE REDUCED SRS DESIGNS

	Nominal	Design No. 1	Design No. 2	Design No. 3	Design No. 4
Controller	-0.36 ± 5.01j	-0.38 ± 4.98j	-0.38 ± 5.05j	-0.38 ± 5.05j	-0.32 ± 4.9j
	-0.41 ± 0.41j	-0.41 ± 0.41j	-0.41 ± 0.41j	-0.41 ± 0.41j	-0.41 ± 0.4j
Estimator	-1.02 ± 5.11j	-1.41 ± 3.17j	-1.16 ± 9.19j	-1.21 ± 9.95j	-0.7 ± 10.3j
	-8.33 ± 8.35j	-0.8 ± 13.2j	-27.6	-22.6	-43.2
			-1.14	-1.21	-1.08

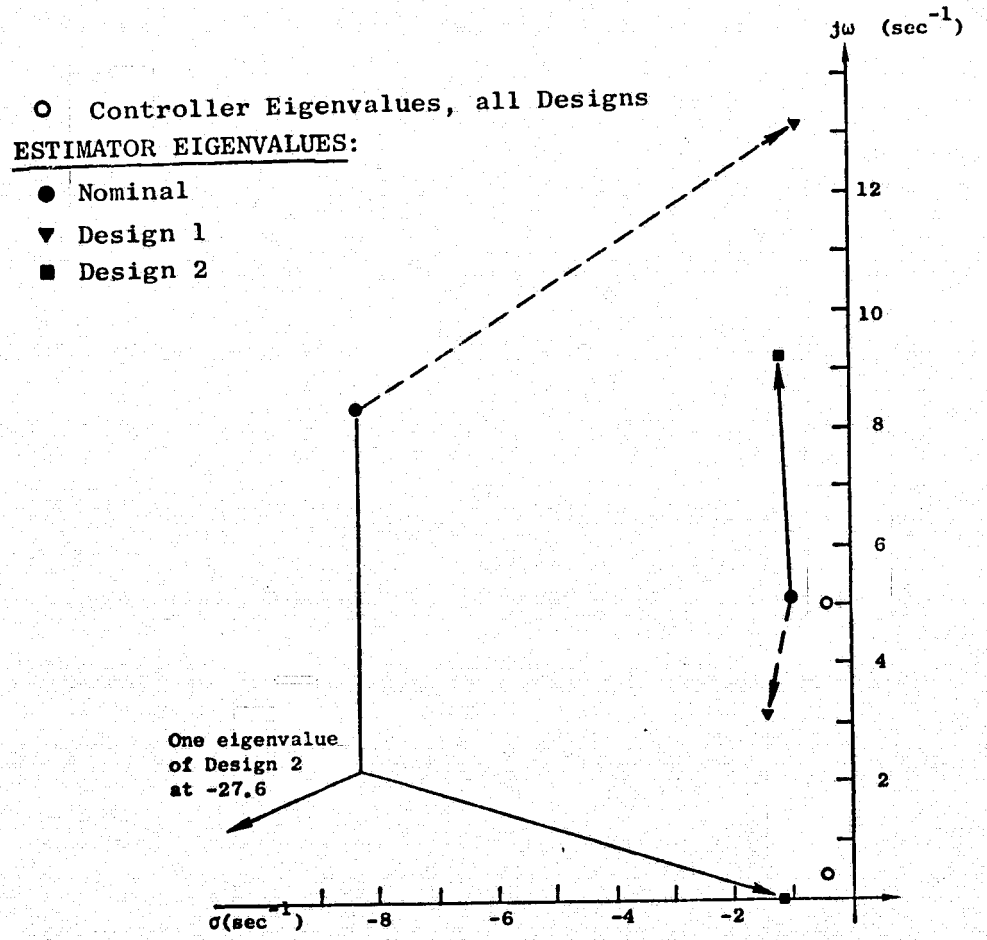

FIG. IV-2 EIGENVALUES OF NOMINAL AND DESENSITIZED DESIGN OF REDUCED STANFORD RELATIVITY SATELLITE.

Note:

1. All roots except root at $-0.36 \pm 5j$ have adjacent zeros and are therefore relatively immobile.

2. Designs 3 and 4 are not shown since they are close to Design 2.

——·—— Nominal

——————— Design 1

— — — — Design 2

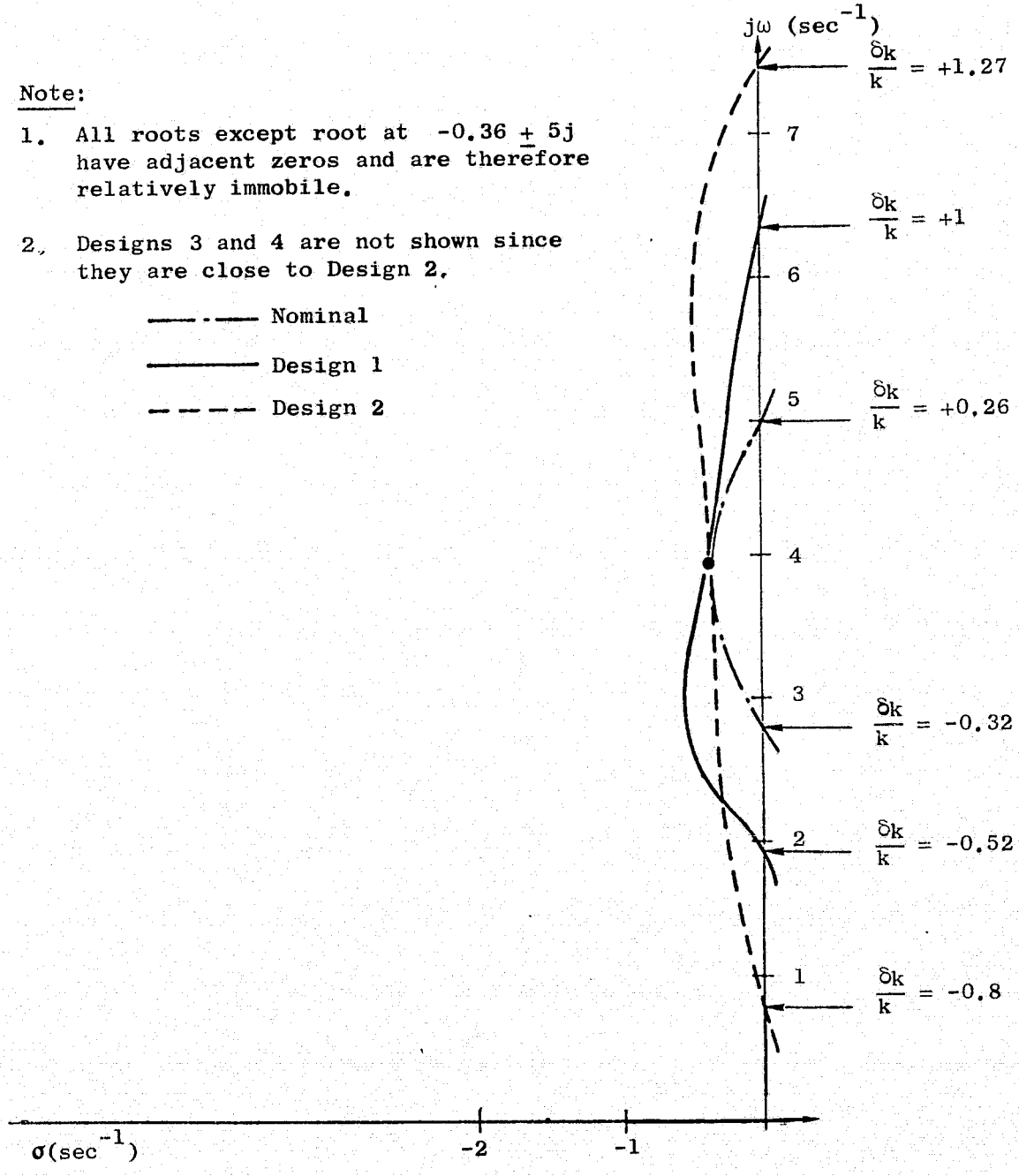

FIG. IV-3 SENSITIVITY ROOT LOCI OF REDUCED RELATIVITY SATELLITE. COMPARISON OF NOMINAL AND DE-SENSITIZED DESIGNS.

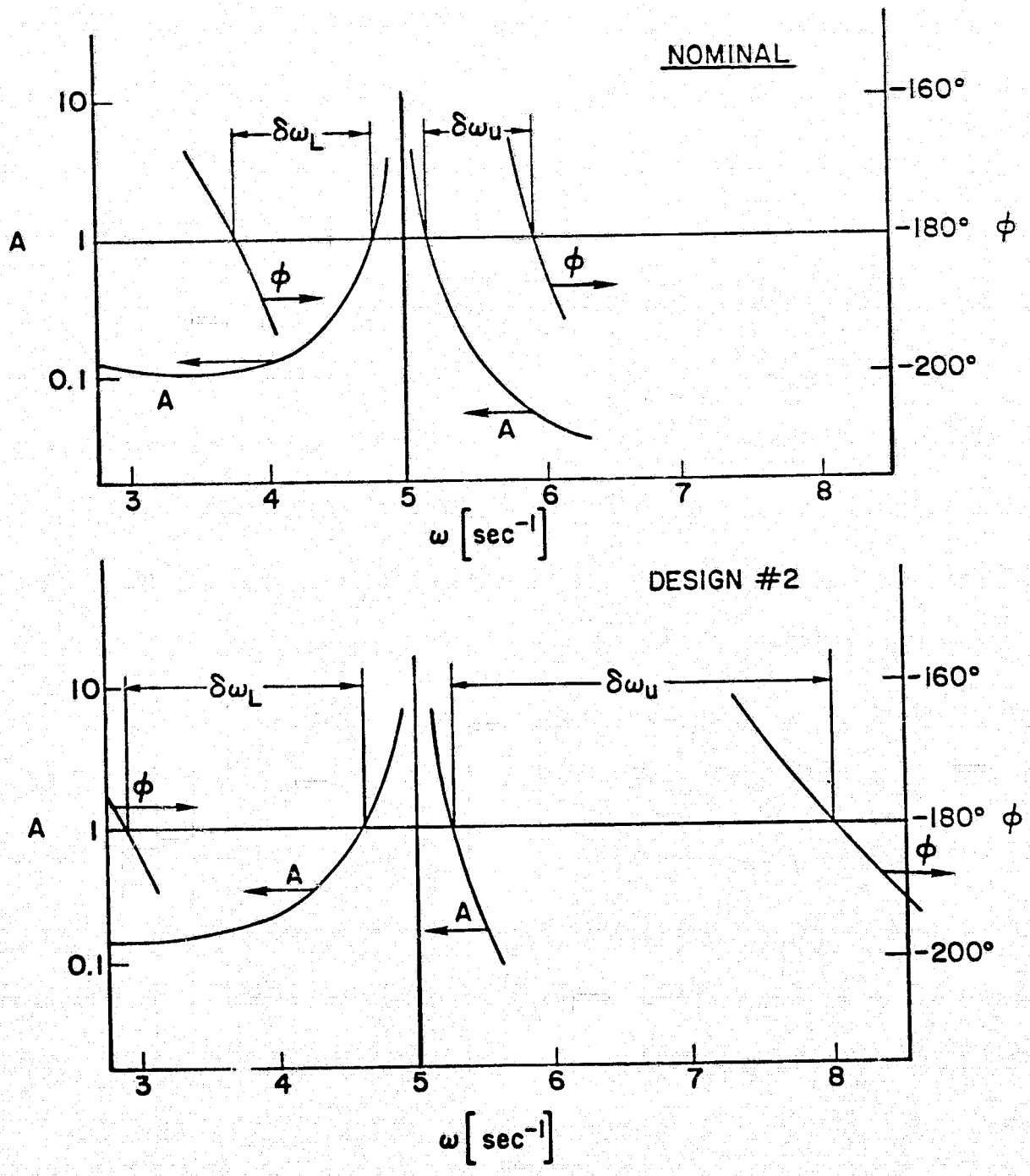

FIG. IV-4 FREQUENCY MARGIN COMPARISON OF NOMINAL AND DESENSITIZED DESIGNS.

Table IV-4

SENSITIVITY PROPERTIES--STABILITY RANGE OF THE REDUCED SRS DESIGNS

		Nominal	Design No. 1	Design No. 2	Design No. 3	Design No. 4
Range of Stability	$+\Delta k/k$	+0.26	+1.0	+1.27	+1.6	+1.92
	$-\Delta k/k$	-0.27	-0.52	-0.8	-0.84	-0.8
	Total $\Delta k/k$	0.53	1.53	1.52	2.07	2.44

(3) Evaluation of the results. (i) As expected, increasing ϵ decreases the sensitivity and increases the output and control noise. In Design 1, the stability range is increased by a factor of approximately 2.5 with an output rms increase of 14% only. If the stability range is increased by a factor of $\approx$ 3.5 (Design 2), the output noise increases by 72%. This design, therefore, constitutes a considerable departure from the nominal optimum. Due to the somewhat artificial nature of the nominal optimum (see IV-C-1), this difference cannot be considered as very significant. A better balance between the increase in output and control noise can probably be achieved by trial and error. It is important to note that the difference in stability range between Designs 1 and 2 does not fully account for the improvement of Design 2 over 1. In Fig. IV-3, it can be seen that in Design 2, the root locus does not approach the imaginary axis appreciably for a range of variations of k that is close to the stability range. Therefore, the practically acceptable range of variations (e.g., $|\text{Re}\,\lambda| > 0.2$) is much larger for this Design than it is for Design 1.

(ii) The lowered sensitivity of Design 2 can also be observed from its frequency margin (Fig. IV-4) which is much larger than that of the nominal system.

(iii) The estimator eigenvalues of Designs 3 and 4, particularly 3, are close to those of Design 2. This indicates that the estimator gains for Design 2 are determined largely by sensitivity considerations.

(iv) The two extreme cases represented by Designs 3 and 4 indicate that for this system the estimator gains may be determined by sensitivity considerations solely, and still give adequate nominal performance.

(v) Even for this simple system, it would have been difficult to determine the minimum sensitivity eigenvalue locations without some general method such as the one that was used. The removal of the eigenvalue at $-1.02 \pm 5.11j$ from the vicinity of the plant eigenvalue at $-0.36 + 5.01j$ looks plausible; but the movement of the eigenvalue at $-8.33 \pm 8.35j$ is difficult to justify intuitively.

C-3 Example 2: Full Stanford Relativity Satellite (SRS)

(1) Program parameters. The augmented system is a 12th order system with two variable parameters--the stiffnesses of the two springs. The variations of these stiffnesses are unrelated and therefore the parameter covariance matrix has only diagonal elements. The design parameters that have to be determined are ϵ, v_{11} and v_{22}.

Different values of these parameters are used for the different designs (Table IV-5). The feedback gains, estimator gains, and assumed values of the spring constants are used as free parameters in all cases (a total of 20 free parameters).

DYNAMICS MATRIX...

COL. 1	COL. 2	COL. 3	COL. 4	COL. 5	COL. 6	COL. 7
0.0	1.000000000 00	0.0	0.0	0.0	0.0	0.0
-4.597750000 03	-1.582150000 02	1.228999710 02	-3.154500000 01	-5.713000000 02	5.003250000 02	4.597750000 03
0.0	0.0	0.0	1.000000000 00	0.0	0.0	0.0
4.842999730 03	1.666543860 02	-1.294556090 02	3.322764970 01	6.210038550 02	-5.270129610 02	-4.842999730 03
0.0	0.0	0.0	0.0	0.0	1.000000000 00	0.0
-2.456132030 02	-9.537122380 00	6.097559450 00	-2.801557940 00	-5.657097160 01	2.519213290 01	2.456132030 02
0.0	0.0	0.0	0.0	0.0	0.0	-2.300000000 01
0.0	0.0	-1.054738910 02	0.0	0.0	0.0	-2.977000000 02
0.0	0.0	0.0	0.0	0.0	0.0	1.030000000 01
0.0	0.0	1.111000000 02	0.0	-6.153599740-01	0.0	2.054000000 02
0.0	0.0	0.0	0.0	0.0	0.0	-4.800000000 00
0.0	0.0	-5.626103900 00	0.0	8.000000000-01	0.0	4.153000000 01

COL. 8	COL. 9	COL. 10	COL. 11	COL. 12	COL.
0.0	0.0	0.0	0.0	0.0	
1.582150000 02	4.704500000 02	3.154500000 01	5.713000000 02	-5.003250000 02	
0.0	0.0	0.0	0.0	0.0	
-1.666543860 02	-4.555443910 02	-3.322764970 01	-6.017738560 02	5.270129610 02	
0.0	0.0	0.0	0.0	0.0	
9.537122380 00	2.555243940 01	2.801557940 00	3.157097160 01	-2.519213290 01	
1.000000000 00	0.0	0.0	0.0	0.0	
0.0	6.988238620 02	0.0	0.0	0.0	
0.0	0.0	1.000000000 00	0.0	0.0	
0.0	-7.361000000 02	0.0	1.984535920 01	0.0	
0.0	0.0	0.0	0.0	1.000000000 00	
0.0	3.727610270 01	0.0	-2.580000000 01	0.0	

STATE WEIGHT...

COL. 1	COL. 2	COL. 3	COL. 4	COL. 5	COL. 6	COL. 7
4.500000000 05	0.0	0.0	0.0	0.0	0.0	0.0
0.0	8.000000000 00	0.0	0.0	0.0	0.0	0.0
0.0	0.0	6.400000000 03	0.0	0.0	0.0	0.0
0.0	0.0	0.0	2.600000000 00	0.0	0.0	0.0
0.0	0.0	0.0	0.0	6.400000000 05	0.0	0.0
0.0	0.0	0.0	0.0	0.0	6.400000000 03	0.0
0.0	0.0	0.0	0.0	0.0	0.0	0.0
0.0	0.0	0.0	0.0	0.0	0.0	0.0
0.0	0.0	0.0	0.0	0.0	0.0	0.0
0.0	0.0	0.0	0.0	0.0	0.0	0.0
0.0	0.0	0.0	0.0	0.0	0.0	0.0
0.0	0.0	0.0	0.0	0.0	0.0	0.0

COL. 8	COL. 9	COL. 10	COL. 11	COL. 12	COL.
0.0	0.0	0.0	0.0	0.0	
0.0	0.0	0.0	0.0	0.0	
0.0	0.0	0.0	0.0	0.0	
0.0	0.0	0.0	0.0	0.0	
0.0	0.0	0.0	0.0	0.0	
0.0	0.0	0.0	0.0	0.0	
0.0	0.0	0.0	0.0	0.0	
0.0	0.0	0.0	0.0	0.0	
0.0	0.0	0.0	0.0	0.0	
0.0	0.0	0.0	0.0	0.0	
0.0	0.0	0.0	0.0	0.0	
0.0	0.0	0.0	0.0	0.0	

FIG. IV-5 DYNAMIC AND WEIGHTING MATRICES OF THE STANFORD RELATIVITY SATELLITE

The initial dynamic and weighting matrices were shown in Fig. IV-5.

Three controllers were designed. They are described in Table IV-5.

Table IV-5

DESIGNS FOR THE STANFORD RELATIVITY SATELLITE

Design No. 1	$\sigma_{k_\gamma}/k_\gamma$	$\sigma_{k_\alpha}/k_\alpha$
1	0.55	0.18
2	2.5	0.81
3	5.0	0.81

The motivation for these various designs is evident from the Table. As explained earlier, the parameter rms values are used as a design tool only for achieving the required sensitivity.

(2) Results. The final values of the free parameters for the different designs are given in Table IV-6. The eigenvalues are shown in Table IV-7. The nominal performance criteria are compared in Table IV-8. The process and measurement noises used for the determination of these criteria are those used in Bull [BU-1].

The sensitivity properties are compared in Table IV-9.

Table IV-6

FREE PARAMETERS (in MKS units) OF THE FULL SRS DESIGNS

			Nominal	Design No.1	Design No. 2	Design No. 3
FEEDBACK GAINS	INNER CONTROLLER	c_{11}	18391.0	same as Nominal Column	18391.0	18391.0
		c_{12}	632.8		631.1	631.2
		c_{13}	1881.8		1880.7	1880.5
		c_{14}	126.1		127.6	127.8
		c_{15}	2285.2		2285.4	2285.5
		c_{16}	-2001.3		-2001.6	-2001.5
	OUTER CONTROLLER	c_{21}	101.4		99.7	99.7
		c_{22}	274.8		254.9	256.1
		c_{23}	115.6		70.9	73.1
		c_{24}	279.8		310.5	310.8
		c_{25}	275.6		278.1	277.9
		c_{26}	372.8		372.9	371.3
ESTIMATOR GAINS		k_1	24.1	23.0	24.2	43.2
		k_2	292.0	297.7	287.2	283.4
		k_3	-2.2	-10.3	-10.9	-19.1
		k_4	-124.0	-205.4	-219.0	-224.0
		k_5	14.9	4.8	-3.6	-10.9
		k_6	-26.0	-41.5	-41.5	-53.6
Plant Parameter Representation In Estimator		$\hat{\omega}_1^2$	625.0	736.0	737.0	736.0
		$\hat{\omega}_2^2$	25.0	25.8	33.2	27.7

Table IV-7

EIGENVALUES OF THE FULL STANFORD RELATIVITY SATELLITE DESIGNS

NOMINAL

REAL	IMAG.
-49.07045521	48.32029403
-49.07045521	-48.32029403
-0.39369490	4.98784394
-0.39369490	-4.98784394
-0.38514360	0.47217532
-0.38514360	-0.47217532
-2.42507047	25.58344618
-2.42507047	-25.58344618
-8.62282277	7.12131077
-8.62282277	-7.12131077
-1.05210676	5.11812296
-1.05210676	-5.11812296

DESIGN 1

REAL	IMAG.
-48.61518571	49.93853088
-48.61518571	-49.93853088
-4.09983984	24.00645133
-4.09983984	-24.00645133
-6.81374959	7.84625316
-6.81374959	-7.84625316
-0.34369446	4.99512259
-0.34369446	-4.99512259
-1.17993306	4.15878479
-1.17993306	-4.15878479
-0.34520706	0.40484027
-0.34520706	-0.40484027

DESIGN 2

REAL	IMAG.
-48.10299920	49.32370542
-48.10299920	-49.32370542
-3.79056988	24.25442200
-3.79056988	-24.25442200
-7.24410743	4.30428075
-7.24410743	-4.30428075
-0.45084515	4.86150763
-0.45084515	-4.86150763
-1.61314669	3.48569047
-1.61314669	-3.48569047
-0.38407223	0.17419996
-0.38407223	-0.17419996

DESIGN 3

REAL	IMAG.
-48.21998588	49.99571976
-48.21998588	-49.99571976
-35.80701057	0.0
-2.54864010	21.88676425
-2.54864010	-21.88676425
-0.41573592	5.03969535
-0.41573592	-5.03969535
-0.80529697	3.78422822
-0.80529697	-3.78422822
-0.38388131	0.18814120
-0.38388131	-0.18814120
-1.61099022	0.0

Table IV-8

NOMINAL PERFORMANCE CRITERIA OF THE FULL SRS DESIGNS
(scaled to initial value)

	Nominal	Design No. 1	Design No. 2	Design No. 3
Nominal PI $[J_o/J_{oi}]$	1.0	1.02	1.15	1.22
Weighted rms $[\sqrt{J_o/J_{oi}}]$	1.0	1.01	1.07	1.1
Output rms $[\sigma_\theta/\sigma_{\theta i}]$	1.0	1.27	1.88	2.4
Inner Control rms $[\sigma_{u1}/\sigma_{u1i}]$	1.0	1.28	1.49	1.44
Outer Control rms $[\sigma_{u2}/\sigma_{u2i}]$	1.0	0.99	1.02	1.02

Table IV-9

SENSITIVITY PROPERTIES OF THE FULL SRS DESIGNS

			Nominal	Design No. 1	Design No. 2	Design No. 3
RANGE OF STABILITY	STIFF SPRING	$+\Delta k_\gamma/k_\gamma$	+0.71	+0.97	+1.3	+3.1
		$-\Delta k_\gamma/k_\gamma$	-0.12	-0.22	-0.24	-0.23
		Total $\Delta k_\gamma/k_\gamma$	0.83	1.19	1.53	3.31
	SOFT SPRING	$+\Delta k_\alpha/k_\alpha$	+0.32	+0.8	+1.4	+1.2
		$-\Delta k_\alpha/k_\alpha$	-0.32	-0.4	-0.44	-0.38
		Total $\Delta k_\alpha/k_\alpha$	0.64	1.2	1.84	1.58
$J_A/J_{A_{nom}}$			1.0	0.76	0.7	0.65

(3) Evaluation of the results. (i) The increase in the output and control rms for this example is much larger than it was for the Example 1 (compare Tables IV-2 and IV-8). This increase, however, is not reflected in the nominal PI (Table IV-8). This PI is a weighted average of the state and control rms values in which other states, beside the output, are weighted. If the rms of some of these states is reduced by the SRP, this reduction can balance the increase in the output rms. A better balance between sensitivity and nominal performance can probably be obtained if only the output and the controls are weighted in the PI.

(ii) The range of stability is not symmetrical about the nominal value especially for the stiff springs. All the designs are more sensitive to the decrease of the spring constant of this spring than to its increase. In Table IV-6 it can be seen that the assumed value of this constant in the estimator is higher than the nominal. It seems, however, that for a more symmetric range, it should be lower. The stability range of a modified design, Design 3A, was therefore found. This design has the estimator gains of Design 3 but the assumed value of the stiff spring constant in the estimator is

$$\omega_1^2 = 500 \text{ sec}^{-2}.$$

(The nominal value is $\omega_1^2 = 625 \text{ sec}^{-2}$). The performance of Design 3A is shown in Table IV-10. Comparing this Design with Design 3, it can be seen that although its total stability range is lower, it still may be preferable since it is more symmetric. There is no obvious way to introduce such considerations into the program but they may lead to modifications of the program results by the designer. The nominal performance criteria are comparable for the two Designs.

Table IV-10

PERFORMANCE OF DESIGN No. 3A

	($\hat{\omega}_1$ = 500 sec^{-1})	
Range of Stability For Stiff Spring	$+\Delta k_\gamma / k_\gamma$	+1.4
	$-\Delta k_\gamma / k_\gamma$	-0.48
	Total $\Delta k_\gamma / k_\gamma$	1.88
Output rms $[\sigma_\theta / \sigma_{\theta i}]$		2.4
Inner Control rms $[\sigma_{u1} / \sigma_{u1i}]$		1.04
Outer Control rms $[\sigma_{u2} / \sigma_{u2i}]$		1.22

(iii) From Table IV-6, it can be seen that the feedback gains are changed very little by the SRP. The principal changes are in the estimator gains. It probably would have been possible to obtain a similar sensitivity reduction by using only the estimator parameters as free parameters. The same effect was also observed in Example 1.

C-4 Conclusions

(a) The method described in this section can provide a considerable reduction in the system sensitivity to parameter variations. If the initial system is optimal, the output and control rms values will increase due to the sensitivity reduction. However, the nature of the optimality of the nominal system has to be considered carefully since it depends on the assumed values of the process and measurement noise intensities. In the examples that were examined, the

sensitivities were reduced by a factor of 2 to 3, while the output rms increased approximately by a factor of 2.

(b) Both examples given in this section use state estimate feedback controllers. In this case the free parameters are the feedback gains and the estimator parameters. The method, however, is by no means limited to such controllers. It is equally applicable to systems with classical compensation networks or other designs that can be represented in state variable form

(c) The computation time for a 12th order system with 20 variable parameters was four minutes on an IBM 360/67 computer. This computation time is almost insensitive to the number of free parameters. It is therefore recommended to define all the parameters that are at the designer's disposition as free parameters, at least for preliminary runs. If some parameters do not vary in those runs, they may be fixed for subsequent runs.

(d) In applying this method, it is recommended to initially select the parameter covariance matrix so that the additional $PI(J_A)$ is much larger than the nominal $PI(J_o)$. A design that is mainly determined by sensitivity considerations results. If the nominal properties of this design are unsatisfactory, other designs with lower sensitivity weightings may be executed.

The comparison between these designs is made conveniently by means of the stability range and the output and control rms values. If the system has specific performance requirements such as time response envelope or gain and phase margin, these can also be used as comparison criteria.

The most satisfactory design, in general, is a matter of subjective designer preference.

V. DESIGN OF A CONTROLLER FOR A TRACKING TELESCOPE

A. INTRODUCTION

In this Chapter, the design of a controller for a tracking telescope is described. It was selected to represent a commonly encountered design problem and is a good example for the use of the design methods of Chapter II. The data and the requirements were obtained from various sources, mainly by private communication, and typify actual systems although they do not necessarily represent a specific one.

Various aspects of the problem of precision pointing and tracking have been treated in the literature and several system designs have been described [CA-1, FI-1, JO-1, WH-1]. The detailed design of a controller for such a system has to consider many specific aspects of the system such as structural details, actuator and sensor characteristics, disturbance inputs, etc. If these aspects are not considered, the system performance will be degraded, especially for a mobile system which operates in a severe and/or changing environment. The design problem is therefore involved and is, in great part, of computational and experimental nature.

Since the principal purpose of this chapter is to demonstrate the application of the design methods of Chapter II, a detailed design for a changing environment is beyond its scope. Even for a simplified ground-based system, structural considerations must be neglected. The actuator and sensor characteristics are, however, taken into account and a plausible disturbance input is assumed. The design of the controller for this simplified but non-trivial system is less involved but the design methods can easily be extended to more complicated tracking problems. The simplified plant is described in Section V-B. The controller specifications are defined in Section V-C, and the controller design is described in Section V-D. The performance of the controller is examined in Section V-E.

B. PLANT REPRESENTATION

B-1 Description

The plant is a ground based telescope, the purpose of which is to track a moving object (target) in the sky. For angular freedom of motion, the telescope is mounted in a three-gimbal structure: inner azimuth, elevation, and outer azimuth. It has unlimited angular freedom in azimuth and -6° to +25° freedom in elevation. A schematic view of the telescope is shown in Fig. V-1.

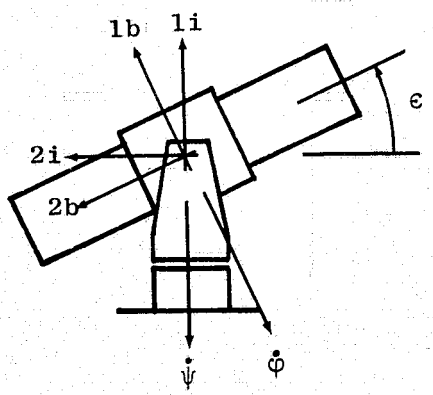

φ inner azimuth gimbal angle (limited to 3°)

ε elevation gimbal angle (limited to -6° to 25°)

ψ outer azimuth gimbal angle

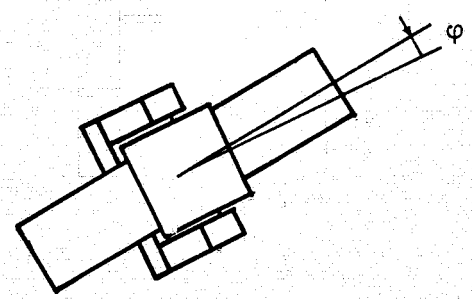

FIG. V-1 TRACKING TELESCOPE ANGLES

Torquers are mounted on all three gimbals. The inner azimuth and the elevation axes have hydraulic torquers. The outer azimuth axis has an electric torquer. The transfer functions from torque command to torque output for the hydraulic torquers are derived in Appendix C. The transfer function of the electric torquer is a pure gain. Since the torquers are subject to saturation acceleration, limiting networks are mounted at their inputs.

The purpose of the two azimuth gimbals is to enable the inner azimuth torquer to operate on a lower inertia and thereby to provide the higher accelerations required for high bandwidth tracking. The outer azimuth gimbal then provides mainly the slewing capability. The relative angular freedom of the inner azimuth gimbal is $\pm$ 3°.

The following measurements are available: (i) the components in azimuth and elevation of the error angle between the target line of sight and the optical axis of the telescope are measured by detectors mounted in parallel to the telescope axis. These measurements are sampled at a rate of 120 meas/sec and are held in a zero order hold. (ii) The integrals of the angular rates about the inner azimuth and elevation axes are measured by rate integrating gyros with their input axes along these directions. (iii) The relative gimbal angles are measured by resolvers. Numerical data for the system are given in Appendix D.

B-2 State Representation

The dynamic equations are derived in Appendix F. Defining $\dot{\alpha} = \dot{\varphi} + \dot{\psi} \cos \epsilon$ (the component of the total angular rate about the 1b axis)

$$M_{\alpha} = I_1 \ddot{\alpha} \tag{5.1a}$$

$$M_{\epsilon} = I_3 \ddot{\epsilon} + I_1 \dot{\psi} \dot{\alpha} \sin \epsilon + (I_3 - I_1 - I_2) \dot{\psi}^2 \sin \epsilon \cos \epsilon \tag{5.1b}$$

$$M_{\psi} = [I_2 \sin^2 \epsilon + (I_3 - I_1) \cos^2 \epsilon + I_4] \ddot{\psi} + I_1 \ddot{\alpha} \cos \epsilon + 2(I_1 + I_2 - I_3) \dot{\psi} \dot{\epsilon} \sin \epsilon \cos \epsilon - I_1 \dot{\alpha} \dot{\epsilon} \cos \epsilon \tag{5.1c}$$

where M_α, M_ϵ, and M_ψ are the external torques acting about the inner azimuth, elevation, and outer azimuth axes. These torques consist of the torquer outputs and disturbance torques. The moments of inertia are defined in Appendix D.

To linearize Eq. (5.1), the following assumptions are made:
(a) The elevation angle remains small so that $\sin \epsilon \approx \epsilon$, $\cos \epsilon \approx 1$.
(b) The terms that consist of products of two angular rates and $\sin \epsilon$ may be neglected. This is equivalent to assuming small deflections of the gimbals from their required orientations.

The coefficient of $\ddot{\psi}$ in Eq. (5.1c) can be written as

$$\begin{aligned} & I_2 \sin^2 \epsilon + (I_3 - I_1) \cos^2 \epsilon + I_4 \\ = \; & I_3 - I_1 + I_4 + (I_2 - I_3 + I_1)\sin^2 \epsilon \\ = \; & I_0 + \Delta I \sin^2 \epsilon \; = \; 2750 + 160 \sin^2 \epsilon \end{aligned}$$

(from the data of App. E).

The linearized equations are

$$M_\alpha = I_1 \ddot{\alpha} \tag{5.2a}$$

$$M_\epsilon = I_3 \ddot{\epsilon} \tag{5.2b}$$

$$M_\psi = I_0 \ddot{\psi} + M_\alpha \, . \tag{5.2c}$$

To put these equations in state form, the torquer equation for the inner azimuth and elevation gimbals as derived in Appendix C, have to be added. Considering Eqs. (C-8) and (C-9) of Appendix C, it can be seen that the linearized elevation equation (5.2b) is decoupled from the azimuth equations. The elevation control, therefore, can be treated separately from the azimuth control. Using Eqs. (5.2a) and (5.2c) and Eq. (C-8) of Appendix C, the azimuth state equations can be written as

$$\begin{bmatrix} \dot{\alpha} \\ \dot{\omega} \\ \dot{a} \\ \dot{q} \\ \hline \dot{\psi} \\ \dot{p} \end{bmatrix} = \left[\begin{array}{cccc|cc} 0 & 1 & 0 & 0 & 0 & 0 \\ 0 & 0 & 1 & 0 & 0 & 0 \\ 0 & -b_3 & -b_1 & b_2 & b_3 & 0 \\ 0 & 0 & b_4 & -b_5 & 0 & 0 \\ \hline 0 & 0 & 0 & 0 & 0 & 1 \\ 0 & 0 & \frac{I_1}{I_o} & 0 & 0 & 0 \end{array}\right] \begin{bmatrix} \alpha \\ \omega \\ a \\ q \\ \hline \psi \\ p \end{bmatrix} + \left[\begin{array}{cc} 0 & 0 \\ 0 & 0 \\ 0 & 0 \\ b_4 & 0 \\ \hline 0 & 0 \\ 0 & 1 \end{array}\right] \begin{bmatrix} u_1 \\ u_2 \end{bmatrix} + \begin{bmatrix} 0 \\ w_1 \\ 0 \\ b_4 w_2 \\ \hline 0 \\ w_3 \end{bmatrix} \qquad (5.3)$$

where (see App. D)

$$b_1 = \frac{B}{v_e} k_2$$

$$b_2 = \frac{B}{v_e} \frac{D_A}{I}$$

$$b_3 = \frac{D_A^2}{I}$$

$$b_4 = \frac{k_A I}{D_A}$$

$$b_5 = \frac{1}{\tau_v}$$

and w_1, w_2 and w_3 are disturbance torques and actuator noises.

In this linearized system, α is the total azimuth angle of the inner gimbal, measured from some reference direction. To add the output equation, (5.3) has to be augmented. The azimuth error detector measures the angle $\alpha - \alpha_c$, after it is sampled and held in a zero order hold. Such a sample-and-hold operation introduces phase lag, and if it is not taken into consideration in the design, a system with insufficient phase margin may result. A linearization of the sampler and hold is done in Appendix G. The linearized sampler and hold is represented by an additional state equation

$$\dot{\beta} = -4f_o\beta - 7.2f_o(\alpha - \alpha_c) \qquad (5.4)$$

where f_o is the sampling rate (120 samples per second).

The measurement is given by

$$y = \beta + 0.9(\alpha - \alpha_c) \ . \qquad (5.5)$$

The effect of using the linearized rather than the exact representation of the sampler is checked by simulation. Replacing the state q by $r = \dot{a}$ in order to get fewer parameters in the state equation, the final state equation (without disturbances) is obtained as

$$\begin{bmatrix} \dot{\beta} \\ \dot{\alpha} \\ \dot{\omega} \\ \dot{a} \\ \dot{r} \\ \hline \dot{\psi} \\ \dot{p} \end{bmatrix} = \left[\begin{array}{ccccc:cc} -4f_o & -7.2f_o & 0 & 0 & 0 & 0 & 0 \\ 0 & 0 & 1 & 0 & 0 & 0 & 0 \\ 0 & 0 & 0 & 1 & 0 & 0 & 0 \\ 0 & 0 & -b_3 & 0 & 1 & b_3 & 0 \\ 0 & 0 & 0 & -m_2 & -m_1 & 0 & 0 \\ \hline 0 & 0 & 0 & 0 & 0 & 1 & 0 \\ 0 & 0 & 0 & \frac{I_1}{I_o} & 0 & 0 & 0 \end{array}\right] \begin{bmatrix} \beta \\ \alpha \\ \omega \\ a \\ r \\ \hline \psi \\ p \end{bmatrix} + \left[\begin{array}{cc} 0 & 0 \\ 0 & 0 \\ 0 & 0 \\ 0 & 0 \\ m_2 & 0 \\ \hline 0 & 0 \\ 0 & 1 \end{array}\right] \begin{bmatrix} u_1 \\ \\ u_2 \end{bmatrix} + \left[\begin{array}{c} 7.2f_o \\ 0 \\ 0 \\ 0 \\ 0 \\ \hline 0 \\ 0 \end{array}\right] \alpha_c \qquad (5.6)$$

$$y = \begin{bmatrix} 1 & .9 & 0 & 0 & 0 & 0 & 0 \\ 0 & 1 & 0 & 0 & 0 & 0 & 0 \\ 0 & 1 & 0 & 0 & 0 & -1 & 0 \\ 0 & 0 & 0 & 0 & 0 & 0 & 1 \end{bmatrix} x - \begin{bmatrix} .9 \\ 0 \\ 0 \\ 0 \end{bmatrix} \alpha_c$$

where

m_1 = $2\zeta\omega_o$, where ω_o is the natural frequency of the hydraulic torquer, and ζ its damping coefficient.

m_2 = ω_o^2

y_1 = the target error detector

y_2 = the rate integrating gyro on the inner azimuth axis

y_3 = the outer azimuth axis resolver

y_4 = the outer azimuth axis rate gyro .

Substituting the numerical values of the entries in the F matrix (from App. C), the open loop eigenvalues (in rad/sec) of the system are found to be

$$\lambda_{1,2} = -80 \pm 615j \qquad \text{(torquer)}$$

$$\lambda_3 = -480 \qquad \text{(sampler-hold)}$$

$$\lambda_4 = -0.024$$

$$\lambda_{5,6,7} = 0 \quad .$$

The parameter b_3 in Eq. 5.6 represents the effect of the outer gimbal motion on the inner torquer output. If this term is neglected, $\lambda_4 = 0$ results. Relative to the other system eigenvalues, the change in λ_4 is small and the term b_3 therefore can be neglected. This eliminates the coupling from the outer azimuth gimbal into the inner azimuth gimbal and decouples the azimuth system into two single input systems, the controllers for which can be designed separately.

By linearizing and neglecting small terms, the coupled system described by Eq. (5.1) has thus been decomposed into three single input subsystems. The inner azimuth and elevation subsystems are almost identical and the controller that is designed for one of them will also be suitable for the other one with small numerical changes.

The inner azimuth system is shown below.

$$\begin{bmatrix} \dot{\beta} \\ \dot{\alpha} \\ \dot{\omega} \\ \dot{a} \\ \dot{r} \end{bmatrix} = \begin{bmatrix} -4f_o & -7.2f_o & 0 & 0 & 0 \\ 0 & 0 & 1 & 0 & 0 \\ 0 & 0 & 0 & 1 & 0 \\ 0 & 0 & 0 & 0 & 1 \\ 0 & 0 & 0 & -m_2 & -m_1 \end{bmatrix} \begin{bmatrix} \beta \\ \alpha \\ \omega \\ a \\ r \end{bmatrix} + \begin{bmatrix} 0 \\ 0 \\ 0 \\ 0 \\ m_2 \end{bmatrix} u + \begin{bmatrix} 0 & 0 \\ 0 & 0 \\ 1 & 0 \\ 0 & 0 \\ 0 & m_2 \end{bmatrix} \begin{bmatrix} w_1 \\ w_2 \end{bmatrix} + \begin{bmatrix} 7.2f_o \\ 0 \\ 0 \\ 0 \\ 0 \end{bmatrix} \alpha_c \qquad (5.7)$$

$$y = \begin{bmatrix} 1 & .9 & 0 & 0 & 0 \\ 0 & 1 & 0 & 0 & 0 \end{bmatrix} x - \begin{bmatrix} .9 \\ 0 \end{bmatrix} \alpha_c + \begin{bmatrix} v_d \\ v_g \end{bmatrix} .$$

Structure of process and measurement noise intensity matrices:

$$Q = \begin{bmatrix} q_1 & 0 \\ 0 & q_2 \end{bmatrix} \qquad (5.8)$$

$$R = \begin{bmatrix} r_d & 0 \\ 0 & r_g \end{bmatrix}$$

Numerical values:

$m_1 = 160 \text{ sec}^{-1}$
$m_2 = 385{,}000 \text{ sec}^{-2}$
} from App. C

$f_0 = 120 \text{ samples/sec}$
$q_1 = 10^{-4} \text{ rad}^2/\text{sec}^3$
$q_2 = 10^{-5} \text{ rad}^2/\text{sec}^3$
$r_d = 10^{-11} \text{ rad}^2/\text{sec}$
$r_g = 2 \times 10^{-14} \text{ rad}^2/\text{sec}$.
} from App. D

Transfer functions:

$$\frac{\alpha(s)}{w_2(s)} = \frac{\alpha(s)}{u(s)} = \frac{m_2}{s^2(s^2 + m_1 s + m_2)} \qquad (5.9a)$$

$$\frac{\alpha(s)}{w_1(s)} = \frac{1}{s^2} \qquad (5.9b)$$

The controller for the outer azimuth gimbal has relatively low performance requirements and its design is straightforward.

The linearization and simplification of complex systems as shown in this section is common in the design of controllers. It should be attempted, whenever possible, since it simplifies the design of the controllers to a large extent. It is important to bear in mind, however, that as a final design step, a simulation of the full nonlinear system should be made using the designed controllers. This simulation should be as close as possible to the real system, including all the nonlinearities and neglected terms. Due to the limited scope of this Chapter such a simulation will not be performed here.

C. CONTROLLER SPECIFICATIONS

For a meaningful evaluation of the controller design, some quantitative specifications are required. These specifications should reflect performance requirements such as tracking and disturbance rejection, as well as hardware limitations such as component saturation. The performance requirements in this Section are based on typical requirements of actual tracking systems. For such systems, tracking requirements are often defined in terms of the permissible error when tracking a target moving in a straight line [FI-1]. It is also customary to require that no steady state output error occur when constant disturbances such as steady wind or unbalance torques act on the system.

The numerical values given in the specifications reflect levels of performance that are plausible with the assumed process and measurement noises, and with the given detector sampling rate. The influence of different noise level assumptions are discussed later. According to this approach, the controller specifications are formulated as follows.

(a) Tracking. The system can track a target moving with constant angular

acceleration with finite steady state error. It is desirable for this error to be less than 100 μrad, which is the value of the detector rms noise, for the entire acceleration range of the outer gimbal (0.65 rad/sec^2). This error corresponds to an acceleration error coefficient of 150 μrad/(rad/sec^2). This requirement is a simplification of the tracking requirement for a target on a straight line flyby. The connection between these two requirements is derived in Appendix E.

(b) Torquer saturation. The torquer input is less than 50% of the acceleration limit when no tracking is required (pointing at a stationary target). This specification is required in order to avoid saturation of the torquer by disturbances and measurement noise and to retain sufficient control authority for the tracking.

(c) Large signal operation. The system remains stable for large output errors up to 30 mrad. This requirement arises because the torquers are subject to saturation (V-B-1). At large error signals, such as may arise during acquisition, saturation instability therefore may occur (Section V-E).

(d) Steady disturbance rejection. No steady state pointing error occurs when steady disturbance torques are acting on the system. The maximum transient error for such a disturbance is

$$\frac{\delta\alpha}{\delta w} < 100\ \mu\text{rad}/(\text{rad}/\text{sec}^2),$$

where w may be either w_1 or w_2 (Eq. 5.7). With this numerical value, a disturbance torque of 25% of the inner azimuth torquer capacity will cause a maximum deflection that is of the order of the measurement noise.

(e) Transient response. The system has "well behaved" tracking and disturbance transient responses by common engineering criteria. The tracking bandwidth is limited by the sampling rate. A bandwidth of 25% to 50% of this rate is considered reasonable.

D. DESIGN OF A CONTROLLER FOR THE INNER AZIMUTH GIMBAL

D-1 Introduction

The design procedure for a state estimate feedback (SEF) controller (Ch. II) consists of the following steps: (a) estimator design, (b) controller design, (c) evaluation. In general, several systems are designed in the first two steps, each one having different state and control weights and, in some cases, different estimator gains. The nature of the evaluation depends on the system specifications. In general, it consists of several stages, and in each stage, some designs are eliminated. In some cases, more than one design cycle is required in order to satisfy the system requirements.

The three-step design procedure outlined above is fairly standard. The nature of each one of these steps, however, depends on the system specifications and on the special features of each specific systems. In the inner gimbal system, the following special features have to be considered: (a) although the system is SISO it has two measurements and different estimators can therefore be designed using various combinations of those measurements. The various designs are described in Section V-D-2. (b) The system has to be augmented by integral control in order to satisfy the tracking and disturbance rejection requirements (requirements a and d in Sec. V-3). The need for this augmentation is established in Section V-D-2 and the controller for the augmented system is designed in Section V-D-3. (c) The evaluation has to include the determination of stability for large input. This is done in Section E-1.

In Section D-4, the various possible designs are compared according to the linear performance criteria and two designs are selected for sensitivity comparison. This comparison is made in Section D-5 and as a result, a final system for further performance evaluation is selected. This evaluation is described in Section E-5.

D-2 Controller and Estimator Structure

Two measurements are available in the system: (a) target detector, (b) gyroscope. The gyroscope can be used in one of two modes: as a rate integrating gyro, or as a rate gyro. The dynamics of the gyroscope in its two modes are described in Appendix H.

The performance specifications call for (a) finite steady state output error for constant acceleration command; (b) zero steady state output for constant disturbances. The satisfaction of these requirements depends on the structure of the system and not on the values of its parameters. The level of the steady state acceleration error and the maximum transient deflection for constant disturbance depend on the parameters.

Several estimator designs will be discussed in this Section, and the structures of the systems incorporating them are examined. The numerical performance criteria such as output and control noise, maximum disturbance deflection, and steady state acceleration error can only be evaluated after both the controller and the estimator are designed. This evaluation is therefore deferred to Section D-4. The discussion in this Section is limited to estimators, the order of which is at most, equal to the order of the system.

(1) Estimator using the detector measurement only. Equations (2.58) and (2.67) define the order of the polynomial equilibrium control required for the tracking of polynomial reference outputs and rejection of polynomial disturbances. Using these equations on the transfer functions of Eq. (5.9) and referring to the controller specifications (V-C), the results are: (a) a constant acceleration reference output, can be tracked with constant equilibrium control. No integration of the output error is therefore required in order to obtain a constant output error for this reference output. (b) A constant disturbance requires a constant equilibrium control for zero output error. One integration of this error is therefore required. The disturbance rejection specification, therefore, determines the requirement for integral control. With this control the output error is zero for a

constant acceleration reference output. In addition to the equilibrium control, error feedback control is required. From Chapter II-D-3 the system with this reference output is completely reducible, i.e., the error state has the same dynamics as the system state. It can therefore be estimated by an estimator that uses the model of the system, the output of which is compared to the target detector output. This estimator can be used for generating the error feedback gains. For zero target motion, it obviously generates the state estimates. The state equations of this estimator are given below.

$$\begin{bmatrix} \dot{\hat{\beta}} \\ \dot{\hat{\alpha}} \\ \dot{\hat{\omega}} \\ \dot{\hat{a}} \\ \dot{\hat{r}} \end{bmatrix} = \begin{bmatrix} -4f_o-k_1 & -7.2f_o-0.9k_1 & 0 & 0 & 0 \\ -k_2 & -0.9k_2 & 1 & 0 & 0 \\ -k_3 & -0.9k_3 & 0 & 1 & 0 \\ -k_4 & -0.9k_4 & 0 & 0 & 1 \\ -k_5 & -0.9k_5 & 0 & -m_2 & -m_1 \end{bmatrix} \begin{bmatrix} \hat{\beta} \\ \hat{\alpha} \\ \hat{\omega} \\ \hat{a} \\ \hat{r} \end{bmatrix} + \begin{bmatrix} k_1 \\ k_2 \\ k_3 \\ k_4 \\ k_5 \end{bmatrix} y + \begin{bmatrix} 0 \\ 0 \\ 0 \\ 0 \\ m_2 \end{bmatrix} u_1$$

$$Q = \begin{bmatrix} q_1 & 0 \\ 0 & q_2 \end{bmatrix} \qquad \Gamma = \begin{bmatrix} 0 & 0 \\ 0 & 0 \\ 1 & 0 \\ 0 & 0 \\ 0 & m_2 \end{bmatrix}$$

$$R = r_d \quad .$$

The structure of a system using it is shown in Fig. V-2.

A controller using this estimator more than satisfies the steady state error requirements since it has zero acceleration error where only a finite error is required. Its transient disturbance response may, however, not be satisfactory. The detector noise level is relatively high (see App. D) and the estimator bandwidth is therefore low.

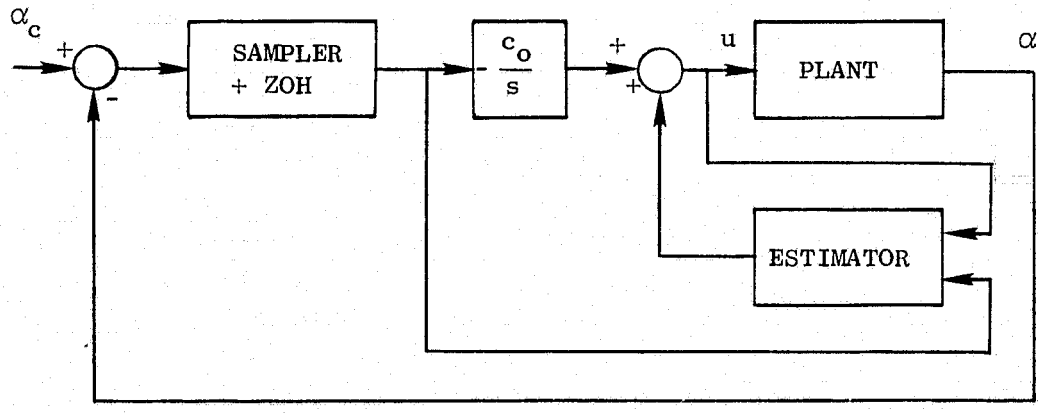

FIG. V-2 SYSTEM WITH DETECTOR MEASUREMENT ONLY

The closed loop transfer functions from the disturbances to the output contain in their denominators, the eigenvalues of both the controller and the estimate error systems. The transient response to these disturbances may therefore be dominated by the estimate error eigenvalues and therefore may be large and relatively slow. In order to improve this response, the gyroscope can be used as an additional measurement in one of its two modes. Estimators using this additional measurement are described below.

(2) Estimator using rate integrating gyro as measurement. As explained in (1), a system using an estimator with detector measurement only may not have satisfactory disturbance response. This is so because the information about output errors due to disturbances is obtained through the detector measurement only, which is relatively noisy and therefore must be filtered by a low bandwidth filter. The gyro has a much lower measurement noise than the detector (App. D).

The disturbance information obtained when the gyro is used as an additional measurement may therefore be filtered through a faster filter and higher stiffness to disturbance outputs may thus be obtained.

The output of a rate integrating gyro is an integral of the torques acting about its output axis. They are: (a) torquer generated torques, T, (b) drift torques, D, (c) torques caused by angular rates about the input axis, ωH. Therefore,

$$\dot{\varphi} = k_D(T + D + \omega H) \ . \qquad (5.10)$$

The total output must be kept close to zero. A command must therefore be applied to the torquer such that it generates torques that balance the drift torques and those due to angular rates. This command may be obtained from the detector signal ϵ such that

$$f(\epsilon) + D + \omega H = 0 \qquad (5.11)$$

where $f(\epsilon)$ is an unspecified function of the signal ϵ. Since, for constant angular rate, a zero error is required, this function must include the integral of the error and can be of the form:

$$f(\epsilon) = a_0\epsilon + a_1 \int \epsilon \, dt \ . \qquad (5.12)$$

The gyro-detector combination is shown in Fig. V-3. If the gyro is used as the sole measurement for the estimator, the gyro output will be kept close to zero by the controller, which adjusts the value of ϵ so that the gyro torques are balanced. The single gyro measurement can be considered to measure a linear combination of system states only if the target motion is viewed as noise, which is a reasonable assumption for an unknown maneuvering target. In that case the measurement is a linear combination of the state α and its two integrals. In order to model this measurement correctly in the estimator, the system model has to be augmented by the two integrals. A seventh-order estimator thus results. Since the order of the estimator is required not to exceed the order of the system, such an estimator cannot be used. An estimator of the order of the system is obtained by using the model of Eq. (5.7) and considering the gyro as a measure of the state α. Since in reality this measurement also contains the error integrals, the estimator does not estimate the actual states and a coupled system results. The block diagram of this coupled system is shown in Fig. V-4. From this figure, it can be seen that the effect of the non-modelled integration is to close an outer loop around the controller from the zero order hold output to the gyro torquer input. Its transfer function is:

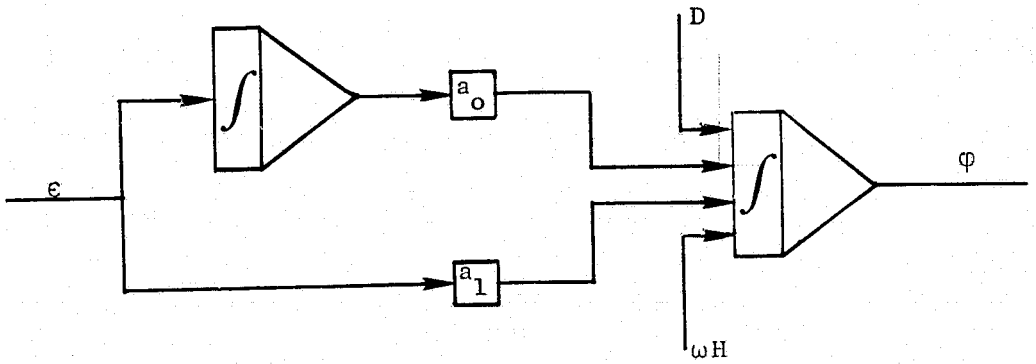

$$\varphi = k_0 \frac{H}{s} \omega + \left[\frac{a_0 + a_1 s}{s^2} \right] \epsilon$$

FIG. V-3 GYRO DETECTOR COMBINATION

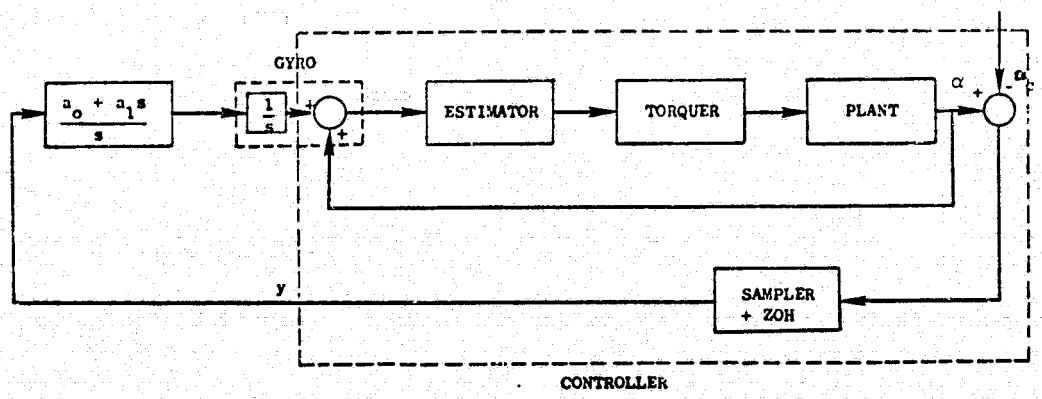

FIG. V-4 BLOCK DIAGRAM OF COUPLED SYSTEMS

$$G_1(s) = \frac{a_0 + a_1 s}{s^2} .$$

This transfer function includes one integration in the gyro. Note that the open loop transfer function of this augmented system has two roots at the origin only after integral control has been added. Therefore, integral control is required in order to obtain finite steady state acceleration error. This is to be compared with the system in which the estimator uses the detector measurement only. There, zero steady state acceleration error is obtained with integral control.

It is to be noted that because of the additional measurement, the steady state tracking and disturbance rejection properties are not obtained from the open loop transfer function of the actuator and plant. From Fig. V-4 it can be seen that the additional measurement has the effect of closing an inner feedback loop. The closed loop transfer function of this inner system is considered as the open loop t. f. for the determination of the steady state properties. If the constants a_0 and a_1 are small (a_0/a_1 much smaller than the eigenvalues of the nominal controller), the outer loop may be neglected and the feedback and estimator gains found by OPTSYS. The actual system eigenvalues will be somewhat shifted from their assumed values. If, however, relatively tight integral control is required in order to obtain a sufficiently small acceleration error, the feedback and estimator gains and the constants a_0 and a_1 have to be found by parameter optimization. The augmented system shown in Fig. V-5 is used for this optimization. Is is performed using the program PAROPT (Ch. IV-B-4) without the sensitivity reduction option.

The weighting matrices and the covariance matrices are the same ones that are used in OPTSYS.

Although the parameter optimization method is somewhat less convenient to use than the optimal controller and filter method, this, by itself, is not a serious drawback of this sytem since the optimization is only carried out a relatively small number of times.

$$
\begin{bmatrix} \dot{i}_1 \\ \dot{i}_2 \\ \hline \dot{\beta} \\ \dot{\alpha} \\ \dot{\omega} \\ \dot{a} \\ \dot{r} \\ \hline \dot{\tilde{\beta}} \\ \dot{\tilde{\alpha}} \\ \dot{\tilde{\omega}} \\ \dot{\tilde{a}} \\ \dot{\tilde{r}} \end{bmatrix} =
\left[\begin{array}{ccccccc|ccccc}
0 & 1 & 0 & 0 & 0 & 0 & 0 & 0 & 0 & 0 & 0 & 0 \\
0 & 0 & 1 & 0.9 & 0 & 0 & 0 & 0 & 0 & 0 & 0 & 0 \\
\hline
0 & 0 & -4f_o & -7.2f_o & 0 & 0 & 0 & 0 & 0 & 0 & 0 & 0 \\
0 & 0 & 0 & 0 & 1 & 0 & 0 & 0 & 0 & 0 & 0 & 0 \\
0 & 0 & 0 & 0 & 0 & 1 & 0 & 0 & 0 & 0 & 0 & 0 \\
0 & 0 & 0 & 0 & 0 & 0 & 1 & 0 & 0 & 0 & 0 & 0 \\
0 & 0 & -m_2c_1 & -m_2c_2 & -m_2c_3 & -m_2(c_4+1) & -m_2c_5-m_1 & m_2c_1 & m_2c_2 & m_2c_3 & m_2c_4 & m_2c_5 \\
\hline
-a_ok_1 & -a_1k_1 & 0 & 0 & 0 & 0 & 0 & -4f_o & -k_1-7.2f_o & 0 & 0 & \\
-a_ok_2 & -a_1k_2 & 0 & 0 & 0 & 0 & 0 & 0 & -k_2 & 1 & 0 & 0 \\
-a_ok_3 & -a_1k_3 & 0 & 0 & 0 & 0 & 0 & 0 & -k_3 & 0 & 1 & 0 \\
-a_ok_4 & -a_1k_4 & 0 & 0 & 0 & 0 & 0 & 0 & -k_4 & 0 & 0 & 1 \\
-a_ok_5 & -a_1k_5 & 0 & 0 & 0 & 0 & 0 & 0 & -k_5 & 0 & -m_2 & -m_1
\end{array}\right]
$$

$$
\begin{bmatrix} \dot{y} \\ \dot{x} \\ \dot{\tilde{x}} \end{bmatrix} =
\begin{bmatrix} A_{11} & A_{12} & 0 \\ 0 & A_{22} & A_{23} \\ A_{31} & 0 & A_{33} \end{bmatrix}
\begin{bmatrix} y \\ x \\ \tilde{x} \end{bmatrix} .
$$

FIG. V-5 SYSTEM WITH ESTIMATOR USING RATE INTEGRATING GYRO OUTPUT EFFECT OF NONMODELED INTEGRATION.

(3) Estimator with rate gyro as sensor. The transformation of a rate integrating gyro into a rate gyro by caging it, i.e., feeding back its output to its torquer, is described in Appendix H. The rate gyro is a second order system for which the natural frequency is determined by the caging loop gain and the damping by the rate integrating gyro time constant. If the natural frequency is sufficiently higher than the system natural frequencies, the gyro transfer function can be approximated by a constant, viz.,

$$\varphi \approx k_g \omega \,. \tag{5.13}$$

The effect of neglecting the gyro dynamics in the estimator model is to couple the estimator and system eigenvalues. The amount of coupling depends on the natural frequency of the gyro. To minimize the coupling, this frequency has to be high but this increases the gyro measurement noise. In Appendix H these effects are discussed and a natural frequency is selected. The conflict between high noise and coupling can be avoided if the rate gyro is modeled in the estimator but this leads to a more complicated estimator (7 states).

Using the approximation of Eq. (5.13), an estimator can be designed using both the detector and rate gyro as measurements. As explained above, the addition of the rate gyro should improve the disturbance response.

Three different realizations of this estimator are considered. (a) One full state estimator using the two measurements. The block diagram of this estimator is shown in Fig. V-6a. (b) One reduced order estimator using the same measurements. Its block diagram is shown in Fig. V-6b. Since its design method is substantially different from the one used for the other estimators, it is described in Appendix K. (c) Two separate full state estimators: • one two-state estimator for α and β (see Fi. V-3a) using the detector as the measurement and the rate gyro as a known input; • one three-state estimator for ω, a, and r using the rate gyro as a measurement.

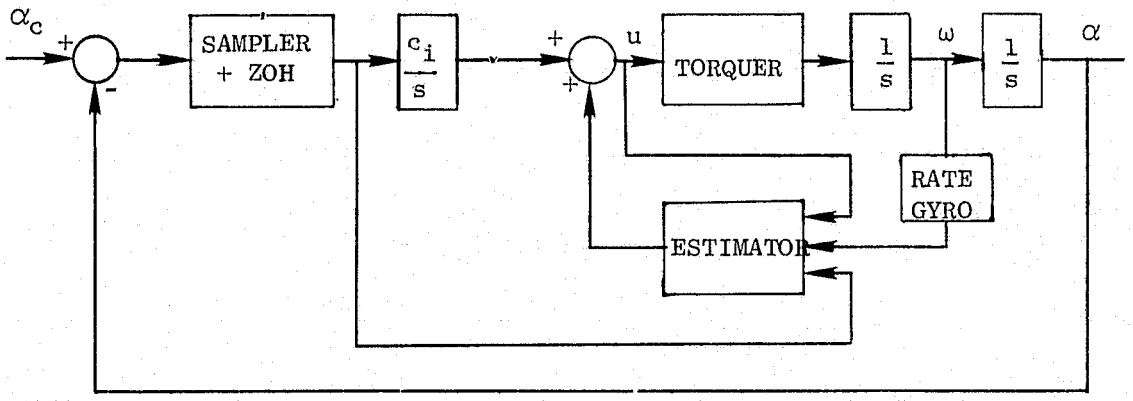

FIG. V-6a FULL STATE ESTIMATOR WITH TWO MEASUREMENTS

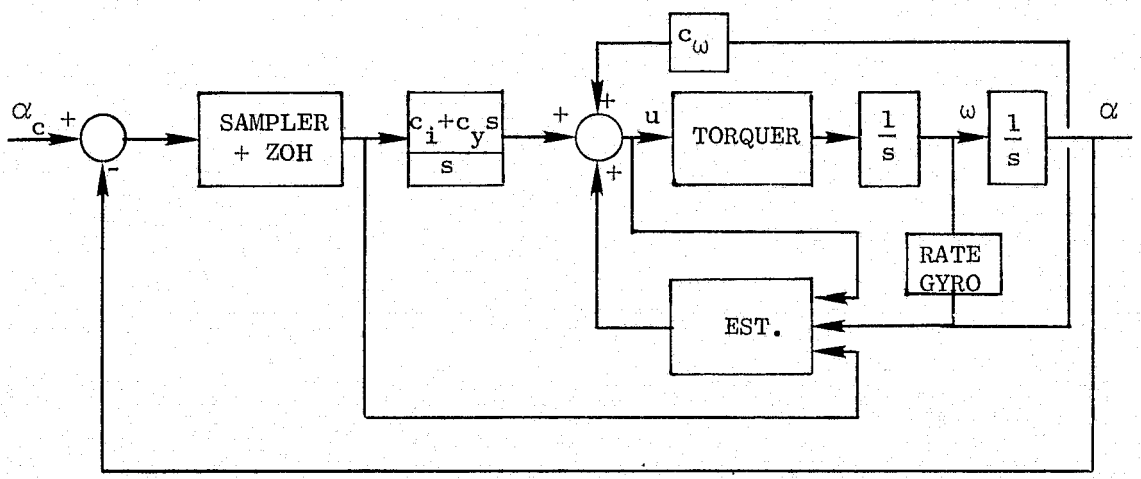

FIG. V-6b REDUCED ORDER ESTIMATOR WITH TWO MEASUREMENTS

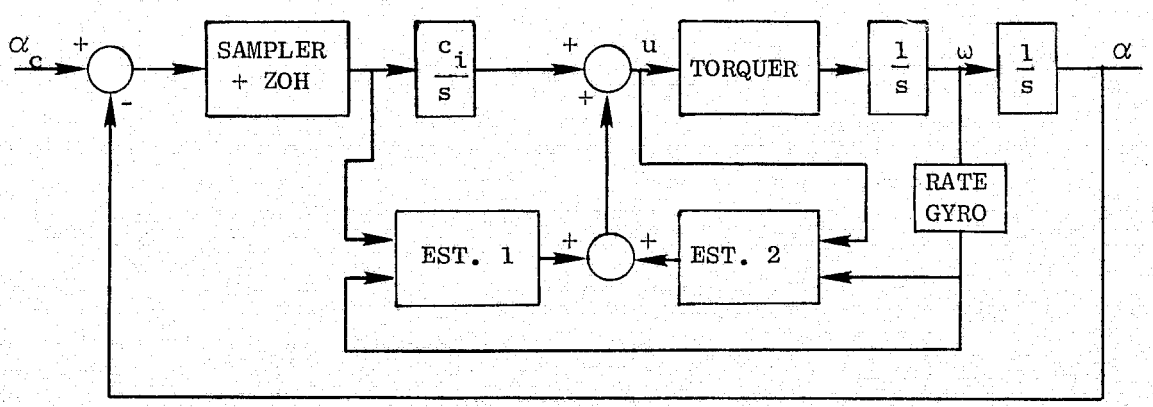

FIG. V-6c TWO SEPARATE FULL STATE ESTIMATORS

The block diagram of this estimator is shown in Fig. V-6c. The dynamic equations of its models are given in Fig. V-7.

$$\begin{bmatrix} \dot{\beta} \\ \dot{\alpha} \end{bmatrix} = \begin{bmatrix} -4f_o & -7.2f_o \\ 0 & 0 \end{bmatrix} \begin{bmatrix} \beta \\ \alpha \end{bmatrix} + \begin{bmatrix} 0 \\ 1 \end{bmatrix} \omega + \begin{bmatrix} 0 \\ 1 \end{bmatrix} w$$

$$y = [1,\ 0.9]x + v$$

$$Q = r_g \quad \text{(rate gyro noise intensity)}$$

$$R = r_d \quad \text{(detector noise intensity)}$$

ω = gyro measurement used as input

v,w = noise

FIG. V.7a MODEL FOR ESTIMATOR NO. 1

$$\begin{bmatrix} \dot{\omega} \\ \dot{a} \\ \dot{p} \end{bmatrix} = \begin{bmatrix} 0 & 1 & 0 \\ 0 & 0 & 1 \\ 0 & -m_2 & -m_1 \end{bmatrix} \begin{bmatrix} \omega \\ a \\ p \end{bmatrix} + \begin{bmatrix} 0 \\ 0 \\ m_2 \end{bmatrix} u + \left[\begin{array}{c|c} 1 & 0 \\ 0 & 0 \\ 0 & m_2 \end{array}\right] \begin{bmatrix} w_1 \\ w_2 \end{bmatrix}$$

$$y = [1\ \ 0\ \ 0]x + v$$

$$Q = \begin{bmatrix} q_1 & 0 \\ 0 & q_2 \end{bmatrix} \quad \text{(see Fig. V.2a)}$$

$$R = r_g \quad \text{(rate gyro noise intensity)}$$

FIG. V-7b MODEL FOR ESTIMATOR NO. 2

Because the system is SISO, the steady state tracking and disturbance rejection properties can be studied from the equivalent transfer function representation of the estimators.

All three designs can be represented by the same transfer function. The block diagrams of this transfer function are shown in Figs. V-8a and V-8b, where Fig. V-8b is a simplification of Fig. V-8a. For the full state estimators, $c_y = 0$ and $c_\omega = 0$.

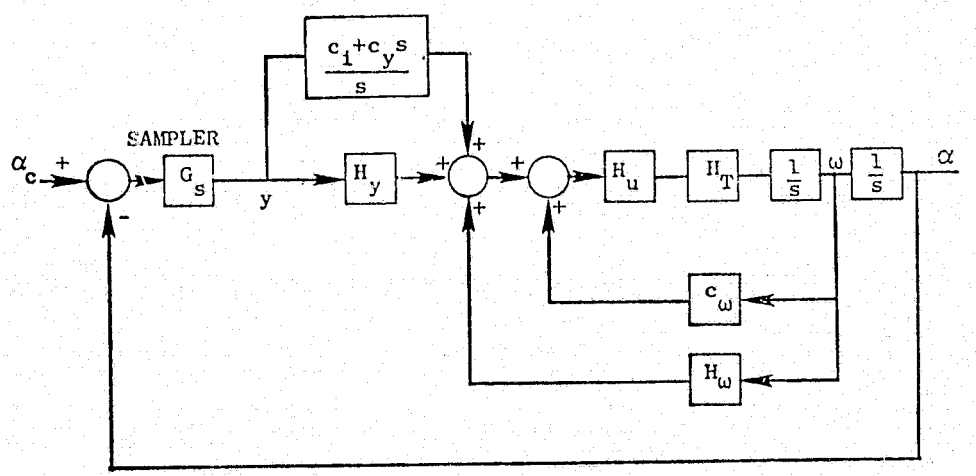

FIG. V-8a

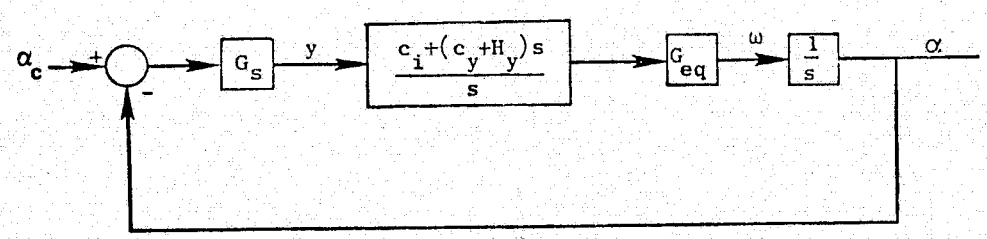

FIG. V-8b

FIGS. V-8a,b EQUIVALENT BLOCK DIAGRAMS OF SYSTEM WITH RATE GYRO AND DETECTOR MEASUREMENT.

From Fig. V-8b, it is observed that the equivalent open loop transfer function, which contains the effect of the integral control and the rate measurement feedback, has two roots at the origin. The systems can therefore track a constant acceleration command with constant control and finite tracking error. To obtain zero tracking error for acceleration command, one additional integration has to be added. The effect of the gyro measurement, both when used as a rate integrating gyro or a rate gyro, is therefore to reduce the system from type (2) to type (1). This disadvantage will be shown to be outweighted by the improved transient response and disturbance rejection discussed in Section D-4 (below).

The five designs that were described in this section cover all the possible combinations of the measurements. There may, however, exist other designs using these same measurements. The structure of the described designsis shown in Table V-1. Later, the gains are calculated and the designs compared.

Table V-1

ESTIMATOR STRUCTURES

DESIGNATION	MEASUREMENTS	METHOD OF DESIGN	Order of Error Free Polynomial		REMARKS
			Tracking	Disturbance	
D	detector	Separate design of controller and estimator by OPTSYS	2	0	
DI	detector and rate integrating gyro	Combined design by parameter optimization	1	0	Coupling between controller and estimator roots
DR 1	detector and rate gyro	same as type D	1	0	
DR 2	detector and rate gyro	same as type D	1	0	two separate estimators
DRR	detector and rate gyro	parameter optimization (see App. J)	1	0	reduced order estimator

D-3 State and Control Weight Selection

In this Section the determination of the state and control weights is described. These weights are then used in an optimal control program for the determination of the feedback gains and closed loop eigenvalues and eigenvectors. Several systems are designed for subsequent evaluation in the next section.

The relation between the weights and the system eigenvalues is determined by the root square locus method. This method was mentioned in Chapter II and is described in more detail in Appendix $\mathcal{J}$. It enables one to determine the weights for single input systems so as to obtain required eigenvalues. The required eigenvalues, however, have to be determined from the given system specifications. The correspondence between these specifications and the eigenvalues is not unique since the time response also depends on the controller eigenvectors and on the estimate error eigensystem. A rough correspondence can, however, be determined by assuming that the controller and not the estimator dominates the time response. Under this assumption, the following criteria for the eigenvalue locations can be established: (a) a high bandwidth is desirable for low tracking error and good disturbance rejection. It is limited by the detector sampling rate ($\omega_s \cong 800$ rad/sec) and the actuator noise requirements. A bandwidth of $\omega = 100$ sec^{-1} seems reasonable as an initial point. (b) The actuator has a natural damping coefficient of 0.13. Although this is somewhat low, high gains may be required in order to increase it and therefore initially this location will be considered satisfactory.

These two criteria sum up to the requirement that the damping of the actuator roots should not decrease and that the magnitude of the real part of the additional roots should be greater than 100 sec^{-1}.

In the remainder of this section, the selection of weights for several systems will be described and candidate systems for the performance evaluation will be determined.

The open loop system for which the controller is designed is the system of Eq. (5.7) augmented by an integral state i such that

$$\frac{di}{dt} = y = \beta + 0.9\alpha \ .$$

The requirement for this state was explained in Section D-2. In order to determine which states have to be weighted, the following rule is used [AN-2]: to ensure stability of the closed loop system, the pair [F,D] has to be observable, where D is any matrix such that $DD^T = A$. From this rule it is obvious that the only state that must be weighted is the integral state i. The effects of the weighting of the states α and ω are also examined. A multiple-parameter root square locus is constructed by first constructing the root square locus for the state i, selecting a temporary weight for this state and considering the closed loop eigenvalues obtained for this weight as denominator eigenvalues for the α root square locus. The same procedure is followed for obtaining the ω root square locus.

The transfer functions to the three weighted states are:

$$G_i(s) = \frac{i(s)}{u(s)} = \frac{0.9m_2(s - 4f_0)}{s^3(s + 4f_0)(s^2 + m_1 s + m_2)} \triangleq \frac{N_i(s)}{D(s)} \qquad (5.14a)$$

$$G_\alpha(s) = \frac{\alpha(s)}{u(s)} = \frac{m_2 s(s + 4f_0)}{D_i(s)} \qquad (5.14b)$$

$$G_\omega(s) = \frac{\omega(s)}{u(s)} = \frac{m_2 s^2(s + 4f_0)}{D_\alpha(s)} \ , \qquad (5.14c)$$

where $D_i(s)$ is the characteristic polynomial obtained when the integral state only is weighted with the selected weight, and $D_\alpha(s)$ is the characteristic polynomial obtained by weighting both i and α. The root square locus for the i, α, and ω states are shown in Figs. V-9 through V-11. From these figures, the influence of increasing the weights of the different states can be assessed as follows:

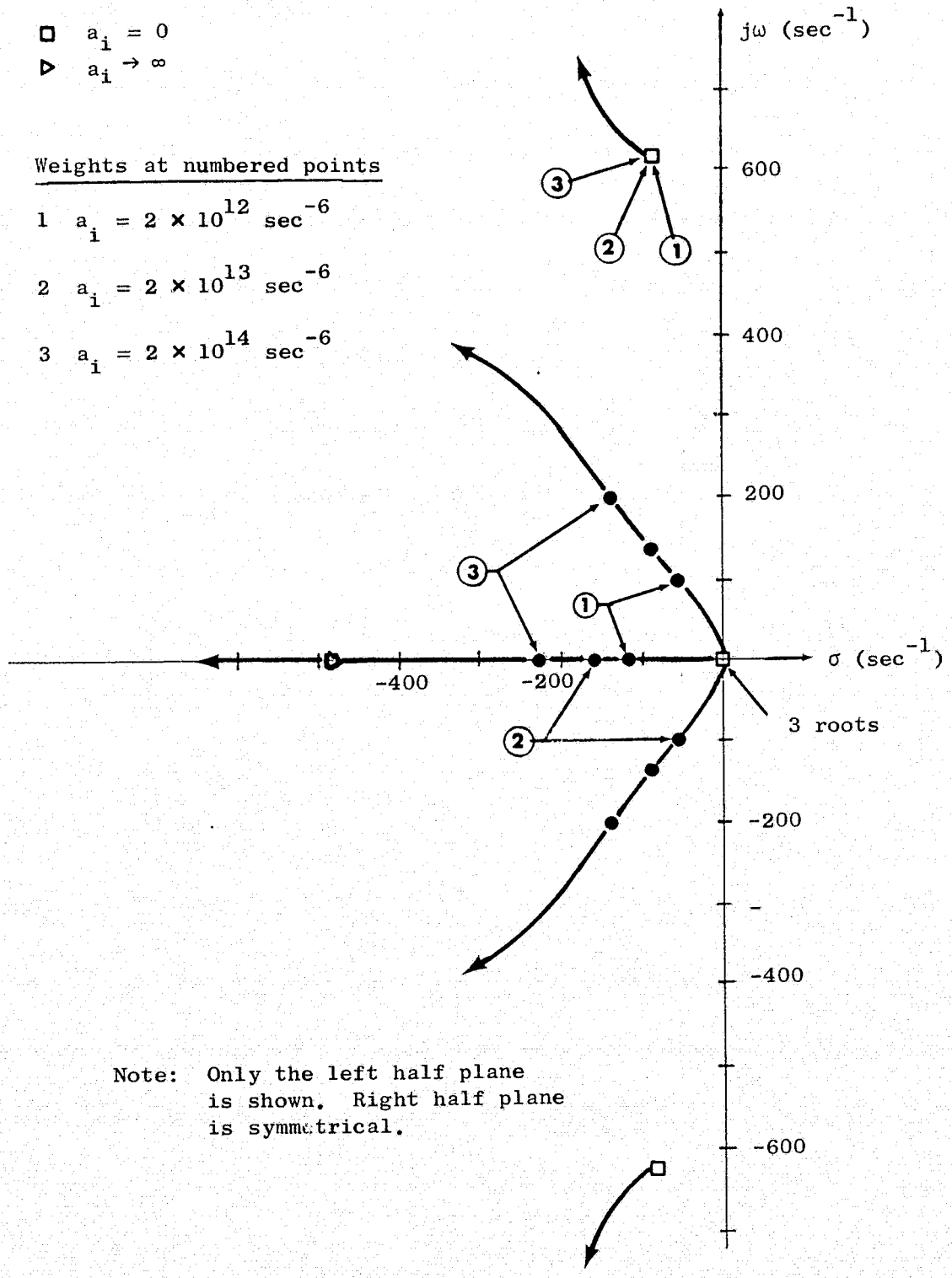

FIG. V-9 ROOT SQUARE LOCUS FOR INTEGRAL STATE WEIGHTING.

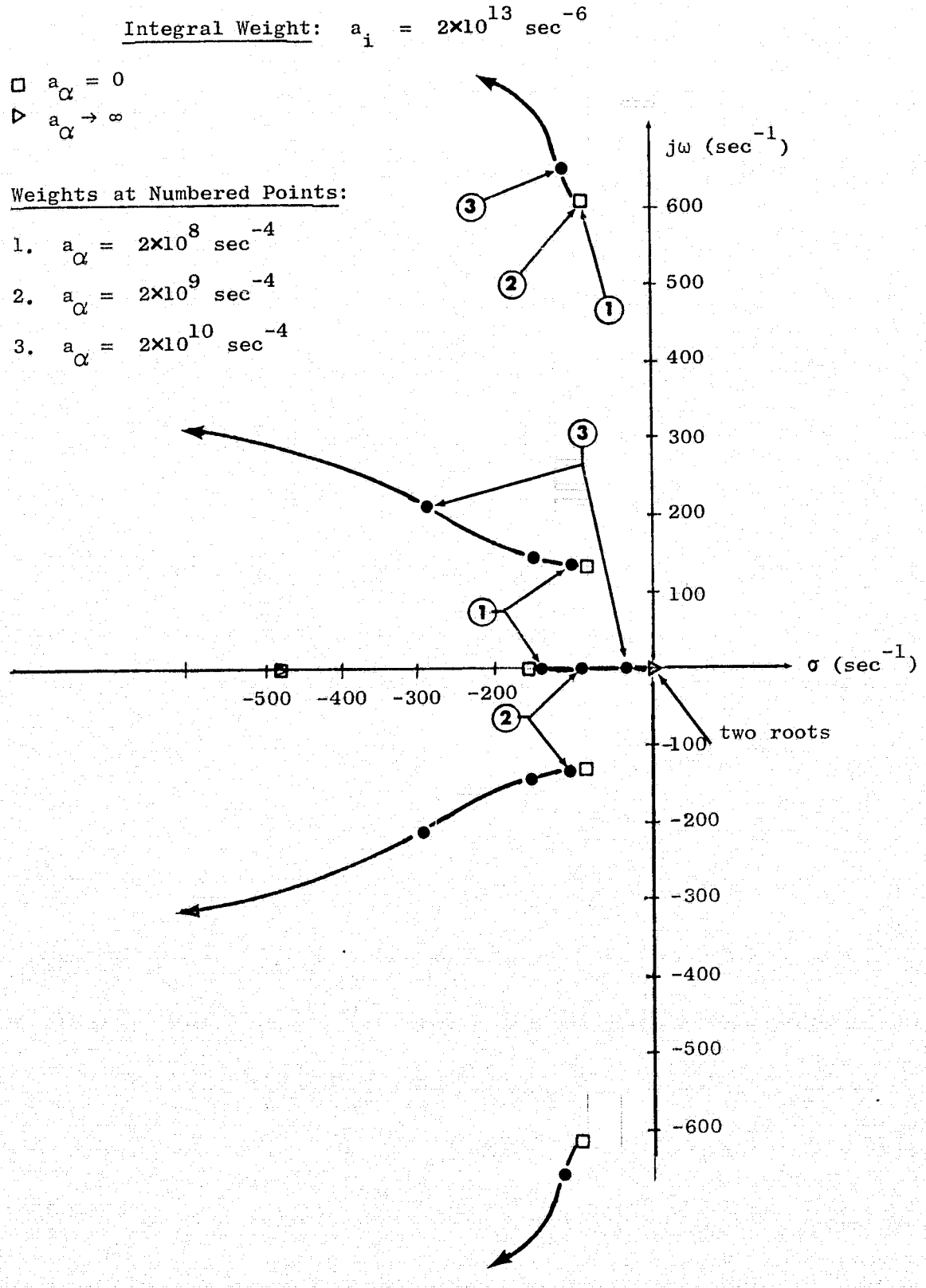

FIG. V-10 ROOT SQUARE LOCUS FOR POSITION STATE WITH FIXED INTEGRAL WEIGHT.

□ $a_\omega = 0$

▷ $a_\omega \rightarrow \infty$

Weights at Numbered Points:

1. $a_\omega = 2\times10^3 \text{ sec}^{-2}$
2. $a_\omega = 2\times10^4 \text{ sec}^{-2}$
3. $a_\omega = 2\times10^6 \text{ sec}^{-2}$

Integral and Position Weights:

$a_i = 2\times10^{13} \text{ sec}^{-6}$

$a_\alpha = 2\times10^9 \text{ sec}^{-4}$

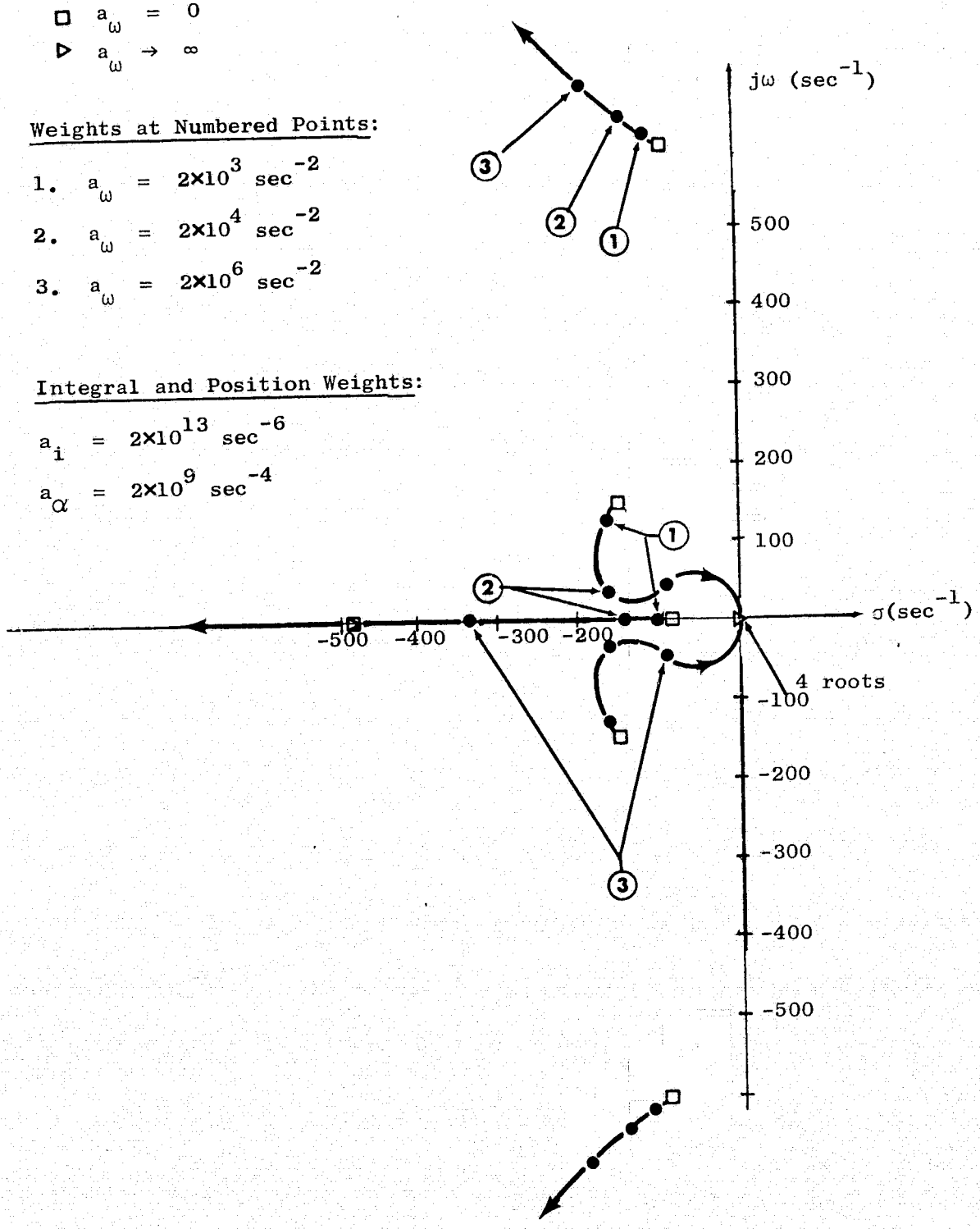

FIG. V-11 ROOT SQUARE LOCUS FOR RATE STATE WITH FIXED INTEGRAL AND POSITION WEIGHTS.

(a) Integral state: • little effect on actuator roots; • other roots move away from the origin with little change in damping of complex roots. (b) Position: • some effect on actuator roots; • real root approaches origin; • complex roots move away from the origin; damping of the complex roots increases; (c) Rate: • increased bandwidth and damping of actuator roots; • real root moves away from the origin; • complex roots initially remain at same distance from imaginary axis with increased damping.

Roughly, therefore, the integral state weight influences primarily the bandwidth, whereas the rate weight affects mainly the damping. The position weight has an intermediate effect. Using these considerations, three designs were selected for further evaluation as shown in Table V-2.

Table V-2

CONTROLLER DESIGNS

Design No.	Characteristics	a_i (sec^{-6})	a_α (sec^{-4})	a_ω (sec^{-2})	Remarks
1	nominal (N)	2×10^{13}	0	0	Point 2 in Fig. V-9
2	high gain (HG)	2×10^{14}	0	0	Point 3 in Fig. V-9
3	high damping (HD)	2×10^{13}	2×10^{9}	8×10^{4}	Point 2 in Fig. V-11

The selection of Design 1 as an initial design was made by considering its acceleration error. If state feedback, without an estimator is used, the steady state acceleration error is:

$$\frac{\epsilon}{a_c} = \frac{\text{rate gain}}{\text{integral state gain}} .$$

For Design 1, this ratio is 1.2×10^{-4} sec^2, or $120\,\mu rad/(rad/sec^2)$. This is less than the required acceleration error but an increase in this error is to be expected if an estimator is used to obtain the

feedback gains (see App. K).

Design 2 has a lower acceleration error, Design 3 a higher one. No design using integral and position weights only was evaluated since this represents an intermediate case between the cases that were selected.

D-4 Estimator Design Evaluation.

The following designs were made and are evaluated in here. (a) The controllers and estimators given in Tables V-1 and V-2 with the noises as given in App. D and H. The influence of different noise assumption is discussed in Section E-3. (b) An additional estimator of type DR 2 (two estimators, one using the rate gyro measurement, and the other the detector measurement). In this design (DR 2H), the gains of the detector estimator were arbitrarily selected at higher values in order to decrease the acceleration error. The connection between the estimator gains and the acceleration error is developed in Appendix K.

The gains for the controllers and the estimators (except Type DI and DRR) were found by the optimal control program, OPTSYS [BRY-3]. The feedback and estimator gains for Type DI and the estimator gains for Type DRR were found by parameter optimization using the sensitivity minimization program, PAROPT, described in Ch. IV-B-4, without the sensitivity reduction option, and with the same state weights as were used for Design 1 in Table V-2. The eigenvalues of the controllers are shown in Figs. V-9 to V-11. The eigenvalues of the estimators are shown in Fig. V-12a. The eigenvalues of the coupled system DI are shown in Fig. V-12b. It is observed in Fig. V-12a that the reduced order estimator has a very slow root. This can be made plausible by considering Eq. J-15 in App. J . Comparing this equation to Eq. (2.31), it can be seen that in the full state estimator, the measurement noise forces the estimate error only, whereas in the reduced order estimator, this noise forces both the state and the estimate error through the estimator gain K. For low output and control noises, a lower gain K is therefore desirable and slower estimator roots result.

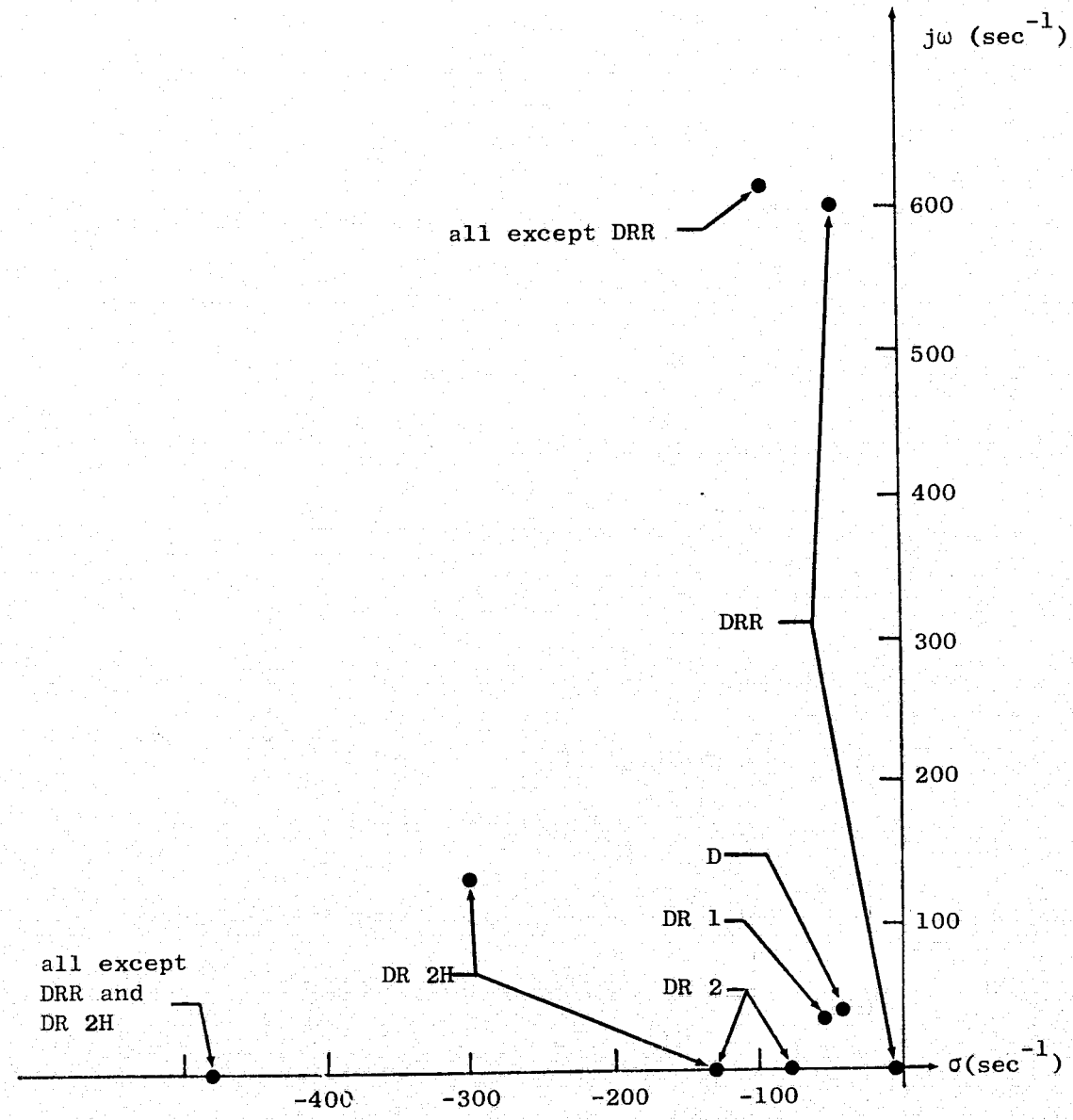

FIG. V-12a ESTIMATE ERROR SYSTEM EIGENVALUES FOR DIFFERENT TRACKER DESIGNS

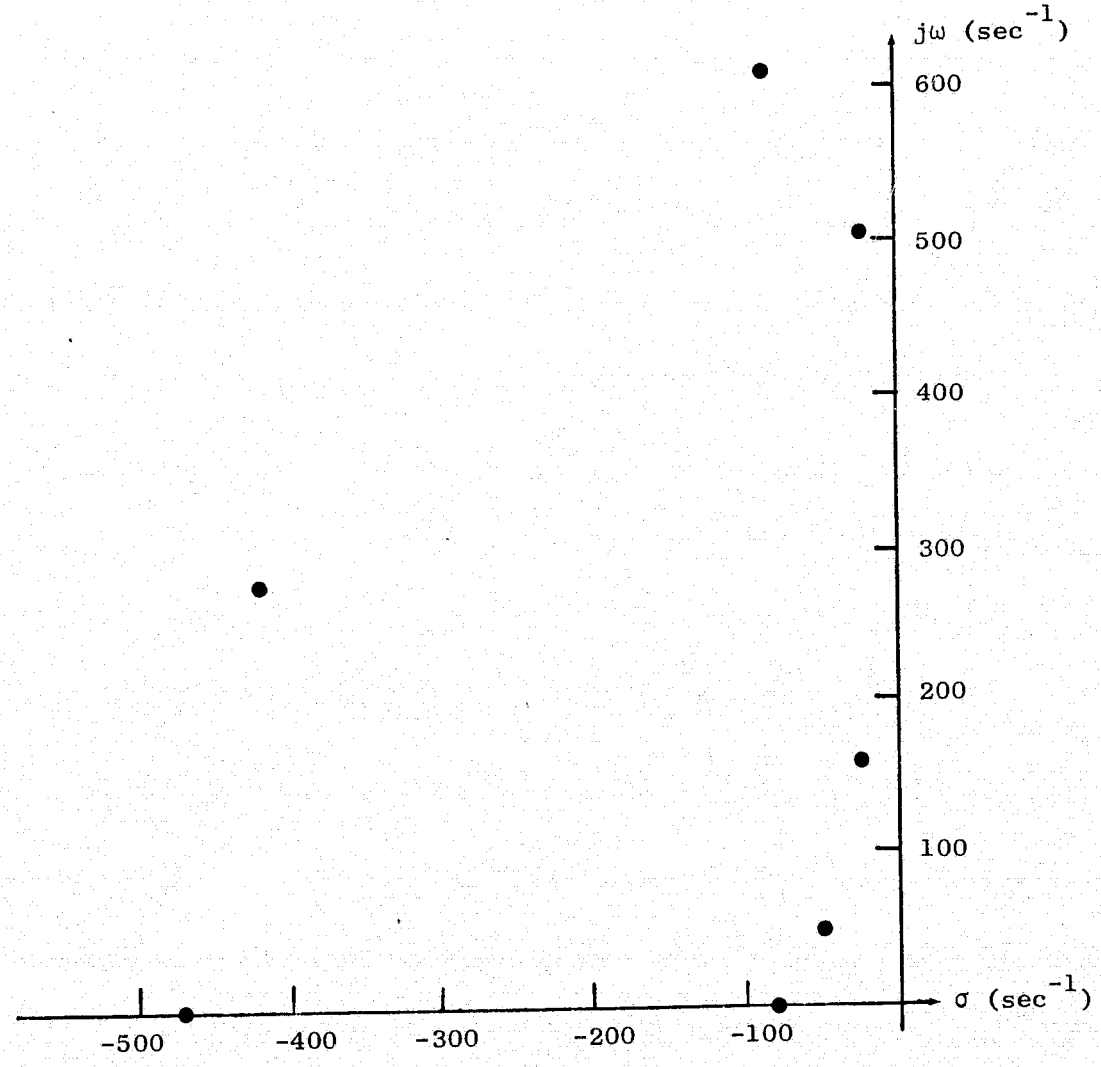

FIG. V-12b EIGENVALUES OF THE DI SYSTEM

The performance of various combinations of these designs was evaluated according to three criteria: (a) steady state error for acceleration input; (b) maximum deflection for step disturbance input; (c) control mean square noise.

For systems using the DI and DR 2 estimators, it is relatively easy to find the analytic expression for the acceleration error. This is done in Appendix K. For systems using the DR 1 estimator, the analytic expression is complicated and the error was calculated numerically using the design program XAGSA [WIT-1]. For systems using the Type D estimator, there is no steady state acceleration error.

The disturbance deflection was found in all cases with the aid of the XAGSA program. The control rms values were found with the aid of the OPTSYS program. The results of these evaluations are given in Table V-3. The time responses of some of the systems are shown in Figs. V-13 and V-14.

Table V-3

PERFORMANCE COMPARISON OF CONTROLLER AND ESTIMATOR DESIGNS

Design No.	Estimator Type	Controller Type	Steady State Error For Acc. Input $\left(\frac{\mu rad}{rad/sec^2}\right)$	Maximum Deflection for Step Disturb. $\left(\frac{\mu rad}{rad/sec^2}\right)$	Control rms noise (rad/sec^2)	Output rms noise (μrad)
1	D	N	0	260	1.8	65
2	DR 1	N	280	145	0.54	29
3	DR 1	HG	205	96	0.94	26
4	DR 1	HD	590	180	0.58	30
5	DR 2	N	400	48	1.05	-
6	DR 2H	N	185	48	1.8	46
7	DR 2H	HG	130	not computed	3.3	53
8	DRR	N	28000!!	18	1.2	28
9	DI	N	240	not computed	2.5	78

N = nominal HG = high gain HD = high damping

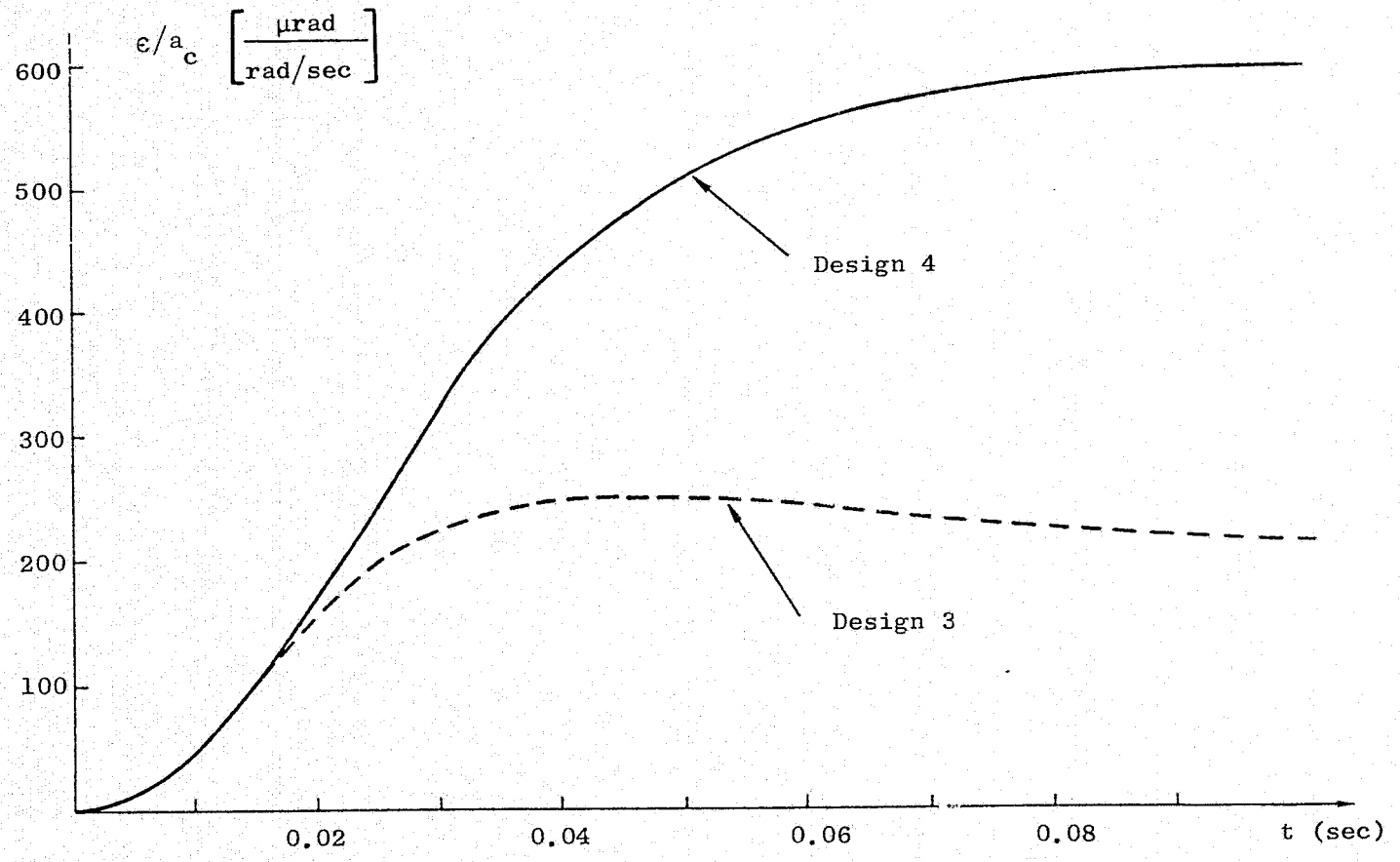

FIG. V-13 OUTPUT ERROR FOR CONSTANT ACCELERATION COMMAND

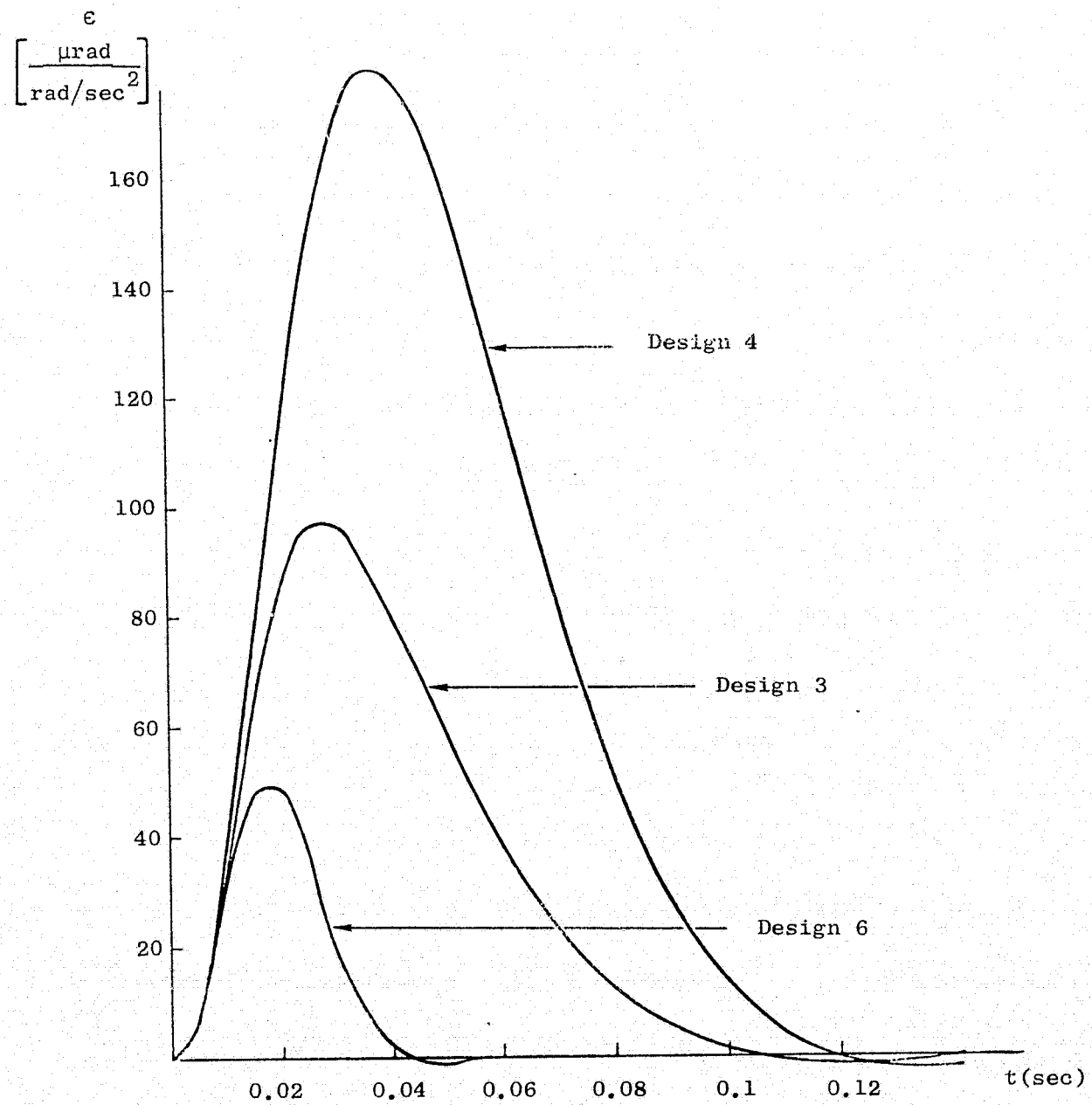

FIG. V-14 CONSTANT DISTURBANCE RESPONSE OF DIFFERENT TRACKER DESIGNS.

A control rms higher than 2 rad/sec^2 is considered unacceptable since it violates the torquer saturation requirement. Other criteria for such designs were therefore not evaluated.

The following observations can be made from Table V-3 and Figs. V-13 and V-14. (1) the addition of the rate measurement to the detector measurement lowers both the control rms and the disturbance deflection (compare Designs 1 and 2). However, it causes the system to have a finite, instead of a zero, acceleration error. (2) Increasing the bandwidth of the system lowers acceleration error and disturbance deflection but increases control rms (compared Designs 2 and 3). This result is to be expected. (3) Increasing the damping increases the acceleration error and the disturbance deflection (compared Designs 3 and 4). The time response of the better damped system has no overshoot (see Fig. V-13). (4) Two partial estimators instead of one full estimator (with the same controller) cause the system to have higher acceleration error and control rms but lower disturbance deflection (compare Designs 2 and 5). (5) The designs using the rate gyro as a second measurement have generally better performance than the one using the rate integrating gyro (DI). (6) The reduced state observer (DRR) has a higher control noise than the full state observer with the same controller, as is to be expected. However, it also has an unacceptably high acceleration error. Its acceleration response is dominated by the low eigenvalue $\lambda_1 = -0.56$ rad/sec.

The ranking of the designs according to the criteria of Table V-3 is given in Table V-4. The designs below the dashed lines in this Table are considered unacceptable for the respective requirements. Note that designs with acceleration errors of up to 200 μrad/(rad/sec) are considered acceptable, although in Section V-C an error of 150 μrad/(rad/sec^2) is specified. This is so because this error is considered as a design goal only and not as a rigid specification. From Table V-3 it can be seen that satisfying this requirement would cause an unacceptably large controller noise.

Table V-4

RANKING OF THE DESIGNS

Acceleration Steady State Error	Disturbance Deflection	Control rms
1	8	2
7	5, 7	4
6	3	3
3		5
9	2	8
2	4	6, 1
v	1	
9		9
8		7

Note that in the above Table, only Designs 3 and 6 are acceptable according to all the criteria. Designs 3 and 6 are comparable and the selection between them will be made according to parameter sensitivity criteria in the next Section.

Design 8, which uses the reduced order observer, is clearly unacceptable as is. It, however, merits some more consideration since it is simpler than all the other designs. Its acceleration error may be decreased by shifting the observer poles but that, of course, will increase its control and state noise. It is reasonable to assume that for parameter sensitivity reduction, the slow eigenvalue has to be moved further from the imaginary axis and therefore the applications of the sensitivity reduction program to this system may also improve its acceleration response. This is done in the next Section also.

D-5 Sensitivity Reduction and Final Selection

The sensitivity of Designs 3 and 6 to the variation of the hydraulic actuator spring constant and damping coefficient is shown in Table V-5. The region of stability is considered as the sensitivity measure. From this Table it can be seen that both designs have low sensitivities to damping variations. The sensitivity to stiffness reduction of Design 3 is unacceptable, whereas for Design 6, it is tolerable.

Table V-5

STABILITY REGION FOR HYDRAULIC ACTUATOR PARAMETER VARIATIONS

		Design 3 (DR 1-HG)	Design 6 (DR 2H-N)
Spring Constant Range	$+ \Delta k/k$	Large	Large
	$- \Delta k/k$	-0.04	-0.18
Damping Coefficient Range	$- \Delta b/b$	Large	Large
	$- \Delta b/b$	-0.7	-1.1

The sensitivity reduction method may be applied to Design 3. Since this is an optimal system, its state and control noises will increase due to this reduction but this is acceptable since the control noise is well below the specified level. Design 6 is not optimal since the gains of estimator No. 1 were selected arbitrarily. Sensitivity reduction may, therefore, increase or decrease its control noise. However, a system with lower control noise will most probably have a higher acceleration error. Since both this error and the control noise are close to their specified limits, the application of the sensitivity reduction method to this system is not feasible. The result of the sensitivity reduction for Design 3 are given in Tables V-6 and V-7.

Table V-6

STABILITY RANGE OF DESIGN 3

		Original	Desensitized
Spring Constant Range	$+ \Delta k/k$	Large	+ 0.31
	$- \Delta k/k$	-0.04	- 0.22
Damping Coefficient Range	$+ \Delta b/b$	Large	Large
	$- \Delta b/b$	-0.7	-0.65

Table V-7

NOMINAL PERFORMANCE CRITERIA OF DESIGN 3

System	Steady State Error For Acc. Input $\left(\frac{\mu rad}{rad/sec^2}\right)$	Maximum Deflection for Step Disturb. $\left(\frac{\mu rad}{rad/sec^2}\right)$	Control rms Noise (rad/sec^2)	Output rms Noise (μrad)
Original	205	96	0.94	26
Desensitized	250	28	2.8	45

Comparing these Tables with Tables V-3 and V-5, it is obvious that Design 6 is preferable by both nominal and sensitivity criteria.

As explained in the previous Section, the sensitivity reduction method is also applied to the reduced order estimator design, No. 8. In this case, this method is used essentially as a pole placement method. The results of its application are given in Table V-8. From this Table it can be seen that

the sensitivity reduction method has, as expected, considerably decreased the acceleration error for this case. The stability ranges of Design 6 and of the desensitized reduced order estimator, Design 8A, are compared in Table V-9. These two designs can be seen to have comparable properties. The nominal properties of Design 6 are slightly better but the sensitivity of Design 8A to reduction of the spring constant is considerably lower. The higher sensitivity of this design to reduction of the damping coefficient is of no importance since the stability range is more than adequate. Since this design is also simpler, it is selected as the final design.

Table V-8

SENSITIVITY REDUCTION OF REDUCED ORDER ESTIMATOR

System	Steady State Error For Acc. Input $\left(\frac{\mu rad}{rad/sec^2}\right)$	Maximum Deflection for Step Disturb. $\left(\frac{\mu rad}{rad/sec^2}\right)$	Control rms Noise (rad/sec^2)	Output rms Noise (μrad)	Estimator Eigenvalues (rad/sec)
Original	28000	18	1.2	28	- 0.54 -36 ± 610j
Desensitized	195	40	2.1	43	- 110 - 94 ± 606j

It is important to note that since the system is noise limited, a different system may have been selected if different values were assumed for the measurement noises and disturbances. In a more detailed design procedure, several designs are usually made using different noise levels and one of the considerations in the selection of the design may also be low sensitivity to assumed noises.

In Fig. V-15, the frequency response to a tracking command is shown. It has a bandwidth of 190 sec^{-1} which is about 25% of the

Table V-9

STABILITY RANGE COMPARISON OF TWO ESTIMATOR DESIGNS

		Design 6	Desensitized Reduced Order Estimator
Spring Constant Range	$+\Delta k/k$	Large	Large
	$-\Delta k/k$	-0.18	-0.33
Damping Coefficient Range	$-\Delta b/b$	Large	Large
	$-\Delta b/b$	-1.0	-0.7

sampling frequency. This is within the range of the specifications discussed earlier (V-C). The output response to a constant acceleration command and to a constant disturbance is shown in Fig. V-16.

D-6 Summary

Among the Designs examined in this Section, two have the best overall performance, with the assumed measurement and process noises:

(a) Design 6, DR 2H. A system using two separate estimators with the gains for the first estimator determined by pole placement.

(b) Design 8, DRR, desensitized. A system using a reduced order estimator. The sensitivity reduction for this design was only used as a pole placement device.

Design 8 was finally selected. Its eigenvalues, performance criteria, and sensitivities were given in Table V-8; its frequency and time responses were shown in Figs. V-15 and V-16.

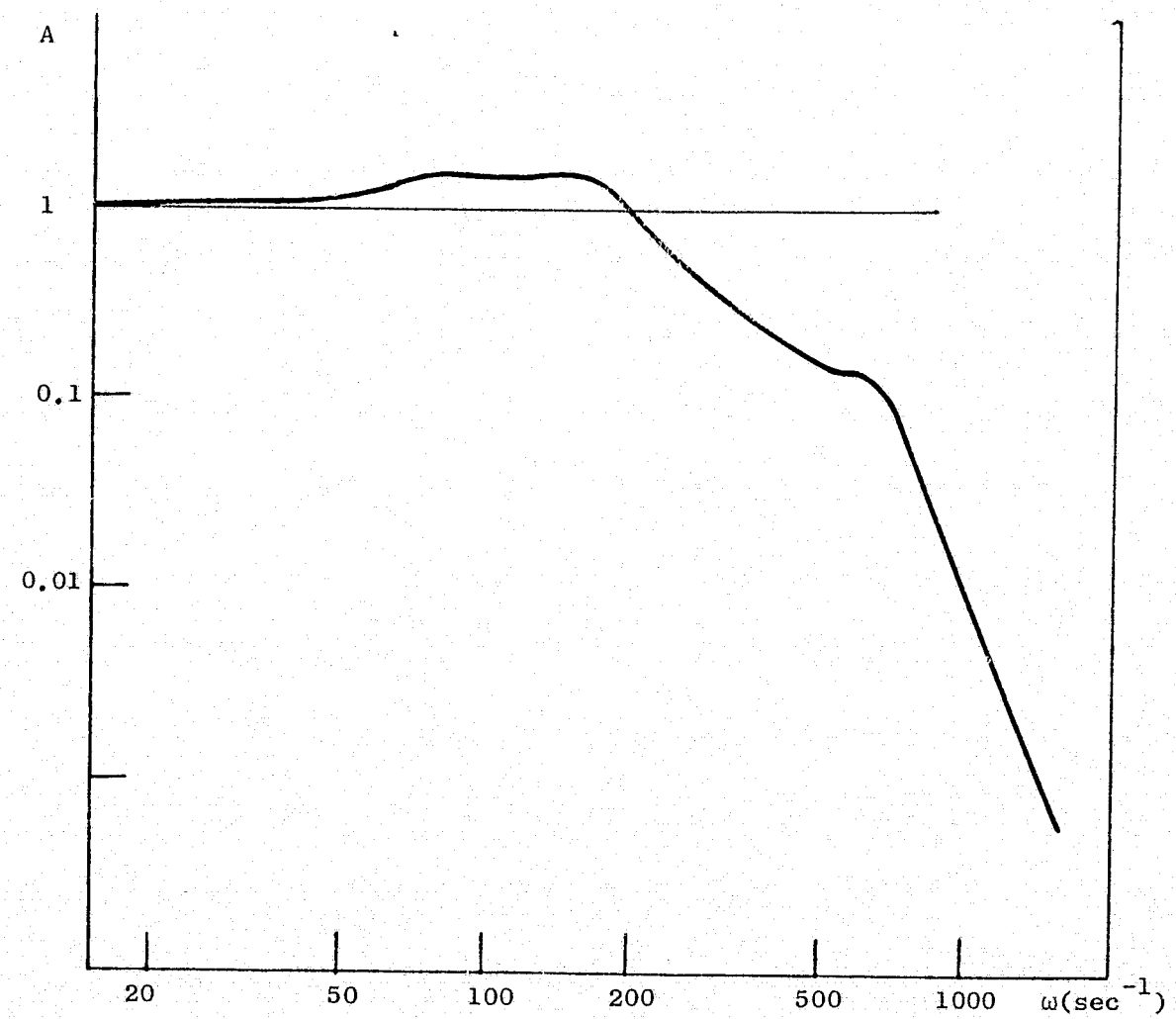

FIG. V-15 FREQUENCY RESPONSE OF REDUCED ORDER ESTIMATOR

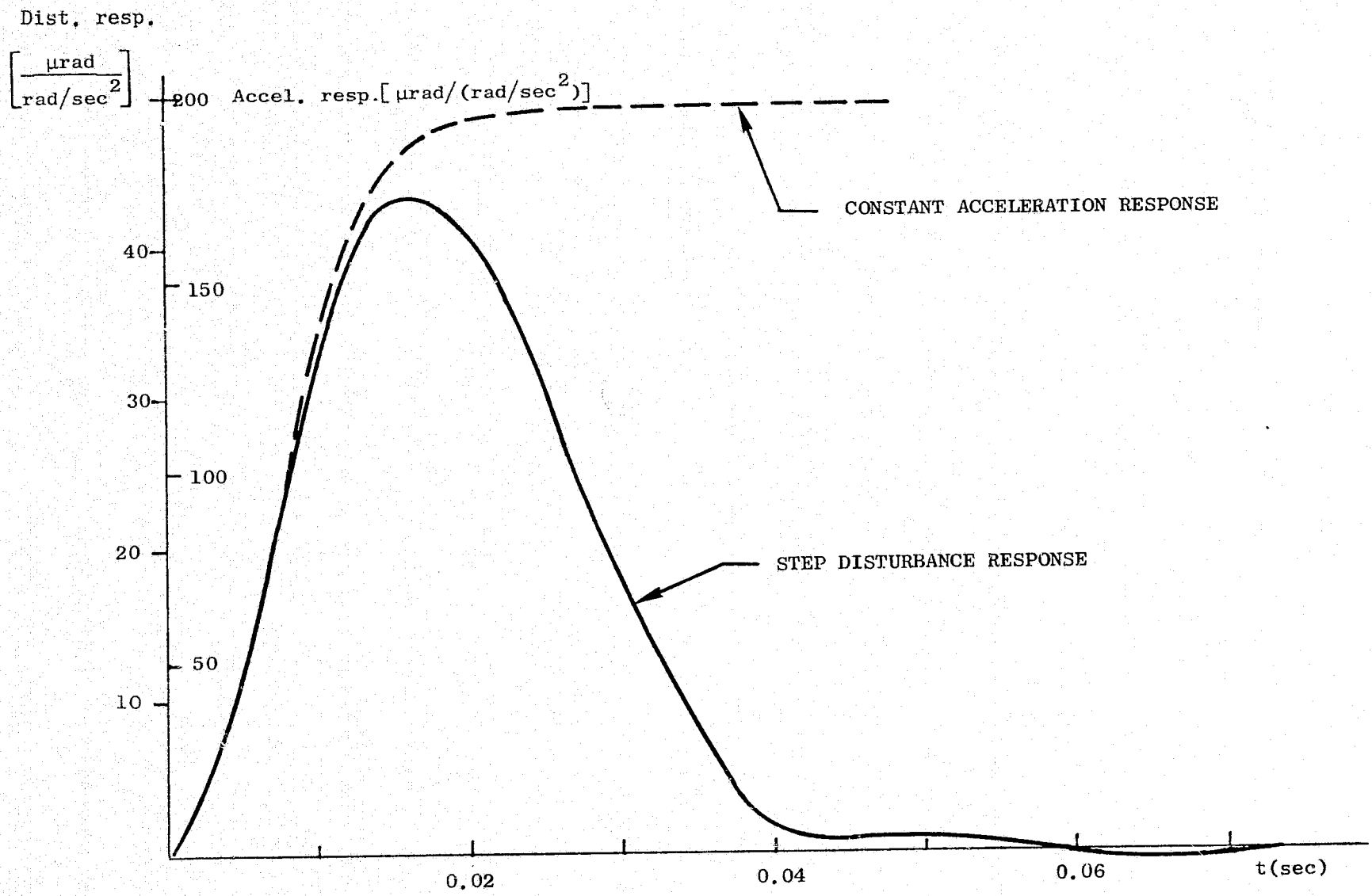

FIG. V-16 DISTURBANCE AND ACCELERATION RESPONSE OF REDUCED ORDER ESTIMATOR

E. PERFORMANCE OF THE SELECTED CONTROLLER

E-1 General

Some aspects of the performance of the selected controller will be examined in this Section. Its large signal operation is examined in the next Section and a nonlinear compensation network is introduced. In Section E-3 the effect of the sampler and hold linearization is assessed. In Section E-4, the tracking performance is compared with that of a similar system using aided tracking, and the effects of assuming a lower measurement noise are evaluated.

E-2 Large Signal Operation

As described in Section V-B, an acceleration command limiter is placed at the input to the torquer. The purpose of this limiter is to protect the torquer from saturation. Its characteristics are shown in Fig. V-17. It is not taken into account in the linear design of Section V-E, the results of which are therefore only valid for conditions in which the control amplitude is below the limit, i.e., for small displacements from the equilibrium condition. During target acquisition, however, the error amplitudes may be large and the acceleration command may exceed the limit. The stability of the system for large error signals, therefore, has to be examined.

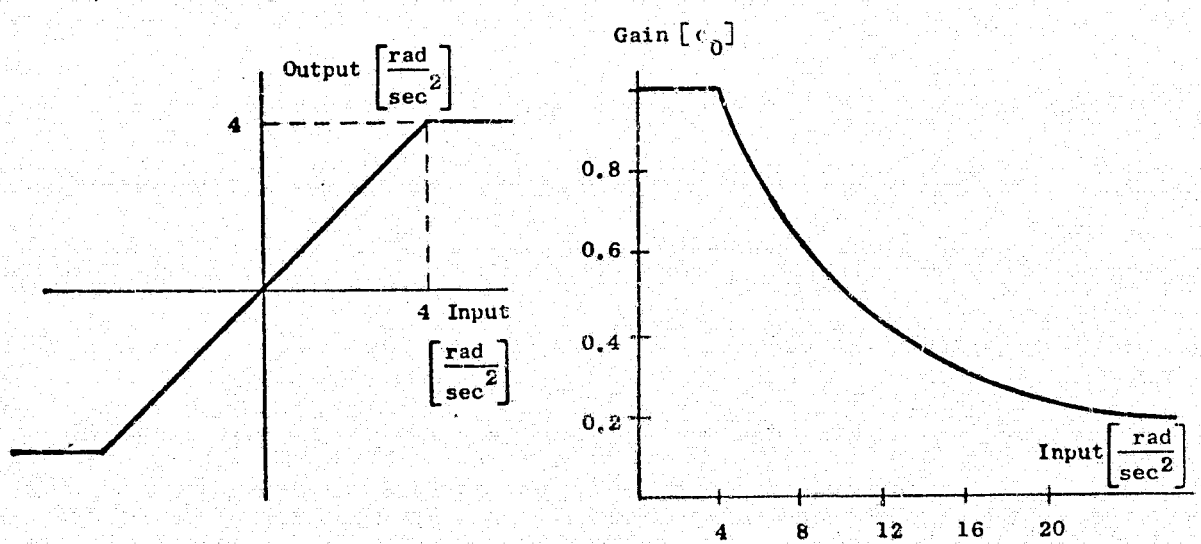

FIG. V-17 CHARACTERISTICS OF ACCELERATION LIMITER

The block diagram of the system with the acceleration limiter is shown in Fig. V-18. Since the control to both the plant and the estimator passes through the limiter, the estimator estimates the states correctly even when the limiter is operative. This is therefore the case described in Chapter II-C-4 of a state estimate feedback single-input single-output controller which has a variable control gain. Its dynamic equation is

$$\dot{x} = Fx + c_0 Gu ,$$

where c_0 is a variable scalar. In Appendix B it is shown that such a system has an infinite gain margin for c_0, but may become unstable if c_0 is decreased. It is also shown that the use of state estimates instead of the actual states for feedback has no influence on the stability considerations, and the stability analysis can therefore be made assuming that state feedback is used.

For the inner azimuth system, it can be seen from Fig. V-17 that for low control amplitudes $c_0 = 1$ and that it decreases with increasing amplitudes. Instability is therefore possible. Assuming that state feedback is used, the closed loop characteristic equation can be written in the form

$$\begin{aligned} & s^3(s + s_0)(s^2 + m_1 s + m_2) \\ & + c_0 m_2[(s+4f_o)(s^4 c_p + s^3 c_a + s^2 c_\omega + s c_\alpha + c_i) \\ & \qquad - 7.2 f_o (s c_y + c_i)] = 0 \end{aligned} \tag{5.15}$$

from which a root locus as a function of c_0 can be constructed.

From this equation is is obvious that for small values of c_0, the system will become unstable since the open loop system ($c_0 = 0$) has three roots at the origin. This is true for any set of the feedback gains as long as integral control is used. Without integral control, the open loop system has only two roots at the origin and therefore will be stable for all values of c_0.

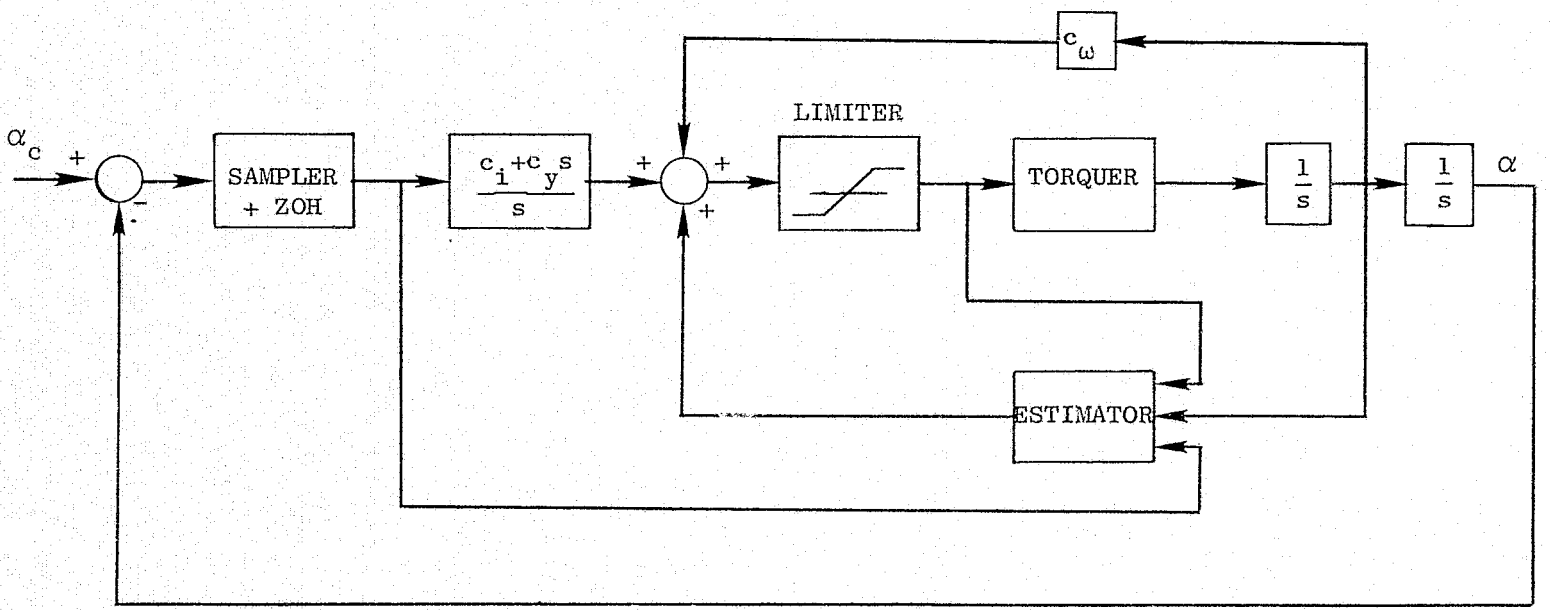

FIG. V-18 BLOCK DIAGRAM OF SYSTEM WITH LIMITER

The c_0 root locus for two values of the integral control gain is shown in Fig. V-19. The reduction of the integral gain can be seen to increase the stability region considerably. Therefore, although the large signal instability cannot be eliminated if integral control is used, it can be made to occur at higher signal levels if the integral control gain is reduced. It is therefore desirable to make the integral gain a function of the control amplitude so that for low signals, the tight integral control required for low tracking error is preserved. This is hard to implement in an analog system but if the control signal is assumed to be roughly proportional to the error signal, the same effect can be obtained by placing a limiter at the input to the integral control integrator. This is shown in Fig. V-20. The characteristics of the limiter are:

$$y_{out} = y_{in} \quad \text{for} \quad y_{in} < y_\ell$$

$$y_{out} = y_\ell \quad \text{for} \quad y_{in} \geq y_\ell .$$

The value of y_ℓ has to be set higher than the error level expected for the maximum acceleration command so as not to interfere with the acceleration tracking capabilities. The error signal level up to which the system remains stable has to be determined experimentally.

E-3 Effect of Sampler Linearization

The state representation of the system as derived in Section B-2 contains a linearization of the sampler and hold. The effect of this linearization has to be determined. The block diagram of V-6c is shown in simplified form in Fig. V-21. The dynamics of the continuous system can be represented as

$$\dot{x} = F_c x + G_c y, \qquad x(0) = x_0 \tag{5.16a}$$

where y is considered as a control. The discrete equivalent of Eq. (5.16a) is

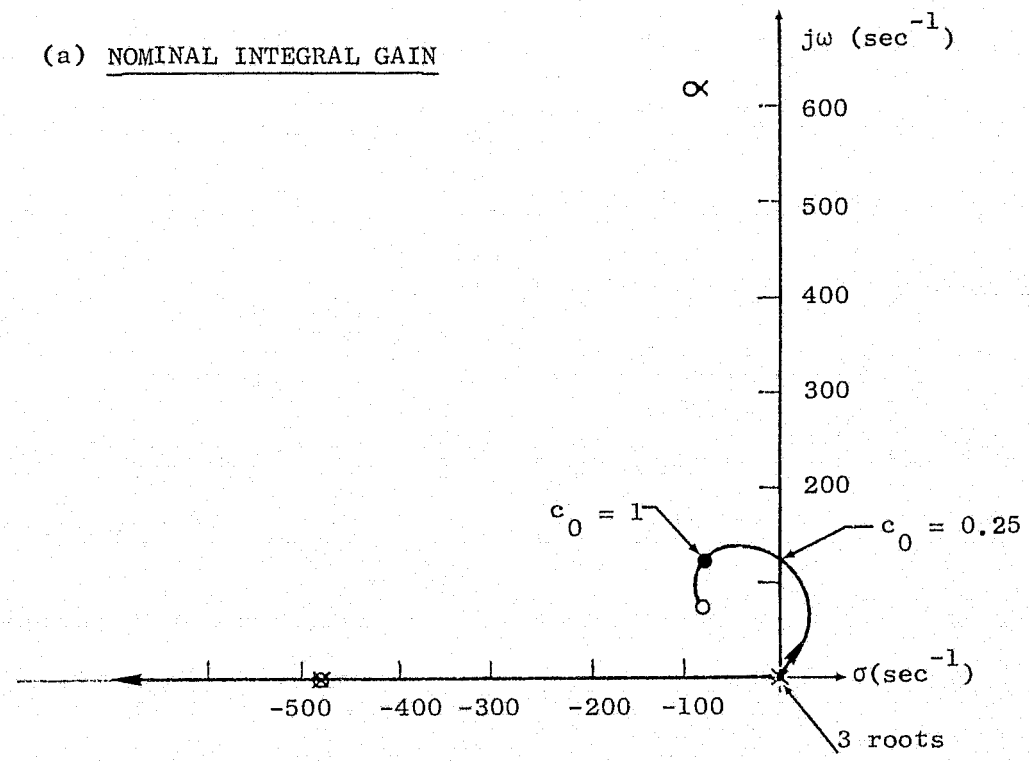

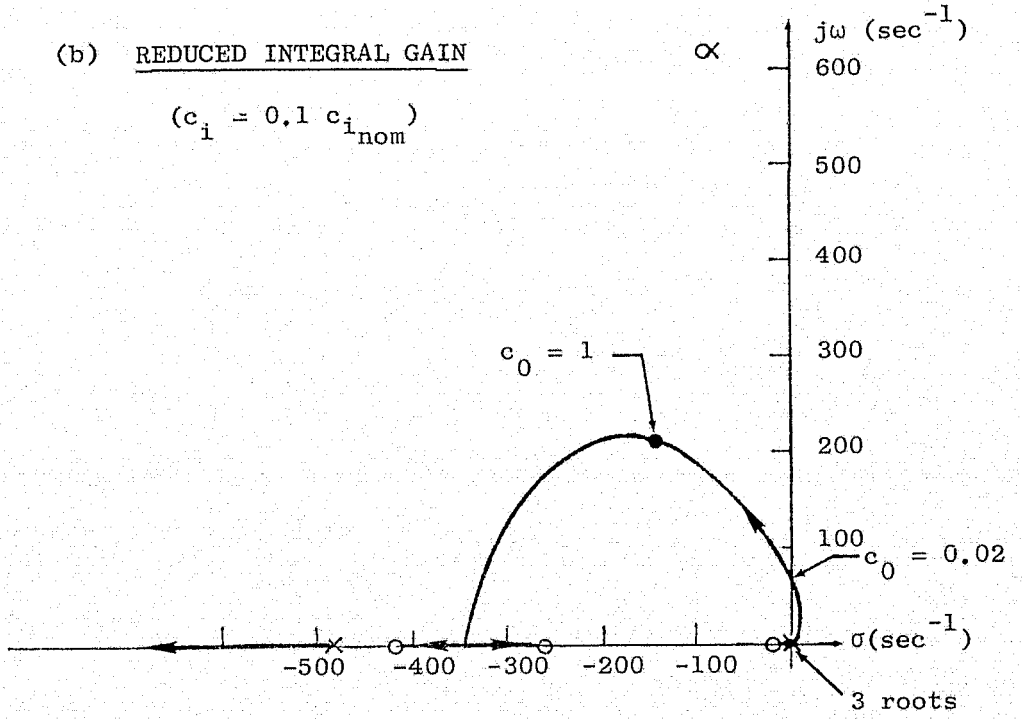

FIG. V-19 ROOT LOCUS AS A FUNCTION OF c_0

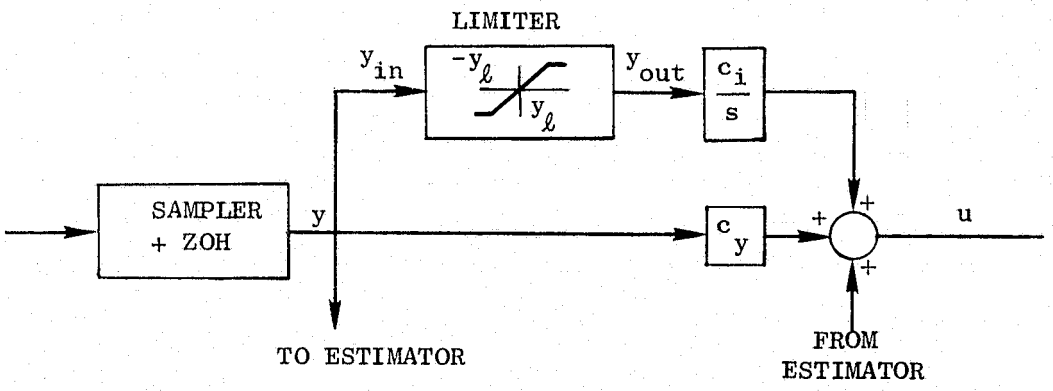

FIG. V-20 LIMITER FOR THE INTEGRAL GAIN

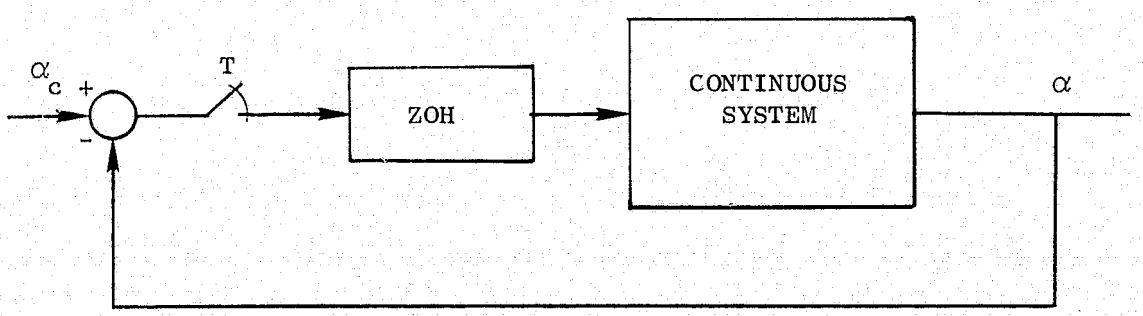

FIG. V-21 SIMPLIFIED REPRESENTATION OF CONTINUOUS SYSTEM WITH SAMPLER AND ZERO ORDER HOLD (ZOH).

$$x_{i+1} = \Phi x_i + \Gamma y_i, \qquad x(0) = x_0 \tag{5.16b}$$

where Φ is the transition matrix of the continuous system. Using

$$y_i = \alpha_{ci} - \alpha_i = \alpha_{ci} - Hx_i \tag{5.17}$$

Eq. (5.16b) becomes

$$x_{i+1} = (\Phi - \Gamma H)x_i + \Gamma\alpha_{ci}, \qquad x(0) = x_0. \tag{5.18}$$

From this equation the time response can be found for α_{ci} and x_0.

This was done with the aid of the computer program SIMUL [KA-1] that determines the state transition matrix Φ and discrete control distribution matrix, Γ, from the dynamics matrices F and G. The same program also calculates the time response of the system.

In Fig. V-22, the true time response, computed by this method, is compared with the one obtained from the system with the linearized sampler and hold. The correspondence is good although the exact system is somewhat less well damped, thus verifying that the effects of the zero order hold for a system with the bandwidth of 1/4 ω_s were adequately modeled by the first order model of Appendix G.

E-4 Comparison With Aided Tracking

1. Aided tracker description. The application of aided tracking to a system similar to the one discussed in this chapter is described by Fitts [FI-1]. In this application, the target motion information is processed by a digital Kalman filter in which the target is modeled as moving in a straight line in inertial coordinates. The output of the Kalman filter is a feedforward signal that is added to the feedback controller signal. Several versions of this method are described and results are presented for targets having both modeled and nonmodeled motion. These results are compared with those of a conventional feedback system and found to be much superior. The type of feedback system

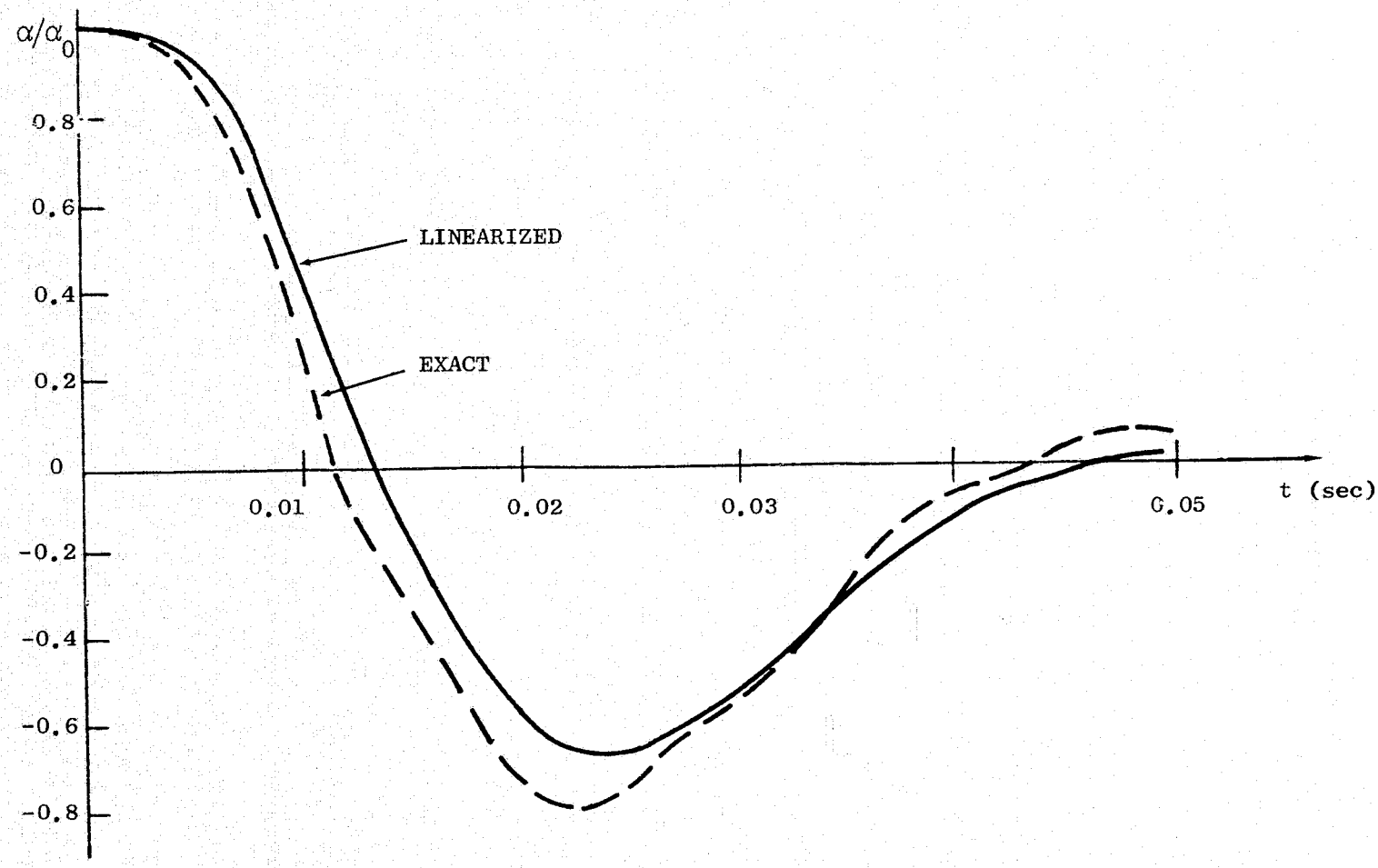

FIG. V-22 COMPARISON OF TIME RESPONSES OF LINEAR AND EXACT SYSTEMS

that is used for comparison is not specified but presumably it is a classical-type design since the acceleration error coefficients given represent the practical limits that are achievable with such a classical design.

In this Section the aided tracker is compared to the controller described in Section D. The application examples by Fitts refer to a system in which the torquer has a natural frequency that is lower than that of the system described in this Chapter. However, from the description of the aided tracking method, it seems that the results would be no different if this method were applied to the system of this Chapter.

The tracking of a target having a modeled motion is examined by Fitts by considering a straight line flyby with a peak angular acceleration of 0.5 rad/sec^2. The results are presented in the form of a rms tracking error defined for this particular profile as

$$\sigma_{az} = \left[\frac{1}{7}\int_1^{\infty} \delta_d^{\,2}\, dt\right]^{\frac{1}{2}} \qquad (5.19)$$

where δ_d is the tracking error. For this target motion, the aided tracker has no constant tracking error. The error is determined by the detector noise only. This noise is assumed to be $\sigma_d = 5$ μrad.

For unmodeled target motion, the results are given in the form of frequency response curves. Zero detector noise is assumed.

2. Comparison of feedback controller and aided tracker. Since the controller designed above is noise limited, a meaningful comparison of this controller with the aided tracker can only be made if the same detector noises are assumed for both designs. The comparison of the modeled target tracking will therefore be made for two noise levels: (a) $\sigma_d = 100$ μrad, as assumed in Section V-D; (b) $\sigma_d = 5$ μrad, as assumed in the paper.

3. $\sigma_d = 100$ μrad. The influence of different detector noise levels is examined by Fitts but only noise levels up to 50 μrad are considered. Extrapolating these results to 100 μrad, a rms tracking

noise of about 70 μrad is obtained.

For the SEF controller, the rms tracking error is caused by two effects: (a) output noise, (b) acceleration error. The numerical values were given in Table V-8. Using these values in Eq. (5.19), the rms tracking error is obtained as

$$\sigma_{az} = 75 \text{ μrad}$$

4. $\sigma_d = 5$ μrad. The rms error for the aided tracker is

$$\sigma_{AT} = 3.8 \text{ μrad.}$$

With this detector noise level, the noise limit on our controller is removed. The system bandwidth is now limited by the sampling rate. The effect of removing the noise limit is considered below for systems using DR 2 and D type estimators (see Table V-1). For the DR 2 system, a high gain controller is used (Design 2) and higher gains are selected for estimator No. 1 according to the acceleration error equation of App. K. The resulting eigenvalues are shown in Fig. V-23.

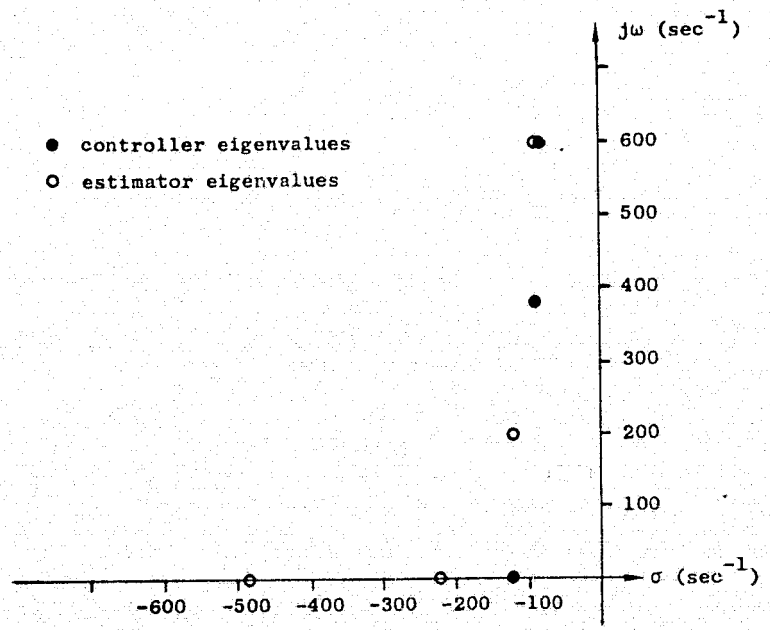

FIG. V-23 EIGENVALUES OF HIGH BANDWIDTH SYSTEM

The correspondence of the time response of this system with that of the exact simulation was found to be satisfactory. Its acceleration error is 70 μrad/(rad/sec^2). The rms tracking error as defined in Eq. (5.19) is

$$\sigma_{FC} = 25 \text{ μrad.}$$

The system using the D-type estimator has zero acceleration error (V-D-2). It was eliminated for the high noise case because it had unsatisfactory disturbance rejection. With the low detector noise, a higher estimator bandwidth is obtained and the disturbance rejection is therefore improved. The maximum deflection for a step disturbance is 85 μrad/(rad/sec^2). This value is still higher than that obtainable when the gyro is used as an additional measurement (see Table V-8).

The frequency response curves for unmodeled target motion as given by Fitts are reproduced in Fig. V-24. The two figures represent two different algorithms. The response of the sampling rate limited DR 2 system described above is overlaid on those curves.

Under the assumption of zero detector noise, the DR 2 system is seen to have lower error for frequencies higher than 1 cycle in all the cases represented in the paper. When nonzero detector noise is considered, the aided tracker has no advantage for even lower frequencies.

5. Evaluation. For nonmodeled targets, the aided tracker is seen to have an advantage over the high bandwidth feedback controller only for low frequencies and if a low detector noise is assumed.

For modeled target motion, comparable errors are obtained in both systems when a high detector noise is assumed. For a low detector noise, where the system is sampling-rate limited, the aided tracker has a lower error unless some disturbance rejection stiffness is sacrificed.

For this case the aided tracker therefore has an advantage. In summary, the high bandwidth controller that can be obtained by using full state feedback can match the performance of the aided tracker in most cases. The aided tracker has an advantage only in the case of

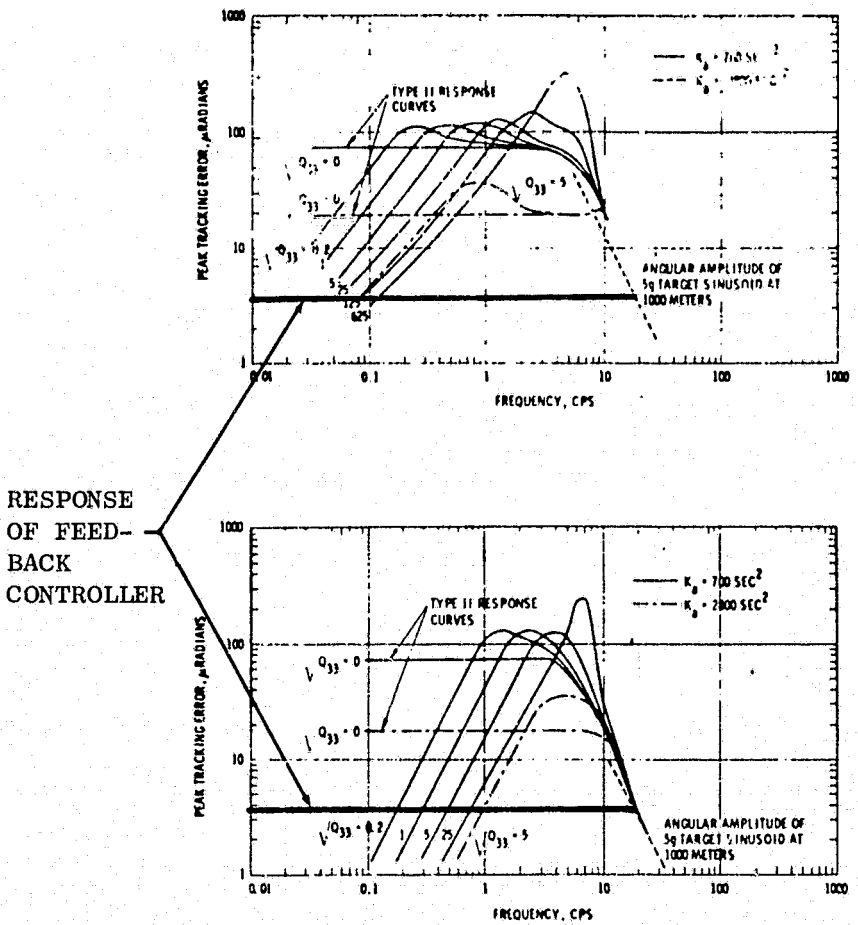

FIG. V-24 FREQUENCY RESPONSE OF AIDED TRACKER [FI-1]

a target that can be modelled and low detector noise. This advantage seems to be outweighed by the added cost of the computing capability and by the complexities of the aided tracker. If it is also taken into consideration that most tracked targets will not follow the model, the state feedback approach to the tracking problem seems to give a better solution.

F. SUMMARY

The design of a controller for the inner azimuth gimbal of a tracking telescope was presented. The controller was designed using state estimate feedback.

To obtain a controller for the entire system, additional controllers for the elevation and outer azimuth gimbals are required. The elevation controller may be identical to the inner azimuth controller except for some minor changes in the numerical values of the parameters due to the different moments of inertia. The outer azimuth controller is straightforward and may be designed by classical techniques.

The special feature of this problem is that the control is applied through an elastic element (the hydraulic torquer), which makes it difficult to obtain adequate damping at high bandwidths. Still, high bandwidth is required in order to obtain a low acceleration error coefficient. The ability of full state feedback to place the closed loop eigenvalues arbitrarily enables the system to obtain the required bandwidth with sufficient damping. The bandwidth and the acceleration error coefficient are limited either by the allowable controller noises or by the measurement sampling rate, depending on the measurement noise levels. These are common limits for controllers designed by state feedback. Stability considerations do not limit the bandwidth of such controllers as they do for many classical designs.

The principal design parameters for state feedback controllers are the state and control weights. However, important performance criteria, such as the acceleration error coefficient, cannot be conveniently expressed in terms of these weights and only general trends can be established. Several designs are therefore made and their performances compared.

Two measurements are available and it is possible to combine them in various ways in the estimator. The comparison between these designs is made according to the functional design criteria. Two measurement noise levels were considered. At the higher noise level, the system is

noise limited. A detailed comparison between several designs was made at this noise level. At the lower noise level the system performance is limited by the detector sampling rate. The influence of removing the noise limit was considered for two of the above designs.

The principal conclusions that were reached from the evaluation of the various designs are as follows.

1. The use of the gyroscope as a measurement, in addition to the target detector, improved the disturbance rejection properties of the system. However, it causes the system to be changed from Type 2 to Type 1.

2. At the high noise level the gyro rate mode is preferable to the rate integrating mode.

3. The ultimately selected system for this noise level is a system using a reduced order estimator. Its performance was made acceptable by the use of the sensitivity reduction method as a pole placement device.

4. Removing the noise limit on the bandwidth results in a decrease by a factor of 3 in the acceleration error of a system using both the gyro and the detector measurement. In a system using the detector measurement only (which has zero acceleration error), the step disturbance rejection is improved by a factor of 3.

5. The representation of the sampler and hold as a linear network proves to be a good approximation for the bandwidths considered, as shown by the closeness of the time responses of the real and the linearized systems.

6. The use of an aided tracker instead of a high bandwidth feedback controller has an advantage for a modeled target and low detector noise only.

In conclusion, the use of state feedback for this system results in a controller that has good transient response and the tracking capabilities which are comparable to those of a much more complicated aided tracker.

VI. CONCLUSIONS

In this thesis, the sensitivity of state feedback controllers (SEF) to parameter variations was investigated; a method was developed to reduce sensitivity, and it was applied to the Stanford Relativity Satellite. In addition, the design of a tracking telescope, partially aided by the sensitivity reduction method, was studied.

The principal conclusions in the area of parameter sensitivty are as follows.

1. The use of state estimate feedback, instead of state feedback, in systems in which there is a lightly damped elastic element between the control and the measurement, results in a considerable increase in the sensitivity to variations of the spring stiffness. Systems of this type are common and include structural resonance, systems with hydraulic actuators and others. Their sensitivity is caused by the multiple points of unity gain of their open loop transfer function and can be characterized by means of the frequency margin of stability. If the elastic element is sufficiently damped so that multiple points of unity gain are avoided, the sensitivity is considerably reduced.

2. The sensitivity reduction method that was developed in this thesis is an effective design tool, as demonstrated by the results of its application to the low order approximation and the full model of the Stanford Relativity Satellite. The range of stability was typically increased by a factor of 2 to 3. For originally optimal systems, the output error and the control effort were thereby increased by a factor of ≈ 2.

3. An efficient computational algorithm of the sensitivity reduction method is essential for this method to be applicable to fairly large systems. Considerable effort was therefore expended in the development of such an algorithm. The resulting computer program has reasonably

low computation times. The sensitivity reduction of a 12th order system requires four minutes approximately on an IBM 360/67 computer.

4. Sensitivity criteria may be a useful tool for the design of estimators. This is demonstrated by the use of the sensitivity reduction method for the design of a reduced order estimator for the tracking telescope.

The following conclusions were derived from the design of the controller for a large tracking telescope.

1. The use of a state estimate feedback controller for this system gives it a tracking capability that is comparable to that obtained by using a much more complicated aided tracker.

2. Since arbitrary pole placement is made possible by the use of full state feedback, there is no stability limit to the system bandwidth. The limit is instead determined either by the allowable control level or by the target detector sampling rate. Of these two limits, the one that is effective depends on the level of the noise inputs.

3. Two measurements are available and different estimator designs are possible using various combinations of these measurements. The relative merits of these estimators cannot be determined a priori and they are therefore compared according to the performance specifications. For noise limited systems, the optimum balance is sought between low controller noise on one hand, and low tracking error and good disturbance rejection on the other hand, with acceptable parameter sensitivity as an additional criterion.

A reduced order estimator using as measurements, the target detector and the gyro in its caged mode was finally selected for this case.

For the sample rate limited system, the estimator selection is more arbitrary.

4. The use of a saturating controller, together with integral control in an inertia-type plant ($1/s^2$), causes an unavoidable large

C.3

signal instability. This instability occurs at larger signals if the input to the integral control integrator is limited.

5. The modeling of the sampler and zero order hold by a linear network is justified in the considered range of bandwidths (up to about 40% of the sampling rate).

In summary, state estimate feedback is found to be an attractive design technique for high performance controllers. Its practical applicability is enhanced by the use of the sensitivity reduction method.

APPENDIX A

GAIN MARGIN OF STATE FEEDBACK CONTROLLERS

Consider a single input system

$$\dot{x} = Fx + c_0 Gu$$

$$u = -Cx$$

where C is a full state feedback gain matrix, and c_0 is a variable scalar parameter, the nominal value of which is unity. The system will have infinite gain margin to changes in c_0 if the roots of the numerator of $C(sI - F)^{-1}G$ are in the left half plane. This is also true if state estimate feedback instead of state feedback is used.

Proof

1. State Feedback

The closed loop characteristic equation of the system is

$$\begin{aligned} \det(sI - F + c_0GC) &= \det(sI - F)\ \det[I + c_0(sI - F)^{-1}GC] \\ &= \det(sI - F)\ [1 + c_0C(sI - F)^{-1}G] \\ &= \det(sI - F) + c_0C\ \mathrm{adj}(sI - F)G\ . \end{aligned}$$

As c_0 increases, m roots of the system tend towards the m roots of $C\ \mathrm{Adj}(sI - F)G$ and the others depart in $n - m$ asymptotic directions. It will now be shown that

$$m = n - 1$$

and that therefore only one root departs on an asymptote, along the

negative real axis.

The diagonal elements of $\text{adj}(sI - F)$ are monic polynomials of degree $n - 1$ in s. This is so because the minors of these elements are the determinants of $(n-1) \times (n-1)$ matrices with s in all their diagonal elements. Therefore, even if G has only one nonzero element the vector $\text{Adj}(sI - F)G$ will have at least one element of order $n - 1$ and since C has no zero elements, $C\ \text{adj}(sI - F)G$ is a polynomial of degree $n - 1$. If the roots of $C\ \text{adj}(sI - F)G$ are in the left half plane, all the roots will therefore remain stable as c_0 increases. QED.

2. State Estimate Feedback

In this case the closed loop characteristic equation is

$$\det(sI - F + c_0GC)\ \det(sI - F + KH)$$

$$= [\det(sI - F) + c_0C\ \text{adj}(sI - F)G]\ \det(sI - F + KH).$$

The estimator roots are therefore unaffected by changes in c_0 and the proof remains valid.

APPENDIX B

PROGRAM PAROPT

1. General

This Appendix contains a partial listing of the program PAROPT and its operating instructions. The listing includes all the subroutines that were developed for the program. For the subroutines that were obtained from the Program Library of the Computer Science Department at Stanford University, only the description is given in the listing. Subroutines from the IBM Library (GMPROD and GMTRAN) are not listed. Sufficient comment lines have been introduced to make the program self explanatory.

2. Operating Instructions

a. Range of the program

Order of system: 12
Number of variable parameters: 5
Number of free parameters: 30
Number of controls: 3

b. Input. The program is stored in compiled form. The input to the program consists of two parts: (1) subroutine SETUP, (2) Data and options.

(1) Subroutine SETUP. This subroutine defines the relationship between the parameters (fixed, free, and variable), the coefficients of the system matrices, and the control gains. It has to be written for each system that is being optimized.

The input to this subroutine consists of the current values of the free parameter vector. The output consists of the F, Γ, and C matrices (see Eqs. 4.3 and 4.9). The subroutine is compiled and adjoined to the compiled program. The program can then be run with different data sets. A sample subroutine SETUP, with the job control language that is

required in order to load it on the IBM 360/67 computer of Stanford University is shown in Fig. B-1. M405. PAROPT on line 39 is the name of the load module that is created. This can be changed to any name selected by the user.

It is recommended that this subroutine be made as general as possible so that different sets of parameters can be defined as free or variable without changing the subroutine.

(2) Data and options. The data cards are:

Card 1: System description: N, NS, NZ, NP, NC, NW

- N Order of system
- NS Number of variable parameters
- NZ Number of free parameters
- NP Number of fixed parameters
- NC Number of controls
- NW Number of disturbances

Format: 5I3

Card 2: Options: NFLAG, NPRINT, NCO. All these parameters are either 0 or 1.

NFLAG = 0. Only initial conditions are required.

NPRINT = 0. Only condensed information is printed about the PI, gradient, and values of the free parameters at each step of the search.

NCO = 0: C is not a function of the free parameters.

Format: 3I3

Card 3: EPS, TOL, DIS

- EPS The relative weight of the additional cost. If EPS $< 10^{-6}$, δX is not evaluated and only the nominal PI minimization problem is solved.
- TOL A measure of the relative precision of the final values of the free parameters. Recommended initial value: 10^{-4}.
- DIS Use 10^{-4}

Format: 3E12.5

```
1.      //PAROPT1 JOB 'M405,301,1.,3','HADASS'
2.      //STEP1  EXEC  FORTHCL,PARM.FORT='OPT=2'
3.      //FORT.SYSIN  DD  *
4.            SUBROUTINE SETUP(Z,A,B,C)
5.            IMPLICIT REAL*8 (A-H,O-Z)
6.            DIMENSION Z(30),A(12,12),B(12,5),C(3,12)
7.            COMMON/PARM/ Q(12,12),R(5,5),V(5,5),QR(3),P(30),S(10),EPS
8.            DO 10 I=1,6
9.            DO 10 J=1,6
10.        10 A(I,J)=0.
11.           DO 20 I=1,5
12.        20 A(I,I+1)=1.
13.           S1=S(1)
14.           A(3,1)=-P(1)*S1
15.           A(3,2)=-P(2)*S1-S1
16.           A(3,3)=-P(3)*S1-S(2)
17.           DO 30 I=1,3
18.        30 A(3,I+3)=P(I)*S1
19.           A(4,4)=-Z(1)
20.           A(5,4)=-Z(2)
21.           A(6,2)=Z(4)-S(1)
22.           A(6,3)=Z(5)-S(2)
23.           A(6,4)=-Z(3)
24.           A(6,5)=-Z(4)
25.           A(6,6)=-Z(5)
26.           DO 40 I=1,6
27.           DO 40 J=1,2
28.        40 B(I,J)=0.
29.           B(3,1)=S1
30.           B(6,1)=S1
31.           DO 50 I=1,3
32.        50 B(I+3,2)=-Z(I)
33.           DO 60 I=1,3
34.           C(1,I)=P(I)
35.        60 C(1,I+3)=-P(I)
36.           RETURN
37.           END
38.     /*
39.     //LKED.SYSLMOD  DD  DSNAME=M405.PAROPT,VOLUME=SER=SYS16,UNIT=2314,
40.     //                  DISP=(NEW,KEEP),SPACE=(TRK,(2,3,1))
41.     //LKED.O  DD  DSNAME=M405.PAROPT,VOLUME=SER=SYS16,UNIT=2314,
42.     //                  DISP=(OLD,KEEP)
43.     //LKED.SYSIN  DD *
44.      INCLUDE O(PAROP)
45.      ENTRY MAIN
46.        NAME PAROP
47.     /*
```

FIG. B-1 SAMPLE OF SUBROUTINE SETUP FOR SIXTH ORDER SYSTEM

Cards 4 and on.

a. Fixed, variable, and free parameters in this order. Six parameters to a card. Each set starts on a new card.

b. The state weight matrix. Read by rows, six numbers to a row.

c. Control weight vector. For this program the control weight matrix is constrained to diagonal form and therefore only the NC diagonal elements are read.

d. The covariance matrix of the variable parameters. Read by rows. Six numbers to a row.

e. The covariance matrix of the disturbances. Read by rows. Six numbers to a row.

Format: 6E12.5

A sample data set with the JCL required to run it on the IBM 360/67 computer is shown in Fig. B-2. M405. PAROPT on line 2 is to be changed to the name selected when loading the subroutine SETUP.

(c) Output. For NFLAG = 0, the printout consists of the initial dynamics, weight, and covariance matrices, initial eigenvalues, and initial nominal and additional PI. For NFLAG = 1, the printout contains, in addition, search information, as well as final values for the free parameters.

A typical printout for NPRINT = 1 is shown in Fig. B-3. For each cost evaluation, the nominal (J_o), additional (J_A), and total PI ($J_o + \epsilon J_A$) are printed out as well as the values of the free parameters. The total PI is given as a fraction of its initial value. At the end of each iteration, more detailed information is printed out.

(3) Suggestions for the use of the program.

(a) Execute an initial run with NFLAG = 0 in order to find the initial relative values of the nominal and additional PI.

(b) Initially select the weighting coefficient, ϵ, and the parameter covariance matrix so that $\epsilon J_A > 10\ J_o$. A design that is mainly determined by sensitivity consideration results. If its nominal properties are unsatisfactory, execute additional runs with lower ϵ.

(c) Limit the time of the run according to the general guidelines given in Section IV-C-4. Even if this causes the run to stop before it is finished, the resulting design may be satisfactory since toward the end the program may become less efficient.

```
//PAROPT2 JOB 'M405,301,1.,5','UAPASS'
//JOBLIB  DD  DSNAME=M405.PAROPT,VOLUME=SER=SYS16,UNIT=2314,
//             DISP=(OLD,PASS)
//STEP1  EXEC PGM=PAROP
//FT06F001  DD  SYSOUT=A
//FT05F001  DD  *
  6  2  5  3  1  2
  0  1  0  0
     1.           1.00E-4     1.00E-6
     .447         .661        1.216
     .4           .3
     .88          .39         -.068       .4          .3
     .2




     1.
     .16                                  .09
     1.                                   1.
/*
```

FIG. B-2   SAMPLE OF DATA FOR SIXTH ORDER SYSTEM

Annotations: Results of 1 PI evaluation; free parameters; J_o; J_A; $J_o + \epsilon J_A$ (relative)

```
0.10258587692476 6D 05     0.54760527622467 9D 03     0.94951985083043 4D 00
  0.18554910996197 5D 02     0.17523269036978 4D 03     0.15466696664650 4D 02
 -0.30790151726539 3D 02     0.26220436984324 6D 02
0.10258587692527 1D 05     0.54760527556050 3D 03     0.94951985023804 3D 00
  0.18554910996197 5D 02     0.17523269035508 3D 03     0.15466696679551 6D 02
 -0.30790151726539 3D 02     0.26220436984324 6D 02
0.10258587692450 6D 05     0.54760527625594 8D 03     0.94951985085726 7D 00
  0.18554910996197 5D 02     0.17523269035508 3D 03     0.15466696664650 4D 02
 -0.30790151711638 1D 02     0.26220436984324 6D 02
0.10258587693378 3D 05     0.54760527678491 8D 03     0.94951985137239 5D 00
  0.18554910996197 5D 02     0.17523269035508 3D 03     0.15466696664650 4D 02
 -0.30790151726539 3D 02     0.26220436999225 8D 02

STATUS AT ITERATION #     1

   CURRENT SOLUTION            GRADIENT                DIRECTION OF SEARCH
 0.18554910996197 5D 02    0.10362025350332 3D-02    -0.17319531013715 7D-01
 0.17523269035508 3D 03    0.43317293749259 5D-02    -0.23368332644259 8D-01
 0.15466696664650 4D 02   -0.35422919318080 0D-01     0.21325760369145 9D 00
-0.30790151726539 3D 02    0.61324685811996 5D-02    -0.39032007908244 5D-01
 0.26220436984324 6D 02    0.40702170692384 2D-01     0.92179890133512 9D-01

APPROXIMATE MINIMUM VALUE OF F:    0.94951985076588 6D 00         ALPHA:    0.36743593100 02
NUMBER OF FUNCTION EVALUATIONS:    16
```

FIG. B-3   TYPICAL PRINTOUT OF PROGRAM PAROPT

LISTING OF PROGRAM PAROPT

```
C            PROGRAM PAROPT
      IMPLICIT REAL*8(A-H,O-Z)
      LOGICAL          PRINT, BRIEF
      DIMENSION Z(30)
      COMMON N,NS,NP,NW,NC,NCO
      COMMON/PARM/ Q(12,12),P(5,5),V(5,5),QR(3),PAR(30),SI(10),EPS,DIS
      COMMON /CRITER/ ETA, TOL, STEPMX, DEPS
      COMMON /LOGICL/ BRIEF, PRINT, UNITL
      EXTERNAL COST,STARTR
  510 FORMAT(6I3)
  511 FORMAT(6F12.5)
  513 FORMAT(4I3)
  512 FORMAT(3F12.5)
  355 FORMAT('0','ORDER OF SYSTEM=',I2,/,' VARIABLE PARAMETERS=',I2,/,'
     1FREE PARAMETERS=',I2,/,' EPS=',F7.3)
  356 FORMAT('0','INITIAL COST ONLY REQUIRED')
  357 FORMAT(' ',6X,'NCO=',I2)
C
C       N IS THE ORDER OF THE SYSTEM
C       NS IS THE NUMBER OF THE VARIABLE PARAMETERS
C       NZ IS THE NUMBER OF FREE PARAMETERS
C       NP IS THE NUMBER OF FIXED PARAMETERS
C       NC IS THE NUMBER OF CONTROLS
C       NW IS THE NUMBER OF DISTURBANCES
C
      READ(5,510) N, NS, NZ, NP, NC, NW
C
C       IF NFLAG=0 ONLY INITIAL CONDITIONS ARE REQUIRED
C       IF NPRINT=0 SEARCH PRINTOUT IS CONDENSED
C       IF NCO=0 C IS NOT A FUNCTION OF THE FREE PARAMETERS
C
      READ(5,513) NFLAG,  NPRINT, NCO ,NXOF
C
C       EPS IS THE RELATIVE WEIGHTING ON THE ADDITIONAL COST
C       TOL IS THE RELATIVE PRECISION OF THE FINAL VALUES OF
C           THE FREE PARAMETERS
C       DIS IS THE RELATIVE PERTURBATION OF THE VARIABLE PARAMETERS
C
      READ(5,512) EPS, TOL, DIS
C
C       PAR- FIXED PARAMETERS
C       SI - VARIABLE PARAMETERS
C       Z  - FREE PARAMETERS
C
      READ(5,511)(PAR(I),I=1,NP)
      READ(5,511)(SI(I),I=1,NS)
      READ(5,511)(Z(I),I=1,NZ)
C
C       Q - THE STATE WEIGHT MATRIX
C       QR- THE CONTROL WEIGHT VECTOR
```

```
C       R - THE COVARIANCE MATRIX OF THE VARIABLE PARAMETERS
C       V - THE COVARIANCE MATRIX OF THE DISTURBANCES
C
      READ(5,511)((Q(I,J),J=1,N),I=1,N)
      READ(5,511)(CR(I),I=1,NC)
      READ(5,511)((P(I,J),J=1,NS),I=1,NS)
      READ(5,511)((V(I,J),J=1,NW),I=1,NW)
      WRITE(6,355)N,NS,NZ,EPS
      WRITE(6,357) NCO
      IF(NFLAG.EQ.1)GO TO 323
      WRITE(6,356)
  323 IF(NPRINT.EQ.0) GO TO 100
      PRINT=.TRUE.
      BRIEF=.FALSE.
      GO TO 110
  100 PRINT=.FALSE.
      BRIEF=.TRUE.
  110 CALL DINIT(COST,NZ,Z)
          IF(NFLAG.EQ.0)GO TO 600
          NLDIM=NZ*(NZ-1)/2
          CALL MINMZF(NZ, Z, NLDIM, COST, STARTR)
  600 STOP
      END
```

```
C-----------------------------------------------------------------------
C
C     SUBROUTINE DINIT
C
C     THIS SUBROUTINE WRITES THE INITIAL DATA AND CALCULATES THE
C     INITIAL PI AND EIGENVALUES USING SUBROUTINE COST
C
C     INPUT TO SUBROUTINE DINIT
C
C     NZ     :  THE NUMBER OF FREE PARAMETERS
C     Z      :  THE FREE PARAMETER VECTOR
C     FUN    :  A SUBROUTINE RETURNING THE VALUE OF THE PI AT THE
C               POINT DEFINED BY THE VECTOR Z.
C
C-----------------------------------------------------------------------
C
      SUBROUTINE DINIT(FUN,NZ,Z)
      IMPLICIT REAL*8(A-H,O-Z)
      DIMENSION A(12,12),B(12,5),Z(30),C(3,12)
      COMMON N,NS,NP,NW,NC,NCO
      COMMON/ROOTS/CR(12),CI(12)
      COMMON/PARM/ Q(12,12),R(5,5),V(5,5),QR(3),PAR(30),SI(10),EPS,DIS
      COMMON/TO/EPI,API
         COMMON/MODES/MODE
      COMMON/EVAL/NEVAL
  201 FORMAT('0',//,2X,'THE INITIAL DYNAMICS MATRIX...')
  208 FORMAT('0',//,2X,'THE DISTURBANCE DISTRIBUTION MATRIX...')
  214 FORMAT('0',//,30X,'INITIAL COST',//,10X,'BASIC COST',11X,'ADDITION
     1AL COST',12X,'TOTAL COST')
  202 FORMAT('0',4X,3(1PD25.15))
  204 FORMAT('0',//,30X,'INITIAL ROOTS',//,20X,'REAL',24X,'IMAG.')
  216 FORMAT('0',//,2X,'THE DISTURBANCE COVARIANCE MATRIX...')
  206 FORMAT(2(13X,F14.8))
  400 FORMAT('0',//,2X,'THE PARAMETER COVARIANCE MATRIX...')
  100 FORMAT('0',//,2X,'THE STATE WEIGHT...')
  101 FORMAT('0',//,2X,'THE CONTROL WEIGHT...')
      CALL SETUP(Z, A ,B, C )
      WRITE(6,201)
      CALL MATOUT(A,12,12,N,N)
      WRITE(6,100)
      CALL MATOUT(Q, 12, 12, N, N )
      WRITE(6,101)
      WRITE(6,202)(QR(I),I=1,NC)
      WRITE(6,208)
      CALL MATOUT(B, 12, 5, N, NW )
      WRITE(6,216)
      CALL MATOUT(V,5,5,NW,NW)
      WRITE(6,400)
      CALL MATOUT(R,5,5,NS,NS)
      NEVAL=0
         MODE=0
      CALL FUN (NZ, Z, F )
      WRITE(6,214)
      WRITE(6,202)EPI,API,F
      WRITE(6,204)
      WRITE(6,206)(CR(I),CI(I),I=1,N)
      RETURN
      END
```

```
C-----------------------------------------------------------------------
C
C      SUBROUTINE COST
C
C      THIS SUBROUTINE CALCULATES THE COST USING SUBROTINE DERIV
C      FOR THE CALCULATION OF X AND DX.
C
C      INPUT TO SUBROUTINE COST:
C
C      NZ     :  THE NUMBER OF FREE PARAMETERS
C      Z      :  THE FREE PARAMETER VECTOR
C
C      OUTPUT FROM SUBROUTINE COST
C
C      PI     :  THE VALUE OF THE PI AT THE POINT DEFINED BY THE
C                VECTOR Z.
C
C-----------------------------------------------------------------------
C
      SUBROUTINE COST(NZ, Z, PI)
      IMPLICIT REAL*8(A-H,O-Z)
      DIMENSION Z(30),XX(12,12),DX(12,12),B(12,5),Q1(12,12),
     1C(3,12)
      COMMON N,NS,NP,NW,NC,NCO
      COMMON/PARM/ Q(12,12),R(5,5),V(5,5),QR(3),PAR(30),SI(10),EPS,DIS
      COMMON/TQ/FPI,API
      COMMON/EVAL/NEVAL
         COMMON/MODES/MODE
         COMMON/STORE/GX(12,12),GDX(12,12),GY(12,12,5),GYY(12,12,5)
  220 FORMAT('0',//,2X,'THE STATE COVARIANCE MATRIX')
      CALL DERIV(XX,DX,Z,C,&650)
      FPI=0.
      API=0.
      IF(NEVAL.GT.0.AND.NCO.EQ.0)GO TO 41
      DO 54 I=1,N
      DO 54 J=1,N
   54 Q1(I,J)=0.
      DO 55 I=1,N
      DO 55 J=1,N
      DO 55 K=1,NC
   55 Q1(I,J)=C(K,I)*C(K,J)*QR(K)+Q1(I,J)
   41 IF(NEVAL.GT.0)GO TO 150
         F1=1.1
       WRITE(6,220)
           CALL MATOUT(XX,12,12,N,N)
  150 DO 50 J=1,N
      DO 50 K=1,N
      FPI=FPI+Q1(K,J)*XX(J,K)
      IF (EPS.LE.1.D-5)GO TO 50
      API=API+Q1(K,J)*DX(J,K)
   50 CONTINUE
      GO TO 60
```

```
650 FPI=1.D6*FPI
    API=0.
 60 PI=FPI+EPS*API
       IF(NEVAL.GT.0)GO TO 68
       F0=PI
       GO TO 65
68     PI=PI/F0
      IF(MODE.EQ.1.OR.PI.GT.F1)GO TO 65
       F1=PI
       DO 66 I=1,N
       DO 66 J=I,N
       GX(I,J)=XX(I,J)
       GDX(I,J)=DX(I,J)
       GX(J,I)=GX(I,J)
66     GDX(J,I)=GDX(I,J)
       DO 67 I=1,N
       DO 67 J=1,N
      DO 67 K=1,NS
67     GYY(I,J,K)=GY(I,J,K)
65  WRITE(6,208)FPI,API,PI
208 FORMAT(3(4X,D25.15))
    WRITE(6,212)(Z(I),I=1,NZ)
212 FORMAT(3(6X,D25.15))
    NEVAL=NEVAL+1
    RETURN
    END
```

```
C-----------------------------------------------------------------------
C
C     SUBROUTINE DERIV
C
C     THIS SUBROUTINE DETERMINES THE VALUES OF X AND DX FOR A
C     GIVEN Z VECTOR.
C
C     INPUT TO SUBROUTINE DERIV:
C
C     Z      : THE FREE PARAMETER VECTOR.
C
C     OUTPUT FROM SUBROUTINE DERIV:
C
C     XX     : THE NOMINAL COVARIANCE MATRIX.
C     DX     : THE ADDITIONAL COVARIANCE MATRIX.
C     C      : THE CONTROL GAIN MATRIX.
C
C-----------------------------------------------------------------------
C
      SUBROUTINE DERIV(XX,DX,Z,C,*)
      IMPLICIT REAL*8(A-H,O-Z)
      DIMENSION XX(12,12),DX(12,12),B(12,5),BV(12,5),BT(5,12),A(12,12),
     1A1(12,12),B1(12,5),C(3,12),C1(3,12),DA(12,12),DB(12,5),DAT(12,12),
     2UL(78,78),IPS(78),CQ(12,12),DAX(12,12),UL1(78,78),IPS1(78),
     3QE(78),COV(78),Y(12,12),Z(30),D(12),INT(12),GA(12,12),
     4GAX(12,12)
      COMMON N,NS,NP,NG,NC,NCO
      COMMON/PARM/ Q(12,12),R(5,5),V(5,5),QR(3),PAR(30),SI(10),EPS,DIS
      COMMON/ROOTS/CWR(12),CWI(12)
         COMMON/MODES/MODE
         COMMON/STORE/GX(12,12),GDX(12,12),GY(12,12,5),GYY(12,12,5)
      CALL SETUP(Z,A,B,C)
         IF(MODE.EQ.1)GO TO 201
C
C       MODE=0- THE INITIAL VALUE OF THE PI OR THE PI ALONG A LINEAR
C               SEARCH POINT IS EVALUATED.
C       MODE=1-THE PI IS EVALUATED FOR GRADIENT DETERMINATION.
C               PERTUBATION EQUATIONS ARE USED.
C
      DO 110 I=1,N
      DO 110 J=1,N
         GA(I,J)=A(I,J)
  110 A1(I,J)=A(I,J)
C
C       EIGENVALUE DETERMINATION. USED TO DETERMINE STABILITY OF
C       SELECTED POINT.
C
      CALL BALANC (12, N, A1, LO, IHI, D )
      CALL ELMHES (12, N, LO, IHI, A1, INT )
      CALL HQR (12, N, LO, IHI, A1, CWR, CWI,  IERR )
      DO 200 I=1,N
      IF(CWR(I).GE.0.)GO TO 720
  200 CONTINUE
```

```
C
C       EVALUATION OF THE RIGHT HAND SIDE OF THE EQUATION
C
C       (1)   A*XX+XX*A'=-B*V*B'.
C
C       THE RIGHT HAND SIDE IS TEMPORARILY STORED IN XX.
C
  201 CALL GMPROD(B,V,BV,N,NG,NG,12,5)
      CALL GMTRAN(B,BT,N,NG,12,5)
      CALL GMPROD(BV,BT,XX,N,NG,N,12,5)
         IF(MODE.EQ.0)GO TO 202
C
C       EVALUATION OF THE ADDED TERMS OF THE RIGHT HAND SIDE OF
C       THE PERTURBATION EQUATION
C
C       (2) A*XX+XX*A'=-B*V*B'-A*GX-GX*A'.
C
C       WHERE GX IS THE COVARIANCE MATRIX AT THE NOMINAL POINT AND
C       XX IS THE PERTURBATION OF THE COVARIANCE MATRIX DUE TO THE
C       PERTURBATION OF Z.
C
          CALL GMPROD(A,GX,GAX,N,N,N,12,12)
          DO 203 I=1,N
          DO 203 J=I,N
          XX(I,J)=XX(I,J)+GAX(I,J)+GAX(J,I)
  203     XX(J,I)=XX(I,J)
          CALL SCOV(GA,XX,UL,QE,COV,IPS,2)
          DO 204 I=1,N
          DO 204 J=I,N
          XX(I,J)=XX(I,J)+GX(I,J)
  204     XX(J,I)=XX(I,J)
          GO TO 205
  202 CALL SCOV(GA,XX,UL,QE,COV,IPS,1)
  205 DO 5 I=1,N
      DO 5 J=1,N
    5 DX(I,J)=0.
      IF(EPS.LT.1.D-6)GO TO 100
C
C       EVALUATION OF DA/DS(I) AND DB/DS(I).
C
      DO 90 M=1,NS
      DSI=DIS*SI(M)
      SID=SI(M)
      SI(M)=SI(M)+DSI
      CALL SETUP(Z,A1,B1,C1)
      SI(M)=SID
      DO 30 I=1,N
      DO 10 J=1,N
   10 DA(I,J)=(A1(I,J)-A(I,J))/DSI
      DO 20 K=1,NG
   20 DB(I,K)=(B1(I,K)-B(I,K))/DSI
   30 CONTINUE
```

```
C
C       EVALUATION OF THE RIGHT HAND SIDE OF THE SYMMETRIC EQUATION
C
C       (3) A*Y+Y*A'=-B*V*(DB/DS(I))-XX*(DA/DS(I))
C
      CALL GMTRAN(DB,BT,N,NG,12,5)
      CALL GMPROD(BV,BT,A1,N,NG,N,12,5)
      CALL GMTRAN(DA,DAT,N,N,12,12)
      CALL GMPROD(XX,DAT,DAX,N,N,N,12,12)
      DO 40 I=1,N
      DO 40 J=I,N
      CQ(I,J)=DAX(I,J)+DAX(J,I)+A1(I,J)+A1(J,I)
   40 CQ(J,I)=CQ(I,J)
         IF(MODE.EQ.0)GO TO 207
C
C       EVALUATION OF THE ADDITIONAL TERMS OF THE SYMMETRIC
C       PERTURBATION EQUATION
C
C       (4) A*DY+DY*A'=-A*GY-GY*A'-B*V*(DB/DS(I))-GX*(DA/DS(I))
C
C       WHERE GY IS THE VALUE OF Y AT THE NOMINAL POINT AND
C       DY IS THE PERTURBATION IN Y DUE TO THE PERTURBATION IN Z.
C
         DO 208 I=1,N
         DO 208 J=1,N
  208    GAX(I,J)=0.
         DO 209 I=1,N
         DO 209 J=1,N
         DO 209 K=1,N
  209    GAX(I,J)=A(I,K)*GYY(K,J,M)+GYY(I,K,M)*A(J,K)+GAX(I,J)
         DO 210 I=1,N
         DO 210 J=1,N
  210    CQ(I,J)=CQ(I,J)+GAX(I,J)+GAX(J,I)
C
C       SOLUTION OF THE SYMMETRIC EQUATION (3).
C
  207 CALL SCOV(A,CQ,UL,QE,COV,IPS,2)
      DO 50 I=1,N
      DO 50 J=1,N
   50 Y(I,J)=CQ(I,J)
C
C       EVALUATION OF THE RIGHT SIDE OF THE ANTISYMMETRIC EQUATION(3).
C
      N1=N-1
      DO 60 I=1,N1
      I1=I+1
      DO 60 J=I1,N
      CQ(I,J)=DAX(I,J)+A1(I,J)-DAX(J,I)-A1(J,I)
         IF(MODE.EQ.0)GO TO 60
C
C       EVALUATION OF THE ADDITIONAL TERMS OF THE ANTISYMMETRIC
C       EQUATION(4).
C
```

```
          CQ(I,J)=CQ(I,J)+GAX(I,J)-GAX(J,I)
   60     CONTINUE
          IF(MODE.EQ.0)GO TO 211
C
C         SOLUTION OF THE ANTISYMMETRIC EQUATION (4).
C
          CALL SCOVA(A,CQ,UL1,QE,COV,IPS1,2)
          GO TO 212
C
C         SOLUTION OF THE ANTISYMMETRIC EQUATION(3).
C
  211  CALL SCOVA(A,CQ,UL1,QE,COV,IPS1,M)
  212  DO 70 I=1,N
       DO 70 J=1,N
   70  Y(I,J)=(CQ(I,J)+Y(I,J))/2.
          IF(MODE.EQ.1)GO TO 213
          DO 214 I=1,N
          DO 214 J=1,N
  214     GY(I,J,M)=Y(I,J)
          GO TO 215
  213     DO 216 I=1,N
          DO 216 J=1,N
  216     Y(I,J)=Y(I,J)+GYY(I,J,M)
C
C         EVALUATION OF THE RIGHT HAND SIDE OF THE EQUATION
C
C         (5) A*DX+DX*A'=-SIGMA(DAT(M)+A1(M)*R(M,M)),    M=1,NS
C
C         WHERE
C             DAT(M)=(DA/DS(M))*Y
C             A1(M)=(DB/DS(M))*V*(DB/DS(M))'
C             NS IS THE NUMBER OF VARIABLE PARAMETERS.
C
  215  CALL GMPROD(DA,Y,DAT,N,N,N,12,12)
       CALL SYMPRD(DB,V,A1,NG,N,12,5)
       DO 80 I=1,N
       DO 80 J=I,N
       DAT(I,J)=DAT(I,J)+DAT(J,I)
   80  DAT(J,I)=DAT(I,J)
       DO 85 I=1,N
       DO 85 J=1,N
   85  DX(I,J)=(DAT(I,J)+A1(I,J))*R(M,M)+DX(I,J)
   90  CONTINUE
          IF (MODE.EQ.0)GO TO 221
C
C         EVALUATION OF THE ADDITIONAL TERMS OF THE RIGHT HAND SIDE
C         OF THE PERTURBATION EQUATION
C
C         (5) A*DDX+DDX*A'=-SIGMA(DAT(M)+A1(M)*R(M,M))-A*GDX-GDX*A'
C                                                          M=1,NS
C
C         WHERE GDX IS THE VALUE OF DX AT THE NOMINAL POINT.
```

```
C
      CALL GMPROD(A,GDX,GAX,N,N,N,12,12)
      DO 217 I=1,N
      DO 217 J=1,N
217   DX(I,J)=DX(I,J)+GAX(I,J)+GAX(J,I)
C
C     SOLUTION OF EQUATIONS(5) OR (6).
C
221   CALL SGDV(A,DX,UL,DE,CCV,IPS,2)
      IF(MODE.EQ.0)GO TO 100
218   DO 220 I=1,N
      DO 220 J=1,N
220   DX(I,J)=DX(I,J)+GDX(I,J)
      GO TO 100
720   RETURN 1
100   RETURN
      END
```

```
C-----------------------------------------------------------------------
C
C     SUBROUTINE SCOV
C
C     THIS SUBROUTINE SOLVES THE EQUATION
C
C       A*X+X*A'=G
C
C     WITH SYMMETRIC G.
C       THE EQUATION IS TRANSFORMED INTO THE FORM
C
C       V*Z=B
C
C     WHERE
C           Z IS THE (N+1)*N VECTOR OF THE ELEMENTS OF X,
C           B IS THE (N+1)*N VECTOR OF THE ELEMENTS OF G,
C           F IS OBTAINED FROM A BY THE TRANSFORMATION OF THIS
C             SUBROUTINE.
C
C     INPUT TO SUBROUTINE SCOV:
C
C     Q      : THE MATRIX G
C     AVCN   : THE MATRIX A
C     MODE   : MODE=1-V IS COMPUTED(EVALUATION OF XX)
C              MODE>1-THE STORED V IS USED(EVALUATION OF Y AND DX)
C
C     OUTPUT FROM SUBROUTINE SCOV:
C
C     UL     : THE LU TRANSFORMATION OF THE V MATRIX
C     QE     : THE VECTOR B
C     COV    : THE VECTOR Z
C     Q      : THE MATRIX X.NOTE THAT THE MATRIX G IS NOT PRESERVED.
C
C-----------------------------------------------------------------------
C
      SUBROUTINE SCOV(AVCN,Q,UL,QE,COV,IPS,MODE)
      IMPLICIT REAL*8(A-H,O-Z)
      DIMENSION AVCN(12,12),Q(12,12),COV(78),QE(78),
     1UL(78,78),L(12,12),IPS(78)
      COMMON/VMAT/V(78,78)
      COMMON N,NS,NP,NG,NC,NCO
      M=N*(N+1)/2
      K = 0
      DO 20 I = 1,N
      DO 20 J = I,N
      K = K+1
      QE(K) =-Q(I,J)
      L(I,J) = K
   20 L(J,I) = K
      IF(MODE.EQ.2)GO TO 90
      DO 30 I = 1,M
      DO 30 J = 1,M
   30 V(I,J) =0.D0
```

```
      DO 40 I = 1,N
      DO 40 J = 1,N
      DO 40 K = 1,N
   40 V(L(I,K),L(J,K)) = AVCN(I,J)+V(L(I,K),L(J,K))
      DO 50 I = 1,N
      DO 50 J = 1,M
   50 V(L(I,I),J)=2.D0*V(L(I,I),J)
   90 CALL LINSY2(MODE,N,V,78,QF,COV,UL,IPS,DIGITS,&141,&142,&143)
      K = 0
      DO 80 I = 1,N
      DO 80 J = I,N
      K = K+1
      Q(I,J) =COV(K)
   80 Q(J,I) = Q(I,J)
      GO TO 155
  141 WRITE(6,151)
      GO TO 155
  142 WRITE(6,152)
      GO TO 155
  143 WRITE(6,153)
      GO TO 155
  151 FORMAT('****MATRIX WITH A ROW OF ALL ZERO ELEMENTS FOUND')
  152 FORMAT('****ZERO PIVOT ELEMENT FOUND')
  153 FORMAT('****MAXIMUM NUMBER OF ITERATIONS REACHED IN IMPROVE')
  155 CONTINUE
      RETURN
      END
```

```
C-----------------------------------------------------------------------
C
C     SUBROUTINE SCOVA
C
C     THIS SUBROUTINE SOLVES THE EQUATION
C
C       A*X+X*A'=G
C
C     WITH ANTISYMMETRIC G.
C       THE EQUATION IS TRANSFORMED INTO THE FORM
C
C       V*Z=B
C
C     WHERE
C           Z IS THE (N-1)*N VECTOR OF THE ELEMENTS OF X,
C           B IS THE (N-1)*N VECTOR OF THE ELEMENTS OF G,
C           F IS OBTAINED FROM A BY THE TRANSFORMATION OF THIS
C             SUBROUTINE.
C
C     INPUT TO SUBROUTINE SCOVA:
C
C     CQ    : THE MATRIX G
C     A     : THE MATRIX A
C     M     : M=1-V IS COMPUTED(FIRST VARIABLE PARAMETER)
C             M>1-THE STORED V IS USED(OTHER VARIABLE PARAMETERS)
C
C     OUTPUT FROM SUBROUTINE SCOVA:
C
C     UL    : THE LU TRANSFORMATION OF THE V MATRIX
C     QE    : THE VECTOR B
C     COV   : THE VECTOR Z
C     CQ    : THE MATRIX X.NOTE THAT THE MATRIX G IS NOT PRESERVED.
C
C-----------------------------------------------------------------------
C
      SUBROUTINE SCOVA(A,CQ,UL,QE,COV,IPS,M)
      IMPLICIT REAL*8(A-H,O-Z)
      DIMENSION A(12,12),CQ(12,12),UL(78,78),IPS(78),
     1QE(78),COV(78)
      COMMON N,NS,NP,NG,NC,NCO
      COMMON/VMAT/V(78,78)
      MN=N*(N-1)/2.
      DO 70 I=1,MN
      DO 70 J=1,MN
   70 V(I,J)=0.
      K=0
      N1=N-1
      DO 80 I=1,N1
      I1=I+1
      DO 80 J=I1,N
      K=K+1
   80 QE(K)=-CQ(I,J)
      MODE=1
      IF(M.GT.1)GO TO 100
      N1=N-1
      DO 15 I=1,N1
      DO 10 J=1,N1
   10 V(I,J)=A(I+1,J+1)
   15 V(I,I)=V(I,I)+A(1,1)
```

```
      DO 60 K=2,N1
      J1=(K-1)*(2*N-K)/2
      K1=K-1
      NK=N-K
      L=0
      DO 30 I=1,K1
      DO 20 J=1,NK
      V(K1+L,J1+J)=-A(I,J+K)
      V(K1+L+J,J1+J)=A(I,K)
      V(J1+J,K1+L)=-A(J+K,I)
      V(J1+J,K1+L+J)=A(K,I)
20    CONTINUE
      L=L+N-I-1
30    CONTINUE
      DO 50  I=1,NK
      DO 40 J=1,NK
40    V(J1+I,J1+J)=A(I+K,J+K)
50    V(J1+I,J1+I)=A(K,K)+V(J1+I,J1+I)
60    CONTINUE
      GO TO 110
100   MODE=2
110   CALL LINSY2(MODE,MN,V,78,QE,COV,UL,IPS,DIGITS,&141,&142,&143)
      K=0
      N1=N-1
      DO 90 I=1,N1
      I1=I+1
      DO 90 J=I1,N
      K=K+1
      CQ(I,J)=COV(K)
      CQ(I,I)=0
90    CQ(J,I)=-CQ(I,J)
      CQ(N,N)=0.
      GO TO 155
141   WRITE(6,151)
      GO TO 155
142   WRITE(6,152)
      GO TO 155
143   WRITE(6,153)
      GO TO 155
151   FORMAT('****MATRIX WITH A ROW OF ALL ZERO ELEMENTS FOUND')
152   FORMAT('****ZERO PIVOT ELEMENT FOUND')
153   FORMAT('****MAXIMUM NUMBER OF ITERATIONS REACHED IN IMPROVE')
155   CONTINUE
      RETURN
      END
```

```
C-----------------------------------------------------------------------
C
C     SUBROUTINE MATOUT
C
C     THIS SUBROUTINE WRITES THE MATRIX A
C
C     INPUT TO SUBROUTINE MATOUT:
C
C     A      : THE MATRIX A(I*J)
C     ND1    : THE NUMBER OF ROWS IN THE STORAGE ARRAY OF A.
C     ND2    : THE NUMBER OF COLUMNS IN THE STORAGE ARRAY OF A.
C
C-----------------------------------------------------------------------
C
      SUBROUTINE MATOUT(A,ND1,ND2,I,J)
      DIMENSION A(ND1,ND2)
      DOUBLE PRECISION A
    1 FORMAT(5HO ROW,7(8X,4HCOL.,I3,1X))
    2 FORMAT(I4,4X,1P7D16.8)
      DO 10 JJ=1,J,7
      J7=JJ+6
      IF(J7.GT.J) J7=J
      WRITE(6,1)(JK,JK=JJ,J7)
      DO 10 II=1,I
   10 WRITE(6,2)II,(A(II,JK),JK=JJ,J7)
      RETURN
      END
```

```
C-----------------------------------------------------------------------
C
C     SUBROUTINE SYMPRD
C
C     THIS SUBROUTINE FINDS THE PRODUCT
C
C           C=A*B*A'
C
C     INPUT TO SUBROUTINE SYMPRD:
C
C     A      : THE MATRIX A(N*M)
C     B      : THE MATRIX B(M*M)
C     I1     : THE NUMBER OF ROWS IN THE STORAGE ARRAY OF A
C     I2     : THE NUMBER OF COLUMNS IN THE STORAGE ARRAY OF A
C
C     OUTPUT FROM SUBROUTINE SYMPRD:
C
C     C      : THE MATRIX C(N*N)
C
C-----------------------------------------------------------------------
C
      SUBROUTINE SYMPRD(A,B,C,M,N,I1,I2)
      IMPLICIT REAL*8(A-H,O-Z)
      DIMENSION A(I1,M),B(I2,M),C(I1,N),D(12,12)
      DO 10 I=1,N
      DO 10 J=1,N
      D(I,J)=0.
   10 C(I,J)=0.

      DO 20 I=1,N
      DO 20 J=1,M
      DO 20 K=1,M
   20 D(I,J)=A(I,K)*B(K,J)+D(I,J)
      DO 40 I=1,N
      DO 40 J=I,N
      DO 40 K=1,M
   40 C(I,J)=D(I,K)*A(J,K)+C(I,J)
      DO 30 I=2,N
      IN=I-1
      DO 30 J=1,IN
   30 C(I,J)=C(J,I)
      RETURN
      END
C
```

```
C-----------------------------------------------------------------------|
C
      SUBROUTINE LINSY2(MODE, N, A, IDIM, B, X, LU, IPS, DIGITS,*,*,*)
C     PROGRAMMER: S. R. DUTROW, JR.
C                 COMPUTER SCIENCE DEPARTMENT, STANFORD UNIVERSITY
C     CONVERTED FOR USE WITH THE WATFOR COMPILER FEBRUARY 1970
C                 MICHAEL MALCOLM, COMPUTER SCIENCE DEPARTMENT, STANFORD
C
C
C     REFERENCES: BASED ON THE SINGLE PRECISION REAL LINEAR SYSTEM
C                 PACKAGE WRITTEN BY JOHN W. WELCH OF SLAC, WHICH IS
C                 IN TURN, AN ADAPTATION OF THE METHODS DESCRIBED IN
C                 FORSYTHE AND MOLER, "COMPUTER SOLUTION OF LINEAR
C                 ALGEBRAIC SYSTEMS", PRENTICE HALL, 1967.
C
C      INDEX OF DOUBLE PRECISION LINEAR SYSTEMS PACKAGE:
          INTEGER MODE, N, IDIM, IPS(N)
          REAL*8 A(IDIM,N), LU(IDIM,N), B(N), X(N)
          REAL DIGITS
C         USES SUBROUTINES DECMP2, SOLVE2, AND IMPRV2 (IF REQUESTED) TO
C         FIND THE SOLUTION TO THE LINEAR SYSTEMS A*X=B. THE MATRIX LU
C         (AND IPS) WILL CONTAIN THE DECOMPOSITION OF A.
C         THE SOLUTION IS TO DOUBLE PRECISION ACCURACY.
C         MODE = 1: DECOMPOSE A, DO NOT IMPROVE THE SOLUTION X.
C         MODE = 2: ASSUME LU CONTAINS THE DECOMPOSITION,
C                   DO NOT IMPROVE X.
C         MODE = 3: DECOMPOSE A AND IMPROVE THE SOLUTION X.
C         MODE = 4: ASSUME LU CONTAINS THE DECOMPOSITION AND IMPROVE X.
          EXTERNAL DECMP2, SOLVE2, IMPRV2
C-----------------------------------------------------------------------|
      SUBROUTINE DECMP2 (N, A, IDIM, LU, IPS, *,*)
          INTEGER N, IDIM, IPS(N)
          REAL*8 A(IDIM,N), LU(IDIM,N), DMAX1, DABS
C         DECOMPOSE THE N*N MATRIX A INTO TRIANGULAR L & U SO THAT
C         L*U = A. IPS IS THE ROW PIVOT VECTOR.
C         MATRIX A WILL BE OVERWRITTEN BY LU IF A AND LU ARE
C         DECLARED TO BE THE SAME MATRIX IN THE CALL OF DECMP2.
C         RETURN 1 FOR ALL ZERO ELEMENTS IN A ROW.
C         RETURN 2 FOR ZERO PIVOT.
C-----------------------------------------------------------------------|
C
      SUBROUTINE SOLVE2 (N, LU, IDIM, B, X, IPS)
          INTEGER N, IDIM, IPS(N)
          REAL*8 LU(IDIM,N), B(N), X(N)
C         SOLVES A*X=B USING LU FROM SUBROUTINE DECMP2.
C         FIRST SOLVES THE TRIANGULAR LINEAR SYSTEM LY = B
C         AND THEN SOLVES THE SYSTEM U*X = Y.
C         IPS IS THE ROW INTERCHANGE VECTOR FROM DECMP2.
C-----------------------------------------------------------------------|
```

```
C
C ********************************** START OF DPPUT,IPTOTL ****************
C                                    UP TO 2/6/73
      SUBROUTINE  DPPUT(A , B)
C
C
C     DPPUT, IPTOTL AND THE FOLLOWING BLOCK DATA SUBPROGRAM
C     ARE USED TOGETHER FOR ACCUMULATING EUCLIDEAN INNER PRODUCTS
C     OF DOUBLE PRECISION VECTORS.   THEY MAY ALSO BE USED FOR
C     CALCULATING OTHER EXTENDED SUMMATIONS.
C
C
C     PROGRAMMER:  GORDON GULLAHORN
C                  STANFORD UNIVERSITY
C                  AUGUST 1969
C
C     REVISED BY:  MICHAEL MALCOLM
C                  COMPUTER SCIENCE DEPARTMENT
C                  STANFORD UNIVERSITY
C                  16 NOVEMBER 1969
C
C     REFERENCE: "AN ALGORITHM FOR FLOATING POINT ACCUMULATION
C                 OF SUMS WITH SMALL RELATIVE ERROR"
C                 COMMUNICATIONS OF THE ACM,VOL 14 NO 11,NOV.1971
C
C     THE SUM IS ACCUMULATED IN AN ARRAY B, WHICH IS IN THE
C     LABELLED COMMON 'DPACCC'.
C
C     THE SUBROUTINES OPERATE AS FOLLOWS:
C
C        BLOCK DATA   :  INITIALIZES THE ACCUMULATOR 'B' TO ZERO.
C                        THE BLOCK DATA SUBPROGRAM OPERATES AS A
C                        DATA STATEMENT.  THE USER SHOULD NOT ATTEMPT
C                        TO CALL IT
C
C        DPPUT(A,B)   :  ADDS THE PRODUCT A*B TO THE ACCUMULATOR
C
C        IPTOTL(X)    :  COMPUTES THE TOTAL OF THE PRODUCTS IN THE
C                        ACCUMULATOR AND ASSIGNS THIS VALUE TO X.
C                        IPTOTL THEN RESETS THE ACCUMULATORS TO ZERO.
C
C     IF NO OVERFLOWS OR UNDERFLOWS OCCUR, THE FINAL RESULT IS GUAR-
C     ANTEED TO HAVE 12 SIGNIFICANT DIGITS.  IF EITHER A OR B IS SMALLER
C     16**(-62), EXPONENT UNDERFLOW IS LIKELY TO OCCUR IN
C     SEPARATING THE HIGH AND LOW ORDER PARTS OF A OR B.
C     SIMILARLY, UNDERFLOW MAY OCCUR IF |A*B| < 10**-50.
C
C
C
```

```
C     ------------------------------------------------------------------
C
      SUBROUTINE BALANC(NM,N,A,LOW,IGH,SCALE)
C
      INTEGER I,J,K,L,M,N,JJ,NM,IGH,LOW,IEXC
      REAL*8 A(NM,N),SCALE(N)
      REAL*8 C,F,G,R,S,B2,RADIX
      REAL*8 DABS
      LOGICAL NOCONV
C
C     THIS SUBROUTINE IS A TRANSLATION OF THE ALGOL PROCEDURE BALANCE,
C     NUM. MATH. 13, 293-304(1969) BY PARLETT AND REINSCH.
C     HANDBOOK FOR AUTO. COMP., VOL.II-LINEAR ALGEBRA, 315-326(1971).
C
C     THIS SUBROUTINE BALANCES A REAL MATRIX AND ISOLATES
C     EIGENVALUES WHENEVER POSSIBLE.
C
C     ON INPUT:
C
C        NM MUST BE SET TO THE ROW DIMENSION OF TWO-DIMENSIONAL
C          ARRAY PARAMETERS AS DECLARED IN THE CALLING PROGRAM
C          DIMENSION STATEMENT;
C
C        N IS THE ORDER OF THE MATRIX;
C
C        A CONTAINS THE INPUT MATRIX TO BE BALANCED.
C
C     ON OUTPUT:
C
C        A CONTAINS THE BALANCED MATRIX;
C
C        LOW AND IGH ARE TWO INTEGERS SUCH THAT A(I,J)
C          IS EQUAL TO ZERO IF
C           (1) I IS GREATER THAN J AND
C           (2) J=1,...,LOW-1 OR I=IGH+1,...,N;
C
C        SCALE CONTAINS INFORMATION DETERMINING THE
C           PERMUTATIONS AND SCALING FACTORS USED.
C
C     SUPPOSE THAT THE PRINCIPAL SUBMATRIX IN ROWS LOW THROUGH IGH
C     HAS BEEN BALANCED, THAT P(J) DENOTES THE INDEX INTERCHANGED
C     WITH J DURING THE PERMUTATION STEP, AND THAT THE ELEMENTS
C     OF THE DIAGONAL MATRIX USED ARE DENOTED BY D(I,J).  THEN
C        SCALE(J) = P(J),    FOR J = 1,...,LOW-1
C                 = D(J,J),        J = LOW,...,IGH
C                 = P(J)           J = IGH+1,...,N.
C     THE ORDER IN WHICH THE INTERCHANGES ARE MADE IS N TO IGH+1,
C     THEN 1 TO LOW-1.
C
C     NOTE THAT 1 IS RETURNED FOR IGH IF IGH IS ZERO FORMALLY.
C
C     THE ALGOL PROCEDURE EXC CONTAINED IN BALANCE APPEARS IN
C     BALANC  IN LINE.  (NOTE THAT THE ALGOL ROLES OF IDENTIFIERS
C     K,L HAVE BEEN REVERSED.)
C
C     QUESTIONS AND COMMENTS SHOULD BE DIRECTED TO B. S. GARBOW,
C     APPLIED MATHEMATICS DIVISION, ARGONNE NATIONAL LABORATORY
C
C     ------------------------------------------------------------------
```

```
C     ------------------------------------------------------------------
C
C
      SUBROUTINE ELMHES(NM,N,LOW,IGH,A,INT)
C
      INTEGER I,J,M,N,LA,NM,IGH,KP1,LOW,MM1,MP1
      REAL*8 A(NM,N)
      REAL*8 X,Y
      REAL*8 DABS
      INTEGER INT(IGH)
C
CC    THIS SUBROUTINE IS A TRANSLATION OF THE ALGOL PROCEDURE ELMHES,
CC    NUM. MATH. 12, 349-368(1968) BY MARTIN AND WILKINSON.
CC    HANDBOOK FOR AUTO. COMP., VOL.II-LINEAR ALGEBRA, 339-358(1971).
CC
CC    GIVEN A REAL GENERAL MATRIX, THIS SUBROUTINE
CC    REDUCES A SUBMATRIX SITUATED IN ROWS AND COLUMNS
CC    LOW THROUGH IGH TO UPPER HESSENBERG FORM BY
CC    STABILIZED ELEMENTARY SIMILARITY TRANSFORMATIONS.
CC
CC    ON INPUT:
CC
CC       NM MUST BE SET TO THE ROW DIMENSION OF TWO-DIMENSIONAL
CC         ARRAY PARAMETERS AS DECLARED IN THE CALLING PROGRAM
CC         DIMENSION STATEMENT;
CC
CC       N IS THE ORDER OF THE MATRIX;
CC
CC       LOW AND IGH ARE INTEGERS DETERMINED BY THE BALANCING
CC         SUBROUTINE  BALANC.  IF  BALANC  HAS NOT BEEN USED,
CC         SET LOW=1, IGH=N;
CC
CC       A CONTAINS THE INPUT MATRIX.
CC
CC    ON OUTPUT:
CC
CC       A CONTAINS THE HESSENBERG MATRIX.  THE MULTIPLIERS
CC         WHICH WERE USED IN THE REDUCTION ARE STORED IN THE
CC         REMAINING TRIANGLE UNDER THE HESSENBERG MATRIX;
CC
CC       INT CONTAINS INFORMATION ON THE ROWS AND COLUMNS
CC         INTERCHANGED IN THE REDUCTION.
CC         ONLY ELEMENTS LOW THROUGH IGH ARE USED.
CC
CC    QUESTIONS AND COMMENTS SHOULD BE DIRECTED TO B. S. GARBOW,
CC    APPLIED MATHEMATICS DIVISION, ARGONNE NATIONAL LABORATORY
C
```

```
      SUBROUTINE HQR(NM,N,LOW,IGH,H,WR,WI,IERR)
C
      INTEGER I,J,K,L,M,N,EN,LL,MM,NA,NM,IGH,ITS,LOW,MP2,ENM2,IERR
      REAL*8 H(NM,N),WR(N),WI(N)
      REAL*8 P,Q,R,S,T,W,X,Y,ZZ,MACHEP
      REAL*8 DSQRT,DABS,DSIGN
      INTEGER MIN0
      LOGICAL NOTLAS
C
C     THIS SUBROUTINE IS A TRANSLATION OF THE ALGOL PROCEDURE HQR,
C     NUM. MATH. 14, 219-231(1970) BY MARTIN, PETERS, AND WILKINSON.
C     HANDBOOK FOR AUTO. COMP., VOL.II-LINEAR ALGEBRA, 359-371(1971).
C
C     THIS SUBROUTINE FINDS THE EIGENVALUES OF A REAL
C     UPPER HESSENBERG MATRIX BY THE QR METHOD.
C
C     ON INPUT:
C
C        NM MUST BE SET TO THE ROW DIMENSION OF TWO-DIMENSIONAL
C          ARRAY PARAMETERS AS DECLARED IN THE CALLING PROGRAM
C          DIMENSION STATEMENT;
C
C        N IS THE ORDER OF THE MATRIX;
C
C        LOW AND IGH ARE INTEGERS DETERMINED BY THE BALANCING
C          SUBROUTINE  BALANC.  IF  BALANC  HAS NOT BEEN USED,
C          SET LOW=1, IGH=N;
C
C        H CONTAINS THE UPPER HESSENBERG MATRIX.  INFORMATION ABOUT
C          THE TRANSFORMATIONS USED IN THE REDUCTION TO HESSENBERG
C          FORM BY  ELMHES  OR  ORTHES, IF PERFORMED, IS STORED
C          IN THE REMAINING TRIANGLE UNDER THE HESSENBERG MATRIX.
C
C     ON OUTPUT:
C
C        H HAS BEEN DESTROYED.  THEREFORE, IT MUST BE SAVED
C          BEFORE CALLING  HQR  IF SUBSEQUENT CALCULATION AND
C          BACK TRANSFORMATION OF EIGENVECTORS IS TO BE PERFORMED;
C
C        WR AND WI CONTAIN THE REAL AND IMAGINARY PARTS,
C          RESPECTIVELY, OF THE EIGENVALUES.  THE EIGENVALUES
C          ARE UNORDERED EXCEPT THAT COMPLEX CONJUGATE PAIRS
C          OF VALUES APPEAR CONSECUTIVELY WITH THE EIGENVALUE
C          HAVING THE POSITIVE IMAGINARY PART FIRST.  IF AN
C          ERROR EXIT IS MADE, THE EIGENVALUES SHOULD BE CORRECT
C          FOR INDICES IERR+1,...,N;
C
C        IERR IS SET TO
C          ZERO       FOR NORMAL RETURN,
C          J          IF THE J-TH EIGENVALUE HAS NOT BEEN
C                     DETERMINED AFTER 30 ITERATIONS.
C
C     QUESTIONS AND COMMENTS SHOULD BE DIRECTED TO B. S. GARBOW,
C     APPLIED MATHEMATICS DIVISION, ARGONNE NATIONAL LABORATORY
C
C     ------------------------------------------------------------------
```

```
C     DRIVING ROUTINE FOR UNCONSTRAINED MINIMIZATION WITHOUT DERIVATIVES
C-----------------------------------------------------------------------
C-----------------------------------------------------------------------
      SUBROUTINE MINMZE( N, NLDIM, FUN, START )
C-----------------------------------------------------------------------
      IMPLICIT REAL*8 ( A-H, L, O-Z )
      LOGICAL         BRIEF, CONV
      COMMON /CRITER/ ETA, TOL, STEPMX
      COMMON /LOGICL/ BRIEF
      DIMENSION       X(30), D(30), L(450), H(30)
      EXTERNAL        FUN, START
C-----------------------------------------------------------------------
C
C     THIS SUBROUTINE USES SUBROUTINE  QNMDIF  TO MINIMIZE A FUNCTION
C     OF N VARIABLES, WITHOUT USING DERIVATIVES.
C
C     THE CALLING PROGRAM MUST DECLARE EXTERNAL THE SUBROUTINES EQUI-
C     VALENT TO  FUN  AND  START.  THE CALL IS THEN OF THE FORM
C                    CALL MINMZE( N, NLDIM, FUN, START ).
C
C     PROGRAMMER:     DAVID SAUNDERS, STANFORD UNIVERSITY.
C     LAST UPDATED:   APRIL, 1973.
C
C     OTHER ROUTINES REQUIRED:
C                     QNMDIF,  LINSCH,  MODCHL,  APROXG,
C                     OUTPUT,  FUN,     START.
C
C     STORAGE FOR ARRAYS  X, D (DIMENSION N) AND  L (DIMENSION NLDIM=
C     N*(N-1)/2)  MAY BE SUPPLIED BY THE CALLER.  HOWEVER, IT WAS CON-
C     SIDERED CLEANER TO DIMENSION ABSOLUTELY ANY LOCAL ARRAYS IN THE
C     OTHER SUBROUTINES.  NO MULTI-DIMENSIONAL ARRAYS ARE USED SO THE
C     USER HAS ONLY TO GIVE ALL LOCAL ARRAYS  ABSOLUTE  DIMENSIONS OF
C     (AT LEAST)  N, WITH ONE EXCEPTION:
C                     MODCHL USES ARRAY  S  WITH DIMENSION  N+1.
C
C     THE USER MUST PROVIDE HIS OWN EQUIVALENTS OF THE 2  SUBROUTINES
C     FUN  AND  START  SUPPLIED HERE AS ILLUSTRATION.
C
C     COMPILERS:      WATFIV  OR  OS/360 FORTRAN H (OPT=2 RECOMMENDED)
C
C-----------------------------------------------------------------------
C
```

```
      SUBROUTINE QNMDIF( N, NLDIM, F, X, L, D, H, CONV, FUN )
C-----------------------------------------------------------------------
      IMPLICIT REAL*8 (A-H, L, O-Z )
      LOGICAL         UNITL, PRINT, BRIEF, CONV, SUCCES
      COMMON /CRITFP/ ETA, TOL, STEPMX, DEPS
      COMMON /NUMBRS/ NUMF
      COMMON /COUNTS/ NFEVAL, ICOUNT
      COMMON /TOTALS/ NFTOTL, NITERS
      COMMON /LOGICL/ BRIEF, PRINT, UNITL
      DIMENSION       X(N), L(NLDIM), D(N), H(N)
      DIMENSION       GK(30), GKPLS1(30), W(30), P(30), PP(30)
      EXTERNAL        FUN
C-----------------------------------------------------------------------
C
C     THIS SUBROUTINE ATTEMPTS UNCONSTRAINED FUNCTION MINIMIZATION,
C     USING A REVISED QUASI-NEWTON METHOD WITHOUT DERIVATIVES.
C     IT IS A TRANSLATION OF THE ALGOL PROCEDURE QNMDIFF IN THE RE-
C     PORT BELOW, TO WHICH THE USER IS REFERRED:
C
C     REFERENCE:  "IMPLEMENTATION OF TWO REVISED QUASI-NEWTON
C                  ALGORITHMS FOR UNCONSTRAINED OPTIMIZATION."
C                  BY GILL, MURRAY, AND PITFIELD (APRIL 1972).
C                  (REPORT DNAC 11 OF THE NPL, LONDON.)
C
C     THE ROUTINE SEEKS THE POINT X AT WHICH THE TWICE CONTINUOUSLY
C     DIFFERENTIABLE FUNCTION F(X) ATTAINS ITS LEAST VALUE. IDEALLY
C     THE VARIABLES SHOULD BE SCALED SO THAT THE HESSIAN  MATRIX OF
C     SECOND DERIVATIVES AT THE SOLUTION IS APPROXIMATELY ROW-EQUI-
C     LIBRATED, WITH THE FUNCTION MULTIPLIED BY A SCALAR SUCH  THAT
C     IT ACHIEVES A MAXIMUM VALUE OF UNITY WITHIN A UNIT SPHERE  A-
C     ROUND THE MINIMUM.  IT MAY NOT BE POSSIBLE TO FULFILL  EITHER
C     OF THESE REQUIREMENTS.
C
C     GIVEN AN INITIAL APPROXIMATION TO THE MINIMUM AND AN ESTIMATE
C     (LOWER BOUND) OF THE MINIMUM VALUE, THE ROUTINE CALCULATES  A
C     LOWER FUNCTION VALUE AT EACH ITERATION.  WHEN THE CONVERGENCE
C     CRITERIA ARE SATISFIED, THE ROUTINE GIVES THE ESTIMATED POSI-
C     TION OF THE MINIMUM, THE FINAL FUNCTION VALUE, AND  THE FINAL
C     CHOLESKY FACTORIZATION OF THE APPROXIMATE HESSIAN MATRIX.
C
C     THE PARAMETERS AND COMMON VARIABLES OF SUBROUTINE QNMDIF  ARE
C     INITIALIZED IN SUBROUTINE  START.  A DESCRIPTION OF THESE  IS
C     GIVEN NOW:
C
C     INPUT TO SUBROUTINE QNMDIF:
C
C     N      : THE NUMBER OF VARIABLES X(I) OF THE FUNCTION F(X).
C     FUN    : A SUBROUTINE RETURNING THE VALUE OF THE FUNCTION,  AT
C              THE POINT DEFINED BY VECTOR X(I).  THE CALL IS OF THE
C              FORM   CALL FUN( N, X, F ).
C     F      : A LOWER BOUND FOR THE MINIMUM VALUE OF THE  FUNCTION.
C     X      : AN INITIAL ESTIMATE OF THE SOLUTION.
```

```
C     L, D  : ARRAYS WHICH WILL NORMALLY NOT BE INITIALIZED BY THE
C             USER (BUT SEE "UNITL" BELOW).
C     H     : A 1-AN ARRAY CONTAINING THE INTERVALS FOR DIFFERENCING
C             F(X) ALONG EACH OF THE COORDINATE DIRECTIONS. TYPICAL
C             VALUE FOR THE H(I) IS DSQRT( DEPS ).
C     DEPS  : THE RELATIVE MACHINE PRECISION.
C     ETA   : THE TERMINATION CRITERION FOR THE LINEAR SEARCH.  IT
C             SHOULD HAVE A VALUE IN THE RANGE 0 TO 1.  THE CLOSER
C             TO ZERO IT IS, THE GREATER THE NUMBER OF EVALUATIONS
C             OF THE FUNCTION THAT WILL BE PERFORMED, WHILE THE
C             CLOSER TO 1 IT IS, THE GREATER THE NUMBER OF ITERA-
C             TIONS LIKELY.  ETA = 0.1 IS SUGGESTED TO START WITH.
C     TOL   : THE OVERALL TERMINATION CRITERION (NORM OF THE GRADI-
C             ENT).  A TYPICAL VALUE IS 1D-6.  (A GOOD ESTIMATE IS
C             APPROXIMATELY DSQRT( DEPS ), BUT THIS CAN BE RELAXED
C             (INCREASED) IF FEWER SIGNIFICANT FIGURES ARE ACCEPT-
C             ABLE.)
C     STEPMX: AN UPPER BOUND ON THE STEP ALLOWED ALONG A DIRECTION
C             OF SEARCH.  THIS CAN BE USED TO PREVENT OVERFLOW IN
C             IN THE COMPUTATION.  IF AN APPROXIMATE SOLUTION ISN'T
C             KNOWN, AND OVERFLOW IN COMPUTING THE FUNCTION IS UN-
C             LIKELY, THEN STEPMX CAN BE SET VERY LARGE (1D11, SAY)
C             SO THAT IT WILL NOT INFLUENCE THE ALGORITHM AT ALL.
C             IF THE SOLUTION IS KNOWN TO BE WITHIN A CERTAIN RANGE
C             OF THE INITIAL ESTIMATE, THEN STEPMX CAN BE SUITABLY
C             LOWERED.
```

```
C     UNITL : A LOGICAL VARIABLE WHICH SHOULD BE SET TO TRUE UNLESS
C             AN APPROXIMATION OTHER THAN THE UNIT MATRIX IS  KNOWN
C             FOR THE HESSIAN MATRIX OF SECOND DERIVATIVES OF F(X).
C             IF UNITL IS TRUE, THE UNIT MATRIX IS SUPPLIED BY  THE
C             SUBROUTINE, ELSE IT IS ASSUMED THAT AN LDL' FACTORIZ-
C             ATION IS GIVEN IN THE ARRAYS  L  AND  D.
C     PRINT : SET THIS LOGICAL VARIABLE TO TRUE IF COMPLETE  OUTPUT
C             IS DESIRED AFTER EVERY ITERATION.
C     BRIEF : SET THIS TO TRUE IF MORE CONCISE OUTPUT IS PREFERRED.
C             FULL INFORMATION FROM THE FINAL ITERATION  IS  STILL
C             PROVIDED EVEN IF PRINT IS FALSE.
C
C     OUTPUT FROM SUBROUTINE GNMDIF:
C
C     NFTOTL: THE TOTAL NUMBER OF FUNCTION EVALUATIONS USED.
C     NITERS: THE TOTAL NUMBER OF LINEAR SEARCHES PERFORMED.
C     CONV  : A LOGICAL VARIABLE SET TO TRUE IF TERMINATION  OCCURS
C             WITH THE CONVERGENCE CRITERIA SATISFIED, AND FALSE IF
C             A LOWER POINT CANNOT BE FOUND ALONG A PARTICULAR DIR-
C             ECTION OF SEARCH.
C     ALSO OUTPUT ARE FINAL VALUES FOR F, X, D, AND L.
C
C-----------------------------------------------------------------------
C
```

APPENDIX C

HYDRAULIC TORQUER DYNAMICS

A schematic of the torquer is shown in Fig. C-1. It consists of two parts:

(a) A hydraulic rotary actuator mounted on the gimbal,

(b) A two-stage electrohydraulic valve that controls the fluid flow to the actuator. Electrohydraulic valves of this type are described in the literature (e.g., GUI-1). The output torque of the actuator is proportional to the differential pressure across its vanes.

The first stage of the electrohydraulic valve is a nozzle and flapper driven by a d-c torque motor. Its output differential pressure, $p_{c1} - p_{c2}$, is proportional to the torque motor current.

The second stage is a two-orifice spool that is displaced by the applied and feedback differential pressures. The fluid flow to the actuator is proportional to the displacement.

The dynamic equations of the torquer are given below. For the spool,

$$m_v \ddot{x}_v = p_c A_1 - p A_2 - b \dot{x}_v , \qquad (C\text{-}1)$$

where

x_v = spool displacement

m_v = spool mass

p_c = $p_{c1} - p_{c2}$, the command differential pressure

p = $p_1 - p_2$, the feedback differential pressure

A_1, A_2 = the areas of application of the command and feedback pressures

b = viscous friction coefficient.

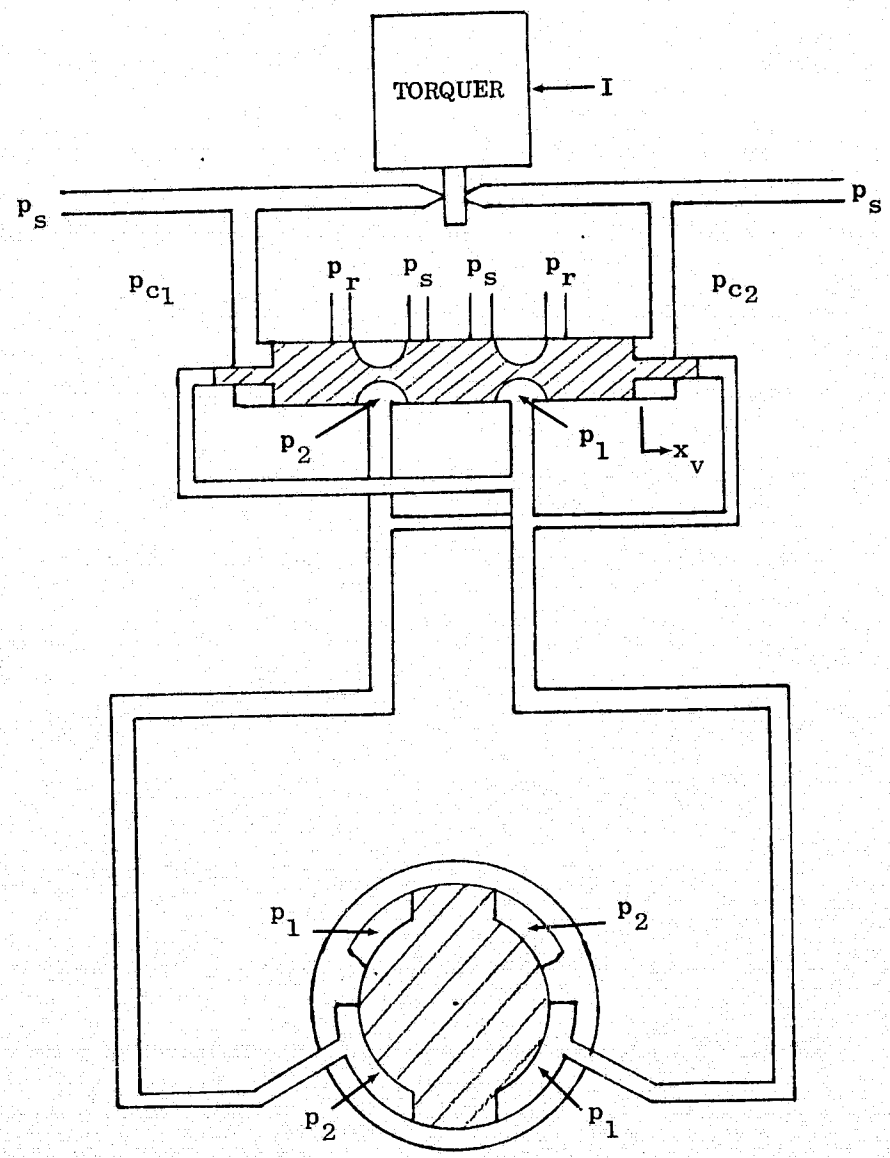

FIG. C-1 SCHEMATIC OF THE HYDRAULIC TORQUER

Assuming a first order lag between the flow rate and the displacement, we get

$$\dot{q} = c_1 x_v - \frac{1}{\tau_v} q , \qquad (C\text{-}2)$$

where

q = load flow rate

c_1 = proportionality constant.

Neglecting the mass of the spool in Eq. (C-1) and assuming $A_1 = A_2 = A$ (required for $p = p_c$ in the steady state), the final equation for the spool is

$$\dot{q} = K_A(p_c - p) - \frac{1}{\tau_v} q \qquad (C\text{-}3)$$

where

$$k_A = \frac{Ac_1}{b} .$$

For the actuator,

$$\dot{p} = \frac{B}{v_e} (q - k_L p - D_A \dot{\theta}), \qquad (C\text{-}4)$$

where

B = bulk modules of the fluid

v_e = volume of the actuator chamber

k_L = leakage coefficient across the vanes

D_A = chamber volume change per unit angular displacement

θ = relative angular displacement between the stationary and moving parts of the actuator.

Equations (C-3) and (C-4) are the state equations for the torquer with p and q as states. They are rewritten below

$$\begin{bmatrix} \dot{p} \\ \dot{q} \end{bmatrix} = \begin{bmatrix} -\frac{B}{v_e} k_L & \frac{B}{v_e} \\ -k_A & -\frac{1}{\tau_v} \end{bmatrix} \begin{bmatrix} p \\ q \end{bmatrix} + \begin{bmatrix} 0 \\ k_A \end{bmatrix} p_c + \begin{bmatrix} \frac{B}{v_e} & D_A \\ 0 & 0 \end{bmatrix} \dot{\theta} .$$

The transfer functions from p_c and $\dot{\theta}$ to the output p:

$$\frac{p}{p_c} = \frac{k_A(B/v_e)}{s^2 + \left(\frac{B}{v_e} k_L + \frac{1}{\tau_v}\right)s + \frac{B}{v_e}\left(\frac{k_L}{\tau_v} + k_A\right)} = \frac{N_1(s)}{D(s)} \qquad (C\text{-}5)$$

$$\frac{p}{\dot{\theta}} = \frac{\frac{B}{v_e} \times \frac{D_A}{\tau_v}}{D(s)} = \frac{N_2(s)}{D(s)} . \qquad (C\text{-}6)$$

Numerical values:

$$\frac{B}{v_e} = 2.75 \times 10^5 \frac{lb}{in^5}$$

$$k_L = 5 \times 10^{-4} \frac{in^5}{lb\ sec}$$

$$k_A = 1.4 \frac{in^5}{lb\ sec^2}$$

$$\frac{1}{\tau_v} = 24\ sec^{-1}$$

$$D_A = 0.3\ in^3/rad$$

$$\frac{p}{p_c} = \frac{1}{\left(\frac{s}{620}\right)^2 + \frac{0.26s}{620} + 1}$$

$$\frac{p}{\theta} = \frac{2\times10^6}{\left(\frac{s}{620}\right)^2 + \frac{0.26s}{620} + 1} \left[\frac{lb}{in^2}\ sec\right] .$$

The damping of this second order system depends mainly on the leakage across the vanes and therefore cannot be determined precisely. The natural frequency is proportional to the bulk modulus which may vary considerably with environmental conditions.

To use the torquer dynamic equations in the system, it is convenient to replace the command and output pressures by command and output accelerations. The relationship is

$$a = p\,\frac{D_A}{I} \qquad (C\text{-}7)$$

where

a = acceleration

I = load moment of inertia.

Substituting (C-7) into (C-3) and (C-4), we get the state equations

$$\begin{bmatrix}\dot{a}\\ \dot{q}\end{bmatrix} = \begin{bmatrix}-\frac{B}{v_e}k_L & \frac{B}{v_e}\frac{D_A}{I}\\ \frac{k_A I}{D_A} & -\frac{1}{\tau_v}\end{bmatrix}\begin{bmatrix}a\\ q\end{bmatrix} + \begin{bmatrix}0\\ \frac{k_A I}{D_A}\end{bmatrix} u_c - \begin{bmatrix}\frac{D_A^2}{I}\\ 0\end{bmatrix}\theta .$$

For the inner azimuth gimbal ($I = I_1 = 680$ in-lb-sec^2):

$$\begin{bmatrix}\dot{a}\\ \dot{q}\end{bmatrix} = \begin{bmatrix}-137 & 121\\ 3200 & 24\end{bmatrix}\begin{bmatrix}a\\ q\end{bmatrix} + \begin{bmatrix}0\\ 3200\end{bmatrix} u_c - \begin{bmatrix}1.3\times10^{-4}\\ 0\end{bmatrix}\dot{\varphi} .$$

For the elevation gimbal ($I = I_3 = 20$ in-lb-sec^2):

$$\begin{bmatrix} \dot{a} \\ \dot{q} \end{bmatrix} = \begin{bmatrix} -137 & 90 \\ 4300 & 24 \end{bmatrix} \begin{bmatrix} a \\ q \end{bmatrix} + \begin{bmatrix} 0 \\ 4300 \end{bmatrix} u_c - \begin{bmatrix} 9.6 \times 10^{-5} \\ 0 \end{bmatrix} \dot{\epsilon}$$

where $\dot{\varphi}$ and $\dot{\epsilon}$ are defined in Figure V-1.

APPENDIX D

NUMERICAL DATA FOR THE TRACKING TELESCOPE

1. Moments of Inertia*

Telescope plus inner azimuth gimbal about 1b axis:

$$I_1 = 680 \text{ in-lb-sec}^2.$$

Telescope plus inner azimuth and elevation gimbals about 2b axis:

$$I_2 = 400 \text{ in-lb-sec}^2.$$

Telescope plus inner azimuth and elevation gimbals about 3b or 1b axes:

$$I_3 = 920 \text{ in-lb-sec}^2.$$

Outer azimuth gimbal about 1_i axis:

$$I_4 = 2500 \text{ in-lb-sec}^2.$$

2. Acceleration Limits

Inner azimuth: 4 rad/sec^2

Elevation: 3.5 rad/sec^2

Outer azimuth: 0.65 rad/sec^2.

3. Measurements

(a) Target detector

Noise: 100 μrad rms at 2000 sec^{-1}

$$r_d = 10^{-11} \text{ rad}^2 \text{ sec}$$

---

* See Fig. V-1 for definition of axes.

(b) Gyro

Time constant: 1.5 msec

Gain : 2.5

Noise: 5 μrad rms at 3000 sec^{-1}

r_g: 2×10^{-14} rad^2 sec

4. Disturbances

Disturbance torques on inner gimbal:

$$\sigma_T = 0.1 \text{ rad/sec}^2 \text{ at } 200 \text{ sec}^{-1}$$

$$q_1 = 10^{-4} \text{ rad}^2/\text{sec}^3$$

Torquer noise (1% of full scale output)

$$\sigma_N = 0.04 \text{ rad/sec}^2 \text{ at } 300 \text{ sec}^{-1}$$

$$q_2 = 10^{-5} \text{ rad}^2/\text{sec}^3 .$$

5. Angular Limits

$$\varphi_{max} = \pm 3°$$

$$\epsilon_{max} = -6°, + 25°$$

Ψ, unlimited.

APPENDIX E

STRAIGHT LINE FLYBY

The geometry of a straight line flyby is shown in Fig. E-1 below.

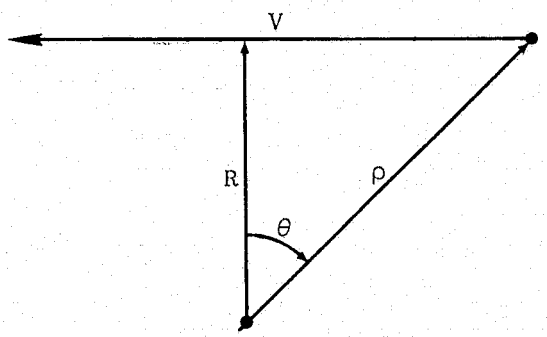

FIG. E-1 GEOMETRY OF A STRAIGHT LINE FLYBY

We have

$$\tan\theta = \frac{Vt}{R} = \tau$$

where t is measured from the time of passage at 0.

$$\dot{\theta} = \frac{V\cos\theta}{\rho} = \frac{V}{R}\cos^2\theta = \frac{V}{R}\frac{1}{1+\tau^2}$$

$$\ddot{\theta} = 2\frac{V^2}{R^2}\cos^3\theta\sin\theta = 2\frac{V^2}{R^2}\frac{\tau}{(1+\tau^2)^2}$$

$$\ddot{\theta}_{max} = 0.65\frac{V^2}{R^2} \text{ at } \tau = \frac{1}{\sqrt{3}} .$$

$\ddot{\theta}$ as a function of τ is shown in Fig. E-2.

The maximum angular acceleration in aximuth that the system can accommodate before the torquer of the outer azimuth gimbal saturates is 0.65 rad/sec^2. For this acceleration we obtain

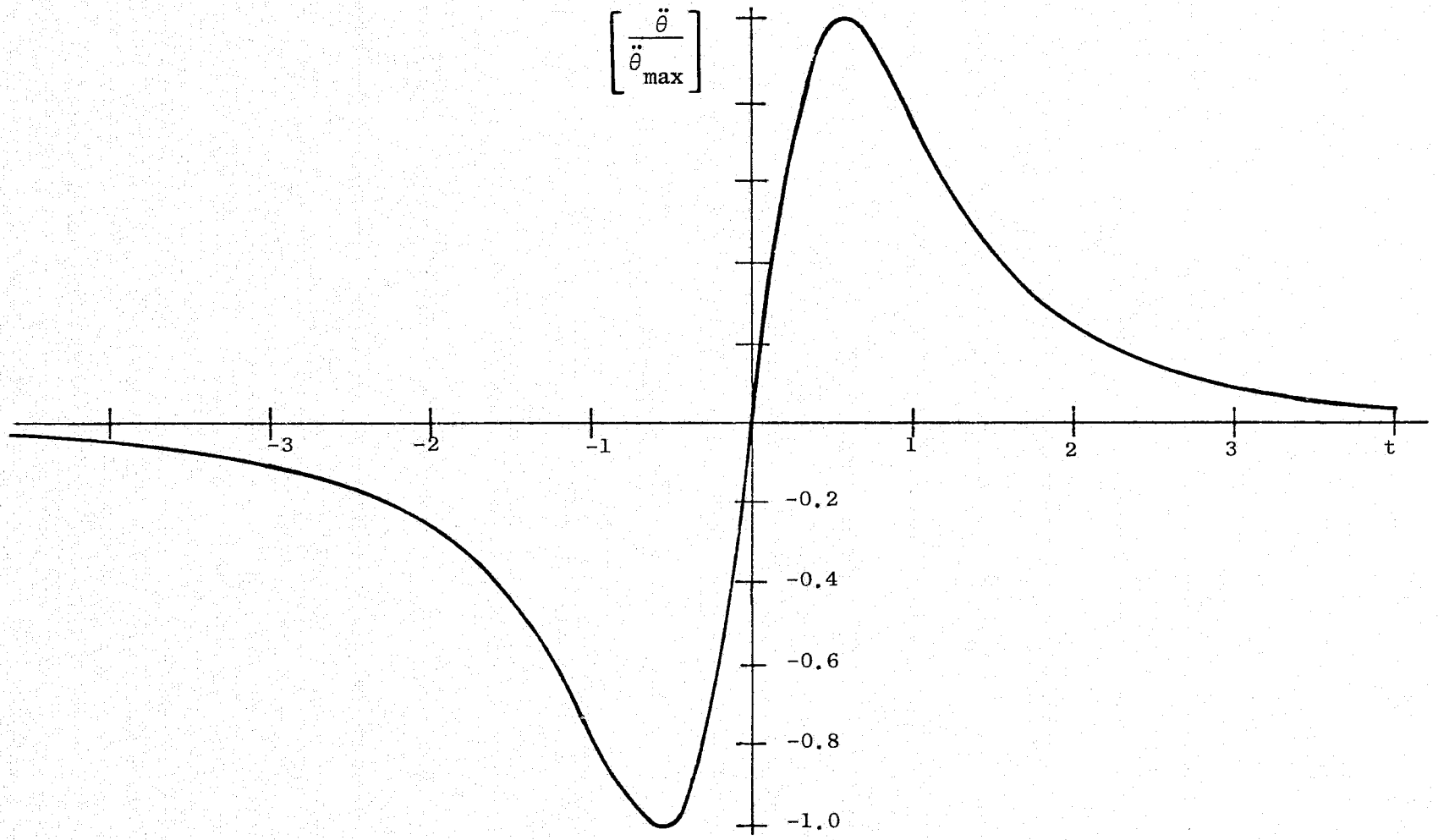

FIG. E-2 STRAIGHT LINE FLYBY IN POLAR COORDINATES

$$\left(\frac{V}{R}\right)_{max} = \sqrt{\frac{\theta_{max}}{0,65}} = 1 \text{ sec}^{-1}.$$

The time at which the maximum acceleration occurs for this ratio is

$$t_{max} = \frac{\tau_{max}}{\left(\frac{V}{R}\right)_{max}} = \frac{1}{\sqrt{3}} = 0,58.$$

The rate of change of the acceleration is low relative to the expected system bandwidth. If a Type 2 (constant acceleration error) system is specified, the error will therefore be approximately proportional to the instantaneous acceleration. The acceptable error at the point of maximum acceleration ($\tau = 1/\sqrt{3}$) can therefore be specified as the maximum error for a constant angular acceleration command. This error should be of the order of the measurement noise.

APPENDIX F

SYSTEM DYNAMIC EQUATIONS

The dynamic equations of the system are found in this Appendix using the Lagrangian method. Referring to Fig. V-1, and to the moments of inertia defined in Appendix D, the kinetic energy of the system is

$$T = \frac{1}{2} I_1(\dot{\varphi} + \dot{\psi} \cos \epsilon)^2 + \frac{1}{2}(I_3 - I_1)\dot{\psi}^2 \cos^2 \epsilon + \qquad \text{(F-1)}$$

$$+ \frac{1}{2} I_3 \dot{\epsilon}^2 + \frac{1}{2} \dot{\psi}^2 \sin^2 \epsilon + \frac{1}{2} I_4 \dot{\psi}^2 \ .$$

The potential energy is $V = 0$; $\therefore L = T$.

The moments about the gimbal axes are given by

$$M_\varphi = \frac{d}{dt} \frac{\partial T}{\partial \dot{\varphi}} - \frac{\partial T}{\partial \varphi}$$

$$M_\epsilon = \frac{d}{dt} \frac{\partial T}{\partial \dot{\epsilon}} - \frac{\partial T}{\partial \epsilon}$$

$$M_\psi = \frac{d}{dt} \frac{\partial T}{\partial \dot{\psi}} - \frac{\partial T}{\partial \psi}$$

$$\frac{\partial T}{\partial \dot{\varphi}} = I_1(\dot{\varphi} + \dot{\psi} \cos \epsilon)$$

$$\frac{\partial T}{\partial \varphi} = 0$$

$$\frac{\partial T}{\partial \dot{\epsilon}} = I_3 \dot{\epsilon} \ ,$$

$$\frac{\partial T}{\partial \epsilon} = (I_2 - I_3 + I_1)\dot{\psi}^2 \cos\epsilon \sin\epsilon - I_1(\dot{\varphi} + \dot{\psi}\cos\epsilon)\dot{\psi}\sin\epsilon$$

$$\frac{\partial T}{\partial \dot{\psi}} = I_1(\dot{\varphi} + \dot{\psi}\cos\epsilon)\cos\epsilon + (I_3 - I_1)\dot{\psi}\cos^2\epsilon + I_2\dot{\psi}\sin^2\epsilon + I_4\dot{\psi}$$

$$\frac{\partial T}{\partial \psi} = 0 \quad .$$

Defining $\dot{\alpha} = \dot{\varphi} + \dot{\psi}\cos\epsilon$ as the total rate about the inner azimuth axis, the moment equations are:

$$M_{\varphi} = I_1\ddot{\alpha}$$

$$M_{\epsilon} = I_3\ddot{\epsilon} + I_1\dot{\alpha}\dot{\psi}\sin\epsilon - (I_2 + I_1 - I_3)\dot{\psi}^2\cos\epsilon\sin\epsilon$$

$$M_{\psi} = [(I_3 - I_1)\cos^2\epsilon + I_2\sin^2\epsilon + I_4]\ddot{\psi} + I_1\ddot{\alpha}\cos\epsilon + 2(I_1 - I_3 + I_2)\dot{\psi}\dot{\epsilon}\cos\epsilon\sin\epsilon - I_1\dot{\alpha}\dot{\epsilon}\sin\epsilon \; .$$

APPENDIX G

LINEARIZATION OF THE ZERO ORDER HOLD (ZOH)

The transfer function of the ZOH (zero order hold) is [OG-1]

$$G_h(s) = \frac{1 - e^{-Ts}}{s} \tag{G-1}$$

The Laplace transform of the sampled signal $x(t)$ is [OG-1]

$$x^*(s) = \frac{1}{T} \sum_{k=-\infty}^{\infty} x(s + j\omega_0 k) \ . \tag{G-2}$$

If most of the incoming signal energy is in frequencies below the sampling frequency, $x^*(s)$ can be approximated by

$$x^*(s) \approx \frac{1}{T} x(s). \tag{G-3}$$

Combining Eqs. (G-1) and (G-3), the transfer function for the sampler and hold is

$$G_{sh}(s) = \frac{1 - e^{-Ts}}{Ts} = \frac{1 - e^{-\alpha}}{\alpha}$$

where

$$\alpha = Ts = \frac{2\pi s}{\omega_0} \ . \tag{G-4}$$

Using

$$\sin h \frac{\alpha}{2} = \frac{1}{2} (e^{\alpha/2} - e^{-\alpha/2}) \ ,$$

(G-4) may be rewritten as

$$G_{sh}(s) = \frac{\sin h \frac{\alpha}{2}}{\alpha/2} e^{-\alpha/2} \ . \tag{G-5}$$

Two approximations to $G_{sh}(s)$ will now be examined

(a) Approximation of $e^{-\alpha}$ in Eq. (G-4) by

$$e^{-\alpha} \cong \frac{1 - \alpha/2}{1 + \alpha/2} ;$$

(b) Approximation of $e^{-\alpha/2}$ in Eq. (G-5) by

$$e^{-\alpha/2} = \frac{1 - \alpha/4}{1 + \alpha/4} .$$

The transfer functions for these approximations are

$$G_a(s) = \frac{1}{1 + \frac{\pi s}{\omega_0}} \tag{G-6}$$

$$G_b(s) = \frac{\sin h \frac{\pi s}{\omega_0}}{\frac{\pi s}{\omega_0}} \frac{1 - \frac{\pi s}{2\omega_0}}{1 + \frac{\pi s}{2\omega_0}} . \tag{G-7}$$

For $s = j\omega$, the amplitudes and phases for these approximations are given in Table G-1.

Table G-1

	Exact	Approx. a	Approx. b
A	$\frac{\sin \frac{\pi\omega}{\omega_0}}{\frac{\pi\omega}{\omega_0}}$	$\frac{1}{\sqrt{1 + \left(\frac{\pi\omega}{\omega_0}\right)^2}}$	Exact
φ	$\pi \frac{\omega}{\omega_0}$	$\tan^{-1} \frac{\pi\omega}{\omega_0}$	$2 \tan^{-1} \frac{\pi\omega}{2\omega_0}$

Numerical values for the amplitudes and phases at different frequencies are given in Table G-2.

Table G-2

	A			φ(°)		
$\frac{\omega}{\omega_0}$	Exact	Approx. a	Approx. b	Exact	Approx. a	Approx. b
0.125	0.974	0.93	0.974	22.5	21.4	22.2
0.25	0.9	0.787	0.9	45.0	38.0	42.8
0.5	0.63	0.53	0.63	90.0	57.5	76.0

From Table G-2 it can be seen that if approximation b is used with a fixed gain of 0.9, the amplitude and phase correspond quite closely to the exact system up to $\omega = 0.25\ \omega_0$. The transfer function for this approximation can be written as

$$G_b(s) = 0.9\ \frac{4f_0 - s}{4f_0 + s} \qquad \text{(G-8)}$$

where f_0 is the sampling frequency.

The block diagram of this transfer function is shown in Fig. G-1. Its state representation is obtained from the block diagram as

$$\begin{aligned} \dot{\beta} &= -4f_0\beta - 7.2f_0\alpha + 7.2f_0\alpha_c \\ y &= \beta + 0.9\alpha - 0.9\alpha_c \end{aligned} \qquad \text{(G-9)}$$

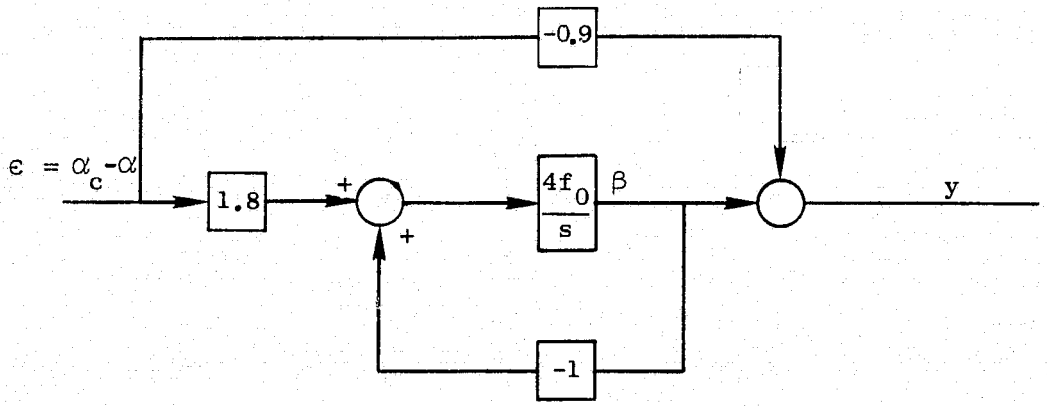

FIG. G-1 BLOCK DIAGRAM OF THE ZERO ORDER HOLD LINEARIZATION

APPENDIX H

GYRO DYNAMICS

The dynamic equation of a rate integrating gyro (RIG), which represents the sum of the moments about its output axis, is

$$J\ddot{\theta}_0 = - c\dot{\theta}_0 + H\omega_i + k_T i_T$$

where

θ_0 = output axis deflection

c = damping coefficient about the output axis

H = angular momentum of the gyro

ω_i = angular rate about the input axis

k_T = torquer scale factor

i_T = torquer current

J = inertia about the output axis.

For a typical RIG (e.g., Honeywell GG 334), the numerical values of the parameters are

$$H = 5 \times 10^4 \text{ gm-cm}^2/\text{sec}$$

$$c = 2 \times 10^4 \text{ gm-cm}^2/\text{sec}$$

$$J = 30 \text{ gm-cm}^2$$

$$k_T = 237 \text{ gm-cm}^2/(\text{sec}^2 \text{ ma}).$$

The transfer function of the gyro is therefore

$$\theta_0 = \frac{1}{s(s + \frac{c}{J})} \left(\frac{H}{J} \omega_i + \frac{k_T}{J} i \right) .$$

With the given values of the parameters

$$\theta_0 = \frac{1}{s(s + 660)}[1660\ \omega_i + 7.9\ i].$$

If c/J is much larger than the system bandwidth, the transfer function from the input axis rate to the output axis deflection is approximately

$$\frac{\theta_0(s)}{\omega_i(s)} \approx \frac{H}{Js}.$$

If the torquer current is made proportional to the output angle,

$$i = -Hk_A\theta_0,$$

the gyro becomes a rate gyro. For this case,

$$J\ddot{\theta}_0 = -c\dot{\theta}_0 - Hk_Ak_T\theta_0 + H\omega_i,$$

and the transfer function is

$$\frac{\theta_0(s)}{\omega_i(s)} = \frac{H}{J}\frac{1}{s^2 + \frac{c}{J}s + \frac{H}{J}k_Ak_T}.$$

The output angle is considered as a measure of the input axis rate.

The steady state scale factor is

$$\frac{\theta_{0ss}}{\omega_{iss}} = \frac{1}{k_Ak_T}.$$

In practice, the torquer current and not the output axis angle is measured.

In control applications the dynamics of the rate gyro is often neglected and the output angle is considered as a direct measurement

of the input rate, viz.,

$$\theta_0(s) = \frac{1}{k_A k_T} \omega_i(s) .$$

The influence of this neglection is to couple the system and gyro eigenvalues with the coupling becoming less pronounced as the gain of the rate gyro is increased.

For the system using the reduced order estimator, a root locus as a function of the gyro gain is shown in Fig. H-1 for values of this gain $[(H/J)k_A k_T]$ ranging from 10^6 to 10^8 sec^{-2}, which corresponds to gyro natural frequencies of 10^3 to 10^4 sec^{-1}. For gains above 10^7 sec^{-2} the root movement is hardly perceptible and even for $[(H/J)k_A k_T] = 10^6$, it is not excessive.

The influence of this gain on the rate gyro output noise will now be considered. The gyro pickoff noise is considered as having an rms of 5 μrad at 3000 sec^{-1} (see Appendix D). The gyro with its pickoff noise may therefore be represented by the block diagram in Fig. H-2. From this block diagram, the state equation of the gyro and its pickoff noise can be represented in state form as

$$\begin{bmatrix} \dot{x}_1 \\ \dot{x}_2 \\ \dot{x}_3 \end{bmatrix} = \begin{bmatrix} -\frac{1}{\tau} & 0 & 0 \\ 0 & 0 & 1 \\ -\frac{kH}{J} & -\frac{kH}{J} & -\frac{c}{J} \end{bmatrix} \begin{bmatrix} x_1 \\ x_2 \\ x_3 \end{bmatrix} \begin{bmatrix} \frac{1}{\tau} \\ 0 \\ 0 \end{bmatrix} v$$

$$y = \omega_0 = [k, \quad k, \quad 0]x,$$

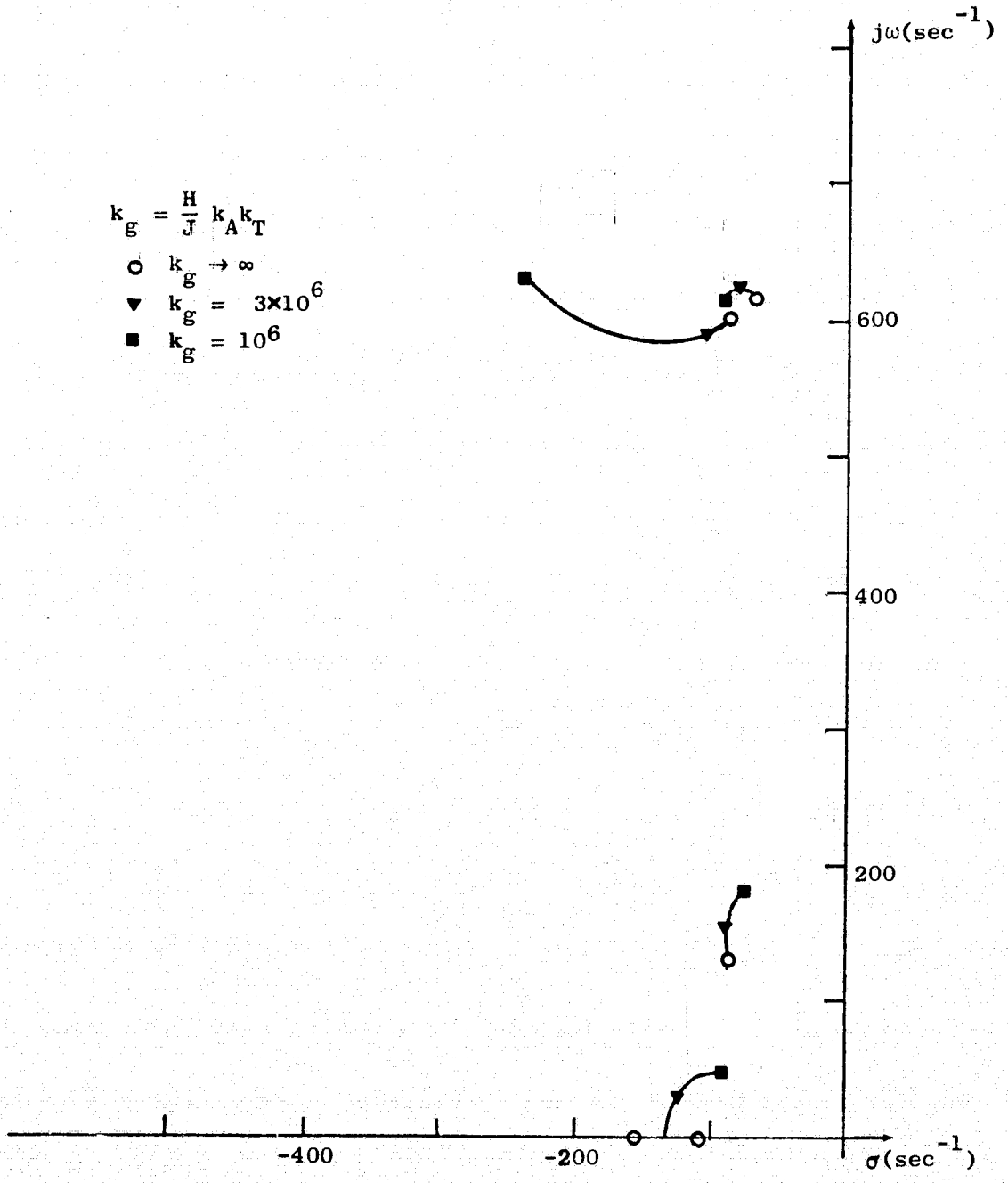

FIG. H-1 ROOT LOCUS AS A FUNCTION OF THE RATE GYRO GAIN

where $k = k_A k_T$. The output noise as a function of k can be obtained from this representation using

$$FX + XF^T = \Gamma Q \Gamma^T$$

where

X = the state covariance matrix

Q = the covariance matrix of the white noise v (see Fig. H-2),

and

$$E(y^2) = k^2[E(x_1^2) + E(x_1 x_2) + E(x_2^2)] .$$

The output rms noise as a function of k is shown in Fig. H-3. The noise can be seen to increase approximately linearly with the gain.

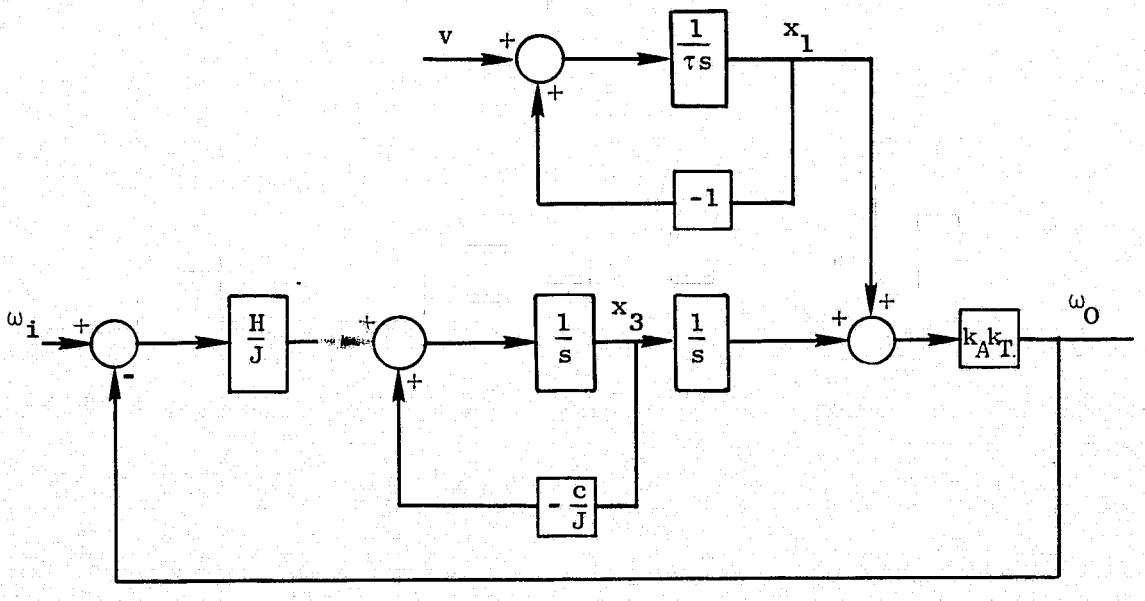

FIG. H-2 BLOCK DIAGRAM OF RATE GYRO WITH NOISE

Considering the eigenvalue coupling as shown in Fig. H-1, the gain

$$\frac{H}{J} k_A k_T = 3 \times 10^6$$

was selected.

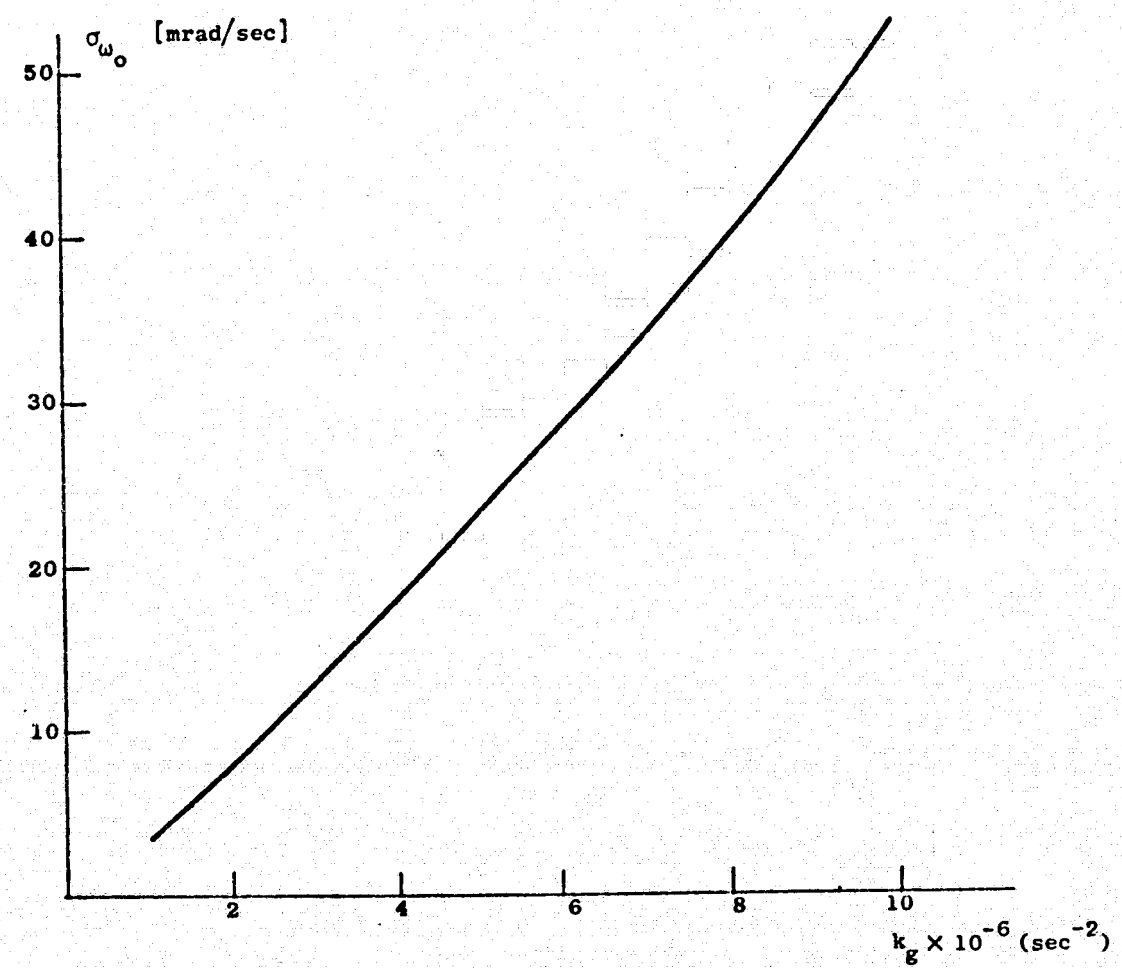

FIG. H-3 RATE GYRO RMS NOISE AS A FUNCTION OF THE GYRO FEEDBACK GAIN.

APPENDIX $\mathcal{J}$

THE ROOT SQUARE LOCUS METHOD FOR DETERMINING STATE WEIGHTS

The closed loop eigenvalues for a system designed by quadratic synthesis are the left half plane eigenvalues of (Eq. 2.6)

$$B + Y^T(-s)AY(s) = 0, \qquad (\mathcal{J}\text{-}1)$$

where

$$Y(s) = (sI - F)^{-1}G$$

is the transfer matrix from the control to the state:

$$x(s) = Y(s)u(s) .$$

For single input systems, Eq. ($\mathcal{J}$-1) can be written as

$$b + tr[AY^T(-s)Y(s)] . \qquad (\mathcal{J}\text{-}2)$$

For a matrix A with diagonal terms only, this equation becomes

$$1 + \sum_{i=1}^{n} \frac{a_{ii}}{b} y_i(-s)y_i(s) , \qquad (\mathcal{J}\text{-}3)$$

where

$$y_i(s) = \frac{N_i(s)}{D(s)}$$

is the transfer function from u to x_i.

If the ratios a_{ii}/b are fixed for all $i \neq k$, the root locus as a function of a_{kk}/b can be found, by writing Eq. (9-3) as

$$D(-s)\,D(s) + \sum_{i \neq k} \frac{a_{ii}}{b}\, Y_i(-s)Y_i(s) + \frac{a_{kk}}{b}\, Y_k(-s)Y_k(s) = 0$$

or, as

$$D_1(-s)D_1(s) = -\frac{a_{kk}}{b}\, Y_k(-s)Y_k(s) \,. \qquad (9\text{-}4)$$

The eigenvalues of the left and the right hand side are symmetric about both the real and the imaginary axis.

APPENDIX J

REDUCED ORDER OBSERVER

The concept of the reduced order observer was introduced by Luenberger [LU-1]. According to this concept, the state of a system can be observed by an observer of order $n - m$ where n is the dimension of the system and m the number of measurements.

Various approaches are available for the actual design of the observer. The approach used here is based on a design method proposed by Gopinath [GO-1].

Consider the observable system:

$$\begin{aligned} \dot{x}_0 &= F_0 x_0 + G_0 u + \Gamma_0 w \\ y &= H_0 x + v \quad . \end{aligned} \tag{J-1a}$$

A state transformation is performed such that the state vector has the form

$$x = \begin{bmatrix} x_r \\ \hline x_n \end{bmatrix}$$

and

$$y = x_n + v. \tag{J-1b}$$

In this representation, only the partial state vector x_r has to be observed since x_n is measured directly.

The dynamic equation of the transformed system can be put in the form

$$\begin{bmatrix} \dot{x}_r \\ \dot{x}_n \end{bmatrix} = \begin{bmatrix} F_r & B_r \\ H_r & F_n \end{bmatrix} \begin{bmatrix} x_r \\ x_n \end{bmatrix} + \begin{bmatrix} G_r \\ G_n \end{bmatrix} u + \begin{bmatrix} \Gamma_r \\ \Gamma_n \end{bmatrix} w \qquad \text{(J-2)}$$

from which the equations for x_r and x_n are

$$\dot{x}_r = F_r x_r + B_r x_n + G_r u + \Gamma_r w \qquad \text{(J-3a)}$$

$$\dot{x}_n = H_r x_r + F_n x_n + G_n u + \Gamma_n w \; . \qquad \text{(J-3b)}$$

From Eq. (J-3b), a "measurement" for the state x_r can be defined as

$$y_r = \dot{y} - F_n y - G_n u = H_r x_r + v_r \qquad \text{(J-4)}$$

where

$$v_r = \Gamma_n w + \dot{v} - F_n v \; . \qquad \text{(J-5)}$$

An observer for x_r using this "measurement" has the form

$$\dot{\hat{x}}_r = F_r \hat{x}_r + B_r y + g_r u + K_r (y_r - H_r \hat{x}_r) \; . \qquad \text{(J-6)}$$

Substituting for y_r from Eq. (J-4), the equation of the observer becomes

$$\dot{\hat{x}}_r = (F_r - K_r H_r)\hat{x}_r + (B_r - K_r F_n)y + (G_r - K_r G_u)u + K_r \dot{y} \; . \qquad \text{(J-7)}$$

In practice, it is of course not feasible to differentiate the measurement y and therefore a new state variable is defined as

$$\theta = \hat{x}_r - K_r y \; . \qquad \text{(J-8)}$$

The dynamic equation for θ is

$$\dot{\theta} = (F_r - K_r H_r)\hat{x}_r + (B_r - K_r F_n)y + (G_r - K_r G_n)u \qquad \text{(J-9)}$$

or

$$\dot{\theta} = (F_r - K_r H_r)\theta + [B_r - K_r F_n + (F_r - K_r H_r)K_r]y + (G_r - K_r G_n)u. \qquad \text{(J-10a)}$$

The estimates obtained from Eqs. (J-8) and (J-9) can be used in a controller for generating the feedback from the nonmeasured states. The control then has the form

$$u = -C_r x_r - C_y y. \qquad \text{(J-10b)}$$

A block diagram of a controller using such an estimator is shown in Fig. J-1.

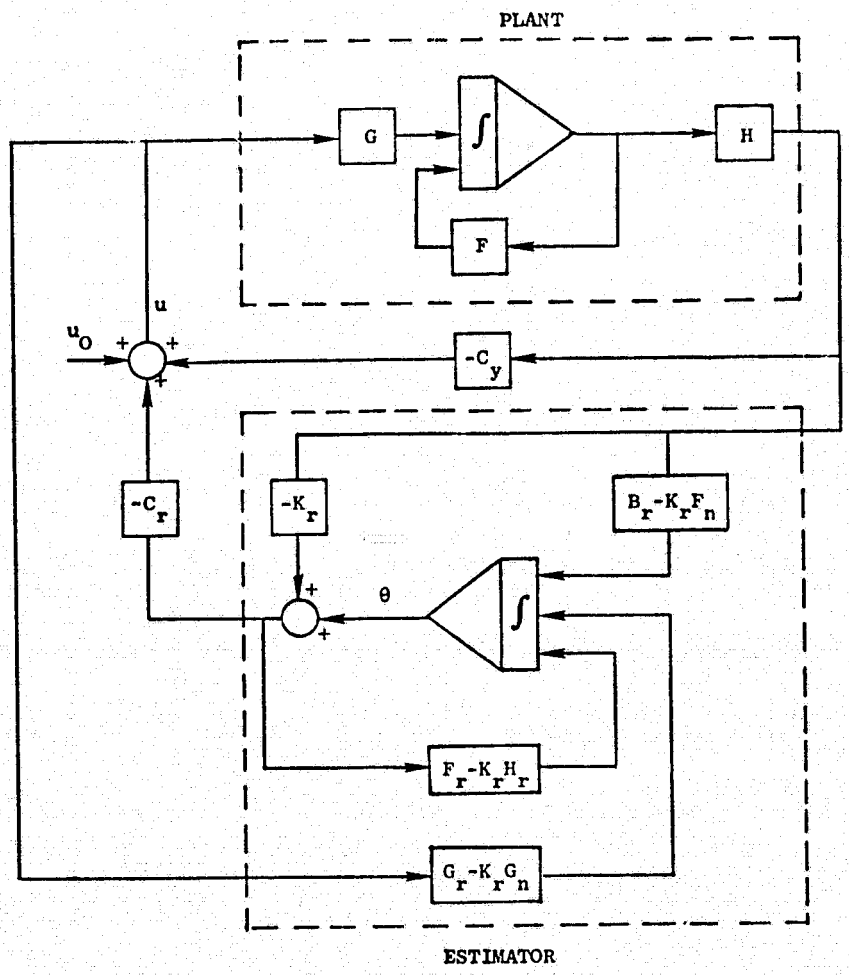

FIG. J-1 CONTROLLER WITH REDUCED ORDER OBSERVER

The error state equation can be obtained by substracting Eq. (J-6) from (J-3a), and using (J-1a). It is

$$\dot{\tilde{x}}_r = (F_r - K_r H_r)\tilde{x}_r - B_r v - K_r v_r + \Gamma_r w. \tag{J-11}$$

Substituting for v_r from Eq. (J-5a),

$$\dot{\tilde{x}}_r = (F_r - K_r H_r)\tilde{x}_r - (B_r - K_r F_n)v + (\Gamma_r - K_r \Gamma_n)w - K_r \dot{v} . \tag{J-12}$$

In order to avoid the use of $\dot{v}$, a new state variable is defined as

$$\tilde{\theta}_r = \tilde{x}_r + K_r v .$$

Its dynamic equation is

$$\dot{\tilde{\theta}}_r = (F_r - K_r H_r)\tilde{\theta}_r - [B_r - K_r F_n + (F_r - K_r H_r)K_r]v + (\Gamma_r - K_r \Gamma_n)w . \tag{J-13}$$

The control equation, (J-10a), can now be rewritten as

$$u = -C_r x_r + C_r \tilde{\theta}_r - C_y x_n - (C_r K_r + C_y)v . \tag{J-14}$$

Substituting Eq. (J-14) in (J-3a), and adding (J-13), the dynamic equations for the augmented system are obtained. They are

$$\begin{bmatrix} \dot{x}_r \\ \dot{x}_n \\ \dot{\tilde{\theta}}_r \end{bmatrix} = \begin{bmatrix} F_r - G_r C_r & B_r - G_r C_n & G_r C_r \\ H_r - G_n C_r & F_n - G_n C_n & G_n C_r \\ 0 & 0 & F_r - K_r H_r \end{bmatrix} \begin{bmatrix} x_r \\ x_n \\ \tilde{\theta}_r \end{bmatrix} + \begin{bmatrix} \Gamma_r & -M_1 \\ \Gamma_n & -M_2 \\ \Gamma_r - K_r \Gamma_n & -M_3 \end{bmatrix} \begin{bmatrix} w \\ v \end{bmatrix} \tag{J-15}$$

where

$$M_1 \equiv G_r(C_r K_r + C_y)$$

$$M_2 \equiv G_n(C_r K_r + C_y)$$

$$M_3 \equiv B_r - K_r F_n + (F_r - K_r H_r)K_r .$$

To apply this method to the inner gimbal system as represented in Fig. V-2a, the detector measurement ϵ must be defined as a state.

From Appendix G,

$$\epsilon = \beta + 0.9\,\alpha \tag{J-17a}$$

$$\dot{\beta} = -4f_0\beta - 7.2f_0\alpha\ . \tag{J-17b}$$

Differentiating (J-17a), inserting (J-17b), and using $\dot{\alpha} = \omega$, the state equation for ϵ is

$$\dot{\epsilon} = -4f_0\epsilon - 3.6f_0\alpha + 0.9\omega\ . \tag{J-18}$$

Using

$$x_r^T = [\alpha,\ a,\ r]$$

$$x_n^T = [\epsilon,\ \omega]$$

the dynamic equation, (J-2), can be written in the explicit form

$$\begin{bmatrix} \dot{\alpha} \\ \dot{a} \\ \dot{r} \\ \hline \dot{\epsilon} \\ \dot{\omega} \end{bmatrix} = \left[\begin{array}{ccc|cc} 0 & 0 & 0 & 0 & 1 \\ 0 & 0 & 1 & 0 & 0 \\ 0 & -m_2 & -m_1 & 0 & 0 \\ \hline -3.6f_o & 0 & 0 & -4f_o & 0.9 \\ 0 & 1 & 0 & 0 & 0 \end{array}\right] \begin{bmatrix} \alpha \\ a \\ r \\ \epsilon \\ \omega \end{bmatrix} + \left[\begin{array}{c} 0 \\ 0 \\ m_2 \\ \hline 0 \\ 0 \end{array}\right] u + \left[\begin{array}{cc} 0 & 0 \\ 0 & 0 \\ 0 & m_2 \\ \hline 0 & 0 \\ 1 & 0 \end{array}\right] \begin{bmatrix} w_1 \\ w_2 \end{bmatrix} \tag{J-19}$$

From this equation, the augmented state equation can be set up. The estimator gain matrix K is then found by parameter optimization, using the PAROPT program. The resulting K matrix is

$$K = \left[\begin{array}{c|c} -0.139 & 1.03\times10^{-4} \\ 1.46\times10^{4} & -8.75\times10^{2} \\ -5.05\times10^{7} & 2.73\times10^{3} \end{array}\right]\ .$$

The observer eigenvalues are: $-36 \pm 610j$, -0.54. Note the very low real eigenvalue.

These results were used in Chapter V-D-4 for comparative evaluation.

APPENDIX K

DETERMINATION OF ACCELERATION ERROR

In this Appendix, the acceleration errors are determined for two types of systems: (1) Type DR I, (2) Type DR H2. The errors are determined by computing the value of the integral state i for a constant rate command. This is equal to the value of the state $\epsilon = di/dt$ for a constant acceleration command. For a constant rate command, $\epsilon = 0$ (Type II system).

1. Type DR I

No control is required for constant rate and the sum of the inputs to the gyro must therefore be zero. From Fig. V-4 this sum is

$$\Sigma u = a_0 i + a_1 \epsilon + \omega_c = 0.$$

Since $\epsilon = 0$ and $\omega = \omega_c$

$$i = \frac{1}{a_0} \omega.$$

This is also the value of the error ϵ for a constant acceleration command and the acceleration error coefficient is therefore

$$\frac{\epsilon}{a_c} = \frac{1}{K_A} = \frac{1}{a_0}.$$

2. Type DR H2 (Fig. V-6c)

The sum of the controls that are obtained from the nonzero estimator states and the integral control must be zero.

From Fig. V-7b, it is obvious that for constant ω

$$\hat{\omega} = \omega$$

$$\hat{a} = \hat{p} = 0 .$$

From Fig. V-7a, the state equation for estimator 1 is

$$\begin{bmatrix} \dot{\hat{\beta}} \\ \dot{\hat{\alpha}} \end{bmatrix} = \begin{bmatrix} -4f_o - k_1 & -7.2f_o - 0.9k_1 \\ -k_2 & -0.9k_2 \end{bmatrix} \begin{bmatrix} \hat{\beta} \\ \hat{\alpha} \end{bmatrix} + \begin{bmatrix} k_1 \\ k_2 \end{bmatrix} \epsilon + \begin{bmatrix} 0 \\ 1 \end{bmatrix} \omega .$$

For $\epsilon = 0$, the steady state transfer functions from $\hat{\beta}$ and $\hat{\alpha}$ to ω can be found. They are

$$\hat{\beta} = \frac{7.2f_0 + 0.9k_1}{3.6f_0k_2}$$

$$\hat{\alpha} = -\frac{4f_0 + k_1}{3.6f_0k_2} \omega .$$

The total control, therefore, is

$$u = 0 = c_i i + c_\beta \hat{\beta} + c_\alpha \hat{\alpha} + c_\omega \hat{\omega}$$

$$= c_i i + \frac{c_\beta(7.2f_o+0.9k_1) - c_\alpha(4f_o+k_1) + 3.6f_o k_2 c_\omega}{3.6\, f_o k_2} .$$

The value of ϵ for a constant acceleration command (equal to i for a constant rate command) is therefore

$$\frac{\epsilon}{a_c} = \frac{1}{k_a} = -\frac{c_\beta(7.2f_0+0.9k_1) - c_\alpha(4f_0+k_1) + 3.6f_0k_2c_\omega}{3.6f_0k_2c_i} .$$

For stability of the characteristic equation of (1), $k_2 > 0$. In general, $c_\beta < 0$, and the three terms in the numerator are therefore additive. Low k_1 can be seen to decrease the error but it also decreases the damping of the characteristic equation of (1) and causes a higher control noise.

For other estimators, the error coefficients can be found in a similar way but since there are many nonzero states in the estimator, the expressions become complicated.

REFERENCES

AC-1 Ackerman, T., "Der Entwurf Linearer Regelungssysteme im Zustandsraum," Regelungstechnik und Prozessodaten-Verarbeitung, Vol. 20, pp. 297-300, 1972.

AN-1 Anderson, B.D.O and D.G. Luenberger, "Design of Multivariable Feedback Systems," Proc. IEEE, Vol. 114, No. 3, Mar 1967.

AN-2 Anderson, B.D.O. and T.B. Moore, Linear Optimal Control, Prentice Hall, Englewood Cliffs, N.J., 1971.

BE-1 Bellman, R., Introduction to Matrix Analysis, McGraw Hill Book Co., New York, 1960.

BI-1 Bingoulac, S.P., "An Alternate Approach to Expanding PA + A'P = -Q," IEEE Trans. Auto. Control, Vol. AC-15, pp. 135-137, Feb 1970.

BO-1 Bode, W.H., Network Analysis and Feedback Amplifier Design, D. Van Nostrand Co., Inc., New York, 1945.

BR-1 Bradt, A.J., "Sensitivity Functions in the Design of Optimal Controllers," IEEE Trans. Auto. Control, Vol. AC 13, No. 1, Feb 1968.

BRY-1 Bryson, A.E., "Control Theory for Random Systems," Invited Lecture, 13th International Congress of Theoretical and Applied Mechanics, Moscow, Aug. 1972. reprinted as SUDAAR No. 447, Dept. Aeronautics & Astronautics, Stanford University, Stanford, Calif., Sept 1972.

BRY-2 Bryson, A.E., and Y.C. Ho, Applied Optimal Control, Ginn-Blaisdell, Waltham, Mass, 1969.

BYR-3 Bryson, A.E., and W.E. Hall, "Optimal Control and Filter Synthesis by Eigenvector Decomposition," Dept. of Aeronautics and Astronautics, Stanford University, Stanford, Calif., SUDAAR No. 436, Dec 1971.

BU-1 Bull, John S., "Precise Attitude Control of the Stanford Relativity Satellite," Ph.D. Dissertation, Dept. Aeronautics and Astronautics, Stanford University, Stanford, Calif. SUDAAR No. 452, Mar 1973.

CA-1 Cameron, Bader, and Mobley, "Design and Operation of the NASA 91.5 CM Airborne Telescope," Applied Optics, Vol. 10, No. 9, 1971.

CAS-1 Cassidy, J., and I. Lee, "On the Optimal Feedback Control of a Large Launch Vehicle to Reduce Trajectory Sensitivity," Proc. 1967 JACC, pp. 587-595.

CAS-2 Cassidy, J., and R.J. Roy, "Sensitivity Design of Output Feedback Controllers," Proc. 1970 JACC, pp. 400-406.

CH-1 Chen, C.T., Introduction to Linear System Theory, Holt, Rinehart & Winston Inc., New York, 1970.

CR-1 Cruz, J.B., System Sensitivity Analysis, Dowden, Hutchison and Ross, Stroudsburg, Penn., 1973.

DA-1 D'Angelo, H., Moe, M.L. and Hendricks, "Trajectory Sensitivity of an Optimal Control System," 4th Allerton Conf. On Circuit & Systems Theory, pp. 489-498, 1966.

DO-1 Dougherty, H.J., I. Lee, and de Russo, "Synthesis of Optimal Feedback Control Systems Subject to Parameter Variations," Proc. 1967 JACC, pp. 125-133.

FI-1 Fitts, J.M., "Aided Tracking as Applied to High Accuracy Pointing Systems," IEEE Trans. Aero. El. Systems, Vol. AES, No. 9, No. 3, May 1973.

FO-1 Forsythe, E.G., M.A. Malcolm, and C.B. Moler, "Computer Methods for Mathematical Computations," Computer Science Dept., Stanford University, Stanford, Calif., Dec 1972.

FR-1 Francis, J.G.F., "The QR Transformations," Computer Journal, Vol. 4, No. 3, pp. 265-272 & pp. 332-345. 1961.

GA-1 Gantmacher, F.R., Matrix Theory, Chelsea Publishing Co., New York, 1959.

GI-1 Gill, P.E., W. Murray, and R.A. Pitfield, "The Implementation of Two Revised Quasi Newton Algorithms for Unconstrained Optimization," National Physics Laboratory, Teddington, Middlesex, England, Report No. NAC 111, Apr 1972.

GO-1 Gopinath, B., "On the Control of Multiple Input Output Systems," Bell Sys. Tech J., Vol. 50, pp. 1063-1081, Mar 1971.

GU-1 Guillon, M., Hydraulic Servo Systems, Plenum Press, New York, 1969.

GUP-1 Gupta, N.K., and A.E. Bryson, "Guidance for a Tilt-Rotor VTOL Aircraft During Takeoff and Landing," Dept. Aeronautics and Astronautics, Stanford University, Stanford, Calif., SUDAAR No. 448, Dec 1972.

GUP-2 Gupta, N.K., and A.E. Bryson, "Automatic Control of a Helicopter With a Hanging Load," Dept. Aeronautics and Astronautics, Stanford University, Stanford, Calif., SUDAAR No. 448, Jun 1973.

HA-1 Hagander, Per, "Numerical Solution of $A^TS + SA + Q = 0$," Information Sci., Vol. 4, pp. 35-50, 1969.

HE-1 Hendricks, T., and H. D'Angelo, "An Optimal Fixed Structure Design With Minimal Sensitivity for a Large Elastic Booster," 5th Allerton Conf. On Circuit & System Theory, pp. 142-150, 1967.

HO-1 Holley, W.W., and A.E. Bryson, "Multi-Input, Multi-Output Regulator Design for Constant Disturbances and Non-Zero Set Points With Application to Automatic Landing in a Crosswind," Dept. Aeronautics and Astronautics, Stanford University, Stanford, Calif., SUDAAR No. 465, Aug 1973.

JO-1 Johnson, C.D., "A Mathematical Analysis of the Problem of Pointing," IEEE Trans. Aero. El Sys., Vol. AES-8, No. 5, Sep 1972.

JO-2 Johnson, C.D., and R.E. Skelton, "Optimal Desaturation of Momentum Exchange Control Systems," AIAA J., Vol. 9, No. 1, Jan 1971.

KA-1 Katz, Paul, "Sample Rate Selection for Digital Control of Aircraft," Stanford University, Aeronautics & Astronautics, Guidance & Control Lab., Stanford, Calif., 94305.

KR-1 Kreindler, E., "On Servo Problems Reducible to Regulator Problems," IEEE Trans. Auto. Control, Vol. AC 14, No. 4, Aug 1969.

KR-2 Kreindler, E., "Closed Loop Sensitivity Reduction of Linear Optimal Control Systems," IEEE Trans. Auto. Control, Vol. AC 13, No. 3, Jun 1968.

KR-3 Kreindler, E., "On Minimization of Trajectory Sensitivity," Int. J. Control, Vol. 8, No. 1, 1968.

KW-1 Kwakernaak , H., "Optimal Low Sensitivity Linear Feedback Systems," Automatica, Vol. 5, No. 3, pp. 279-286.

KW-2 Kwakernaak, H., and R. Sivan, Linear Optimal Control Systems, Wiley - Interscience, New York, 1972.

LA-1 Lamont, G.B. and S.J. Kahne, "Time Domain Sensitivity Comparisons," 5th Allerton Conf., pp. 161-169, 1967

LU-1 Luenberger, D.G., "Observing the State of a Linear System," IEEE Trans. Mil. El., Vol. MIL-8, Apr 1964.

LU-2 Luenberger, D.G., "Observers for Multivariable Systems," IEEE Trans. Auto. Control, Vol. AC-11, No. 2, Apr 1966.

LUH-1 Luh, J.Y.S., and E.R. Cross, "Optimal Controller Design for Minimum Trajectory Sensitivity," 5th Allerton Conf. On Circuit & System Theory, pp. 152-159, 1967.

OG-1 Ogata, K., Modern Control Engineering, Prentice Hall, Inc., Englewood Cliffs, N.J., 1970.

PA-1 Pace, I.S., and S. Barnett, "Comparison of Numerical Methods for Solving Lyapunov Matrix Equations," Int. J. of Control, Vol. 15, No. 5, 1972.

PAL-1 Palsson, T., and Whitta[illegible]er, "Parameter Uncertainties in Control System Design," Proc. 1972 JACC, pp. 248-254.

PO-1 Porter, B., and R. Crossley, Modal Control, Barnes & Noble, New York, 1972.

RA-1 Ramaswami, B., and K. Ramar, "A New Method for Solving Optimal Servo Problems," IEEE Trans. Auto. Control, Vol. AC 17, No. 1, Feb 1972.

RE-1 Rediess, H.A., and H.P. Whitaker, "A New Model Performance Index for Engineering Design of Flight Control Systems," AIAA J. of Aircraft, Vol. 7, Nov 1970.

RI-1 Rillings, J.H., and R.J. Roy, "Analog Sensitivity Design of Saturn V Launch Vehicle," IEEE Trans. Auto. Control, Vol. AC-15, No. 4, Aug 1970.

RY-1 Rynasky, E.G., and R.F. Whitbeck, "Theory and Application of Linear Optimal Control," Cornell Aeronautical Laboratory, Buffalo, New York, 14221, Report No. CAL. 1H-1943-F-1, Oct 1965.

RY-2 Rynasky, E.G., R.F. Whitbeck, and B.W. Dolbin, "Sensitivity Considerations of a Flexible Launch Vehicle," Cornell Aeronautical Laboratory, Buffalo, New York, 14221, Report No. CAL BE-2311-F-1.

SA-1 Sannuti, P., J.B. Cruz, et al, "A Note on Trajectory Sensitivity of Optimal Control Systems," IEEE Trans. Auto. Control, Vol. AC 13, No. 1, Feb 1968.

SC-1 Schultz and Melsa, State Functions and Linear Control Systems, Mc Graw Hill, Inc., New York, 1967.

ST-1 Stavroulakis, P., and P.E. Sarachik, "Low Sensitivity Feedback Gains for Deterministic and Stochastic Systems," Int. J. of Control, Vol. 19, No. 1, Jan 1974.

TA-1 Tashker, M.G., "Integral Control of a Spinning Drag-Free Satellite," Ph.D. Dissertation, Dept. Aeronautics and Astronautics, Stanford University, Stanford, Calif., 94305, SUDAAR No. 472, Apr 1974.

WH-1 Whittaker, Burdin, "A Gyro Stabilized Heliostat for Airborne Astronomy," ISA Trans., Vol. 5, No. 2, 1966.

WI-1 Wilkie, D.F., and W.R. Perkins, "Essential Parameters in Sensitivity Analysis," Automatica, Vol. 5, pp. 191-197, 1969.

WIT-1 Witsmeer, A.J., "Preliminary Design Studies of Attitude Control Systems for the Stanford Relativity Satellite," Dept. Aeronautics and Astronautics, Stanford University, Stanford, Calif., 94305, SUDAAR No. 337, Jan 1968.